# CATALYSIS BY PILLARED MONTMORILLONITES EXCHANGED WITH TRANSITION METALS

*Thesis submitted to*

*Cochin University of Science and Technology*

*in partial fulfillment for the requirements for the degree of*

**Doctor of Philosophy**

**In**

**Chemistry**

In the Faculty of Science

*By*

**MANJU KURIAN**

*Department of Applied Chemistry*

*Cochin University of Science and Technology*

*Kochi-22*

**April 2004**

*To my beloved parents*

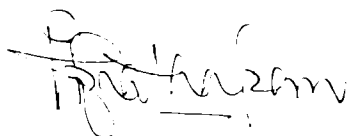*......... for I owe them a lot more than I can express.*
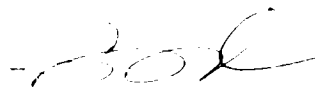
T73
MAN

541.395
MAN

# CERTIFICATE

Certified that the present work entitled **"Catalysis by pillared montmorillonites exchanged with transition metals"** submitted by Ms. Manju Kurian is an authentic record of research work carried out by her under our supervision in the Department of Applied Chemistry in partial fulfillment of the requirements for the Degree of Doctor of Philosophy of Cochin University of Science and Technology, and further that no part thereof has been submitted previously for the award of any degree.
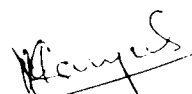
Kochi-22

15- 2- 2004


**Dr. S Prathapan**

(Supervising Guide)

Dept. of Applied Chemistry,

Cochin University of

Science and Technology,

Kochi-22,

India.

**Dr. S Sugunan**

Professor and Head

(Supervising Co Guide)

Dept. of Applied Chemistry

Cochin University of

Science and Technology

Kochi-22,

India.

# DECLARATION

I hereby declare that the work presented in the thesis entitled **"Catalysis by pillared montmorillonites exchanged with transition metals"** is based on the original work done by me independently under the combined guidance of Dr. S Prathapan (Reader, Organic Chemistry) and Dr. S Sugunan (Professor and Head, Physical Chemistry) in the Department of Applied Chemistry, Cochin University of Science and Technology. I further declare that this thesis has not formed the basis for the award of any degree or diploma, fellowship or associateship or similar title of any University or Institution.

MANJU KURIAN

Kochi-22
15- 4- 2004

## PREFACE

Catalysis is probably one of the most ancient chemical phenomena to find an application in that; many of the early molecules were formed by catalytic processes involving metal or photo catalysis. The very first synthesis by a catalyst in nature took place many millions of years ago and ever since; catalysis has been responsible for life in all its manifestations on this globe.

The use of clay for mainly clay figures, pottery and ceramics was already known by primitive people about 25,000 years ago. Today clays are important materials with a large variety of applications in ceramics, oil drilling and the metal and paper industry. Clays are furthermore used as adsorbents, decolouration agents, ion exchangers and molecular sieve catalysts. For the application as molecular sieve catalysts, a group of expandable clays known as smectites is employed. Although, the idea of expanding clays has a history of about 50 years, the rapid advances in the field of zeolites overshadowed this possibility. There is now a renewed interest in pillared clays, since by varying the size of the pillars and the distance between the pillars; one can tune the pore size for specific applications in fine chemical synthesis.

The present work is oriented to obtain a comparative evaluation of the physicochemical properties and catalytic activities of iron, aluminium and iron aluminium mixed pillared montmorillonites and their transition metal exchanged analogues. Reactions of industrial importance like Friedel Crafts alkylations, catalytic wet peroxide oxidation of phenol and MTBE synthesis have been selected for the present study. The thesis is structured into seven chapters. First chapter deals with a brief introduction and literature survey on pillared clays. Second chapter explains the materials and methods employed in the work. Results and discussions on the characterisation techniques are described in the third chapter. The subsequent three chapters describe the catalytic activities of pillared clays in the industrially important reactions. Last chapter comprises the summary of the investigations and the conclusions drawn from the earlier chapters.

..

# Acknowledgements

my deep sense of appreciation to my present labmates Sanjay, Sunaja, Radhika, Binitha, Shali, Maya, Ramanathan, Kochurani and Ajitha. I remember with thanks the help provided by Mr. Saravanan, Department of Physics, Mr. Gopi Menon, Mr. Jose and Mr. Kashmiri, Department of Instrumentation, Mr. Murali, Department of Electronics and Mr. Suresh, Chemito during the technical difficulties.

I would like to thank my parents for the immense moral support rendered to me in times of shade. It will be highly ungrateful of me not to acknowledge the cooperation given by my in laws without which I would not have been able to complete the work in time. I would like to apologise my daughters and my husband for the long hours spent on research than with them. My husband had been the epitome of encouragement and assistance throughout the entire period and my words fail to convey my gratitude towards him.

# CONTENTS

## Chapter 3    Physicochemical Characterisation

## Chapter 4    Friedel Crafts Alkylations

## Chapter 5    Phenol Hydroxylation

# 1

# INTRODUCTION

*Heterogeneous catalysis is an interdisciplinary area and modern industries are learning more and more about the applications and benefits of catalysts. Catalyst technologies generally involve less capital investment, lower operating costs, higher purity products and reduced environmental hazards. Pillar interlayered clays constitute a novel class of microporous materials with good thermal stability, high surface area and pronounced Brönsted and Lewis acidity. These materials result from a two step modification of naturally occurring swelling clay minerals; the propping apart of clay layers by intercalation with oligo or polymeric cationic metal complexes and calcination of the intercalated clays transforming the inserted complexes into nanosized pillars of metal oxides cross linked to the clay layers. Thus pillared clays present a category of innovative materials for molecular sorption, chemical synthesis and shape selective catalysis. A brief introduction and literature review on catalysis as well as pillared montmorillonites are presented in this chapter. The details of the various reactions selected for the present study are also outlined. Finally a short outlook on the objectives of the present work is summarised.*

## 1.0 INTRODUCTION

Catalysis is probably one of the most ancient chemical phenomena to find an application in that, many of the early molecules were formed by catalytic processes involving metal or photo catalysis. The very first deliberate synthesis of a catalyst (an enzyme) took place many millions of years ago and ever since, catalysis has been responsible for life in all its manifestations on this globe. Today, more than 60% of all chemical products and almost 90% of chemical processes are based on catalysis, attesting the ubiquitous presence and necessity of this discipline throughout the chemical industry.

The history of catalysis began from 1876 with the studies by von Marum on dehydrogenation of alcohols using metals. J Roebuck used a catalyst industrially for the first time in the manufacture of $H_2SO_4$ by the oxidation of $SO_2$ (Lead Chamber process). However, the term catalysis was defined by J.J Berzelius in 1836, as a process in which a relatively small amount of a foreign material, called catalyst augments the rate of a reaction without being consumed in the reaction. Early developments occurred in inorganic industrial chemistry with processes for carbon dioxide, sulphur trioxide and chlorine production in 1800s[1]. At the moment, most of the catalysts are used in three major industries: chemical processing, petroleum refining and pollution control. In terms of physical volume, catalyst consumption continues to be dominated by petroleum refining[2]. But cost wise, pollution abatement catalysts being mostly made of platinum group metals, match the catalysts consumed in petroleum refining.

## 1.1 HETEROGENEOUS CATALYSIS

Conventionally, the field of catalysis is divided into homogeneous and heterogeneous catalysis. A catalytic reaction in which the reactants and catalyst are in same phase is homogeneous catalysis and if the reactants and catalyst are in

different phases, it is heterogeneous catalysis. Each of these has their own advantages and disadvantages. Homogeneous systems often accomplish better selectivity, activity and reproducibility. However, they are vulnerable to extraneous materials and cost of production is high, owing to low thermal stability and short catalyst lifetime. The advantages of heterogeneous catalytic processes include easy separation of final reaction mass from the catalyst, reusability of the catalyst and possibility of continuous operation in reactor without interruption. Also heterogeneous processes are more environmentally benign and have little disposal problems. Thus, the so-called E- factor or ratio of the amount of by products to amount of products is usually low for heterogeneous processes and hence the field is one of the rapidly advancing areas in chemical industry.

Heterogeneous catalysts perform by interacting with reactants and enhance the rate of chemical reactions. This interaction may be chemical or physical processes or steps, which are fundamental to any heterogeneous catalytic system. Each of these steps contributes to a greater or lesser extent to the overall reaction rate. The general steps involved in heterogeneous catalysis are:

- External diffusion: Transfer of reactants from bulk fluid phase to fluid-solid interface and external surface of the catalyst particle.

- Internal diffusion (for porous particles): Internal transfer to catalyst particle

- Adsorption: Physisorption and chemisorption of reactants at the surface (sites) of the catalyst particle.

- Surface reaction: Chemical reaction of adsorbed species giving adsorbed products; this is the intrinsic or true chemical reaction step.

- Desorption: Release of adsorbed products from the catalyst.

- Internal diffusion: Transfer of products to outer surface of catalyst particle.

- External diffusion: Transfer of products from fluid-solid interface into reaction stream.

3

An exceptional heterogeneous catalyst must possess both high activity and long-term stability. But the most important quality is selectivity, which reflects its ability for direct conversion of reactants in a specific way. The properties of a good catalyst for industrial use may be divided into two categories[3].

- properties that determine catalytic activity and selectivity directly. Here, factors such as bulk and surface chemical composition, local microstructure and phase composition are important.
- properties that ensure their successful implementation in the catalytic process. Here, thermal and mechanical stability, porosity, shape and dimensions of the particle enter.

Heterogeneous catalysts can be classified in several ways. Based on their physicochemical characteristics, they can be classified as metal oxides (simple metal oxides, mixed metal oxides, supported metal oxides and modified metal oxides), supported metals/bimetallic catalysts, zeolites/molecular sieves, clays, hydrotalcites and solid supported heteropolyacids. Another mode of classification is based on their behaviour in a particular reaction, as structure sensitive and structure insensitive. Rates of structure sensitive catalytic reactions alter markedly when the crystallite size of the system is changed whereas rate is independent of crystallite size in structure insensitive catalytic reactions. Apart from these, they can be classified on the basis of their functions as shape selective, phase transfer, redox and acid base catalysts.

In recent years, a large variety of organic transformations have been reported over heterogeneous catalysts like zeolites and other microporous materials like clays, oxides and mixed oxides[4]. Reactions on surfaces may be classified in terms of reactant or product classes or on the basis of mechanistic similarities[5].

i. Acid base (ionic) reactions. Catalytic cracking, hydration, dehydration, hydrolysis, isomerisation and a host of other reactions pertain to this type. Acid base

property of a heterogeneous surface is the important factor in determining the catalytic efficiency of these reactions.

ii. Oxidation reduction (electronic) reactions. Reactions pertaining to this type are oxidation, reduction, hydrogenation, dehydrogenation, decomposition of unstable oxygen containing compounds and others. The reactions are catalysed by solid possessing free or easily excited electrons i.e. metals and semiconductors.

## 1.2 SMECTITES

The swelling phyllosilicate minerals known as smectites constitute a naturally occurring class of inorganic catalysts. These omnipresent minerals are often found as large mineralogically pure deposits[6]. Due to small particle size ( < 2 micrometres) and unusual intercalation properties, they afford an appreciable surface area for adsorption of organic molecules[7]. The probable catalytic role of smectites has been recognised in several natural processes like chemical transformations in soils[9], petroleum forming reactions[8] and reactions related to chemical evolution[10]. In fact, clays are considered to have served as micro reactors in prebiotic synthesis, effecting the formulation of life itself! More than 70 years ago, Eugene Houndry found that acid modified smectites gave gasoline in high yield when used as petroleum cracking catalysts[11] and were used extensively as commercial catalysts until the mid 1960's. Today smectites are important materials with large variety of applications in ceramics, oil drilling and the metal and paper industry. Besides, they are used as adsorbents, decolouration agents and ion exchangers.

## 1.3 SMECTITE STRUCTURES

Smectites have layer lattice structures in which two dimensional oxy anions are separated by layers of hydrated cations. The oxygen atoms define the upper and lower sheets of tetrahedral sites and a central sheet of octahedral sites. The extremely stable $SiO_4$ tetrahedral structural unit polymerise to form two dimensional

5

sheets of composition $T_2O_5$ by sharing three oxygens (basal oxygens) at the corners of the tetrahedra[12]. The fourth oxygen, called apical oxygen, points normally away from the tetrahedral sheet and is linked to the octahedral sheet of aluminium. It turns out to be geometrically possible for oxygens to be shared between two types of sheets lying on top of the other. As a result, the oxygen of Si-O becomes the oxygen of Al-OH, producing the link Si-O-Al. The tetrahedral sheet has no further spare apical oxygen, so an Oct- Tet- Oct sandwich is not possible. As the octahedral sheet has spare OH groups, formation of Tet- Oct- Tet layer is possible. The members of the smectite group of clays are distinguished by the type and location of cations on the oxygen framework. In a unit cell formed from twenty oxygens and four hydroxyl groups there are eight tetrahedral sites and six octahedral sites. When two-thirds of the octahedral sites are occupied by trivalent cations, the mineral is classified as dioctahedral 2:1 phyllosilicate and if all octahedral sites are filled with bivalent cations, the mineral is termed trioctahedral 2:1 phyllosilicate.

In smectites, isomorphous substitution occurs during their formation in dirty geochemical environments. In the tetrahedral layer, an occasional $Si^{4+}$ is replaced by an $Al^{3+}$ ion. Consequently, the valencies of coordinated oxygens are no longer saturated. In order for electronuetrality to be maintained, cations come into the interlamellar space, in between two adjoining platelets and condense next to the negatively charged silicate sheet. Likewise, in a random manner, an $Al^{3+}$ is replaced with a divalent ion such as $Mg^{2+}$, $Mn^{2+}$ or $Fe^{2+}$. Again, counter ions in the interlamellar space compensate the electrical imbalance exactly. Thus, the primary structure of smectites is lamellar, with parallel layers of tetrahedral silicate and octahedral aluminate sheets. Secondary structure stems from valence deficiencies in primary structure. The tertiary structure is a consequence of secondary structure. This is a result of the effect of interstitial cations that are trapped as freely moving ions between the negatively charged layers[13].
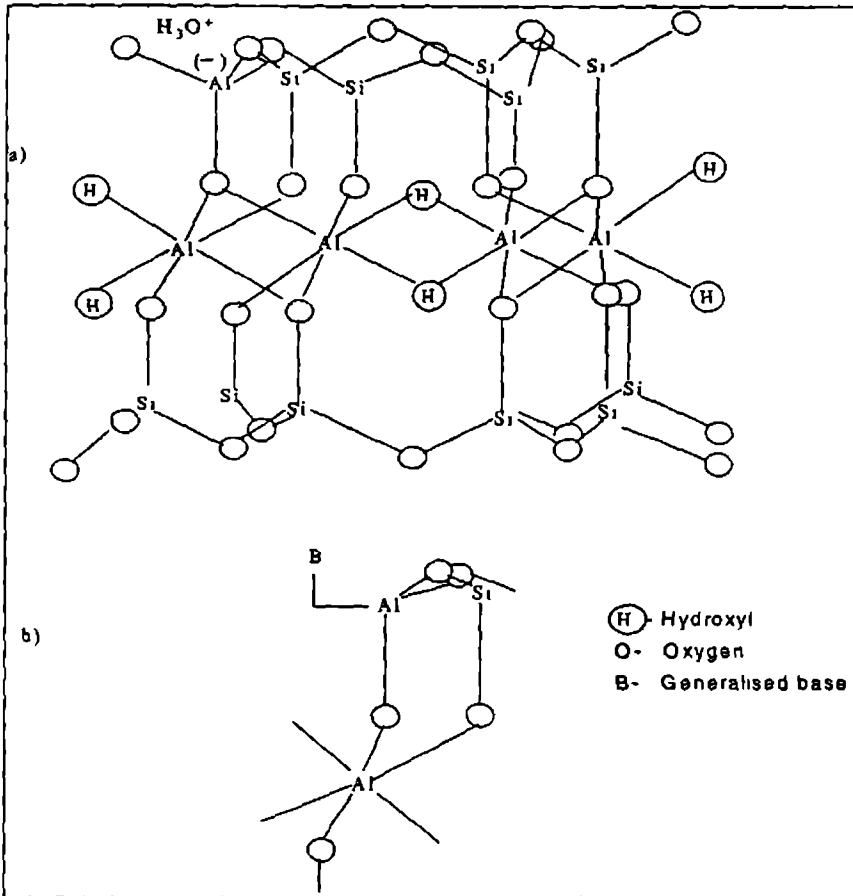
Figure 1.1 a) off axis projection of a 2:1 dioctahedral mineral with Brönsted acid site.
b) possible configuration of a Lewis acid site.

An $H_3O^+$ associated with the negatively charged octahedral layer acts as a Brönsted acid site. Brönsted acidity also stems from terminal hydroxyl groups and from bridging oxygens. Aluminium in threefold coordination, perhaps occurring at an edge, or arising from a Si-O-Al rupturing dehydroxylation of Brönsted site, would correspond to a Lewis site (Figure1.1). An octahedral $Al^{3+}$ located at a platelet edge after thorough dehydration, will be electron pair acceptors and will function as aprotic

acids in the Lewis sense. Obviously, water will convert the Lewis site into Brönsted site, a fact that limits the study of Lewis sites to relatively anhydrous systems[14].

The most common and familiar smectite is the montmorillonite with formula, $M_{x/n} \cdot yH_2O[Al_{4.0-x}Mg_x]Si_8O_{20}(OH)_4$. In the tetrahedral sheet, tetravalent Si is sometimes partly replaced by trivalent Al. Nevertheless, the extent to which this occurs is less than the frequency of substitution of $Al^{3+}$ ions by others in octahedral sites[15]. In the octahedral sheet, there may be replacement of trivalent Al by divalent Mg without complete filling of third vacant octahedral position resulting in the cropping up of layer charge. Al atoms can be replaced by Fe, Cr, Zn, Li or other atoms. The small size of these atoms permits them to take the place of the small Si and Al atoms; therefore the replacement is often referred to as isomorphous substitution[16].

## 1.4 PROPERTIES OF SMECTITES

Smectites possess a combination of cation exchange, intercalation and swelling properties that makes them unique.

**1.4.1 Cation exchange:** Smectites can adsorb cations and retain them in exchangeable form. Cation exchange capacity (CEC) can be defined as the sum of exchangeable cations that mineral adsorbs at a specific pH, i.e. a measure of negative charges carried by the mineral. These negative charges can be derived from, i) isomorphous substitution within structure ii) broken bonds at edges and external surfaces iii) dissociation of accessible hydroxyl groups.

Negative charges due to isomorphous substitution within the mineral structures are known as permanent charge and are independent of conditions such as pH and ion activity whereas those from latter two sources are dependant[17]. The negative charge of montmorillonites arises mainly from isomorphous substitution within structure. Only a small variable charge is present, since all disposable hydroxyl groups are present in subsurface planes covered by a network of oxygen

atoms. Since exchangeable cations compensate the unbalanced charge in the interior of layers due to isomorphous substitutions, CEC is a measure of the degree of substitution. The essence of this phenomenon is that cations of interlamellar space have no fixed sites in the lattice and if the mineral is immersed in electrolyte, exchanges governed by the principle of equivalence will take place between the external and internal cations[18].

**1.4.2 Swelling:** Smectites can expand beyond a single molecular layer. The retention of water by clays and finely divided materials is due to adsorption and capillary condensation. The adsorption creates pillars between clay layers and a water film on external surfaces of particles or aggregates which induce the increase of spacing between clay layers and of the distance between particles. This is the swelling mechanism. Adsorption forces that induce swelling are equilibrated by capillary condensation forces[19]. The extent of interlayer swelling depends on the nature of swelling agent, exchange cation, layer charge and its location. Thus, if a sodium or calcium smectite is transformed into a potassium mineral, swelling is altogether suppressed[20]. Several models were recommended to explain the swelling mechanism in smectites. A macroscopic energy balance model for crystalline swelling of 2:1 phyllosilicates was suggested by Laird[21]. Crystalline swelling for a static system was modelled by balance among potential energies of attraction, repulsion and resistance. Politowicz *et.al.* suggested a lattice model for explaining the influence of swelling on reaction efficiency[22].

**1.4.3 Intercalation:** Intercalation is the insertion of guest species in interlayer space with preservation of layered structure. Neutral molecules other than water can be intercalated between the layers. Several binding mechanisms may operate in the intercalation processes[23-25]. One particularly important mechanism involves complex formation between exchanged cations and intercalant as in the binding of pyridine to $Cu^{2+}$ exchanged forms of smectites[26]. Another one is the reaction of hydrated cation

9

functioning as Brönsted acid site and intercalant acting as base as in the case of binding of ammonia as ammonium ion in Mg montmorillonite[27].

Naturally occurring clays may not be efficient for acid catalysed reactions, especially if the unit cell composition is neutral and is balanced with alkali or alkaline earth metals. The best way of activating the clay is by acid leaching and by pillaring with polyhydroxy metal cations. Acid activation generally involves treatment with dilute acids. $H^+$ ions attack the silicate layers via the interlayer region and exposed edges, displacing octahedral ions like $Al^{3+}$ and $Mg^{2+}$, which then occupy interlayer sites, causing little damage to silicate layer. Rate of dissolution of octahedral sheet increases with concentration of acid, temperature, contact time and increasing Mg content[28,29]. Modifications can also be effected on smectite by impregnation of metal oxides like vanadia, chromia and alumina[30,31]. The structure, composition of metal oxide and extent to which they interact with the clay support may all influence the catalytic activity[32]. Impregnation also modifies acidity, due to varying dispersion and interaction with oxide surface and contributes to conversion and selectivity[33]. One new class of intercalates incorporates metal complex catalysts between the silicate layers. Although the immobilisation of complex catalysts in clay structures makes it possible to conduct solution-like reactions in the solid state and to minimise many of the technical and economic barriers associated with the use of homogeneous solution catalysts, the advantages of catalyst intercalation go beyond mere immobilisation. By mediating the chemical and physical forces acting on interlayer reactants, one can often improve catalytic specificity relative to homogeneous solution[18]. Though various modifications can be effected on clay surface, the process called pillaring is by far resourceful in competency as well as widespread application.

## 1.5 PILLARED CLAYS

Intercalation of clays via exchange of cations located in their interlayer space with hydroxy metal cations, followed by a thermal treatment is an effective approach

to obtain catalysts, catalyst supports, sensors or adsorbents[34]. The materials thus prepared are referred to as pillar interlayered clays (PILCs). By varying the size, charge and shape of the entering ions, a homogenous network of micropores can be obtained with pore openings ranging in size from 16-30 Å. These pores are easily accessible for adsorption of gases. Pillared clays are characterised by high surface area, pore dimensions larger than in zeolites and substantial intrinsic acidity[35-38].

The preparation of these solids can be considered as a logical sequence of two facts: First, the intercalation of large organic molecules in the interlayer space of layered clays has been reported earlier and the intercalation chemistry has been widely studied[39]. Second, the existence and structure of a positively charged polymeric aluminium species had been established[40-42]. The basic phenomenon used in the preparation of pillared clays is the exchange of interlamellar cations by bulky cationic species that props apart clay layers keeping the structure open. Thus only swelling clays capable of cation exchange can be pillared. Pillaring mechanism essentially consist of the exchange of charge balancing cations (preferably $Na^+$) by a cationic oligomer $P_n^{v+}$ made from n cations bound by oxo or hydroxo bridges and with a total charge $v^+$. If M is the symbol representing clay, then

$$MNa_v + P_n^{v+} \rightarrow MP_n + vNa^+ \qquad (I)$$
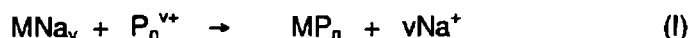
The gallery height or basal spacing increases by a length somewhat lower than the radius of oligomer. The oligomer itself results from condensation reactions such as

$$nP^{Z+} \leftrightarrow P_n^{v+} + (nZ-v) H^+ + xH_2O \qquad (II)$$
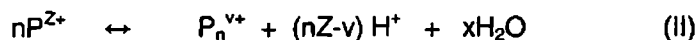
involving hydronium and water. Therefore, the overall pillaring reaction necessarily involves reactions I and II and chemical properties of clay surfaces such as its acidity play an important role. Microporosity is created in the resulting intercalated clay by removing hydration water by thermal activation. The nature and extent of crosslinking action of $P_n^{v+}$ on adjacent microcrystals depend on the nature of both the surface of clay and that of pillar. The solid stabilised in the temperature range of 400- 500°C is

the actual pillared clay. Since the pillaring oligomers are cationic, they will be distributed on the surface as far as possible to reduce mutual electrostatic repulsion. The pillaring process can be schematically shown as,
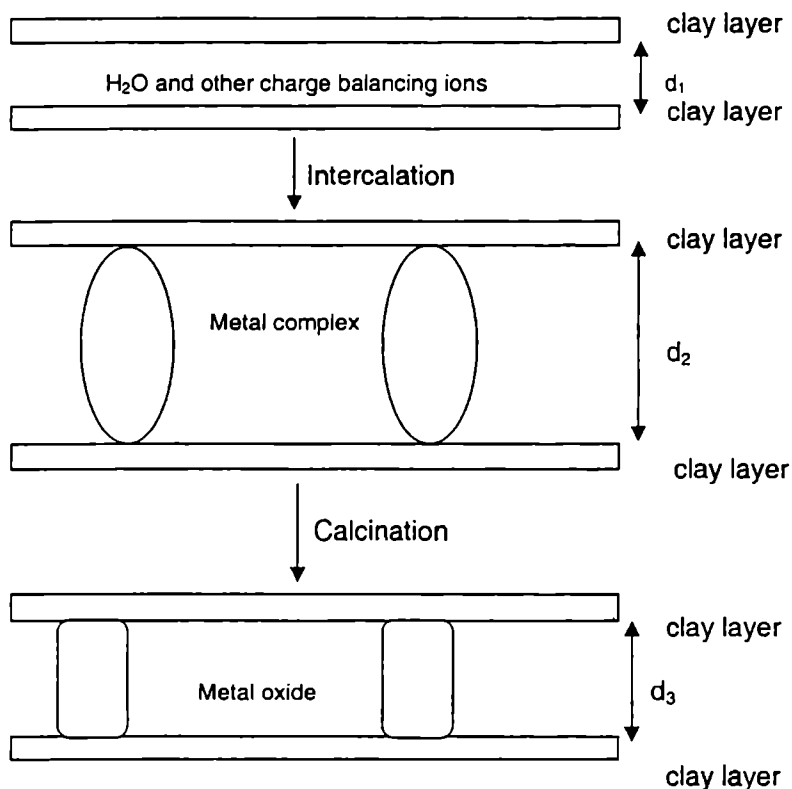


Figure1. 2. Schematic description of pillaring ($d_1 < d_3 < d_2$)

Microporous structure of pillared clays is characterised by the distance between intercalated oxides (pillars). These are the interlayer and interpillar spacings showing two or three dimensional microstructure respectively. The interlayer spacing depends on chemical nature and height of intercalating species. On the other hand, interpillar distance is mainly related to density of pillars, which in turn depends strongly on the extent, and distribution of charge density on clay layers and also on size of pillars[43].

Drying of the intercalated product has profound influence on the structure of resultant pillared solid. Air-drying favours face-to-face orientation of layers whereas freeze-drying preserves the structure of flocculated clay, which exhibits substantia edge-to-face orientation, or a card house structure. The material is then said to be delaminated. Delaminated clays and pillared clays have different pore structures[44]. The differences in stacking morphology for the two clays are illustrated in figure 1.3.
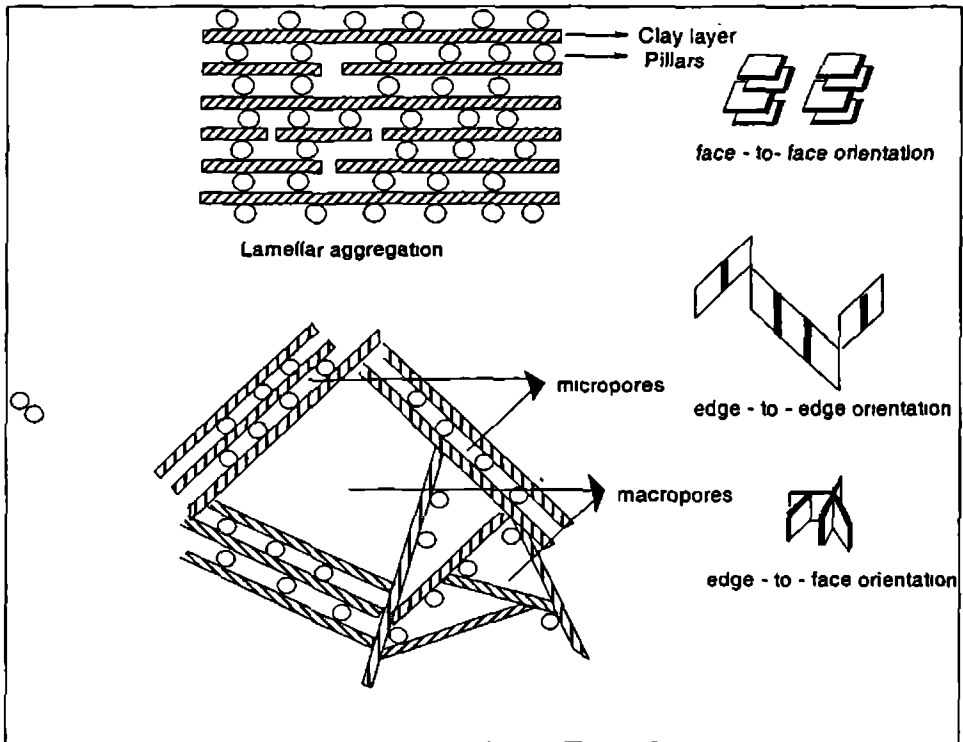


Figure 1.3. Stacking morphology of pillared and delaminated clays

In general terms, the experimental procedure for the synthesis of pillared clay is as follows. A suspension containing layered clay is mixed with a solution containing polyoxocation. This solution has been previously partially hydrolysed and aged in order to polymerise a multivalent cation. The reaction between polyoxocation

and clay consisting of the substitution of exchangeable cations is known as cationic exchange reaction or intercalation. After the reaction, the resulting suspension is separated and washed, giving rise to the intercalated clay. Its calcination at moderately high temperature stabilises the polymeric cation, preventing the collapse of interlayer space and generating a stable porous structure. Plee *et.al* investigated the process of pillaring using MASNMR of $^{29}$Si and $^{27}$Al and found that in uncalcined pillared products, only electrostatic bonding exists between the negatively charged layers and pillaring oligocations[45]. Tichit *et.al* concluded from XRD and FTIR measurements that dilatation of the sheet occurs on calcination, though structural integrity of the original clay sheet was preserved[46].

Apart from the general procedure of pillaring, several other variations, which concern different parameters in the synthesis like starting clay, intercalating solution, intercalation process and drying and calcination steps among the others. These modifications in chemical aspects include

- pillaring with mixed solutions containing more than two cations[47-48]
- using coordination or organometallic compounds[49-50]
- using polymers and surfactants[51-52]
- pillaring of acid activated clays[53-54]
- enhancement of pillared clay acidity[55-56]
- pillaring using metal oxide sol[57-58].

## 1.6 CHARACTERISTICS OF PILLARED CLAYS

The versatile applications of pillared clays as catalysts, catalyst supports, adsorbents and sensors require regular distribution of pillars and pores in interlayer region. The basal spacing, specific surface area, pore size distribution and thermal stability are essential physical characteristics of pillared solids. The preparation conditions are very critical for the ultimate size of the molecules that have access to

the gallery. A broad spectrum of different pillared clays can be formed by control of experimental variables prior to addition of the clay, during clay addition and post pillaring reactions. This ability to tailor the products to a specific purpose is of much importance in the formulation of catalysts for different applications.

The structural evolution of pillars does not involve clay lattice reconstruction, at least when calcination is carried out below the temperature at which clay octahedral layer dehydroxylates. Thus, it should be stated that pillaring decreases the temperature for dehydroxylation of clay layers[59]. Upon dehydroxylation, the bond between the pillar and clay is thought to shift from ionic to near covalent, which results in stabilisation of porous network. The pillar spacing is decided by the radius of hydrated cations. Interlayer spacing in the order of 12-16 Å requires pillars with about six or more oxygen layers. These pillaring species are likely to be nanosized colloidal particles on the positive side of their zero point charge[60]. The hydrothermal stability of the clay depends on nature of interlayer cations. The clay sheet by itself is remarkably stable and hence collapse of pillared clay is then attributed to sintering of pillars. Two factors appear to control the process: density of pillars and their distribution within the particle[61]. This phenomenon has some similarity with sintering of pure oxides.

## 1.7 ACIDITY OF PILLARED CLAYS

Smectite surfaces are acidic. This results from the high degree of dissociation of water of hydration and is a consequence of the bidimensional structure[62-63]. It is well known that the residual water molecules belonging to hydration shell of exchangeable cations are very acidic[59]. The exchangeable cation clay association is like a cation anion association but the anion viz. the clay lattice has an infinite radius of curvature. Thus, the electric field created by the cation strongly polarises a hydration water molecule in the first coordination shell. The proton is probably delocalised on the network of water filling the space between

cations, while the remaining OH⁻ remains coordinated to cation. The strong dependence of Brönsted acidity on structural OH groups has been evidenced[64]. Al-O-Al and Al-O-Mg linkages comprise most of the structural OH groups and only a small part of the structural OH groups can become Brönsted acid sites on adsorption. Hall[65] and Davidtz[66] pointed out that co-ordinately unsaturated Al exposed at crystal edges can become either Brönsted or Lewis sites. However, their contributions are limited by site density.

Pillaring the clay will modify the surface acidity in at least two ways. i) the polycationic pillars displace the cations originally present on the surface of clay and ii) pillar's own acidity may create Si-OH-Al bridges in smectites with Al, Si substitution in the tetrahedral layer. These OH may provide an anchoring point to the pillar. These two facts are fundamental to the nature of crosslinking mechanisms. There is a general agreement on the presence of higher proportion of Lewis sites than Brönsted sites in pillared clays[61,67-69]. In calcined forms, the pillars being usually metal oxide clusters, contribute mainly to Lewis acidity. However, unavoidable contribution to Brönsted acidity by the pillars has also been evidenced[70-72]. The structural hydroxyl groups are a major source of Brönsted acidity in dried samples, disappearing slowly during thermal activation[64]. This is attributed to migration of protons of interlayer space into clay lattice sites where the negative charges originate. These sites are in the octahedral sheet in cases where octahedral isomorphous substitution occurs and in tetrahedral sheet when isomorphous substitution occurs in tetrahedral sheet. Figueras has explained several categories of acidic sites, which indeed are known to exist in the surface[35].

- one type connected with initial sites of ion exchange, not occupied by pillars, representing approximately 30% of the initial CEC of the clay.
- second type can be the Si-O-Al linkages.

- third type can be connected with the pillars, since hydrolytic reactions of the following type can occur.

$$[Al_{13}O_4 (OH)_{24}(H_2O)_{12}]^{7+} \rightarrow [Al_{13}O_4 (OH)_{24+x}(H_2O)_{12-x}]^{(7-x)+} + x H^+$$

Coexistence of different types of acidity complicates the situation and hence localisation of acid sites is much more difficult than for well crystallised structures like zeolites.

## 1.8 PILLARING AGENTS

Oxidic pillaring usually proceeds via insertion of hydroxy oligomeric cationic species between aluminosilicate layers and stabilisation by heat treatment[18,35-37]. A second method is the insertion of organocationic complexes into interlamellar space, followed by heating which removes the organic part leaving oxidic micro pillars[73-75]. A large variety of metals can be used for pillaring clay suspensions and the list of metal oxides used in pillaring various smectites has rapidly expanded and already comprises quite a few metals. Examples are aluminium[76-78], zirconium[79-81], titanium[82-84], silicon[85-86], iron[87-89], chromium[90,91], niobium[92], gallium[93,94], tantalum[95], molybdenum[96], tin[97], vanadium[98,99], magnesium[100], lead[101,102], lanthanum[103], copper[104], nickel[105,106], uranium[107], bismuth[108] and organometallics[109-110]. Mixed metal oxide pillars containing two and more cations have also been prepared. Usually the first cation polymerises easily and addition of small molar fractions of a second cation improves the thermal adsorptive and/or catalytic properties of final solids. Mixed pillars include Al-Zr[111,112], Al-Fe[113,114],Al-Ga[115,116],Al-Si[117,118],Al-Cr[119,120], Al-La[121,122], Al-Ce[123], Al-Ru[124,125], Al-Cu[126], Al-Mo[127], Fe-Cr[129-132], Cr-Zr[133], Ni-La[134], Si-Ti[135,136], Si-Fe[137,138], Si-Cr[139], Al-Ce-Mg[128], Al-La-Ca[140] and Sm-Mn-Al[141].

## 1.9 ALUMINIUM PILLARED CLAYS

Intercalation compounds obtained from montmorillonite and aluminium polyhydroxy polymers have been studied extensively because of their thermal

stability and rather large specific surface areas[142-146]. The aluminium polymer is obtained by partial hydrolysis of aluminium salt (usually nitrate or chloride) with NaOH or $Na_2CO_3$ solutions, at required OH/Al ratios[147,148] or by dissolving Al powder in $AlCl_3$[149,150]. Hydroxy aluminium pillaring of concentrated clay suspensions (40%) also can be achieved using dialysis bags[151,152].

Basal spacings of about 18 Å and specific surface areas of 250- 300 $m^2/g$ were reported by Pinnavia[18] and Vaughan *et.al*[153]. These authors suggested that the intercalated species giving rise to this stable basal spacing is the so called $Al_{13}$ polyhydroxy polymer or Keggin cation which has been characterised by small angle X-ray scattering[154] and $^{27}Al$ NMR[155]. This polymer with structural formula, $[AlO_4Al_{12}(OH)_{24}(H_2O)_{12}]^{7+}$ is a tri-decamer composed of one aluminium tetrahedra surrounded by 12 aluminium octahedra. It exists in aluminic solutions having 1 < OH/Al < 2.5 and its concentration increases with increasing OH/Al. It contains four layers of superimposed oxygen atoms needed for expanding the clay basal spacings to 18 Å. The lateral expansion however, is limited. The surface area occupied by one polymeric unit or pillar is 10 $Å^2$. The gyration radius of this polymer with its anionic and hydration cloud is about 10 $Å^{40,156}$. The total positive charge (between 4+ and 7+ depending on the number of OH or $H_2O$ in Al octahedral) is partially screened by firmly attached anions[157]. After ionic exchange with clay counterions, $Al_{13}$ pillars have about the same structure as in solution, as evidenced by $^{27}Al$ MASNMR[45]. During calcination, pillars dehydrate by the reaction,

$$[AlO_4Al_{12}(OH)_{24}(H_2O)_{12}]^{7+} \rightarrow 6.5\ Al_2O_3\ +\ 7\ H^+\ +\ 20.5\ H_2O.$$
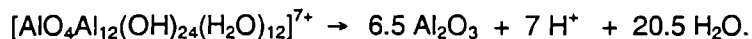
The protons liberated, diffuse into the octahedral layer and do not apparently play a significant role in pillared clay acidity[158]. Comparison of model isotherms based on cylindrical pore geometry with the help of hybrid density functional theory and experimentally observed pore volume distribution showed that the nature of clay surface was nearly unaffected by pillaring reaction. This result and atomic force

microscopy (AFM) images lent to the conclusion that Keggin ions added are inside the interlamellar space[159].

Bergaoui *et.al* pointed out that the amount of Al never exceeds one $Al_{13}$ per 6 unit cells, due to constraints in solid liquid interface. Layer charge plays a role in the competition between flocculation and intercalation[160]. Low charged smectites were shown to flocculate easily, thereby slowing down the intercalation process. Charge balance is achieved through hydrolysis of pillaring species[161]. Jones *et.al* have shown that Al pillars exhibit an ion charge slightly above 3 instead of 7 as assumed for $Al_{13}$, which explains why more Al is introduced in the clay interlayer than a 7+ charged $Al_{13}$ would allow[162]. Depending on drying conditions, Kodama *et.al* obtained three types of Al pillared montmorillonites. Extremely dry conditions led to a phase exhibiting basal spacing of 18.8 Å. An intermediate phase was formed under ambient conditions. Upon aging, both phases transformed to a third phase displaying a basal spacing of 28 Å with regular interstratified structure of non expanding layers of spacing, 9.6 Å and expandable layers of spacing, 18.8 Å in a ratio of 0.46: 0.54[163,164].

From titration curves and NMR results, Bottero *et.al* suggested that the other aluminic species present in solution are either monomeric $Al(OH)_x(H_2O)$ or dimeric $Al_2(OH)_xH_2O$[165]. Plee *et.al* proposed that these species in equillibrium with $Al_{13}$ are probably preferentially adsorbed because of lower steric hindrance to diffusion within interlamellar space[45]. As pillaring proceeds, Al monomer is progressively removed from interlamellar space to the benefit of $Al_{13}$ polymer until maximum uptake of this species occurs and this requires a relatively high concentration of $Al_{13}$, which in turn is favoured by high OH/Al and or high Al/ clay ratios. Molecular simulation of $Al_{13}$ intercalated montmorillonite revealed that there is no two dimensional ordering of $Al_{13}$ cations in the interlayer and therefore no regular stacking of layers can be expected in intercalated montmorillonite[166]. Dimov *et.al* proposed a structural model involving deformed pillars for Al pillared montmorillonite. Four pillar types were obtained and

the model explains increased ordering along *c* axis[167]. Cheng *et.al* suggested that micropore dimensions of pillared clays could be tailored to optimise the microporosity of these materials[168]. These results were furthered by Hutson *et.al*[169]. The effects of post synthesis ion exchange using differently sized alkali and alkaline earth cations to modify the microporous character of $Al_2O_3$ pillared clays were also reported[170].

## 1.10 IRON PILLARED CLAYS

The first pillared clay with iron as a constituent of pillars was from organic cage like structures such as Fe (II)-1,10 phenanthroline[26] and Fe (II) tribipyridyl[171]. However, these clays could not be used for catalytic purposes because of their low thermal stability and surface area[172]. Fe pillared clays are cheaper to prepare and would not only have acidic properties but also contain pillars which in themselves would be catalytically active and have redox and magnetic properties[173]. Hence a large volume of literature has been dedicated for the characterisation and applications of iron pillared clays[174-178].

The aqueous chemistry of iron(III) yields polymeric cations of substantial size[179]. Studies on hydrolytic polymerisation of iron (II) nitrate revealed the presence of discrete high polymeric component[180]. The isolated polymer fraction disclosed the polycations $[FeO_{x/2}(H_2O)_2^{(3-x)+}]_n$ where x lies between 2.3 and 2.5. Polymerisation of iron typically begins at low pH (<1.5) and propagates by deprotonation of coordinated water molecules (olation) and hydroxy groups (oxolation)[181].

$$[Fe(OH)_2^+]_n + Fe^{3+} + H_2O \rightarrow [Fe(OH)_2^+]_{n+1} + 2H^+$$
$$[Fe(OH)_2^+]_n \rightarrow [FeO(OH)]_n + H_n^+$$
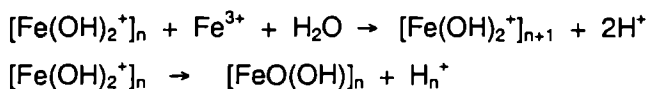
The hydrolysis reactions of $Fe^{3+}$ lead to discrete spherical cations as large as 30 Å in diameter[182,183]. Aggregation of two to six spheres produces rods and eventually rafts. The polycations are hydrated and extensively bound to the nitrate counter ions, which neutralise their high charge density.

In general, different routes have been described to synthesise Fe polycations in solution. Burch *et.al* observed an increase in microporous surface area and micropore volume due to pillaring plus an increase in mesoporous surface area and volume due to changes in stacking of clay platelets generating a secondary structure[184]. Washing the clay after exchange increased the product crystallinity suggesting that hydrolysis of intercalated polycations continued during washing[185]. $^{57}$Fe Mossbauer spectrum of iron pillared montmorillonite at room temperature revealed $Fe^{3+}$ to be located essentially in trans octahedral sites[186]. Organic cage like structures like Fe(II) 1,10 phenanthroline[174,175] and trinuclear aceto Fe(III) ions[178,187] were also used for pillaring. Pillared clays with partially delaminated structures were produced. The pillars showed unusually high resistivity against hydrogen reduction even at high temperatures, which made them possible catalysts for Fischer Tropsch synthesis with high shape selectivity.

## 1.11 IRON ALUMINIUM PILLARED CLAYS

The thermal stability and catalytic properties of single oxide pillared clays can be improved by incorporating a second component into pillars. Several authors have reported successful pillaring with intercalating solutions containing Fe and Al[188-191]. Lee *et.al* postulated formation of $[Al_{12.5}Fe_{0.5}O_4(OH)_{24}]^{7+}$ polycations in intercalating solution but in the final pillared solid, discrete alumina and iron oxide pillars were found[192]. No evidence was found for isomorphous substitution of iron for aluminium in $Al_{13}$ Keggin type cations by Kirisci *et.al*[193,194]. Instead, mixed pillars containing $Al_{13}$ cations and hydrous iron oxide oligomers were found. Lenarda *et.al* reported Fe-Al mixed pillared systems with high oxidising activity and strong acid properties, which was confirmed by dehydrogenation of 2-propanol to acetone[124,125]. Canizares *et.al* studied the effect of Al/Fe ratio on the structure of mixed pillared clay[87]. In samples with high Al/Fe ratio Keggin structure predominated whereas the pillar structure in materials with low Al/Fe metal ratio was similar to that of iron pillared clays.

Formation of mixed $Al_{13-x}Fe_x$ pillars, based on the Fe content of pillared solids was proposed by Bergaua et.al[195,196]. These were found to be more stable with respect to sintering and carbide formation than other iron containing catalysts. Incorporation of iron into alumina pillar decreases the Brönsted acid concentration and surface acid strength of resulting pillared clays[197]. Studies on mixed Fe-Al species at different Fe/Al ratios demonstrated the presence of short range ordered materials of different chemical composition, size and nature[198]. Mixed Fe-Al pillaring on clays gave broken pillars that do not sinter during subsequent oxidising stages[199]. Catalytic activity of Fe-Al mixed pillared systems for isopropanol decomposition was related to surface acidity by $NH_3$-TPD[200]. The products were mainly propene and diisopropyl ether with a propene selectivity of 0.8-0.9. The adsorption of cyclic and linear chain/cyclic nonaromatic hydrocarbons was studied with Fe-Al pillared systems. The separation could be effected at 200-350°C[201]. Catalytic transformation of gases evolved during HDPE decomposition was carried over Fe-Al pillared systems. Thermal decomposition of plastic gave light gases and aromatic species, which suggested presence of dehydrocyclisation sites associated with pillars[202].

## 1.12 PILLARED CLAYS AS CATALYST SUPPORTS

Recently, the suitability of pillared clays as catalyst supports has been explored because of their textural and acidic properties. Potential applications of pillared clays in catalytic processes of redox nature would require the pillared clay structure to accommodate transition metal ions known to change oxidation states. Usually, transition metals are deposited on pillared clays by means of ion exchange, incipient wetness or dry impregnation of calcined samples. Copper, vanadium and platinum have been the preferred active phases and to a lesser extent nickel, manganese, cobalt and other elements.

Copper doped pillared clays have been widely studied. Using ESR, Kukkadappu et.al studied the nature of Cu species in Zr and Al pillared

montmorillonites[203,204] and Al pillared laponites[205]. They concluded that nature and coordination of existing Cu species depended on the method of preparation of support. Three Cu species were found: octahedral $Cu^{2+}$ in between layers, square planar species corresponding to $Cu^{2+}$ within pillars bonded to hydroxyl groups and square planar species corresponding to $Cu^{2+}$ within pillars bonded to oxygen atoms. ESR and ESEM spectroscopic studies on the coordination of Cu(II) cations exchanged with Al and Zr pillared montmorillonites gave evidence for coordination of Cu(II) cations to pillars. In Zr pillared sample, part of the Cu(II) was freely tumbling between the clay and pillars and was hexacoordinated to water[206]. Braddell *et.al* have reported EPR studies of $Cu^{2+}$ and $VO^{2+}$ in pillared clays[207,208]. The spectra showed mobile (with hindered free rotation) as well as immobile species (adsorbed on pillars) for the two ions. Bahranowski *et.al* employed Cu doped Al pillared montmorillonite for phenol hydroxylation and obtained activities comparable to titanium silicalite, the commercial catalyst. Characterisation by ESR spectroscopy showed that copper species are located in the interlayer region of the clays either as isolated $Cu^{2+}$ species located in the interlayer region or as patches of amorphous $CuO$[209]. Bergaoui *et.al* introduced $Cu^{2+}$ into pillared saponites and obtained inner sphere complexes in which the AlO surface groups act as ligands, rather than a simple ion exchange process[210]. Cu doped AZA and FAZA catalysts have been investigated for the SCR of NO with $NH_3$ and propane[211]. The presence of Cu led to an improvement in reduction activity and to a decrease in $N_2O$ formation. Yang *et.al* reported Cu supported on Al, Zr and Ti pillared clays and Fe, Ce, Co, Ag and Ga supported on Ti pillared clays as catalysts for SCR of NO by ethylene, methane and ammonia[212-215]. Catalytic activity could be related to redox properties of Copper(II) and strong acidity of catalysts, which in turn were related to the method of preparation. Studies on copper doped Al, Zr and Ti pillared systems showed formation of clustered copper ions on the clay. Sensitivity of the mesoporous system of Ti pillared clay was attributed to crystallisation effects in extra framework titania[216].

23

Vanadium containing Al, Zr and Ti pillared montmorillonites were prepared by the addition of $VOSO_4$[217-220]. A careful ESR study showed that the vanadium species were bound to pillars. The unpaired electron of the vanadyl species became partially delocalised and in-plane $\pi$-covalent bonding was enhanced in cointercalated solids. The catalysts were used for oxidative dehydrogenation of propane, ammoxidation of *m*-xylene and SCR of NO by ammonia. Occelli *et.al* studied the effect of vanadium on pillared rectorite samples and found that initially V species was preferentially located in micropores, but calcination caused clay platelets with vanadium enriched surface to form[221].

Excellent results were obtained by employing CoMo/Al and NiMo/Al pillared clays for hydrotreating of crude oil[222]. Several Al pillared montmorillonites were used as catalyst supports in the preparation of nickel sulphide catalysts by Klopprogge *et.al.* Catalytic performance of the samples was evaluated for thiophene hydrodesulphurisation[223]. Monnier *et.al* employed NiMo/Al pillared montmorillonites for hydrocracking of denitrogenated synthetic crude gas oil. XPS studies indicated that nickel was present as Ni silicate or Ni aluminate phases[224]. 10% $MnO_2$ doped Al and Zr pillared clays were prepared and characterised by Gandia *et.al*[225]. After calcination, presence of $\alpha$–$MnO_2$ and $\beta$–$Mn_2O_3$ was detected, suggesting weak interaction between manganese oxides and pillared clays.

## 1.13 REACTIONS SELECTED FOR THE PRESENT STUDY

Pillar interlayered clays constitute one of the widely studied families among the new group of microporous materials developed by molecular engineering. These solids also known as crosslinked clays are obtained by exchanging the interlayered cations of layered clays with bulky inorganic polyoxocations, followed by calcination. The intercalated polycations increase the basal spacing of clays and upon heating, are converted to metal oxide clusters by dehydration and dehydroxylation. As a result, a two dimensional porous network is generated. Maintenance of a well-

defined porous network upto relatively high temperatures along with the presence of acid sites immediately suggest potential catalytic applications for these solids. The reactions selected for evaluating the catalytic performance of prepared pillared clay catalysts are,

## 1.13.1 Friedel Crafts alkylations

Friedel-Crafts alkylation is an important means of attaching alkyl chains to aromatic rings. Diphenylmethane and substituted diphenylmethanes are industrially significant compounds used as heat transfer fluids, aromatic solvents, fragrances and monomers for polycarbonate resins[226,227]. Traditionally, homogeneous acid catalysts like $AlCl_3$, $BF_3$ and $H_2SO_4$ are used for Friedel-Crafts alkylation reactions[228]. However, use of Lewis acid catalysts is laden with several problems like difficulty in separation and recovery, disposal of spent catalyst, corrosion, high toxicity and other undesirable reactions like alkyl isomerisations and *trans* alkylation reactions[229]. Hence worldwide efforts have been made to replace the present environmentally unfriendly catalysts with highly acidic solid acid catalysts.

## 1.13.2 *Tert*-butylation of phenol

*Tert*-butyl phenols (TBP) find a wide variety of applications in industry. 2-TBP is used for the synthesis of antioxidants and agrochemicals. 4-TBP is used on a large scale for the production of phenol formaldehyde resins, used as binders in paints and varnishes and calixeranes used as clathrates. 4-TBP find extensive applications as stabilisers in rubber and chlorinated hydrocarbons, chain length regulator in the production of polycarbonate resins and antioxidant. 2,4-DTBP is expansively used in the production of UV absorbers and stabilisers and is an indispensable building block in high molecular mass light protection agents and antioxidants.

### 1.13.3 Catalytic Wet Peroxide Oxidation of Phenol

Phenol is a major water pollutant. Presence of phenol even in trace amounts has been proven to be fatal to living beings. Removal of phenol from effluents can be brought about by oxidation with hydrogen peroxide. An added advantage of this reaction is that oxidation of phenol produces catechol and hydroquinone, two important intermediates in agrochemical and fine chemical industries. Catechol and hydroquinone are also used as photographic developers and antioxidants. Among catalysed wet oxidations, Wet Peroxide Oxidation (WPO) is preferred because the active oxygen content of hydrogen peroxide is much higher than that of other oxidants. Also, aqueous hydrogen peroxide is a stable reagent, provided it is handled and stored in the correct manner[230]. Water is the only by product formed.

### 1.13.4 Methyl *Tert*-butyl Ether Synthesis

Pollution from motor vehicles is responsible for ozone forming smog, hazardous carbon monoxide pollution and other toxic air pollutants. Methyl *tert*-butyl ether is widely used as oxygenate for gasoline[231] not only to enhance the octane number but also to make fuel burn more cleanly[232]. It also acts as a volume extender, by adding volume to the gasoline pool and by reducing the severity of naphtha reforming and related conversion operations. Decomposition of the ether is also of industrial interest as it represents a route for producing pure isobutene[232].

### 1.14 MAIN OBJECTIVES OF THE PRESENT WORK

The main objectives of the present work can be summarised as,

❖ to prepare iron, aluminium and mixed iron aluminium pillared montmorillonites and their metal exchanged analogues by single step exchange using 1 M metal salt solution. The metals selected include V, Mn, Ni, Co, Cu and Zn.

❖     physico-chemical characterisation of the prepared systems using instrumental techniques likeCEC determination, EDX, BET surface area and pore volume measurements, XRD, FTIR, $^{27}$Al NMR, $^{29}$Si NMR, TG-DTA, and UV DRS studies.

❖     to explore the surface acidic properties by three independent techniques, viz. ammonia TPD studies, perylene adsorption studies and test reactions like cumene cracking and cyclohexanol decomposition.

❖     to investigate the catalytic efficiency of the systems towards industrially important Friedel-Crafts benzylation using different benzylating agents viz. benzyl chloride, benzyl alcohol and a combination of the two reagents. Assessment of the activity of the systems towards vapour phase *tert*-butylation of phenol also is intended.

❖     to examine the redox properties by catalytic wet peroxide oxidation of phenol, a major industrial pollutant.

❖     to evaluate the catalytic activity of the systems for vapour phase synthesis of methyl *tert*-butyl ether.

## REFERENCES

1.  E.L Bruce, "Applied Industrial Catalysis", Vol.1, McGraw Hill, New York (1987).
2.  F Greek, *Chem. Eng. News*, 6, 22 (1989).
3.  J.A Schwarz, C Contescu, A Contescu, *Chem. Rev.*, 95, 477 (1995).
4.  W.F.H Foelderich, H.V Bekkum, *Stud. Surf. Sci. Catal.*, 58, 631 (1991).
5.  M.A Barteau, *Chem. Rev.*, 96, 1413 (1996).
6.  R.E Grim, "Clay Mineralogy", 2$^{nd}$ ed, McGraw Hill, New York (1968)
7.  J.J Fripiat, M.I Cruz-Cumplido, *Annu. Rev. Earth Planet. Sci.*, 2, 239 (1974).
8.  A Shimoyama, W.D Johns, *Nature*, 232, 140 (1971).

9.  S.W Bailey, J.L White, *Residue Rev.*, 32,19 (1970).

10. H Lahav, D White, S Chang, *Science*, 201, 67 (1978).

11. B Ryland, M.W Tamele, J.N Wilson, "Catalysis", P.H Emmett (ed), Reinhold, New York (1960).

12. C.J.B Mott, *Catal. Today*, 2, 199 (1988).

13. P Laszlo, *Science*, 235 (1987).

14. J.P Rupert, W.T Granquist, T.J Pinnavia, " Chemistry of Clays and Clay Minerals", A.C.D Newman (ed) (1987).

15. J.M Thomas, C.R Theocharis, Perspectives in catalysis, J.M Thomas, K.I Zamarev (eds) (1922).

16. H van Olphen, "An Introduction to Clay Colloid Chemistry", John Wiley & Sons, New York, (1977).

17. "Clay mineralogy: Spectroscopic and Chemical Determinative Methods",p-312, Chapman & Hall (1994).

18. T.J Pinnavia, *Science*, 220, 365-372 (1983)

19. R Prost, A Benchara, E Huard, *Clays. Clay Miner.*, 46, 117-131 (1998).

20. "Chemistry of Clays and Clay minerals", Mineralogical Society, Monograph No.6, A.C.D Newman (ed), 275 (1987).

21. D.A Laird, *Clays Clay Miner.*, 44, 553-559 (1996)

22. P.A Politowicz, J.J Kozak, *J. Phy. Chem.*, 92, 6078-6081 (1988).

23. M.M Mortland, *Adv. Argon*, 22, 70 (1970).

24. M.M Mortland, *Trans. $9^{th}$ Int. Cong. Soil Sci.*, 1, 691 (1968).

25. R.K.G Theng, "The Chemistry of Clay-Organic Reactions", John Wiley, New York (1974).

26. V Berkheiser, M.M Mortland, *Clays. Clay Miner.*, 25, 105 (1977).

27. K.V Raman, M.M Mortland, *ibid.*, 16, 393 (1968).

28. D.A Morgan, D.B Shaw, M.J Sidebottom, T.C Soon, R.C Taylor, *J. Am. Oil Chem. Soc.*, 62,292 (1985).

29. W Cranquit, G.S Gardner, *Clays Clay Miner.*, 292 (1959).

30. S Narayanan, K Deshpande, *Appl. Catal. A: Gen.*, 199, 1-31 (2000).

31. B.M Choudary, M Sateesh, M.L Kantam, K.V.R Prasad, *Appl. Catal. A: Gen.*, 171, 155-160 (1998).

32. T Nishimura, S Ohtaka, A Kimura, E Hayama, Y Haseba, H Takeuchi, S Uemera, *Appl. Catal. A: Gen.*, 194-195, 415-425 (2000).

33. K Manju, S Sugunan, *React. Kin. Catal. Lett.*, (in press).

34. F Bergaya, N Hassoun, L Gatineau, J Barrault, "Preparation of Catalysts", G Poncelot *et.al* (eds), Elsevier Science Publishers B.V, Amsterdam, 329-337(1991)

35. F Figueras, *Catal. Rev. Sci. Eng.*, 30 (3) 457-499 (1988).

36. J.T Kloprogge, *J. Porous Mat.*, 5 5-41 (1998).

37. A Gil, L.M Gandia, M.A Vicente, *Catal. Rev. Sci. Eng.*, 42,145-212 (2000).

38. D.E.W Waughan, *Catal. Today*, 2, 178-192 (1988)

39. R.M Barrer, D.M MacLeod, *Trans. Faraday Soc.*, 51,1920 (1955)

40. J.Y Bottero, D Tchoubar, J.M Cases, F Fissinger, *J. Phy. Chem.*, 86, 3667 (1982).

41. W.V Rauschband, H.D Bale, *J. Chem. Phy.*, 40, 3391 (1964).

42. G Fu, L.F Nazar, A.D Bain, *Chem. Mater.*, 3, 602 (1991).

43. Z Ge, D Li, T.J Pinnavia, *Microporous. Mater*, 3,165 (1994).

44. T.J Pinnavia, M.S Tzou, S.D Landau, R.H Raytatha, *J. Mol. Catal.*, 27, 195 (1984).

45. D Plee, F Borg, L Gatineau, J.J Fripiat, *J. Am. Chem. Soc*, 107, 2362-2369 (1985).

46. D Tichit, F Fajula, F Figueras, *Clays. Clay Miner.*, 36, 369-375 (1988).

47. H.Y Zhu, E.F Vansant, J.A Xia, G.Q Lu, *J. Porous Mater.*, 4,17 (1997).

48. C Flego, L Galasso, R Millini, I Kirisci, *Appl. Catal. A: Gen.*, 168, 323 (1998)

49. S.M Thomas, J.M Bertrand, M Occelli, F Huggins, S.A.C Gould, *Inorg. Chem.*, 38, 2098 (1999).

50. G Guiu, P Grange, *J. Catal.*, 168, 463 (1997)

51. H Khalaf, O Bouras, V Perrichon, *Microporous Mater.*, 8,141 (1997).

52. E Montrags, L.J Michot, P Ildefons, *Microporous Mesoporous Mater.*,28, 83 (1999)

53. F Kooli, W Jones, *Clay Miner.*, 31, 501 (1996).

54. F Kooli, W Jones, *J. Mater. Chem.*, 8, 2119 (1998).

55. E Iwamatsu, E Hayashi, Y Sanada, S Ahmed, S.A Ali, A.K.K Lee, H Hamid, T Yoneda, *Appl. Catal A: Gen.*, 179, 139 (1999).

56. T Yamaguchi, *Appl. Catal. A: Gen.*, 61,1 (1990).

57. S Sivakumar, K.G.K Warrier, A.D Damodaran, *Polyhedron*, 12, 2587-2591 (1993).

58. S Ghosh, P Mukundan, K.G.K Warrier, A.D Damodaran, *J. Mat. Sci. Lett.*, 10, 1193 (1991).

59. J.J Fripiat, *Catal. Today.*, 2, 281-295 (1988).

60. M.L Occelli and D.H Finceth. *J. Catal.*, 99, 316 (1986)

61. D Tichit, F Fajula, F Figueras, J Bosquet, C Guegen, "Catalysis by Acids and Bases", B Imelik *et.al* (eds), Elsevier, Amsterdam, p. 725 (1985).

62. J.J Fripiat, "Handbook of Heterogeneous Catalysis", G Ertl, H Kozinger, J Weitkamp (eds), p.387, Germany, (1997).

63. M.M Mortland, K.V Raman, *Clays. Clay Miner.*, 16, 398 (1968).

64. H.M Yuan, L Zhonghui, M Enze, *Catal. Today.*, 2, 321-338 (1988).

65. P.L Hall, *Clay Miner.*, 15,321 (1985).

66. J.C Davidtz, *J. Catal.*, 43, 260 (1976).

67. D Plee, A Schutz, G Poncelot, J.J Fripiat, "Catalysis by Acids and Bases", B Imelik *et.al* (eds), Elsevier, Amsterdam, p. 725 (1985).

68. M.L Occelli, *Ind. Eng. Chem. Prod. Res. Dev.*, 22, 55 (1983).

69. J.F Lambert, G Poncelot, *Topics Catal.*, 4, 43 (1997).

70. J Kijenski, A Baiker, *Catal. Today.*, 5, 12 (1989).

71. M.L Occelli, R.M Tindwa, *Clays. Clay Miner.*, 31,22 (1983).

72. M.L Occelli, J Lester, *Ind. Eng. Chem. Prod. Res. Dev.*, 24, 27 (1985).

73. S.P Skaribas, P.J Pomonis, P Grange, B Delmon. *J. Chem. Soc. Faraday Trans.*, 88, 3217 (1988).

74. S Yamanaka, M Hattori, *Catal. Today.*, 2, 261-270 (1988).

75. L Li, X Liu, R Xu, J Rocha, J Klinowski, *J. Phy. Chem.*, 97,10389-10393 (1993).

76. M.J Avena, R Cabrol, C.P de Pauli, *Clays. Clay Miner.*, 38, 356-362 (1990).

77. D.T Karamanis, X.A Aslanoglou, P.A Assimakopolous, N.H Gangas, A.A Pakou, N.G Papayannakos, *Clays. Clay Miner.*, 45, 709-717 (1997).

78. B Gu, H.E Doner, *Clays. Clay Miner.*, 38, 493-500 (1990).

79. M.L Occelli, R.J Bennard, *Catal. Today.*, 2, 309-319 (1988).

80. G.J.J Bartley, *Catal. Today.*, 2, 233-241 (1988).

81. A Gil, P Grange, *Microporous. Mater.*, 4, 369-378 (1995).

82. L.K Boudali, A Ghorbel, D Tichit, B Chiche, R Dutartre, F Figueras, *Microporous Mater.*, 2, 525-535 (1994).

83. J Sterte, *Clays. Clay Miner.*, 34, 658-664 (1986).

84. H Yoneyama, S Haga, S Yamanaka, *J. Phy. Chem.*, 93, 4833-4837 (1989).

85. A Galarneauu, A Barodawalla, T.J Pinnavia, *Nature*, 374, 629 (1995).

86. G Fetter, D Tichit, P Massaini, R Dutatre, F Figueras, *Clays. Clay Miner.*, 42, 161 (1994)

87. P Canizares, J.L Velverde, M.R SunKou, C.B Molina, *Microporous Mesoporous Mater.*, 29, 267-281 (1999).

88. D.D Carstea, *Clays. Clay Miner.*, 16, 231 (1968).

89. P Rengaswamy, J.M Oades, *Aust. J. Soil Res.*, 15, 221 (1977).

90. M.S Tzou, T.J Pinnavia, *Catal. Today.*, 2, 243-259 (1988).

91. C Volzone, *Clays. Clay Miner.*, 43, 377 (1995).

92. S.P Christiano, J Wang, T.J Pinnavia, *Inorg. Chem.*, 24,1222-1227 (1985).

93. A.V Coelho, G Poncelot, *Appl. Catal. A: Gen.*, 77, 303 (1991).

94. S.M Bradley, R.A Kydd, *Catal. Lett.*, 8, 185 (1991). ·

95. G Guiu, P Grange, *J. Chem. Soc. Chem. Commun.*, 1729-1731 (1994).

96. S.P Christiano, T.J Pinnavia, *J. Solid State Chem.*, 64, 232-239 (1986).

97. D Petridis, T Bakas, A Simopoulos, N.H.J Gangas, *Inorg. Chem.*, 28, 2439-2443 (1989).

98. B.M Choudary, V.L.K Valli, *J. Chem. Soc. Chem. Commun.*, 1115-1116 (1990).

99. B.M Choudary, V.L.K Valli, A.D Prasad, *J. Chem.Soc.Chem.Commun.*,721 (1990).

100. G.W Brindly, C.C Kao, *Clays. Clay Miner.*, 26, 21 (1980).

101. M Uehera, A Yamazaki, R Otsuka, *Clay Sci.*, 9, 1 (1993).

102. M Uehera, A Yamazaki, M Suzuta, *Clays. Clay Miner.*, 43, 744 (1995)

103. S.P Skaribas, P.J Pomonis, P Grange, B Delmon, *J. Chem. Soc. Faraday Trans.*, 88, 3217 (1992).

104. O. Braddell, R.C Barklie, D.H Doff, N.H.J Gangas, A. McKim, *J. Phy. Chem.*, 151, 157 (1987).

105. S Yamanaka, G.W Brindley, *Clays. Clay Miner.*, 26, 21 (1978).

106. J Gaaf, R van Santen, A Knoester, B van Wingerden, *J. Chem. Soc. Chem. Commun.*, 655-657 (1983).

107. S.L Suib, J. F Tanguay, M.L Occelli, *J. Am. Chem. Soc.*, 108, 6972-6977 (1986).

108. S Yamanaka, G Yamashita, M Hattori, *Clays. Clay Miner.*, 28, 281-284, (1980).

109. F Tsvetkov, J White, *J. Am. Chem. Soc.*, 110, 3183-3187 (1988).

110. E.P Giannelis, E.G Rightor, T.J Pinnavia, *J. Am. Chem. Soc.*, 110, 3880-3885 (1988).

111. A Gil, P Grange, *Microporous Mater.*, 4, 369-378 (1995)

112. T.J Bandosz, J Jagiello, J.A Schwarz, *J. Phy. Chem.*, 99, 13522-13527 (1995).

113. N.D Skoularikis, R.W Coughlin, A Kostapapas, K Corrado, S.L Suib, *Appl. Catal. A: Gen.*, 39, 61 (1988).

114. C Breen, P.M Last, *J. Mater. Chem.*, 9, 813, (1999).

115. M.J Hernando, C Pesquera, C Blanco, I Benito, F Gonzalez, *Chem. Mater.*, 8, 76 (1996).

116. S.M Bradley, R.A Kydd, R Yamdagni, *Magn. Reson. Chem.*, 28, 746 (1990).

117. A Gil, G Guiu, P Grange, M Montes, *J. Phy. Chem.*, 99, 301-312 (1995).

118. D Zhao, Y Yang, X Guo, *Inorg. Chem.*, 31, 4727-4732 (1992).

119. K.A Carrado, S.L Suib, N.D Skoularkis, R.W Coughlin, *Inorg. Chem.*, 25, 4217 (1986).

120. T Mandalia, M Crespin, D Messad, F Bergaya, *J. Chem. Soc. Chem. Commun.*, 2111 (1998).

121. D Zhao, Y Yang, X Guo, *Mater. Res. Bull.*, 28, 939 (1993).

122. F Gonzalez, C Pesquera, I Benito, S Mendioroz, G Poncelot, *J. Chem. Soc. Chem. Commun.*, 491 (1992).

123. E Booij, J.T Klopprogge, J.A.R van Deen, *Appl. Clay Sci.*, 11, 155 (1995).

124. M Lenarda, R Ganzerla, L Storraro, S Enzo, R Zanoni, *J. Mol. Catal.*, 92, 201 (1994).

125. L Storraro, R Ganzerla, M Lenarda, R Zanoni, *J. Mol. Catal. A: Chem.*, 97, 139 (1995).

126. J Barrault, C Bouchoule, K Echachoui, N.F Srasra, M Trabelsi, F Bergaya, *Appl. Catal. B: Environ.*, 15, 269 (1998).

127. A Gil, M Montes, *Ind. Eng. Chem. Res.*, 36, 1431 (1997).

128. C Flego, L Galasso, R Millini, I Kiricsi, *Appl. Catal. A: Gen.*, 168, 323-331 (1998).

129. T Mishra, K Parida, *Appl. Catal. A: Gen.*, 174, 91-98 (1998).

130. I Heylen, N Maes, P Cool, M deBock, E.F Vansant, *J. Porous Mater.*, 3, 217, (1996).

131. N Maes, I Heylen, P Cool, E.F Vansant, *Appl. Clay Sci.*, 12, 43 (1997).

132. A Molinard, E.F Vansant, *Adsorption*, 49, (1995).

133. J Jamis, A Drljaca, L Spiccia, T.D Smith, *Chem. Mater.*, 7, 2078 (1995).

134. A.K Ladavos, P.J Pomonis, "Preparation of Catalysts", G Poncelot *et.al* (eds), Elsevier Science Publishers B.V, Amsterdam, 329-337 (1991)

135. P.B Malla, S Komernani, *Clays. Clay Miner.*, 41, 472 (1993).

136. H He, L Zhang, J Klinowski, M.L Occelli, *J. Phy. Chem.*, 99, 6980 (1995).

137. Y.S Han, S Yamanaka, *J. Porous Mater.*, 5, 111, (1998).

138. Y.S Han, J. H Choy, *J. Mater. Chem.*, 8, 1459 (1998).

139. Y.S Han, S Yamanaka, J.H Choy, *J. Solid State Chem.*, 144, 45 (1999).

140. H.Y Zhu, E.F Vansant, J.A Xia, G.Q Lu, *J. Porous Mater.*, 4, 17 (1998).

141. L.M Gandia, M.A Vicente, P Oelker, P Grange, A Gil, *React. Kin. Catal. Lett.*, 64, 145 (1998).

142. J Pires, M.B de Carvalho, A.P Carvalho, J.M Guil, J.A Perdigon Melon, *Clays. Clay Miner.*, 48, 385-391 (2000).

143. D Tichit, F Fajula, F Figureas, B Ducourant, G Mascherpa, C Guegen, J Bosquet, *Clays Clay Miner.*, 36, 369-373 (1988).

144. A Gil, M Vicente, L.M Guandia, *Microporous Mesoporous. Mater.*, 34, 115-125 (2000).

145. S Goldberg, R.A Glaubig, *Clays. Clay Miner.*, 35, 220 (1988).

146. S Moreno, R SunKou, R Molina, G Poncelot, *J. Catal.*, 182, (1999) 174-185.

147. M Tokarz, J Shabtai, *Clays. Clay Miner.*, 33, 91-96 (1985).

148. J Ahenach, P Cool, E.F Vansant, *Microporous Mesoporous Mater.*, 26, 185-192 (1998).

149. C.J Tsiao, K.A Carrado, R.E Botto, *Microporous Mesoporous Mater.*, 21, 45-51 (1998).

150. M Trombetta, G Busca, M Lenarda, L Storaro, R Ganzerla, L Piovasan, A.J Lopez, M.A Rodriguez, E.R Castellon, *Appl. Catal A: Gen.*, 193,55-69 (2000).

151. R Molina, A.V Coelho, G Poncelot, *Clays. Clay Miner.*, 40, 480-482 (1992).

152. R.A Schoonheydt, H Leeman, *Clay Miner.*, 27, 249-252 (1992).

153. D.E.W Vaughan, R.J Lussier, "Preparation of molecular sieves based on pillar interlayered clays", L.V.C Rees (ed), Heyden London, 94-101.

154. W.I Rausch, H.D Bale, *J. Chem. Phy.*, 40, 3391-3397 (1964)

155. A.K Helmy, E.A Ferreiro, S.G deBussetti, *Clays. Clay Miner.*, 42, 444-450 (1994).

156. J.Y Bottero, S Partyka, F Fissinger, *Thermochimica Acta.*, 59, 221-229 (1982).

157. M Axelos, D Tchoubar, J.Y Bottero, F Fissinger, *J. Physique.*, 46, 1587-1593 (1985).

158. D.T.B Tennacoon, W Jones, J.M Thomas, *J. Chem. Soc. Faraday. Trans.*, 82, 545 (1986).

159. J.P Olivier, M.L Occelli, *J. Phy. Chem. B.*, 105, (2001)

160. L Bergaoui, J.F Lambert, R Franck, H Suquet, J.L Robert, *J. Chem. Soc. Faraday Trans.*, 91, 2229 (1995).

161. R Keren, *Clays. Clay Miner.*, 34, 534 (1986).

162. J.R Jones, J.H Purnell, *Catal. Lett*, 18, 137 (1993).

163. H Kodama, S.S Singh, *Solid State Ionics*, 32/33, 363 (1989).

164. S.S Singh, H Kodama, *Clays Clay Miner.*, 36, 397-402 (1988).

165. J.Y Bottero, J.M Cases, F. Fissinger, *J. Phy. Chem.*, 84, 2933-2939 (1980).

166. P Capkowa, A.J Driessen, M Numan, H Schenk, Z Weiss, Z Klika, *Clays. Clay Miner.*, 46, 232-239 (1998).

167. V.I Dimov, A.V Ilieva, N.G Khaltakova, *Clays. Clay Miner.*, 48, 1-9 (2000).

168. L Cheng, R.T Yang, *Microporous Mater.*, 8, 177 (1977).

169. N.D Hutson, M.J Hoekstra, R.T Yang, *Microporous Mesoporous Mater.*, 28, 447-459 (1999).

170. N.D Hutson, D.J Gualdoni, R.T Yang, *Chem. Mater.*, 10, 3707 (1998).

171. M.F Traynor, M.M Mortland, T.J Pinnavia, *Clays. Clay Miner.*, 27, 201 (1979).

172. R.H Loeppert, M.M Mortland, T.J Pinnavia, *Clays. Clay Miner.*, 2, 201 (1979).

173. C.I Warburton, *Catal. Today.*, 2, 271-280 (1988).

174. D.H Doff, N.H.J Gangas, J.E.M Allen, J.M.D Coey, *Clay Miner.*, 23, 167 (1988).

175. R Herrera, M Peech, *Soil Sci. Soc. Amer. Pro*, 34, 740.

176. P Rengaswamy, J.M Oades, *Aust. J. Soil Res.*, 15, 235 (1977).

177. S Yamanaka, T Doi, S Sako, M Hattori, *Mat. Res. Bull.*, 19, 161 (1984).

178. S Yamanaka, M Hattori, *Catal. Today.*, 2, 261-270 (1988).

179. R.N Sylva, *Rev. Pure Appl. Chem.*, 115,22 (1972).

180. T.G Spiro, S.E Allerton, J Rennes, A Terzis, R Bils, P Saltman, *J. Am. Chem. Soc.*, 88, 2721-2726 (1996).

181. C.M Flynn Jr, *Chem. Rev.*, 84, 31 (1984).

182. P.J Murphy, A.M Posner, J.P Quirk, *Aust. J. Soil Res.*, 13, 189 (1975).

183. P.J Murphy, A.M Posner, J.P Quirk, *J. Coll. Inter. Sci.*, 52, 229 (1975).

184. R Burch, C.I Warburton, *Appl. Catal.*, 33 395 (1987).

185. E.G Rightor, M.S Tzou, T.J Pinnavia, *J. Catal.*, 29 (1991).

186. C.M Cardile, J.H Johnston, *Clays. Clay Miner.*, 34, 307-313 (1986).

187. M.A.M Luengo, H.M Carvalho, J Ladrie, P Grange, *Clay Miner.*, 24, 495 (1989).

188. I Palinko, K Lazar, I Hannus, I Kirisci, *J. Phy. Chem. Solid*, 57, 1067 (1996).

189. L Storaro, M Lenarda, R Ganzerla, A Rinaldi, *Microporous Mater.*, 6,55 (1995).

190. J Barrault, C Zivkov, F Bergaua, L Gatineau, N Hassoun, H vanDamme, G Mari, *J. Chem. Soc. Chem. Commun.*, 1403 (1988).

191. I Kirisci, A Molnar, I Palinko, K Lazar, *Stud. Surf. Sci. Catal.*, 94, 63 (1995).

192. W.Y Lee, R.H Raythatha, B.J Tatarchuk, *J. Catal.*, 115, 159 (1989).

193. I Palinko, A Molnar, J.B Nagy, J.C Bertrand, K Lazar, J Valyon, I Kirisci, *J. Chem. Soc. Faraday Trans.*, 93,1591 (1997).

194. J Valyon, I Palinko, I Kirisci, *React. Kin. Catal. Lett.*, 58, 249 (1996).

195. F Bergaua, N Hassoun, J Barraoult, L Gatineau, *Clay Miner.*, 28, 109 (1993).

196. J Barraoult, L Gatineau, N Hassoun, F Bergaua, *Energy Fuels*, 6, 760 (1992).

197. D Zhao, G Wang, Y Yang, X Guo, Q Wang, *Clays Clay Miner.*, 41, 317 (1993).

198. C Colombo, A Violante, *Clays Clay Miner.*, 44, 113-120 (1996).

199. T Bakas, A Moukarika, V Papaefthymiou, A Ladavos, *Clays Clay Miner.*, 42, 634-642 (1994).

200. V.N Stathopoulos, A.K Ladavos, K.M Kolonia, S.P Skaribas D.E Petrakis, P.J Pomonis, *Microporous Mesoporous Mater.*, 31, 111-121 (1999).

201. A deSteffanis, G Perrez, A.A.G Tomlinson, *J. Mater. Chem.*, 4, 959 (1994).

202. C Breen, P.M Last, *J. Mater. Chem.*, 9, 813 (1999).

203. R.K Kukkadappu, L Kevan, *J. Chem. Soc. Faraday Trans.*, 86, 691 (1990),

204. R.K Kukkadappu, L Kevan, *J. Phy. Chem.*, 92, 6073 (1988)

205. R.K Kukkadappu, L Kevan, *J. Phy. Chem.*, 93, 1654 (1989).

206. J.M Comets, L Kevan, *J. Phy. Chem.*, 97, 12004-12007 (1993).

207. O Braddell, R.C Barklie, D.H Doff, *Clay Miner.*, 25, 15 (1990).

208. R.C Barklie, O Braddell, D.H Doff, "Pillared Layered Structure: Current Trends and Applications", I.V Mitchell (ed), Elsevier, London (1990).

209. K Bahranowski, M Gasior, A Kielski, J Podobinski, E.M Serwicka, L.A Vartikian, K Wodnicka, *Clays and Clay Miner.*, 46, 98-102 (1998).

210. L Bergaoui, J.F Lambert, H Suquet, M Che, *J. Phy. Chem.*, 99, 2155 (1995).

211. S Perathoner, A Vaccari, *Clay Miner.*, 32, 123 (1997).

212. R.T Yang, N Tharapivatan, R.Q Long, *Appl. Catal. B: Environ.*, 19, 28 (1998).

213. M Srilumpen, R.T Yang, N Tharapivatan, *J. Mol. Catal A: Chem.*, 137, 273 (1999).

214. W.B Li, M Srilumpen, R.T Yang, *Appl. Catal B: Environ.*, 11, 347 (1997).

215. R.T Yang, W.B Li, *J. Catal.*, 155, 414 (1995).

216. K Bahranowski, A Kielski, E.M Serwicka, E.W Walsh, K Wodnicka, *Microporous Mesoporous Mater.*, 41, 201-215 (2000).

217. K Bahranowski, E.M Serwicka, *Geol. Carpathica Clays*, 44, 17 (1993).

218. K Bahranowski, E.M Serwicka, *Colloid Surf. A: Phy. Eng. Aspects*, 72, 153 (1993).

219. K Bahranowski, M Labnowska, E.M Serwicka *Appl. Magn. Reson.*, 10, 477 (1996).

220. K Bahranowski, J Janas, T Machej, E.M Serwicka, L Vartikian, *Clay Miner.*, 32, 665 (1997).

221. M.L Occelli, J.M Dominguez, H Eckert, *J. Catal.*, 141, 510 (1993).

222. C.E Ramos-Galvan, G Sandoval-Robles, A Castillo-Mares, J.M Dominguez, *Appl. Catal. A: Gen.*, 150, 37 (1997).

223. J.T Klopprogge, W.J.J Welters, E Booy, V.H.J deBeer, R.A vanSatan, J.W Geus, J.B.H Jansen, *Appl. Catal A: Gen.*, 97,77 (1993).

224. J Monnier, J.P Charland, J.R Brown, M.F Wilson, "New Frontiers in Catalysis", Vol. 75, Elsevier, Amsterdam (1993).

225. L.M Gandia, M.A Vicente, A Gil, *Appl. Catal. A: Gen.*, 196, 281-292 (2000).

226. D.E James, N.R Nowicki, US patent 4, 822,527 (1989).

227. L.A DeWitt, H Su, C.T Mathew, US patent 5, 723,676 (1998).

228. G.A Olah, "Friedel Crafts Chemistry", Wiley, New York (1973).

229. P Ratnaswamy, A.P Singh, S Sharma, *Appl. Catal. A: Gen.*, 135, 25 (1996).

230. M.G Clerici, "Heterogeneous Catalysis and Fine Chemicals III" M Guisnet, J Baebier (eds) Wiley, New York (1988).

231. J.E Peeples, *Fuel Reform.*, 1, 27 (1991).

232. G.R Hadder, *Energy*, 97, 99 (1992).

233. Q.H Xia, K Hidajat, S Kawi, *J. Catal.*, 209, 433-444 (2002).

# 2

# MATERIALS
# AND METHODS

*The performance of a catalyst is influenced by the method of catalyst preparation and pretreatment conditions. The materials and methods used for synthesis, physicochemical characterisation and catalytic activity studies are listed in this chapter. The various notations given for the prepared systems are also specified. A detailed but precise description of the various techniques used for characterisation of samples viz. CEC determination, EDX, XRD, surface area and pore volume measurements, FTIR, NMR, TG, UV-DRS and SEM is outlined in this chapter. The acidic structure of prepared materials was followed by $NH_3$-TPD, perylene adsorption studies and test reactions like cumene cracking and cyclohexanol decomposition. The catalytic reactions chosen for the present study are industrially important Freidel Crafts reactions, tert-butylation of phenol, phenol hydroxylation and MTBE synthesis.*

## 2.0 INTRODUCTION

The aim of active research in catalysis is to produce and reproduce a commercial product, which can be used as stable, active and selective catalyst. Subtle changes in the preparative details can result in dramatic alteration in the properties of final catalyst. In spite of numerous studies, preparation of heterogeneous catalysts is still regarded as an art, often kept secret by the producer. However many preparative routes are sought so as to furnish catalysts with sufficient surface area, good porosity and suitable mechanical strength.

## 2.1 PREPARATION OF CATALYSTS

Iron, aluminium and mixed iron aluminium pillared montmorillonites were prepared. The pillared clays were doped with transition metal oxides of first series viz., vanadium oxide, manganese oxide, nickel oxide, cobalt oxide, copper oxide and zinc oxide.

| *Materials* | *Suppliers* |
|---|---|
| 1.  Montmorillonite KSF | Aldrich |
| 2.  Aluminium(II) nitrate | Merck |
| 3.  Iron(III) nitrate | Merck |
| 4.  Sodium carbonate | Qualigens |
| 5.  Ammonium metavanadate | Qualigens |
| 6.  Manganese(II) nitrate | Merck |
| 7.  Cobalt(II) nitrate | Merck |
| 8.  Nickel(II) nitrate | Merck |
| 9.  Copper(II) nitrate | Merck |
| 10. Zinc(II) nitrate | Merck |

## 2.1.1 PREPARATION OF PILLARED MONTMORILLONITES

The pillared clays were synthesised by partial hydrolysis method. Pillaring by partial hydrolysis method involves four steps.

- Preparation of pillaring solution.
- Intercalation of polymeric species into the clay layer.
- Washing of reaction mixture.
- Drying and subsequent calcination.

0.1 M solution of corresponding nitrate was hydrolysed by drop wise addition of 0.3 M $Na_2CO_3$ solution under vigorous stirring for 3 hours. This solution was agitated for another hour. $N_2$ gas was bubbled through the solution to remove excess $CO_2$ and aged for 24 hours at room temperature. In the meantime, a suspension of the clay in distilled water was swollen for 24 hours. Intercalation of pillaring species into the clay layers was done by treating the pillaring solution with clay suspension for 25 hours [OH/M ratio of 2 and M/clay ratio of 20 mmol/g clay]. For iron aluminium mixed pillared systems, equimolar ratio of metals was taken. For aluminium pillaring, temperature for preparation of pillaring solution and intercalation process was 70°C and for iron and iron aluminium pillared clays it was 80°C. The clay after exchange was washed several times with distilled water and filtered. This was dried in air oven at 110°C overnight, followed by calcination for 6 hours at 450°C in muffle furnace.

## 2.1.2 PREPARATION OF TRANSITION METAL EXCHANGED CATALYSTS

Exchange with transition metals was done using 0.1 molar aqueous solutions of the corresponding metal nitrate. For exchange with vanadium, requisite amount of ammonium metavanadate was dissolved in oxalic acid. Pillared clays were stirred mechanically with salt solutions for 24 hours at room temperature. The clay after exchange was washed 5-6 times with distilled water. This was filtered and dried in air oven at 110°C overnight and calcined for 5 hours at 500°C.

## 2.2 NOTATIONS FOR CATALYSTS

The pillared clays synthesised for the present study are notated as,

M                   Montmorillonite

Fe PM               Iron pillared montmorillonite.

Al PM               Aluminium pillared montmorillonite

FeAl PM             Iron aluminium mixed pillared montmorillonite.

The notations for transition metal exchanged pillared montmorillonites are as given below.

| Exchanged transition metal | Notation for iron pillared systems | Notation for aluminium pillared systems | Notation for mixed pillared systems |
|---|---|---|---|
| Vanadium | V/Fe PM | V/Al PM | V/FeAl PM |
| Manganese | Mn/Fe PM | Mn/Al PM | Mn/FeAl PM |
| Cobalt | Co/Fe PM | Co/Al PM | Co/FeAl PM |
| Nickel | Ni/Fe PM | Ni/Al PM | Ni/FeAl PM |
| Copper | Cu/Fe PM | Cu/Al PM | Cu/FeAl PM |
| Zinc | Zn/Fe PM | Zn/Al PM | Zn/FeAl PM |

Table 2.1 Notations for the prepared systems.

## 2.3 CHARACTERISATION TECHNIQUES

Catalyst characterisation is a lively and relevant discipline in catalysis. A thorough characterisation of the prepared systems was undertaken using different spectroscopic as well as quantitative methods. A brief discussion of the characterisation methods adopted along with its experimental aspects is given in the following sections. Before each experiment except thermogravimetric analysis, catalysts were activated at 500°C for two hours.

| *Materials* | *Suppliers* |
|---|---|
| 1. Glacial acetic acid | Merck |
| 2. Ammonium hydroxide | Merck |
| 3. Sodium hydroxide | Qualigens |
| 4. Liquid nitrogen | Sterling gases |
| 5. Magnesium oxide | Merck |

## 2.3.1 CATION EXCHANGE CAPACITY (CEC)

Clay minerals can adsorb cations and retain them in an exchangeable form. Cation exchange capacity can be defined as the sum of exchangeable cations that a mineral adsorbs at a specific pH, i.e. measurement of the negative charges carried by a mineral. These negative charges in clay minerals can be derived from,

- isomorphous substitution within structure.
- broken bonds at edges and external surfaces.
- dissociation of accessible hydroxyl groups.

Negative charges due to isomorphous substitution within the mineral structures are known as permanent charge and are independent of conditions such as pH and ion activity whereas those from the latter two sources are dependant. The high levels of CEC can to some extent be attributed to their large external surface area accessible to hydrated cations[1].

The negative charge of montmorillonites arises mainly from isomorphous substitution within structure. Only a small variable charge is present, since all the disposable hydroxyl groups are present in subsurface planes covered by a network of oxygen atoms. Since the exchangeable cations compensate the unbalanced charge in the interior of layers due to isomorphous substitutions, CEC is a measure of the degree of substitution.

For pillared clays, it has been proposed that interpillar rather than interlayer distance controls the pore size distribution[2]. This distance depends on the number of pillars introduced in the clay layer, which in turn is mainly related to the amount of exchangeable cations (CEC). Therefore, CEC can be a key factor for the synthesis of pillared clays with desired pillar population[3]. A minimum of CEC is required in the layered material to obtain thermally stable pillared clay. On the other hand, excessively high CEC value can cause a negative effect due to the presence of very high number of pillars that decrease accessibility to the porous network[4].

Cation exchange capacity of the clay samples was quantified by titration of total exchangeable metallic cations as ammonium ions in ammonium acetate extract method. Accurately weighed clay was transferred into a conical flask and shaken intermittently for 3 hours with 1N $NH_4OAc$ solution. The exchanged ammonium ions were quantified by micro Kjeldahl method. CEC can be determined by other methods employing triethylenetetramine and tetraethylenepentamine complexes of $Cu(II)$[5], exchange with Ba ions[6], potentiometric titrations[7] etc

## 2.3.2 ENERGY DISPERSIVE X-RAY SPECTROSCOPY (EDX)

Energy Dispersive X-ray spectroscopy (EDX) is a promising as well as a widely used technique for elemental analysis. Use of this technique accelerated since 1960s as a result of development of solid-state detectors, nuclear electronics and small computers. An electron beam of energy typically in the range of 10- 20 keV strikes the surface of a conducting sample. This causes X-rays to be emitted. The interaction of X-rays with an object causes secondary (fluorescent) X-rays to be generated, which can be detected and displayed as a spectrum of intensity against energy. Each element present in the object produces X-rays with different energies. The positions of peaks identify which elements are present and peak heights identify how much of each element is present. Thus qualitative as well as quantitative elemental mapping is possible. The typical applications of this method include

surface contamination analysis, corrosion evaluations, coating composition analysis, rapid material alloy identification, small component material analysis and phase identification and distribution. Electron microscopic analysis of elements provides some advantages compared to wet chemical analysis:

- *X-ray sampling is non-destructive*
- natural heterogeneity is retained
- analysis can be conducted on microgram quantities
- adjacent structures can be directly compared
- excellent probe size (20 to 200 nanometers)

EDX is accurate and fast and the effort for sample preparation is minimal. If conditions are optimised minimum detection limits can be below the nanogram level for small laboratory instruments and into the femtogram region for more advanced instrumentation[8]. But, it is not sensitive enough to measure low concentrations such as trace elements (those present at levels below about 0.1%). Again, it is not responsive to elements lighter than sodium.

EDX analysis of the prepared samples was done in a JEOL JSM-840 A (Oxford make model I6211 with a resolution of 1.3 eV). Samples were prepared by dusting the clay powder onto double sided carbon tape, mounted on a metal stub.

## 2.3.3 X-RAY DIFFRACTION (XRD)

X-ray diffraction (XRD) by crystals is the most widely employed method for determining three dimensional structure of solid substances. Recording X-ray diffraction pattern of powdered polycrystalline samples by powder diffractometer method has many applications like qualitative phase analysis, quantitative phase analysis, determination of unit cell parameters, study of preferred orientation and determination of particle size. For pillared clay catalysts, the technique can be employed for the determination of the d spacing as a result of pillaring.

The use of X-rays for structure determination is rather simple in concept, though complicated in its fine details. Monochromatic X-rays (like Cu K$\alpha$ or Mo K$\alpha$ source) are reflected by planes in the polycrystalline material when the Bragg equation, 2d sin$\theta$ = n$\lambda$, is fulfilled, where d is the interplanar spacing, $\theta$ is angle between planes and X-ray beam (Bragg angle), $\lambda$ is X-ray wave length and n, order of reflection[9].

Every crystalline structure has a unique X-ray powder pattern since line positions depend on size, and line intensity depends on the type of atoms present and their arrangement in the crystal. Materials are identified from these values in conjunction with 'Joint Committee on Powder Diffraction Standards' (JCPDS) Powder Diffraction File. This contains cards containing X-ray data for known crystalline phases that include d spacing and relative intensity values, Miller indices, unit cell dimensions etc. The experimental data, especially those of the three strongest peaks are matched with standard values using appropriate card[10].

The diffractometer traces of the catalyst samples were taken in RIGAKU D/MAX-C instrument using Cu K$\alpha$ radiation ($\lambda$ = 1.5405Å).

## 2.3.4 SURFACE AREA AND PORE VOLUME MEASUREMENTS

The Brunauer, Emmett and Teller (BET) method has been adopted as standard procedure for surface area determination of powdered catalysts[11]. The BET theory of adsorption is an extension of Langmuir model to multilayer adsorption. The basic assumptions of BET model are (i) heat of adsorption for an adsorbate-adsorbant system does not change with surface coverage which means that all the adsorption sites on a given surface are energetically homogeneous (ii) adsorption is multilayer and the heat of adsorption of the second and subsequent layers are the same as heat of condensation of the adsorbate and (iii) dynamic equilibrium occurs within each layer.

The BET equation is conveniently expressed in the form,

$$P/[V(P_0-P)] = [1/V_mC] + [(C-1)/V_mC] (P/P_0)$$

where P is adsorption equilibrium pressure, $P_0$ is saturated vapour pressure of adsorbate, V is volume occupied by molecules adsorbed at equilibrium pressure, $V_m$ is volume of adsorbate required for monolayer coverage and C is a constant related to heat of adsorption. A plot of $P/[V (P_0-P)]$ against $P/P_0$ is a straight line with slope $(C-1)/V_mC$ and intercept $1/V_mC$. From the slope and intercept, $V_m$ can be calculated and the specific surface area can be calculated using the relation,

$$A = V_mN_0A_m / W \times 22414$$

where $N_0$ is Avagadro number, $A_m$ is molecular cross sectional area of adsorbate (for $N_2$ being 0.162 $nm^2$) and W is weight of the sample. Adsorption of nitrogen gas at its boiling point is generally used for surface area measurements using BET method. The linearity of BET plot is severely restricted within the $P / P_0$ range of 0.05- 0.30. A very high or low C value will create considerable error in calculating the effective adsorbate cross sectional area. High C values are likely to be associated with localised monolayer adsorption or with micropore filling.

The microporous surface areas of the samples were calculated by the t-plot[12,13]. In this method, the adsorbed $N_2$ volume is plotted against statistical thickness (t) of adsorbed $N_2$ layer to yield micropore volumes on the basis of,

$$V = V_{micro} + 10^{-4} S_0t.$$

where $V_{micro}$ is volume of $N_2$ adsorbed in micropores. A universal t-curve of $N_2$ has been established which gives,

$$t = [13.99/ (0.034 - log (P/P_0)]^{0.5}$$

$V_{micro}$ can be converted to an equivalent microporous surface area using the relation,

$$S_{micro} = KV_{micro}$$ where K is a constant with value 4.37 $m^2cm^{-3}$.

The simultaneous determination of surface areas and pore volumes of the catalyst samples was done on a Micromeritics Gemini analyser. Previously activated

samples were degassed at 200°C under nitrogen atmosphere for 2 hours and then brought to nitrogen boiling point.

## 2.3.5 FOURIER TRANSFORM INFRARED (FTIR) SPECTROSCOPY

Infrared absorption spectroscopy is a rapid, economical and non-destructive physical method universally applicable for structural analysis. The technique is so versatile that it can be used both as a source of the physical parameters of crystal lattice determinations and for eliciting purely empirical qualitative relationships between samples. The number, position, bandwidth and intensity of absorption bands may be correlated with the electronic and molecular structure. It also provides important information about the intramolecular forces acting between atoms in a molecule, intermolecular forces in condensed phase and nature of chemical bond.

Infrared spectroscopy is a direct method for monitoring transitions between quantised vibrational levels induced by absorption of light in infrared region. A vibration that interacts with the electromagnetic field absorbs the radiation into the molecule, the interaction being provided by an oscillating dipole moment. The spectrum is generally recorded by passing a beam of polychromatic infrared light through a sample and monitoring the radiant power of transmitted light at each frequency of source.

The technique can be applied to solids as crystals or powder; liquids as solutions or melt; gases, films and adsorbed species. IR analysis can be used to almost any type of sample as long as the material is composed of compounds. Areas of application include catalysis, polymer chemistry, fast reaction dynamics, charge transfer complexes etc. Its utilisation is spreading to other areas like layer thickness measurements, reflectivities and refractive index. The use of IR spectroscopy for clay samples is controlled by the constraints of overall symmetry of unit cell and local site symmetry of each atom within the unit cell.

FTIR spectra of the samples were measured by the KBr disc method in the range 400- 4000 $cm^{-1}$ using a Perkin Elmer RX-1 spectrometer.

## 2.3.6 NUCLEAR MAGNETIC RESONANCE (NMR) SPECTROSCOPY

Nuclear resonance spectroscopy is a reliable and relatively new technique used in the characterisation of catalysts. In comparison to structural analysis by X-rays, which requires relatively large crystals, NMR spectroscopy can be applied to microcrystalline material, crystalline powders and even to amorphous materials.

The physical foundation of NMR spectroscopy lies in the magnetic properties of atomic nuclei. Interaction of nuclear magnetic moment with an external magnetic field, according to rules of quantum mechanics, leads to a nuclear energy level diagram because magnetic energy of the nucleus is restricted to certain discrete values $E_i$, the eigen values. Associated with each eigen values are the eigen states, the only state in which the elementary particle can exist. Through a high frequency transmitter, transitions between the eigen states within the energy level diagram can be stimulated. The absorption of energy can be detected, amplified and recorded as resonance signal. In this way spectra can be generated for compounds containing atoms whose atomic nuclei have non zero magnetic moments[14].

Solid state NMR studies of heterogeneous catalysts are usually carried out by 'Magic Angle Spinning' (MAS) i.e. rapid rotation of the sample about an axis subtended at an angle 54°44' with respect to magnetic field. This technique removes line broadening from dipolar interactions, chemical shift anisotropy and quadrupolar interactions to the first order since all interactions contain the angular term $3 \cos^2\theta - 1$ which is zero for $\theta = 54.7°$. The number of signals in solid state NMR spectrum gives the number of different structural environment of observed nucleus in the sample while relative signal intensities correspond to relative occupancies of different environments[15]. High resolution solid state NMR provides information about bonding

situation, symmetry properties and dynamic behaviour of solid state structures. For structure elucidation of clays, $^{27}Al$ and $^{29}Si$ NMR measurements are usually done.

$^{29}Si$ NMR is often preferred to $^{27}Al$ NMR because quadrupole interaction in the latter case can produce very broad NMR peaks. Also studies have been restricted to clays with low iron content because of relaxation effects of paramagnetic centres. $^{27}Al$ NMR shows unambiguously the distinction between octahedrally and tetrahedrally coordinated Al atoms. Thus, octahedral Al appears around 0 ppm where as tetrahedral Al shows resonance between 60-70 ppm. Not all the Al present need give rise to an observable Al NMR peak; the inference being that the nuclei concerned are present in highly distorted environments and/or large polymeric ions.

NMR spectra of samples were recorded by a 300 DSX Brooker spectrometer with static magnetic field of 8.5T. The ordinary single pulse sequence was used and number of scans was adjusted depending on concentration of Si and Al in systems.

## 2.3.7 THERMOGRAVIMETRY (TG)

Thermogravimetry (TG) is a well established technique in heterogeneous catalysis for evaluating the thermal stability of the catalyst. It finds widest applications in the determination of different parameters on preparation of catalyst, nature and composition of active phase, effect of added promoters or presence of impurities on the catalyst, dispersion of active phase and active phase support interactions, nature and heterogeneity of active sites on catalyst surface, nature of different bound states of adsorbates on catalyst surface, mechanistic aspects of the reaction under investigation, transient chemical changes that occur on surface, catalyst deactivation and regeneration. The technique can also be used for quality control and catalyst characterisation through finger print spectra of different batches of the same catalyst.

The technique involves the pursuit of weight of sample over a period of time while its temperature is raised linearly. Recording analytical balances with provision

for controlled heating of sample, records the temperature curve. In a thermogravimetric curve, horizontal portions point out regions where there is no weight change, whereas weight loss is indicated by curved portions. In derivative thermogravimetric curve (DTG), plateaus correspond to no weight change. Any decomposition of sample is indicated by a dip in the curve and hence provide an idea about species lost during heating step.

Shimadzu TGA-50 instrument was used for carrying out thermogravimetric studies. About 10 mg of the sample was used at a heating rate of 20°C per minute in the temperature range of 50-600°C.

## 2.3.8 ULTRAVIOLET DIFFUSE REFLECTANCE SPECTROSCOPY (UV-DRS)

The measurement of radiation in the ultraviolet region reflected from a mat surface constitutes the area of spectroscopy known as ultraviolet diffuse reflectance spectroscopy (UV-DRS). The technique is widely used for the study of solid or powdered solid samples although it can be used for the study of liquids or paste like materials also. Since only the surface of the sample is responsible for reflection and absorption of incident radiation, it is used in the chemistry and physics of surfaces. In situ identification and determination of a variety of substances is possible.

The most appropriate theory treating diffuse reflections and transmission of light scattering layers is the general theory developed by Kubelka and Munk. For an infinitely thick, opaque layer the Kubelka- Munk equation can be written as,

$F(R_\infty) = (1-R_\infty)^2 / 2R_\infty = k/s$ where $R_\infty$ is the diffuse reflectance of the layer relative to a nonabsorbing standard such as MgO, k is molar absorption coefficient of sample and s is scattering coefficient. Provided s remains constant, a linear relationship should be observed between $F(R_\infty)$ and k[16].

In catalysis, the information given by DRS mainly includes the active phase – support interactions, chemical changes during modification procedure leading to

active phase and nature of active surface species. Metal centred (d-d) transitions and charge transfer transitions can be clearly differentiated by UV-DRS and assignment of these gives a picture about the oxidation state and coordination environment of the transition metals.

Ultraviolet diffuse reflectance spectra of the samples were recorded using a conventional spectrophotometer (Ocean Optics-2000) with CCD detector using MgO as reference.

## 2.3.9 SCANNING ELECTRON MICROSCOPY (SEM)

Scanning Electron Microscopy (SEM) is one of the widely used tools of modern science as it allows study of both morphology and composition of biological and physical materials. By scanning an electron probe across a specimen, high resolution images of the morphology or topography of a specimen with great depth of field at very low or very high magnifications can be obtained. This reveals the beauty and complexity of the microstructure in amazing clarity. Compositional analysis of a material may also be obtained by monitoring secondary X-rays produced by the electron-specimen interaction[17]. Thus detailed maps of elemental distribution can be produced from multi-phase materials or complex, bioactive materials. Characterisation of fine particulate matter in terms of size, shape, and distribution as well as statistical analyses of these parameters, may be performed.

Scanning electron microscopy examines structure by bombarding the specimen with a scanning beam of electrons and then collecting slow moving secondary electrons that the specimen generates. These are collected, amplified, and displayed on a cathode ray tube. The electron beam and the cathode ray tube scan synchronously so that an image of the specimen surface is formed. Specimen preparation includes drying the sample and making it conductive to electricity, if it is

not already. Useful magnifications upto 100,000 times are possible with large depth of field. Potential applications of SEM include,

- Surface topography if low energy secondary electrons are collected
- Atomic number or orientation information if higher energy backscattered electrons are used for imaging
- Differentiation between surface roughness, porosity, granular deposits, stress-related gross microcracks
- Observation of grain boundaries in unetched samples
- Critical dimension measurements
- Outstanding diagnostic instrument for micro fabrication.

The main drawback of this technique is that the scan results may not represent the entire sample. Taking the images at different locations can remunerate this.

The SEM pictures were taken in a JEOL JSM-840 A (Oxford make model I6211 with a resolution of 1.3 eV). Samples were prepared by dusting the clay powder onto double sided carbon tape, mounted on a metal stub. The samples were then sputter coated with a thin film of gold to reduce charging effects.

## 2.4 SURFACE ACIDITY MEASUREMENTS

Acidity plays an important role in virtually all organic reactions occurring over solid catalysts. The stability and selectivity of solid acids are determined to a large extent by their surface acidity. i.e. the number, nature, strength and density of acid sites. The acidity required for catalysing the transformation of reactants into valuable products can be quite different. For a long time, the acid strength has been recognised as an important parameter in the field of acid catalysis. In the 1920's Brönsted and Pederson and further Hammett and Deyrup quantified the relationship between the acid strength of an acid in solution and rate of the reaction catalysed by the acid. Stronger the acid, easier it is to activate a bond to form transition state

complex. Similar attempts were undertaken for heterogeneous catalysis also. Efforts to quantitatively correlate reaction rates to acid strength have to take two points into account. First, the exact value of acid sites in catalysts cannot be determined directly as in solution. Second, for any solid acid, a range of sites of different strengths exists. Thus it is not possible to know the exact acidity of each site. Hence, domains of acid strengths and number of sites belonging to the domain only can be defined[18].

A number of physicochemical methods have been developed and accepted to evaluate the strength and density of surface acid sites. A large variety of probe molecules have been utilised to ascertain acidity quantitavely as well as to provide an insight on acid site distribution[19]. However, range of applicability of most of these methods is limited to a narrow sphere of solids and a given experimental procedure.

The materials used for surface acidity measurements are given below.

| *Materials* | *Suppliers* |
| --- | --- |
| 1. Sulphuric acid | Merck |
| 2. Sodium carbonate | Qualigens |
| 3. Perylene | Merck |
| 4. Benzene | Merck |
| 5. Cumene | Merck |
| 6. Cyclohexanol | CDH |

A thorough characterisation of the surface acidity was undertaken using three independent techniques viz.,

1. temperature programmed desorption of ammonia ($NH_3$ -TPD)
2. perylene adsorption studies
3. test reactions for the characterisation of acid-base properties
   a) cumene cracking
   b) cyclohexanol decomposition.

## 2.4.1 TEMPERATURE PROGRAMMED DESORPTION OF AMMONIA (NH₃-TPD)

Among the various physicochemical methods to characterise acidity, temperature programmed desorption is the most promising technique, facilitating direct determination of cumulative acidity and acid site distribution. Ammonia is the most important basic probe molecule used, since it can titrate acid site of any strength and is easily accessible to even micro pores due to the small size. When chemisorbed on a surface possessing acid properties, ammonia can interact with acidic protons, electron acceptor sites and hydrogen from neutral or weakly acidic hydroxyls and thus can detect most types of acid sites[20]. In pillared clays, interaction with ammonia produces new acidic hydroxyls, some of which undergo proton transfer to ammonia and seven types of hydroxyls have been discriminated based on nature and location[21]. Three different surface reactions have been detected with ammonia: ammonolysis of surface bonds, exchange reactions and scrambling of hydroxyls.

The TPD measurements were performed in a conventional flow type apparatus made of a steel reactor (30 cm long and 1 cm in diameter), at a heating rate of 10°C min$^{-1}$ in $N_2$ atmosphere. Pelletised sample (0.5g) was treated inside the reactor with $N_2$ at 300°C for 2 hours and cooled to room temperature. Ammonia was injected into the sample in the absence of $N_2$ flow and kept as such for 15 minutes for the equilibrium adsorption of ammonia to all acidic sites. Excess and physisorbed ammonia were flushed off for 30 minutes at room temperature. The desorbed ammonia was collected at a temperature interval of 100°C into 0.02 N $H_2SO_4$ solution. This was quantified by direct titration with $Na_2CO_3$ solution using methyl orange indicator. The amount of ammonia desorbed at 35-200, 201-400 and 401-600°C were assigned as weak, medium and strong acid sites respectively.

## 2.4.2 PERYLENE ADSORPTION STUDIES

The determination of surface sites which act as acceptors of single electrons is based on the measurement of the amount of adsorbed molecules, which can

easily donate one electron. Thus, investigation of the interaction between one electron acceptor sites and adsorbed donor molecules is an indirect determination of electron deficient sites. This method is very successful in gaining information about Lewis acidity in presence of Brönsted sites. The principle is based on the ability of catalyst surface to accept electron from an electron donor like perylene to form a charge transfer complex. The amount of adsorbed species can be measured by spectroscopic means[22]. Perylene has an electron affinity of 1.17 eV, which accounts for the ease with which it can form cation radical in liquid solutions[23].

The adsorption experiments were carried out in a 50 mL stoppered U- tube by stirring 5 mL of freshly prepared perylene in benzene solutions of varying perylene strength and accurate amounts of the catalyst for 4 hours. The concentration range of perylene was varied from 0.01- 0.02 mol $L^{-1}$ in benzene. The contents were filtered after 24 hours and the absorbance measured after dilution by ten times. In all cases, bsorbance measurements were performed in the adsorbate concentration range where Beer Lambert law is valid. Since perylene gets adsorbed on the Lewis acid sites of the catalyst, its concentration will be less in the solution after adsorption. From Langmuir plots, limiting amount of perylene adsorbed on the catalyst surface, which is a measure of Lewis acidity is obtained. The chemical interaction between adsorbate and sample can be described by Langmuir adsorption isotherm,

$$C / X = 1 / BX_m + C / X_m,$$ where C is concentration of perylene solution, B, a constant and $X_m$ is limiting amount of perylene adsorbed.

The quantitative estimation of Lewis acidity by perylene adsorption is not an absolute method since it suffers from the drawback that perylene being a bulky molecule is not accessible to all Lewis sites in experimental conditions. The absorbance measurements were done in a Shimadzu UV-160A spectrophotometer at $\lambda_{max}$ 439 nm using a 10 mm quartz cell.

## 2.4.3 TEST REACTIONS FOR ACID-BASE PROPERTIES

The multifunctional character of a catalytic system is manifested through the wide diversity of products obtained with a given reactant. Vapour phase cumene cracking is a model reaction in identifying the Lewis-Brönsted acidity of a catalyst. Cumene is cracked to benzene and propene over Brönsted acid sites as opposed to the dehydrogenation to *a*-methyl styrene over Lewis acid sites. Thus, the relative amount of benzene to *a*-methyl styrene in the product mixture is a good indication of the acidity possessed by the catalyst[24]. Cyclohexanol decomposition reaction is adopted to evaluate the acid-base properties of the system. Alcohols being amphoteric in nature can interact with both acidic and basic centres[25,26]. Hence for cyclohexanol, dehydration to cyclohexene occurs over acidic sites while a concerted action of acidic and basic sites is required for dehydrogenation to cyclohexanone.

The vapour phase test reactions were carried out at atmospheric pressure in a fixed bed, downflow vertical glass reactor (1 cm diameter, 40 cm length) inside a double zone furnace. 0.5 g catalyst activated at 500°C was immobilised inside the reactor using glass wool, sandwiched between inert silica beads. A thermocouple positioned near the catalyst bed monitored the reaction temperature, regulated using a temperature controller. The reactant was fed into the reactor with the help of a syringe pump at a controlled flow rate. The product was collected downstream the reactor in a receiver connected through a water condenser and analysed gas chromatographically by comparison with authentic samples.

## 2.5 CATALYTIC ACTIVITY MEASUREMENTS

The liquid phase catalytic reactions performed were benzylation of benzene with benzyl chloride, benzylation of *o*-xylene with benzyl alcohol, benzylation of *o*-xylene with benzyl alcohol in presence of benzyl chloride and oxidation of phenol.

All the liquid phase reactions were carried out in a 50 mL round bottomed flask equipped with an oil bath, a magnetic stirrer and a water condenser. The oil bath was attached to a dimmerstat so that the temperature of the oil bath can be adjusted between room temperature and refluxing temperature of the mixture. At specified intervals, the catalyst was filtered off from the reaction mixture. The product was subjected to gas chromatography and product identification was achieved by comparing the retention times with those of standard compounds. The analysis conditions are specified in table 2.1.

Applicability of liquid phase reaction is often limited by the low temperature requirement. Temperatures higher than the refluxing temperature of reaction mixture can be attained by gas phase experiments. The vapour phase experiments selected for present study are *tert*-butylation of phenol and methyl *tert*-butyl ether synthesis.

In a typical vapour phase experiment, the reactor (1 cm diameter, 40 cm length) was first charged with the activated catalyst. A screen of silica beads was placed at the top and bottom of the reactor to ensure that the catalyst remains in middle portion. The upper portion of the reactor served as vapouriser cum preheater and a thermocouple positioned at the centre of catalyst bed monitored the exact temperature. The liquid reactants were fed into the reactor by a syringe pump. Products of reaction were collected downstream from the reactor in a receiver connected through cold water circulating condenser at specified intervals and analysed by gas chromatography. Comparing the GC retention times of expected products with those of standard chemicals accomplished identification of products. The products of the various reactions were analysed using Chemito 8610 Gas Chromatograph equipped with Flame Ionisation Detector and appropriate coloumn. The details of the analysis are given in table 2.2.

| Catalytic reaction | Analysis conditions | | | |
|---|---|---|---|---|
| | Coloumn | Temperature programme | Injector (°C) | Detector (°C) |
| Cumene cracking | FFAP | 120°C- isothermal | 230 | 230 |
| Cyclohexanol decomposition | Carbowax | 120°C- isothermal | 200 | 200 |
| Benzene benzylation | SE-30 | 80°C-2-3°C-200°C* | 230 | 230 |
| o-xylene benzylation | SE-30 | 100°C-2-3°C-230°C | 230 | 230 |
| Tert-butylation of phenol | SE-30 | 120°C-2-8°C-210°C | 230 | 230 |
| Phenol oxidation | OV-17 | 140°C-2-8°C-230°C | 250 | 250 |
| MTBE synthesis | OV-101 | 60°C- isothermal | 150 | 250 |

*Initial temperature-duration in minutes-rate of increase-final temperature.

Table 2.2 Analysis conditions for various catalytic reactions

## REFERENCES

1.  "Clay mineralogy: Spectroscopic and Chemical Determinative Methods", 312, Chapman & Hall (1994).

2.  M Horio, K Suzuki, H Masuda, T Mori, *Appl. Catal. A: Gen.*, 72, 109 (1991).

3.  K Suzuki, M Horio, T Mori, *Bull. Chem. Soc. Jpn.*, 64, 732 (1991).

4.  A Gil, M Vicente, L.M Guandia, *Microporous. Mesoporous Mater.*, 34, 115-125 (2000).

5.  L.P Meir, G Kahr, *Clays. Clay Miner.*, 47, 386-388 (1999).

6.　A.K Helmy, E.A Ferreiro, S.G de Bussetti, *Clays. Clay Miner.*, 42, 444-450 (1994).

7.　C Ma, R.A Eggleton, *Clays. Clay Miner.*, 47, 174-180 (1999).

8.　"Encyclopaedia of Analytical Chemistry", R.A Mayers (ed), John Wiley.

9.　Clive Whiston, "X-ray Methods-Analytical Chemistry by Open Learning", F.E Prichard (ed), John Wiley, ch.3 (1987).

10.　H Lipson, H Steeple, "Interpretation of X-ray powder diffraction patterns", Macmillan, London (1970).

11.　S Brunauer, P.H Emmett and E Teller, *J. Am. Chem. Soc.*, 60, 309 (1938).

12.　J.H de Boer, B.C Lippens, B.G Linsen, J.C.P Broekhoff, T.J Osinga, *J. Colloid Interface Sci.*, 21, 405-414 (1966).

13.　M.J Remy, G Poncelet, *J. Phy. Chem.*, 99, 773-779 (1995).

14.　Harald Günther, "NMR Spectroscopy", John Wiley, 2nd ed (1998).

15.　E.R Andrew, *Intern. Rev. Phy. Chem.*, 1, 195, (1981).

16.　"Modern aspects of Reflectance Spectroscopy", W.W Wendlandt (ed), Plenum Press, New York, (1968).

17.　A Howie, "Characterisation of Catalysts", J Thomas, R.M Lambert (eds), John Wiley, New York (1989).

18.　D Barthomenf, "Catalysis by Acids and Bases", B Imelik (eds), Elsevier, Amsterdam, 75-90, (1985).

19.　P.A Jacobs, "Characterisation of Heterogeneous Catalysts", F Delanney (eds), Elsevier, Amsterdam, 311 (1985).

20.　F Lonyi, J Valyon, *Microporous. Mesoporous Mater.*, 47, 293-301 (2001).

21.　S Bodoardo, R Chiappetta, B Onida, F Figueras, E Garrone, *Microporous. Mesoporous Mater.*, 20, 187-196, (1998).

22.　B.D Flockart, J.A.N Scott, R.C Pink, *J. Am. Chem. Soc. Faraday Trans.*, 62, 730 (1966).

23.　A Stritweser, I Schwager, *J. Phy. Chem.*, 66, 2316 (1962).

24.　S.M Bradly, R.A Kydd, *J. Catal.*, 141, 239 (1993).

25.  S.J Kulkarni, R.R Rao, M Subramanyam, A.V.R Rao, *J. Chem. Soc. Chem. Commun.*, 273 (1994).

26.  C.G Ramankutty, S Sugunan, B Thomas, *J. Mol. Catal. A*, 187, 105-117 (2002).

# 3

# PHYSICOCHEMICAL
# CHARACTERISATION

*Understanding catalysis requires an understanding of surface chemistry, which deals with the bonding and reaction of an adsorbate with the surface and the influence of the surface on the bonding and reaction between the adsorbates. An important aspect of this understanding is the ability to characterise the physical and chemical properties of the surface. The characterisation of the prepared systems was done by versatile techniques like cation exchange capacity determination, energy dispersive X ray analysis, surface area and pore volume measurements, X ray diffraction, infrared spectroscopy, $^{27}Al$ and $^{29}Si$ NMR spectroscopy, thermogravimetry, UV diffuse reflectance spectroscopy and scanning electron microscopy. The nature and density of the acidic sites were examined by three independent techniques, viz., ammonia TPD, perylene adsorption and cumene cracking test reaction. The acid base property of the systems was evaluated by cyclohexanol decomposition reaction. The results and the conclusions drawn from the analysis are detailed in this chapter.*

## 3.0 INTRODUCTION

Heterogeneous catalysis deals with reactions between species, which are adsorbed on the surface a catalyst. The role of catalyst surface is to provide an energetically favourable pathway for the reaction. Thus to explain catalytic activity of systems, it is essential to look at surface properties rather than collective properties of the bulk of the catalyst. Catalytic properties of the surface are determined by the composition and structure on atomic scale. It is essential to know the exact structure of surface including defects as well as exact location of active sites. Thus from a fundamental point of view, ultimate goal of catalyst characterisation should be a look at the surface, atom by atom and under reaction conditions. Establishing empirical relations between factors that govern catalyst composition, pore dimensions, particle size and shape and catalyst performance are very useful in catalyst development.

### 3.1.1 CATION EXCHANGE CAPACITY (CEC)

Cation exchange capacity of pillared clays is only partially compensated by the charge of oligomers. Even if the oligomer to clay ratio is very high, a part of exchangeable cations remains unchanged. The residual CEC provides an estimation of the fraction of layer charge, which is not compensated by cationic pillaring species. During exchange process, some monomeric forms of the pillaring species could as well be exchanged. The protons that are formed in final calcination step of pillaring process, when intercalated oligomeric cation is decomposed into metal oxide pillars can also restore CEC of clay. Since, in the present study, pillared clays were exchanged with ammonium acetate solution (pH at which amphoteric character would play limited role), it may be assumed that residual CECs have a comparable value and that most ammonium ions occupy the accessible exchange positions[1]. The residual CEC of various pillared clays determined by ammonium acetate extract method is given in table 3.1.

| Catalyst | Residual CEC (mmol g$^{-1}$) | (Residual CEC/Initial CEC) x100 (%) |
|----------|------------------------------|-------------------------------------|
| M | 0.91 | 100 |
| Fe PM | 0.32 | 35.2 |
| Al PM | 0.56 | 61.5 |
| FeAl PM | 0.36 | 40.1 |

*Table 3.1 Cation Exchange Capacity of pillared clays.*

The residual CEC gives a measure of effectiveness of pillaring process. Table 3.1 reveals that pillaring with iron has been most effective. Montmorillonite shows a cation exchange capacity of 0.91 mmol g$^{-1}$. Iron pillaring exchanges 64.8% of the exchange capacity with Fe polymeric species. Aluminium polymeric solution contains Al monomeric and dimeric species and they also are considered to be exchangeable. Hence residual CEC of Al PM is the CEC that has not been exchanged with Al$_{13}$ polymer or it is an indication of effectiveness of pillaring with Al$_{13}$ polymer. The high value of residual CEC for Al PM indicates that pillaring with aluminium oligomeric solution is not so successful in intercalating clay interlayers with Al$_{13}$ polymer. Poncelet *et.al* measured residual CEC of Al pillared clays and found that polycations compensated 43 to 82% of the original CEC of clays, the rest remaining unchanged[2]. The same authors estimated residual CEC of clays after pillaring with Al, Zr and mixed Al-Zr species and found 16 to 35% of original CEC retained[3]. The mixed iron aluminium pillaring exchanges 59.9% of the initial CEC of the parent montmorillonite. Hence, it can be concluded that exchange with mixed iron aluminium oligomeric species is an effective way for pillaring montmorillonite.

Presence of residual CEC implies that these materials can further exchange ther layer charge with other metals. Therefore, room temperature exchange with transition metals of first series was tried to improve textural and catalytic properties.

## 3.1.2 ENERGY DISPERSIVE X-RAY ANALYSIS (EDAX)

Energy dispersive X-ray analysis yields chemical composition of the prepared samples. The elemental compositions of individual systems are presented below.

### 3.1.2.1 Iron pillared systems

The results of EDX analysis of iron pillared systems are tabulated in table 3.1.2.1. The Si/Al ratio of parent montmorillonite is 3.18. After pillaring the clay with iron oligomeric species, Si/Al ratio remains 3.1. The parent clay has considerable amount of exchangeable cations, viz., Na, Mg, K and Ca. A drastic reduction in the amount of these elements occurs as a result of pillaring with iron and the amount of iron increases by 23.54%. Room temperature exchange with transition metals incorporates about 1- 2.5% of the metals into the pillared system. Vanadium and zinc exchange best while copper and manganese exchange least.

| Catalyst | Element (%) | | | | | | | |
|---|---|---|---|---|---|---|---|---|
| | Na | Mg | Al | Si | K | Ca | Fe | TM* |
| V/Fe PM | 0.29 | 1.38 | 14.09 | 46.96 | 1.11 | 0.41 | 33.43 | 2.33 |
| Mn/Fe PM | 0.31 | 1.52 | 14.71 | 46.85 | 1.07 | 0.44 | 35.1 | 1.19 |
| Co/Fe PM | 0.37 | 1.34 | 14.09 | 46.52 | 1.85 | 0.50 | 33.36 | 1.97 |
| Ni/Fe PM | 0.44 | 1.85 | 14.78 | 47.06 | 1.54 | 0.49 | 33.84 | 1.93 |
| Cu/Fe PM | 0.36 | 1.03 | 14.46 | 47.94 | 1.61 | 0.42 | 32.97 | 1.21 |
| Zn/Fe PM | 0.34 | 1.84 | 14.12 | 47.12 | 1.64 | 0.46 | 31.22 | 2.26 |
| Fe PM | 0.33 | 1.42 | 14.88 | 45.55 | 1.91 | 0.56 | 35.21 | - |
| M | 2.18 | 2.81 | 17.74 | 56.47 | 4.11 | 5.01 | 11.67 | - |

Table 3.1.2.1 Elemental composition of iron pillared systems

* - Exchanged transition metal

Si/Al ratio of a system, before and after treatment, is an important parameter exhibiting structural stability. Differences in the ratio indicate dealumination from

structural framework. This effect, highly important for zeolites is not usually observed in clays. Thus, conservation of Si/Al ratio indicates that pillaring does not affect structural framework of clay. Increase in iron content with corresponding decrease in amount of exchangeable cations points to successive replacement of interlamellar cations with stable iron oxide pillars. The reduction in CEC values on pillaring supports this point. Transition metal exchange again replaces the exchangeable cations from interlamellar spaces, in particular potassium with the respective metal.

### 3.1.2.2 Aluminium pillared systems

The elemental composition of aluminium pillared systems is given in table 3.1.2.2. It can be seen from the table that Si/Al ratio of parent clay decreases from 3.18 to 2.0. Aluminium content increases by 9.14% with corresponding decrease in amount of exchangeable cations. Exchange with transition metals incorporates about 1-2% of the metal at the expense of interlamellar cations. Vanadium exchanges best.

| Catalyst | Element (%) | | | | | | | |
|---|---|---|---|---|---|---|---|---|
| | Na | Mg | Al | Si | K | Ca | Fe | TM |
| V/Al PM | 0.45 | 1.54 | 24.85 | 57.71 | 2.7 | 0.34 | 10.0 | 2.36 |
| Mn/Al PM | 0.49 | 2.19 | 24.51 | 58.65 | 2.42 | 0.33 | 10.38 | 1.03 |
| Co/Al PM | 0.63 | 1.67 | 23.19 | 59.55 | 2.65 | 0.64 | 10.59 | 1.08 |
| Ni/Al PM | 0.88 | 2.03 | 24.08 | 58.32 | 2.7 | 0.46 | 10.05 | 1.15 |
| Cu/Al PM | 0.49 | 1.25 | 23.28 | 59.42 | 2.46 | 0.74 | 10.24 | 1.06 |
| Zn/Al PM | 0.69 | 1.24 | 22.20 | 58.4 | 2.63 | 0.82 | 10.78 | 1.62 |
| Al PM | 1.44 | 2.96 | 26.87 | 54.42 | 3.16 | 0.94 | 10.91 | - |

Table 3.1.2.2 Elemental composition of aluminium pillared systems

Decrease in Si/Al ratio is a direct consequence of the increase in aluminium content as a result of pillaring rather than structural instability of the clay layers. From the data, it can also be concluded that pillaring occurs at interlamellar sites in the

place of exchange cations. This fact is supported by CEC measurements. Exchange with the transition metals of the first series further replaces these cations.

### 3.1.2.3 Iron Aluminium pillared systems

Table 3.1.2.3 reveals the chemical composition of the catalysts of iron aluminium mixed pillared series. The data shows that Si/Al ratio of the original clay decreases from 3.18 to 2.65 on mixed pillaring. Fe and Al content of pillared system increases from the original clay by 5.62% and 3.67%. Exchange with transition metal incorporates about 1-3% of metal. Zinc and manganese is loaded to greater extent.

Pillaring process involves exchange of interlamellar cations with bulky oligomeric species and this does not affect the structural stability of original clay. The decrease in Si/Al ratio is due to increase in aluminium content as a result of mixed pillaring and not due to dealumination. Insertion of oligomeric species occurs at the expense of exchangeable cations as indicated by marked decrease in the amount of Na, K, Mg and Ca. The decrease in CEC on pillaring supports this view. Exchange with metals further replaces these cations as suggested by CEC measurements.

| Catalyst | Element (%) | | | | | | | |
|---|---|---|---|---|---|---|---|---|
| | Na | Mg | Al | Si | K | Ca | Fe | TM |
| V/FeAl PM | 0.23 | 1.48 | 20.69 | 56.18 | 1.8 | 0.35 | 17.08 | 1.99 |
| Mn/FeAl PM | 0.21 | 1.58 | 19.95 | 56.07 | 2.19 | 0.39 | 16.9 | 2.51 |
| Co/FeAl PM | 0.22 | 1.59 | 21.29 | 56.0 | 2.02 | 0.41 | 17.01 | 1.26 |
| Ni/FeAl PM | 0.28 | 1.78 | 21.22 | 56.26 | 2.04 | 0.4 | 17.02 | 1.3 |
| Cu/FeAl PM | 0.32 | 1.46 | 20.73 | 55.85 | 2.24 | 0.31 | 17.29 | 1.8 |
| Zn/FeAl PM | 0.22 | 1.83 | 19.94 | 55.0 | 1.57 | 0.43 | 16.73 | 3.18 |
| FeAl PM | 0.31 | 1.97 | 21.41 | 56.61 | 2.67 | 0.54 | 17.29 | - |

Table 3.1.2.3 Elemental composition of iron aluminium pillared systems

In order to show the effects of exchange process on the original constituents of the clay, the elemental weights can be recalculated to 100% after excluding the fixed transition metal oxide. This calculation indicated that transition metal oxide was introduced without a significant deleterious effect on the clay structure and the pillars. Thus on exchange with transition metal, metal oxides are incorporated into the pores or in between the pillars rather than exchanged in the location of pillars.

## 3.1.3 SURFACE AREA AND PORE VOLUME MEASUREMENTS

The determination of surface area and pore volume in clays is a subject of controversy[4]. The most convenient approach for textural characterisation of these materials is to obtain the adsorption isotherm at a temperature lower than or equal to critical adsorbate temperature. $N_2$ (at 77.2 K) is traditionally used as adsorbate. As gas pressure increases, adsorption proceeds by pore filling, starting from smaller pores. The potential energy fields from neighbouring surfaces overlap and the total interaction energy with adsorbate molecules becomes substantially enhanced giving rise to high gas volume adsorption at very low relative pressures. The surface areas of pillared clays are typically obtained by applying BET equation. The range of validity of BET equation for these materials is usually between $P/P_0 = 0.01$ and 0.1. However, in microporous solids like pillared clays where the interlamellar distance is of the order of a few molecular diameters, monolayer formation on clay silicate layers occurs. Thus surface areas approximated by Langmuir equation are reasonable representations of pillared clay surface areas[5]. Hence in the present study, BET and Langmuir surface areas of various systems obtained directly are tabulated. The external and microporous surface areas were calculated from $t$-plot[6,7].

### 3.1.3.1 Iron pillared systems

The surface areas and pore volumes of iron pillared systems are given in table 3.1.3.1. Montmorillonite has a BET surface area of 14.3 $m^2g^{-1}$ and Langmuir

surface area of 27.9 $m^2g^{-1}$. As a result of pillaring, surface area and pore volume increases drastically. Fe PM exhibits maximum surface area and pore volume. 71.8% of the total surface area is microporous in nature. Pore volume also increases significantly on pillaring. Transition metal exchange decreases the surface area and pore volume, mainly in external surface area. Minimum surface area is exhibited by zinc exchanged system. Decrease in surface area can be roughly correlated to the amount of metal oxide incorporated as obtained from EDX measurements.

Pillaring is the process by which stable metal oxide clusters are incorporated into interlayer space of swellable clays. As a result, a three dimensional porous network is created. Hence, surface area and pore volume increases extensively, especially the microporous surface area. The external surface area in pillared clays arises from mesopores which are mainly interparticle voids[8,9]. Transition metal exchange deposits the metal oxides inside the porous network and hence the decrease in surface area and pore volume. The exchanged metal oxides have been evidenced to be attached to pillars[10] and hence decrease in external surface area.

| Catalyst | Surface Area ($m^2g^{-1}$) | | | | Pore volume ($ccg^{-1}$) |
|---|---|---|---|---|---|
| | BET | Langmuir | Microporous | External | |
| V/Fe PM | 160.7 | 234.2 | 118.2 | 42.5 | 0.1991 |
| Mn/Fe PM | 194.1 | 285.4 | 132.3 | 61.8 | 0.2086 |
| Co/Fe PM | 178.3 | 250.8 | 128.6 | 49.7 | 0.1957 |
| Ni/Fe PM | 164.8 | 226.5 | 116.3 | 48.5 | 0.1920 |
| Cu/Fe PM | 171.2 | 248.2 | 120.9 | 50.3 | 0.1992 |
| Zn/Fe PM | 147.7 | 234.8 | 108.6 | 39.1 | 0.1857 |
| Fe PM | 194.2 | 269.7 | 139.4 | 54.8 | 0.2157 |
| M | 14.3 | 27.9 | - | - | 0.0058 |

Table 3.1.3.1. Surface area and pore volume of iron pillared systems

### 3.1.3.2 Aluminium pillared systems

Table 3.1.3.2 furnishes the surface area and pore volumes of various aluminium pillared systems. In this case also, surface area and pore volume of montmorillonite increases as a result of pillaring, but not to the same extent as iron pillaring. Aluminium pillaring increases BET surface area to 132.9 $m^2g^{-1}$ and Langmuir surface area to 192.3 $m^2g^{-1}$. The pore volume increases to 0.1623 $ccg^{-1}$. About one third of the area can be attributed to external surface. As a result of transition metal exchange, surface area and pore volume decreases. Zinc and vanadium exchange brings about this effect to the maximum. Decrease in surface area and pore volume can be correlated well with the amount of metal oxide incorporated into the pillared system.

| Catalyst | Surface Area ($m^2g^{-1}$) | | | | Pore volume ($ccg^{-1}$) |
|---|---|---|---|---|---|
| | BET | Langmuir | Microporous | External | |
| V/Al PM | 105.2 | 154.3 | 71.2 | 34.0 | 0.1432 |
| Mn/Al PM | 120.7 | 163.9 | 74.6 | 46.1 | 0.1493 |
| Co/Al PM | 125.2 | 171.8 | 73.8 | 51.4 | 0.1539 |
| Ni/Al PM | 121.3 | 165.2 | 72.0 | 49.3 | 0.1502 |
| Cu/Al PM | 126.9 | 179.1 | 74.9 | 52.0 | 0.1592 |
| Zn/Al PM | 116.8 | 168.9 | 70.2 | 46.6 | 0.1498 |
| Al PM | 132.9 | 192.3 | 86.9 | 46.0 | 0.1623 |

Table 3.1.3.2. Surface and pore volume of aluminium pillared series.

Increase in surface area and pore volume can be ascribed to the pillaring process. From CEC measurements it was obtained that 38.5% of original CEC was replaced by $Al_{13}$ polymer. But a lower surface area was obtained for the final pillared solid. This can be due to breaking of pillars on calcination. Similar observations were reported by Bakas et.al[1]. Breaking of pillars disrupts the porous network and hence

decreased percentage of microporous surface area compared to iron pillared systems. Transition metal exchange deposits the metal oxides nearby the pillars resulting in lower percentage of external surface.

### 3.1.3.3 Iron Aluminium pillared systems

The surface areas and pore volumes of mixed pillared systems are depicted in table 3.1.3.3. The values increase on pillaring as expected. Here also, two third of the surface area can be attributed to microporous surface. Transition metal exchange decreases the surface area and pore volume of FeAl PM, mainly in external surface.

| Catalyst | Surface Area ($m^2g^{-1}$) | | | | Pore volume ($ccg^{-1}$) |
|---|---|---|---|---|---|
|  | BET | Langmuir | Microporous | External |  |
| V/FeAl PM | 158.3 | 229.9 | 102.3 | 56.0 | 0.1753 |
| Mn/FeAl PM | 156.0 | 219.2 | 100.7 | 55.3 | 0.1703 |
| Co/FeAl PM | 164.9 | 229.5 | 108.6 | 56.3 | 0.1871 |
| Ni/FeAl PM | 142.2 | 203.9 | 98.5 | 43.7 | 0.1673 |
| Cu/FeAl PM | 144.5 | 207.6 | 95.6 | 48.9 | 0.1658 |
| Zn/FeAl PM | 147.2 | 233.6 | 100.3 | 46.9 | 0.1635 |
| FeAl PM | 170.6 | 253.7 | 114.9 | 55.7 | 0.1894 |

Table 3.1.3.3. Surface and pore volume of iron aluminium pillared series.

Increase in surface area and pore volume is a direct consequence of pillaring. Thus, it can be concluded that mixed pillaring with iron aluminium species is very effective in propping apart clay layers. Exchange with transition metals causes pore blocking by deposition of oxides inside the porous network.

### 3.1.4 X-RAY DIFFRACTION (XRD)

Pillared clays are produced by intercalating bulky polymeric species into the interlayer space of the swellable clays. Insertion of the metal oxide clusters in

between the planes, brings about propping apart of these planes. Obviously, pillar intercalation increases the interlayer distance. Apart from surface area and pore volume measurements, the easiest way to determine whether pillar intercalation is successful is to record the X-ray diffraction pattern of an oriented film of the product.
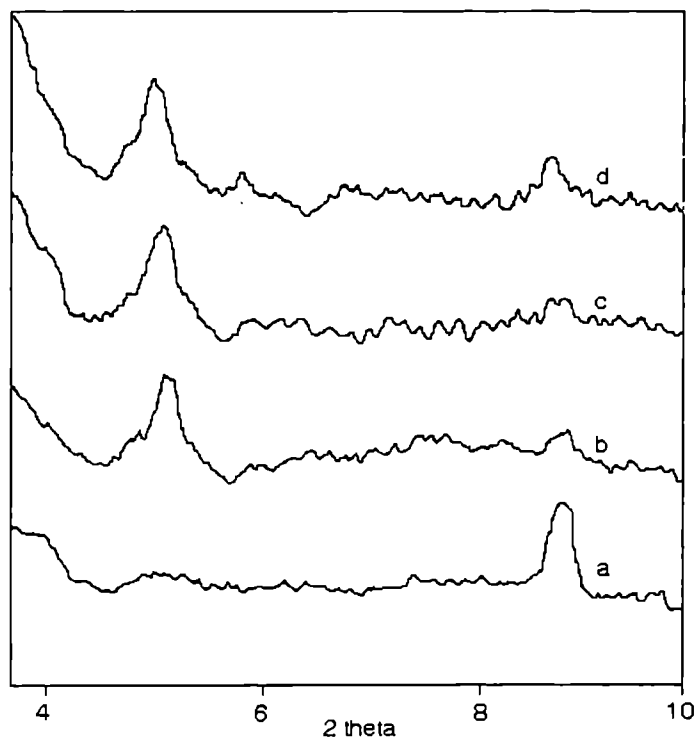


Figure 3.1.4 Low angle XRD profile of the pillared clays

a) M      b) Al PM      c) FeAl PM      d) Fe PM

Figure 3.1.4 depicts XRD patterns of montmorillonite and the three pillared clays. Pillared clays are semi crystalline in nature. The broad bands obtained in the XRD spectrum, instead of sharp peaks can be attributed to semi crystalline nature of clays. Hence, indexing of the spectrum is not possible for this type of solid acids. The only data that can be obtained is the d spacing of (001) plane, which indicates the

extent of propping apart of clay layers. X-ray diffraction peaks shows that long range face to face layer aggregation is present in the pillared sample. Thus, it can be safely commented that the sample is not an edge to face delaminated clay.

The characteristic $d_{001}$ spacing of montmorillonite is seen at $2\theta$ value of 9.8Å. For Al PM, this value increased to 17.3 Å. The d spacing increased to 19.2 Å and 17.8 Å as a result of iron pillaring and mixed iron aluminium pillaring, respectively. Shifting of $2\theta$ values clearly suggest expansion of clay layer during pillaring process.

The major intercalated species giving rise to stable basal spacing in Al PM is the so called $Al_{13}$ polyhydroxy polymer or Keggin cation which has been characterised by small angle X-ray scattering[12] and $^{27}Al$ NMR[13]. This polymer with structural formula, $[AlO_4Al_{12}(OH)_{24}(H_2O)_{12}]^{7+}$ is a tri-decamer composed of one aluminium tetrahedra surrounded by 12 aluminium octahedra. It contains four layers of superimposed oxygen atoms needed for expanding clay basal spacings to 18 Å. The expansion of (001) plane of clay layer near this value suggests that the intercalated species is the $Al_{13}$ polymer in Al PM. The hydrolysis reactions of $Fe^{3+}$ lead to discrete spherical cations[14,15]. Aggregation of two to six spheres produces rods and eventually rafts. Insertion of these species also leads to expansion of the clay layer. The thermal stability and catalytic properties of single oxide pillared clays can be improved by incorporating a second component into pillars. Formation of mixed $Al_{13-x}Fe_x$ pillars, based on the Fe content of the pillared solids was reported by Bergaua et.al[16,17]. The d spacing of (001) plane increased from 9.8 Å to 17.8 Å in the present case indicating the presence of Fe substituted $Al_{13}$ like polymers.

The relative intensity of the peaks, gives a measure of the extent of pillaring. In all cases, maximum intensity (100%) was for the peak corresponding to increase in basal spacing. Hence the relative intensity was calculated comparative to the intensity of this peak. The d spacings and relative intensities of the three pillared systems are tabulated in table 3.1.4. From the table, it can be concluded that iron

pillaring was far more efficient in propping apart the clay layers, both in the pillar size as well as extent of pillaring. Insertion of iron oxide pillars increases the basal spacing up to 19.2 Å and the corresponding relative intensity is 42.39. Aluminium pillaring led to mediocre network as indicated by the table. The mixed pillaring resulted in a much stable pillared species. Thus, XRD patterns underline the conclusions drawn from surface area and pore volume measurements. It is interesting to note that the order of extent of pillaring is the same as that obtained from residual CEC measurements.

| Catalyst | d spacing (Å) | Relative intensity (I/I$_0$) |
|----------|---------------|------------------------------|
| Al PM    | 17.3          | 56.23                        |
| Fe PM    | 19.2          | 42.39                        |
| FeAl PM  | 17.8          | 49.25                        |

Table 3.1.4. Basal spacings and relative intensities of the pillared clays

The effect of exchange with transition metals on the XRD patterns of the three pillared systems were studied for representative samples. The XRD patterns were exactly identical to that of the parent pillared sample. Thus, it can be concluded that insertion of the second metal after the formation of stable pillars does not destabilise the porous network. Additional peaks corresponding to the exchanged metal oxides were not noticed. This may be due to the diminutive amounts (1-3%) of the exchanged metal in these samples.

## 3.1.5 FOURIER TRANSFORM INFRARED SPECTROSCOPY

The structural evolution of the aluminosilicate layer was characterised by FTIR spectroscopy. The IR spectra of the parent montmorillonite and the three pillared systems are given in figure 3.1.5.
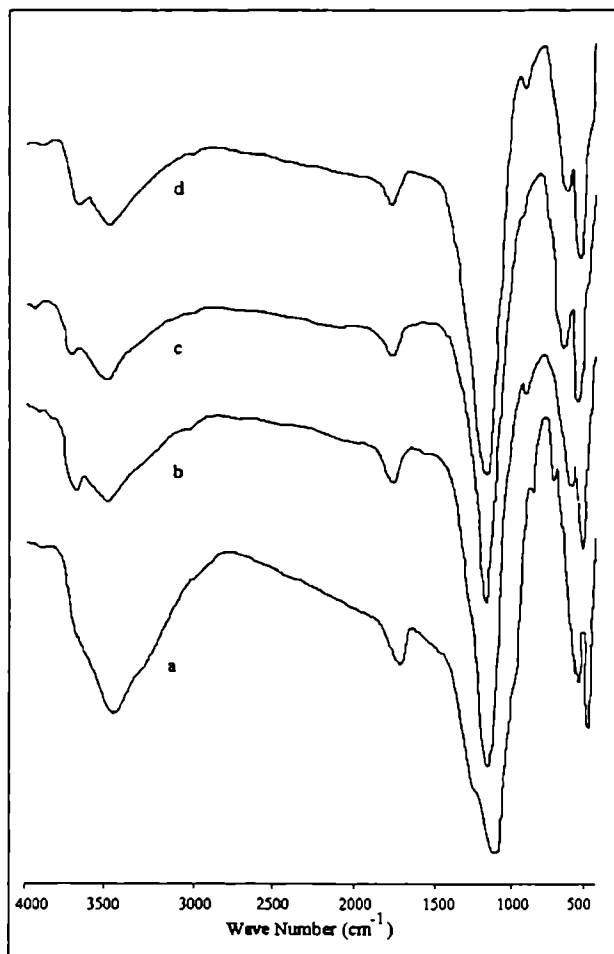
Figure 3.1.5  FTIR spectra of the pillared clays

a) M        b) Al PM        c) Fe PM        d) FeAl PM

The parent montmorillonite points up a large band at 3620 $cm^{-1}$, typical of smectites with large amount of Al in the octahedra[18]. Intensity of this peak decreases upon pillaring. Formation of a new band in the range of 3740-3770 $cm^{-1}$ is an important observation. The identification of hydroxyl species on pillared clays is extremely difficult, because of the complexity of the system and the opaqueness of

the sample in the corresponding IR region. It has been reported that isotopic exchange with mild deuterating agent $C_6D_6$ has allowed to identify two acidic hydroxyls, with OH stretching modes at 3660 and 3740 $cm^{-1}$, the former referring to the unstructured band of the parent montmorillonite and the latter which seem to arise from the sealing of montmorillonite layer and the pillar[19]. These can be represented as Si-O-Al-OH or Al-O-Si-OH. Thus FTIR spectra of the three pillared samples also are indicative of effective pillaring.

The IR spectra in the fingerprint region are characterised by absorptions at 1200-1000 $cm^{-1}$ due to asymmetric stretching vibrations of apical oxygens of $SiO_2$ tetrahedra and the large band due to combined stretching and bending vibrations of the Si-O bonds related to basal oxygens[20]. The band around 900 $cm^{-1}$ often provides information on the composition of the octahedral sheets. In montmorillonite, it reflects partial substitution of octahedral Al by Mg. Absorptions at 526-471 $cm^{-1}$ echo bending Si-O vibrations. Thus, the framework vibrations contain information about the structural characteristics of the material and their preservation after thermal treatments may be considered as a proof of the structural stability on pillaring. Absence of additional peaks suggests that no bond formation occurs between the montmorillonite and the pillars unlike other clays like saponite[21].

### 3.1.6 ^{27}Al NMR SPECTROSCOPY

Clay minerals and pillared clays have been the subject of several solid state NMR investigations[22-24]. ^{27}Al NMR can detect the co-ordination of Al atoms in clays containing as little as 0.26% of $Al_2O_3$[25]. Therefore this technique is of particular utility in studying octahedral and tetrahedral sites in the extra framework Al species contained in aluminium pillared samples. The ^{27}Al NMR spectra of the pillared clays are illustrated in figure 3.1.6.1.
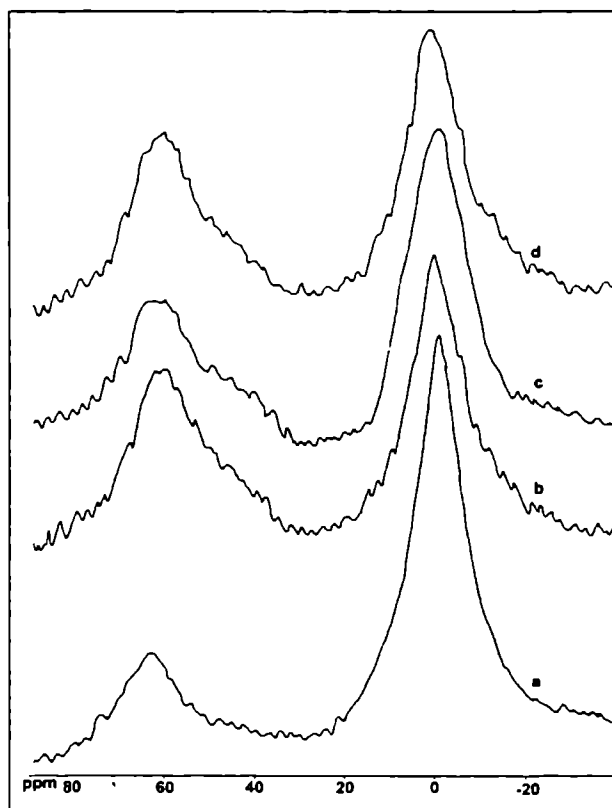
Figure 3.1.6.1. $^{27}$Al NMR spectra of the pillared clays

a) M        b) Al PM        c) Fe PM        d) FeAl PM

Montmorillonite shows two resonances; one at +1.38 ppm that can be ascribed to octahedral Al atoms and other at +66.0 ppm attributable to tetrahedrally coordinated Al atoms. For aluminium pillared samples, $\delta$ ppm values for octahedral Al atoms shifts to +1.98 ppm. This is due to overlapping of signals of Al atoms of intercalating polymer with that of original signal. Two resonances can be distinguished at tetrahedral region: resonance at +66.4 ppm belonging to clay tetrahedral sites and undoubtedly resonance at +60.3 ppm corresponds to tetrahedral sites in the pillar. An important conclusion is that the intercalated species

76

is not transformed into a spinel like structure. When aluminium hydroxides like gibbsite and boehmite are the pillars, corresponding resonances are between +8 to +9 ppm and above +68 ppm, signifying spinel like structure. Further, no resonance is observed at around +30 ppm demonstrating the absence of pentacoordinated Al atoms. Thus it can be unambiguously concluded that pillared species is the Keggin $Al_{13}$ polymer for Al pillared systems. The Keggin cation contains a central Al tetrahedra linked to 12 Al octahedra and has the formula $[AlO_4Al_{12}(OH)_{24}(H_2O)_{12}]^{7+}$.

For iron pillared systems, intensity of $^{27}Al$ NMR peaks at the octahedral and tetrahedral Al sites are almost similar to that of montmorillonite. Thus, as expected, there is non existence of Al atoms in the extra framework region. But the peaks are somewhat broader. This can be due to relaxation effects of paramagnetic centres.

The $^{27}Al$ NMR spectrum in the mixed iron aluminium pillared systems shows the $Al^{IV}$ signature of Keggin cation at +65.8 ppm. Resonance corresponding to octahedral Al atoms also is shifted to +1.97 ppm. Thus the pillaring solution would be made from these cations in which $Al^{3+}$ is partially replaced by $Fe^{3+}$. The nature of substitution is not known, but in view of Al by Fe in octahedral layers of micas, it is likely that some of the octahedral Al atoms in Keggin structure are replaced by Fe atoms[26]. Thus, structure of iron aluminium mixed pillared systems is similar to Al polymeric species and not hydroxy iron oligomers. Here also, relaxation effects caused by paramagnetic centres are operative. Hence FWHM (full width at half maximum) of the peaks is greater, compared to montmorillonite.

The effect of transition metal exchange on structural stability of pillared clays was examined by taking $^{27}Al$ NMR spectra of copper and cobalt doped iron and aluminium pillared systems as representative systems. Figure 3.1.6.2 shows $^{27}Al$ NMR spectra of Al PM and Fe PM in comparison with their cobalt and copper exchanged analogues. As a result of exchange with transition metals, peak width as well as peak positions do not vary. This shows that incorporation of transition metals

does not affect the structural stability of layers and pillars. Hence $^{27}$Al NMR data supports the inference drawn from surface area and pore volume measurements, that metal oxides are incorporated into porous network rather than attached to pillars.



Figure 3.1.6.2 $^{27}$Al NMR spectra of exchanged systems

a) Al PM    b) Co/Al PM    c) Cu/Al PM    d) Fe PM    e) Co/Fe PM    f) Cu/Fe PM

## 3.1.7 $^{29}$Si NMR SPECTROSCOPY

For Si nucleus (spin I = 1/2), chemical shift is affected mainly by the electron density on oxygen atoms of Si tetrahedron. Therefore nature of neighbouring atoms coordinated to these oxygen atoms can influence the shift. The spread of these shifts

is not only a function of the structural disorder but depends also on nature of second neighbours. The connectivity of Si nuclei in silicate species is described by the usual $Q^n$ notation. Q represents a silicon nucleus connected to four oxygen forming a tetrahedron. The superscript n is the number of other Q units attached to central $SiO_4$ tetrahedron. Thus $Q^0$ denotes monomeric orthosilicate anion $SiO_4-$, $Q^1$ denotes end groups of chains, $Q^2$ denotes middle groups in chains or cycle, $Q^3$ denotes chain branching sites and $Q^4$, three dimensionally cross linked groups.
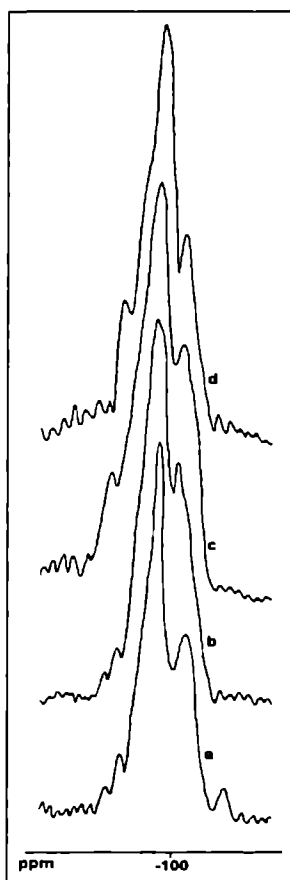


Figure 3.1.7.1 $^{29}Si$ NMR spectra of pillared clays

a) M        b) Al PM        c) Fe PM        d) FeAl PM

Figure 3.1.7.1 illustrates the $^{29}$Si NMR spectra of pure montmorillonite and various pillared clays. Montmorillonite shows a single resonance centred on $-93$ ppm. The peak shows a main peak at $-93.98$ ppm and two shoulder peaks: a large one at $-104.5$ ppm and a diminutive one at $-90.3$ ppm. The peak at $-93.98$ ppm can be attributed to $Q^3$ (Si1Al) units representing Si(IV) atoms linked through oxygen atoms to three other Si(IV) and to one Al(VI) (or Mg) in the clay octahedral layer. The shoulder peak at $-104.5$ ppm can be ascribed to $Q^3$ (Si0Al) where Si is linked to Si only through oxygens and small peak at $-90.3$ ppm is due to $Q^3$ (Si2Al). Thus majority of the silicon tetrahedra is linked to 3 Si atoms and one Al atom. A very small portion is linked to 2 Al atoms and 2 Si atoms while a part of Si tetrahedra is linked to Si atoms alone. This distribution of silicon tetrahedra into various environments is not affected by pillaring. A slight shift in ppm values can be noticed for pillared samples and this is tabulated in table 3.1.7.

| Catalyst | $Q^3$ (Si0Al) (ppm) | $Q^3$ (Si1Al) (ppm) | $Q^3$ (Si2Al) (ppm) |
|---|---|---|---|
| PM | -90.3 | -93.98 | -104.5 |
| Fe PM | -91.6 | -95.6 | -105.98 |
| Al PM | -90.9 | -94.29 | -105.23 |
| FeAl PM | -91.02 | -94.34 | -105.45 |

Table 3.1.7. Distribution of Si atoms to different environments

From the table it can be inferred that Lowenstein rule is obeyed. Lowenstein rule is the avoidance rule, which states that two tetrahedral Al cannot be next neighbours. Also, the shift in ppm values is in the order Fe PM > FeAl PM > Al PM. The order is the same as the order of d spacing obtained from X-ray diffraction studies. Thus the shift in ppm, which indicates strain in the local environment of Si atoms, is proportional to the size of intercalated species.

Several authors have pointed out that inversion of silicon tetrahedra can occur with intercalation of polymeric species in clays like beidellite and saponite where the layer charge is localised in tetrahedral layer[21,23]. Such an inversion is not anticipated in montmorillonites since layer charge is not localised. $^{29}$Si NMR spectra confirm this point since the shift in $\delta$ ppm values is less than 1- 2 ppm in all pillared samples. The contributions of different Si environments also remain the same. This gives confirmation to the nonexistence of chemical bonds between exchanged polymeric species and clay layers. Thus as anticipated, pillaring which is only a cation exchange process does not affect the short range order within clay layers. Had any bond that forms Al-O-Si linkage between the pillars and silicate layers been formed, the spectra would have contained $Q^3$ (Si3Al) resonance.

The more negative shift in Si spectrum in pillared samples can also be due to neutralisation of layer charge by migrating protons liberated from dehydration of pillars. The migration of protons was evidenced by Malla *et.al* by treatment with $NH_3$, which subsequently converted to $NH_4^+$ in interlayers[27].

The effect of exchange with transition metals on the structural stability of clay as well as pillaring process was exposed by taking the $^{29}$Si NMR spectra of two of the exchanged systems of the iron and aluminium pillared series, viz., cobalt and zinc exchanged systems. The spectra are depicted in figure 3.1.7.2. From the figure, it can be inferred that $\delta$ ppm values do not alter much as a result of exchange with transition metals. Thus incorporation of transition metals on the pillared systems does not alter the local environment of Si atoms. Hence, it can be inferred that metal oxides are not in the immediate environment of Si layer. They may be present in the porous network of the pillared system. This has been evidenced by surface area data and $^{27}$Al NMR spectra.
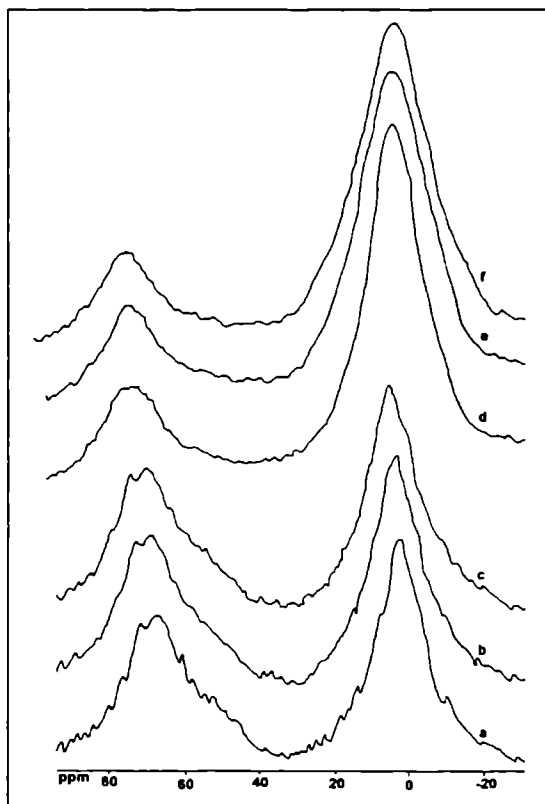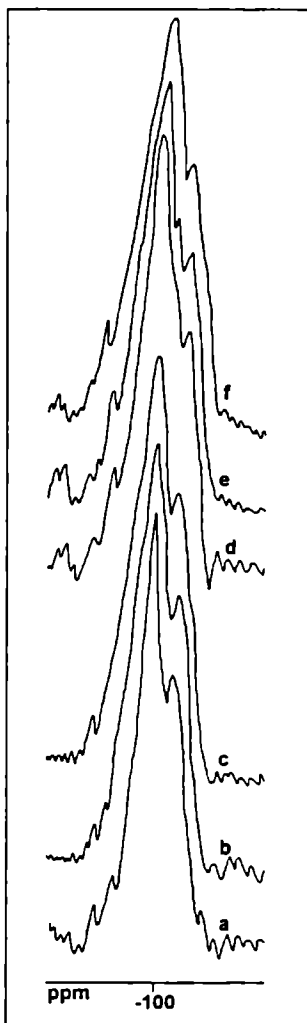
Figure 3.1.7.2 $^{29}$Si NMR spectra of exchanged systems

a) Al PM     b) Co/Al PM     c) Cu/Al PM     d) Fe PM     e) Co/Fe PM     f) Cu/Fe PM

## 3.1.8 THERMOGRAVIMETRY (TG)

Lack of thermal stability is the common drawback attributed to pillared clays. In order to find out thermal stability of prepared pillared clays, they were subjected to

thermogravimetric analysis in the temperature range of 80- 800°C. TG- DTA profiles of the samples are sketched in figure 3.1.9. Endothermic peaks corresponding to release of water alone are detected. Weight loss occurred in two steps for montmorillonite. After losing weight at 100-120°C, weight of montmorillonite remained almost constant to about 650°C. Al PM followed the same trend; only difference being in the temperature of second dip at about 600°C. However, iron containing systems exhibited three weight losses. An additional dip 9around 300°C was noticed for these systems. For Fe PM, the third weight loss occurred around 500°C where as for FeAl PM, it was observed in the range of Al PM (600°C).
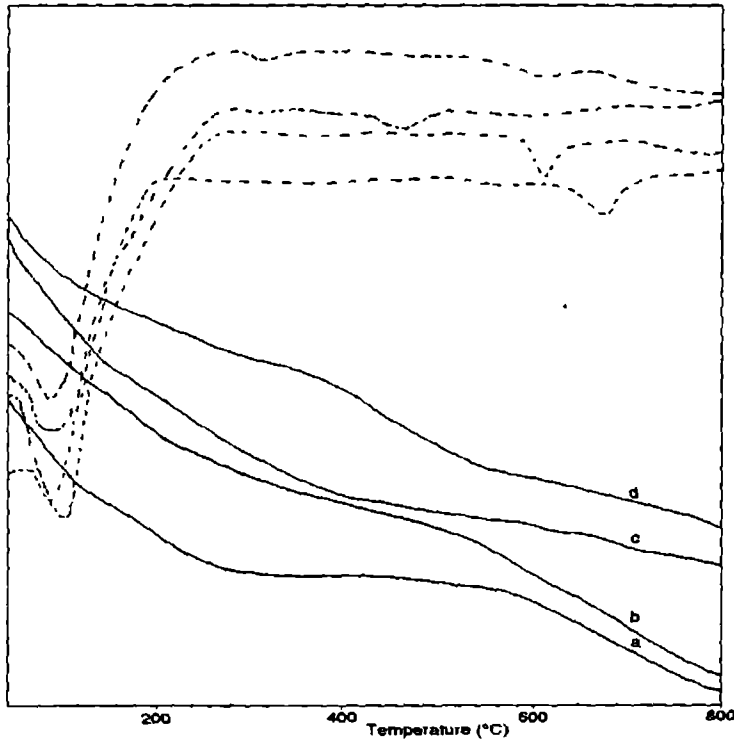


Figure 3.1.9. TG- DTA profile of the pillared clays

a) M        b) Al PM        c) Fe PM        d) FeAl PM

From the figure, it can be concluded that pillared clays possess substantial thermal stability. At each weight loss step, only water was released either by simple desorption or by hydroxylation of OH groups. The latter process occurred at high temperature while weight loss at 100-120°C characterised dehydration of samples. The dehydroxylation of montmorillonite occurred at 650°C. The temperature of dehydroxylation can be related to thermal stability of the pillared sample. Hence stability of pillared clays is in the order Al PM > FeAl PM > Fe PM. The second dip for iron containing pillars, occurring around 300°C can be attributed to conversion of oligomeric species to stable iron oxide pillars. Similar observations were reported by Zhao et.al[28]. However, this effect was not observed for aluminium pillared systems. The introduction of pillars in montmorillonite increases the amount of water released in dehydroxylation range.

## 3.1.9 ULTRAVIOLET DIFFUSE REFLECTANCE SPECTROSCOPY (UV- DRS)

UV diffuse reflectance spectroscopy has increasingly been applied to investigate structures of solid catalysts due to charge transfer spectra in ultraviolet region[29]. Iron containing systems show absorption bands at UV to near IR wavelengths, caused by electronic transitions within incompletely filled $3d^5$ shell of Fe(III)[30]. Differences between the spectra of iron oxide minerals occur because of different linkages of the octahedra. Distortions of octahedra alter (O, OH) distance and lower the symmetry, factors which alter legend field and shift band positions[31]. DRS can favourably complement surface studies of transition metal compounds, although it is restricted to information on first shell (metal- oxygen interaction)[32].

The UV- DR spectra of montmorillonite and pillared systems are presented in figure 3.1.9.1. A band centred at 250-280 nm is present in all systems. This is due to presence of Si in tetrahedral coordination. This band becomes higher for aluminium pillared and mixed pillared samples due to contribution of tetrahedrally coordinated aluminium in Keggin structure[33]. Thus, UV- DRS also supports the presence of

Keggin cation in these systems. The spectra for iron pillared and mixed pillared systems show one band at 300 nm that could be assigned to polyoxoiron complexes. The hydrolysis reactions of Fe(III) are known to yield discrete spherical polycations with an estimated diameter of 15-30 Å[34]. As expected, the intensity of this peak is higher for single oxide system than the mixed pillared system.
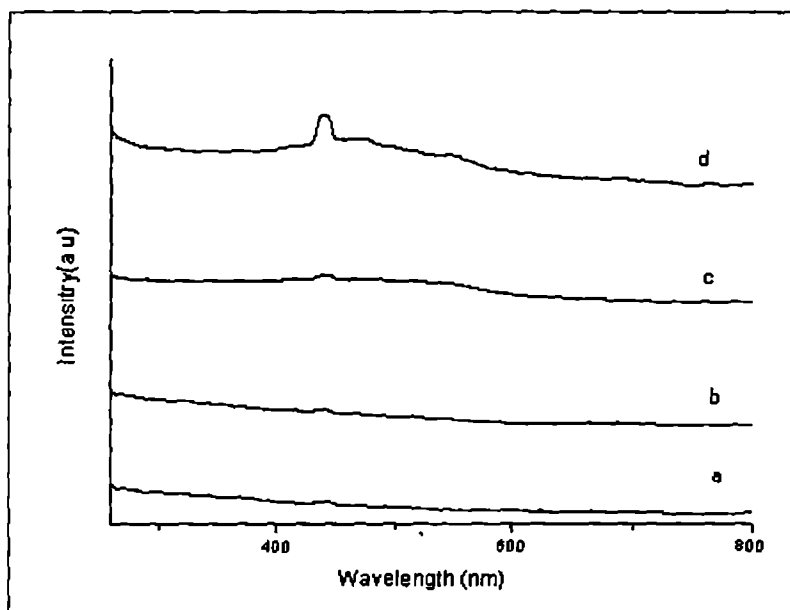


Figure 3.1.9.1 UV- DR spectra of pillared clays

a) M        b) Al PM        c) Fe PM        d) FeAl PM

UV- DR spectra of transition metal exchanged pillared clays are presented in figure 3.1.9.2. Exchange with transition metals does not alter the spectra much. Though, bands due to d-d and charge transfer transitions can be expected in metal oxides like vanadium and zinc, they are not observed in the present case. This may be due to low concentration (1-2%) these metals in the systems.
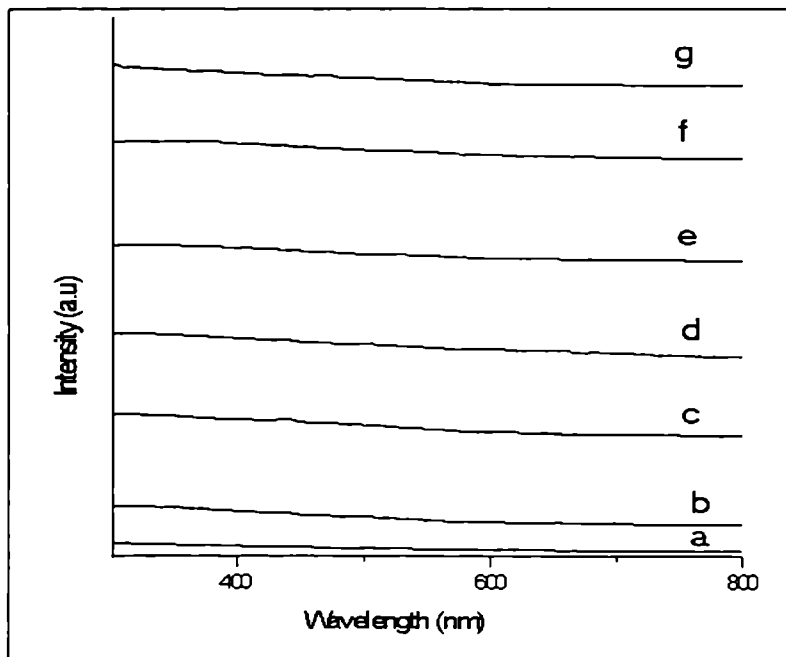
Figure 3.1.9.1. UV- DR spectra of transition metal exchanged pillared clays.

## 3.1.10 SCANNING ELECTRON MICROSCOPY (SEM)

SEM images reveal the beauty and complexity of microstructure in amazing clarity. The SEM pictures of the prepared pillared clays are given in figure 3.1.11. The SEM images of the prepared systems reveal important structural details. The parent montmorillonite is composed of small flaky particles. Pillaring with aluminium transforms these powder forms to large discrete particles. Iron pillaring and mixed iron aluminium pillaring modifies the size and shape of montmorillonite, but not to a significant extent. The effect of transition metal exchange was traced by taking the SEM pictures of doped samples also. Incorporation of transition metals does not alter the structure of pillared clays, in the microgram level.
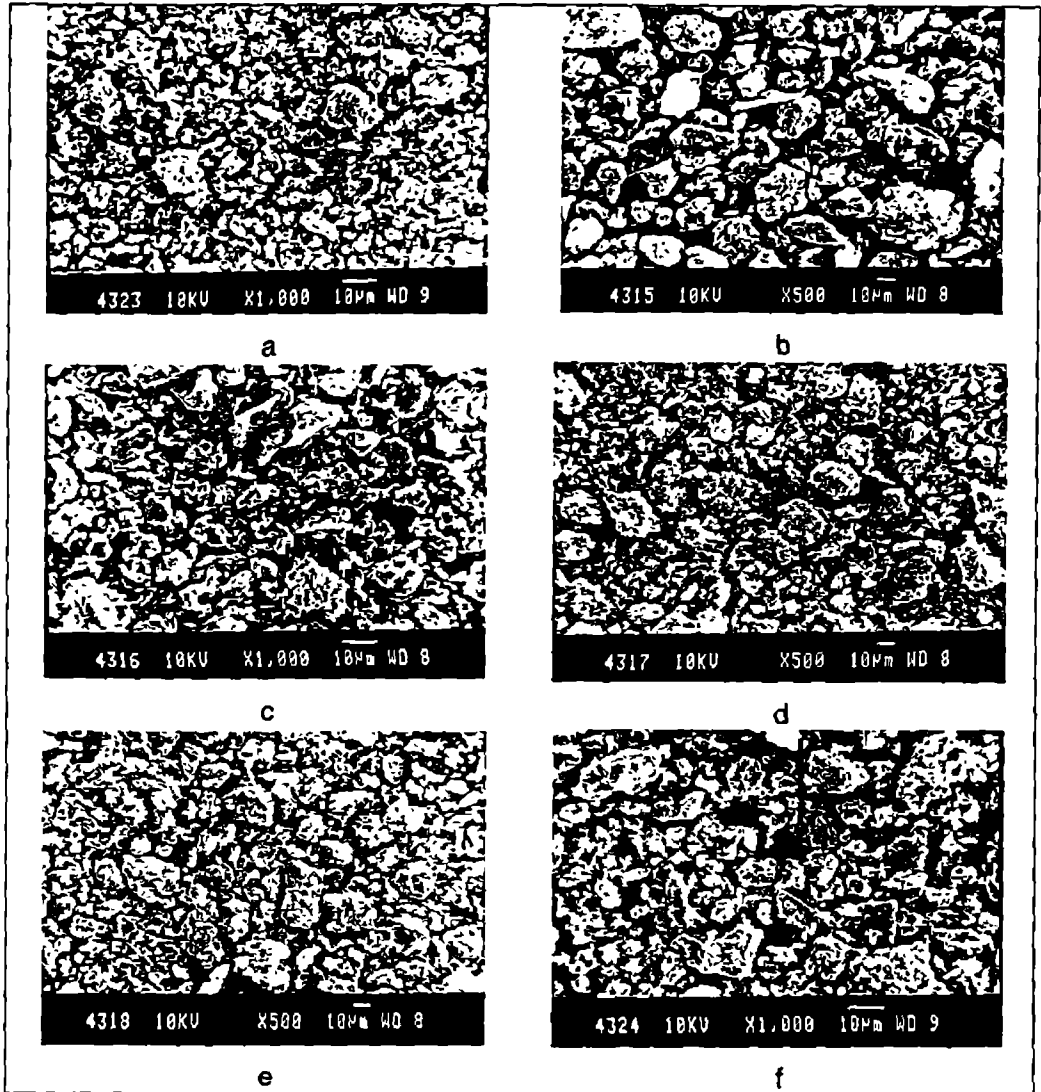
Figure 3.1.11. SEM images of the pillared clays

a) M          b) Al PM          c) Fe PM          d) FeAl PM          e) V/Fe PM          f) Co/Fe PM

The comparatively large particles observed in aluminium pillared system can be ascribed to the combination of large number of particles. Such combinations do

not occur to a substantial amount in iron containing systems. As can deduced from the SEM pictures, exchange with transition metals does not affect the external structure of pillared clays. Thus, SEM images also support the conclusion that exchanged metal oxides are incorporated inside the porous network.

## 3.2 ACIDITY OF PILLARED CLAYS

Acidity of pillared clays comes from at least three sources: the original clay, the pillaring cation and binding between clay and pillar[35]. The generally accepted view of acidity of pillared clays is that Lewis sites are mainly resident on metal oxide pillars whereas Brönsted acid sites are associated with structural OH groups present on the layers of the host clay[36]. Pillaring process releases $Na^+$ ions from blocked six member silicate rings, creating many accessible structural OH groups and possible Brönsted sites, which are accessible to probe molecules and which are removed upon heating[37]. The number of Brönsted acid sites decreases with increase in temperature and these sites are practically lost at temperatures above 500°C. Protons from different sources may be at the origin of acidity of pillared clays. The water molecules belonging to the hydration shell of charge balancing cations are submitted to a strong electrical polarising field and therefore have a degree of dissociation several orders of magnitude larger than liquid water. Water molecules hydrating the pillars are from that point of view a potential source of acidity whereas it is known that hydroxyl groups of clay octahedral layer do not contribute to acidity[38].

The acidity of the prepared systems have been characterised by three independent methods. The results and the conclusions that can be drawn from the observations are discussed in the following sections of the chapter.

## 3.2.1 TEMPERATURE PROGRAMMED DESORPTION OF AMMONIA

It is generally recognised that ammonia is an excellent probe molecule for testing acidic properties of solid catalysts as its strong basicity and small molecular

size allow detection of acidic sites located in very narrow pores also. Usually, IR spectroscopy[39], differential scanning calorimetry[40,41] and temperature programmed desorption techniques[3,42] are employed to achieve information on the interaction of ammonia with solid acids. Although, there is widespread use of TPD in the studies of surface acidity, $NH_3$-TPD spectra are often poorly resolved[43]. However, the procedure is a standardisation method since ammonia allows the determination of both protonic and cationic acidities by titrating acid strengths of any strength.

Ammonia adsorption on pillared clays can be physical ($\Delta H \approx 13$ Kcalmol$^{-1}$) or chemical ($\Delta H \approx 33$ Kcalmol$^{-1}$) type. Acid site distribution profiles show the presence of weak (ammonia desorbed between 35-200°C), medium (201-400°C) and strong (401-600°C) acid sites. The acid site distribution at various temperatures has been calculated as functions of mass of the sample as well as BET surface area. The former expression helps in quantifying acid sites per gram of clay while the latter helps in understanding the acidic structure of catalysts as a surface property.

### 3.2.1.1 Iron pillared systems

The acid site distribution of Fe PM and the transition metal analogues as functions of mass and surface area are given in tables 3.2.1.1 and 3.2.1.2

| Catalyst | Weak (35-200°C) | Medium (201-400°C) | Strong (401-600°C) | Cumulative (mmolg$^{-1}$) |
|---|---|---|---|---|
| V/Fe PM | 0.722 | 0.159 | 0.088 | 1.068 |
| Mn/Fe PM | 0.715 | 0.311 | 0.182 | 1.208 |
| Co/Fe PM | 0.420 | 0.191 | 0.057 | 0.688 |
| Ni/Fe PM | 0.997 | 0.350 | 0.258 | 1.505 |
| Cu/Fe PM | 0.696 | 0.287 | 0.153 | 1.136 |
| Zn/Fe PM | 0.592 | 0.112 | 0.080 | 0.784 |
| Fe PM | 0.48 | 0.354 | 0.084 | 0.918 |

Table 3.2.1.1 Acid site distribution/mass of iron pillared series

| Catalyst | Weak (35-200°C) | Medium (201-400°C) | Strong (401-600°C) | Cumulative ($\times10^{-3}$ mmolm$^{-2}$) |
|----------|-----------------|--------------------|--------------------|-------------------------------------------|
| V/Fe PM | 1.80 | 0.398 | 0.22 | 2.418 |
| Mn/Fe PM | 1.51 | 0.66 | 0.386 | 2.556 |
| Co/Fe PM | 0.77 | 0.350 | 0.473 | 1.593 |
| Ni/Fe PM | 2.49 | 0.876 | 0.645 | 4.011 |
| Cu/Fe PM | 2.07 | 0.856 | 0.457 | 3.383 |
| Zn/Fe PM | 1.56 | 0.296 | 0.211 | 2.067 |
| Fe PM | 1.23 | 0.91 | 0.216 | 2.356 |

Table 3.2.1.2 Acid site distribution/surface area of iron pillared series

The tables reveal that iron pillared montmorillonite shows considerable acidity. Weak and medium strength acid sites predominate the strong sites. Exchange with transition metals increases the amount of cumulative as well as strong acid sites. V, Mn, Ni and Cu doping of the pillared clay improves the acidity.

NH$_3$-TPD method lacks in discriminating the type of acid sites (Brönsted and Lewis). However it is generally accepted that evacuation of ammonia adsorbed at 400°C removes most of the Brönsted acid sites[44]. For pillared clays, it has been documented that ammonia adsorbs in Brönsted sites at temperatures around 250°C[3]. Again, it is implied that coordinatively bound ammonia on strong Lewis site can be desorbed only at high temperatures and hence acidity in strong region can be correlated to the amount of Lewis sites. In pillared clays, Lewis acidity is considered to originate from pillars where as Brönsted acidity arises from structural framework of aluminosilicates. Pore volume values indicate presence of exchanged cations inside the porous network. Hence, increase in number of strong sites can be attributed to contribution of these cations in pillars. This is substantiated by the fact that amount of medium acid sites (correlated to Brönsted acidity), arising from structural framework

decreases as a result of transition metal exchange. This may be due to shielding of these sites by the deposition of metals in the pores, near the structural framework.

Comparison of data in the two tables discloses that acidity is dependant on the surface area in microporous solids. This is most pronounced for Cu/Fe PM and Zn/Fe PM. These systems, due to the low surface area exhibit higher amounts of acid sites/surface area. This can be highly significant in surface catalysed reactions.

### 3.2.1.2 Aluminium pillared systems

The acidic structure of aluminium pillared catalysts as obtained from $NH_3$-TPD is presented in tables 3.2.1.3 and 3.2.1.4. Al PM exhibits high acidity compared to the iron pillared system. Exchange with transition metals does not improve the acidity and weak and medium acid sites predominate the strong sites. Thus a good distribution of weak and strong acid sites is present. Acidity in the medium strength region decreases as a result of incorporation of metals. Acidity expressed as a function of surface has values comparable to Al PM.

| Catalyst | Weak (35-200°C) | Medium (201-400°C) | Strong (401-600°C) | Cumulative (mmolg$^{-1}$) |
|---|---|---|---|---|
| V/Al PM | 0.521 | 0.133 | 0.223 | 0.894 |
| Mn/Al PM | 0.530 | 0.248 | 0.100 | 0.868 |
| Co/Al PM | 0.655 | 0.394 | 0.079 | 1.128 |
| Ni/Al PM | 0.669 | 0.334 | 0.192 | 1.195 |
| Cu/Al PM | 0.514 | 0.253 | 0.058 | 0.825 |
| Zn/Al PM | 0.53 | 0.427 | 0.169 | 1.126 |
| Al PM | 0.652 | 0.441 | 0.105 | 1.198 |

Table 3.2.1.3 Acid site distribution/mass of aluminium pillared series

| Catalyst | Weak (35-200°C) | Medium (201-400°C) | Strong (401-600°C) | Cumulative ($\times 10^{-3}$ mmolm$^{-2}$) |
|---|---|---|---|---|
| V/Al PM | 1.52 | 0.387 | 0.648 | 2.56 |
| Mn/Al PM | 1.66 | 0.778 | 0.314 | 2.75 |
| Co/Al PM | 1.44 | 0.869 | 0.174 | 2.48 |
| Ni/Al PM | 2.04 | 1.11 | 0.639 | 3.79 |
| Cu/Al PM | 1.30 | 0.638 | 0.146 | 2.08 |
| Zn/Al PM | 1.92 | 1.61 | 0.615 | 4.14 |
| Al PM | 1.68 | 1.13 | 0.272 | 3.08 |

Table 3.2.1.4 Acid site distribution/surface area of aluminium pillared series

It has been reported that acidity varies with intercalated hydroxycation. Aluminium pillars are found to be much more acidic than iron pillars[45]. The effect is pronounced in all types of acidity, especially the strong acidity. An effective distribution of acid sites of varying strength is present. Consequently, they can be used as suitable catalysts in acid catalysed reactions. Exchange of transition metals blocks the hydroxyl groups in the structural framework, reducing the Brönsted acidity. Decrease in surface area as a result of pore blocking increases the acidity of samples when expressed as a surface property.

### 3.2.1.3 Iron Aluminium pillared systems

The acid site distribution of the mixed pillared systems as functions of mass and surface area of samples used are given in tables 3.2.1.5 and 3.2.1.6. Fe Al PM desorbs considerable amount of ammonia in the weak and medium regions and nominal acidity in strong acid region. Transition metal exchange increases the acidity in all regions especially acidity in strong acid region. V/FeAl PM and Co/FeAl PM exhibits maximum acidity in the series owing to increased concentration of weak acid sites. Ni/FeAl PM displays exceptionally high acidity in the strong acid region.

| Catalyst | Weak (35-200°C) | Medium (201-400°C) | Strong (401-600°C) | Cumulative (mmolg$^{-1}$) |
|---|---|---|---|---|
| V/FeAl PM | 0.844 | 0.382 | 0.202 | 1.428 |
| Mn/FeAl PM | 0.637 | 0.246 | 0.191 | 1.074 |
| Co/FeAl PM | 1.401 | 0.440 | 0.147 | 1.988 |
| Ni/FeAl PM | 0.524 | 0.224 | 0.299 | 1.047 |
| Cu/FeAl PM | 0.413 | 0.159 | 0.050 | 0.627 |
| Zn/FeAl PM | 0.449 | 0.163 | 0.112 | 0.724 |
| FeAl PM | 0.473 | 0.161 | 0.048 | 0.682 |

Table 3.2.1.5 Acid site distribution/mass of iron aluminium pillared series

| Catalyst | Weak (35-200°C) | Medium (201-400°C) | Strong (401-600°C) | Cumulative (x10$^{-3}$ mmolm$^{-2}$) |
|---|---|---|---|---|
| V/FeAl PM | 1.65 | 0.75 | 0.396 | 2.796 |
| Mn/FeAl PM | 1.40 | 0.542 | 0.42 | 2.362 |
| Co/FeAl PM | 1.99 | 0.568 | 0.21 | 2.768 |
| Ni/FeAl PM | 1.24 | 0.528 | 0.705 | 2.473 |
| Cu/FeAl PM | 1.07 | 0.412 | 0.13 | 1.612 |
| Zn/FeAl PM | 0.94 | 0.340 | 0.234 | 1.514 |
| FeAl PM | 1.08 | 0.366 | 0.109 | 1.555 |

Table 3.2.1.6 Acid site distribution/surface area of iron aluminum pillared series

The increase in acidity, especially in the strong acidity region as a result of transition metal deposition is due to the increase in acidity of pillars. It has been evidenced from NMR spectroscopy that the doped metals are present near the pillars and not in structural framework. The efficient distribution of acid sites in the three regions suggests potential application of these materials in acid catalysed reactions.

## 3.2.2 PERYLENE ADSORPTION MEASUREMENTS

Adsorption studies of electron acceptors like perylene, pyrene and chrysene give information regarding the presence of Lewis acid sites in presence of Brönsted sites. Perylene, being an electron donor, transfer one electron to Lewis acid sites and get adsorbed as perylene radical cation[46]. The limiting value of perylene that is adsorbed on catalyst surface is a measure of Lewis acidity of the sample. A clear picture of adsorption and limiting value can be obtained by plotting the amount of perylene adsorbed against equillibrium concentration. These graphs convince Langmuir type of adsorption over solid surfaces[47]. Perylene was adsorbed on the catalyst and unadsorbed perylene in the solution was estimated by UV visible spectrophotometry. The limiting amounts of perylene adsorbed for the three series of catalysts are given in the subsequent sections.

An important point while comparing the acidity data obtained from perylene adsorption and $NH_3$-TPD is the large difference in magnitude of acidity values. Ammonia being smaller and stronger base, can detect almost all types and strengths of acid sites where as perylene being large along with its sole ability for binding with electron acceptor centres has access only to exposed Lewis acid sites. Though perylene measures only Lewis acidity, the large difference in the values cannot be attributed to Brönsted acidity alone. The low values for perylene adsorption is also due to shape selective nature of the porous network hindering the access of bulky one electron donor into the Lewis acid sites present inside the pillars.

### 3.2.2.1 Iron pillared systems

The results of perylene adsorption studies for iron pillared systems are presented in table 3.2.2.1. Montmorillonite does not adsorb perylene. Substantial amount of perylene gets adsorbed on Fe PM. Introduction of transition metals, even in small amounts, increases significantly the limiting value of the one electron donor

adsorbed on catalyst surface. However, exchange with zinc reduces the one electron adsorption capacity of Fe PM.

| Catalyst | Perylene adsorbed ($\times 10^{-6}$ molg$^{-1}$) |
|----------|--------------------------------------------------|
| V/Fe PM  | 8.3 |
| Mn/Fe PM | 9.3 |
| Co/Fe PM | 8.8 |
| Ni/Fe PM | 9.5 |
| Cu/Fe PM | 9.2 |
| Zn/Fe PM | 4.1 |
| Fe PM    | 5.1 |
| M        | -   |

Table 3.2.2.1 Perylene adsorption data for iron pillared systems

It has been reported that the Lewis acid sites in pillared clays originate from the pillars. The nonadsorption of perylene in pure montmorillonite supports this fact. Introduction of iron oxide pillars brings in Lewis acidity into the system and hence the substantial adsorption of perylene molecules. Exchange with transition metals increases the Lewis acidity of the material. It was observed from NH$_3$ -TPD measurements that ammonia adsorption in the strong acid region of the pillared clay, benefited from transition metal exchange.

### 3.2.2.2 Aluminium pillared systems

Table 3.2.2.2 demonstrates the amount of perylene adsorbed over aluminium pillared catalysts. Al PM shows much reduced Lewis acidity compared to Fe PM. Introduction of transition metals of first series into the porous network does not improve the acidity much, Mn/Al PM and Co/Al PM being exceptions.

| Catalyst | Perylene adsorbed $(\times10^{-6}\ molg^{-1})$ |
|----------|-----------------------------------------------|
| V/Al PM  | 0.43 |
| Mn/Al PM | 3.6  |
| Co/Al PM | 2.83 |
| Ni/Al PM | 0.97 |
| Cu/Al PM | 0.60 |
| Zn/Al PM | 0.62 |
| Al PM    | 0.46 |

Table 3.2.2.2 Perylene adsorption data for aluminium pillared systems

The decreased adsorption of perylene molecules into the Lewis acid sites of Al PM can be ascribed to incompetent pillaring in this material rather than the decreased amount of Lewis acid sites. From XRD and surface area measurements, it is evident that intercalation of aluminium polymers into interlayer space of montmorillonite is not successful. Hence, perylene molecules may be experiencing steric hindrance for the accessibility of Lewis acid sites situated inside the pores, leading to lowered perylene adsorption. Exceptionally high Lewis acidity for Mn/Al PM and Co/Al PM may be due to the formation of some complex structures in some local areas of the surface, which results in an overall electronegativity of the surface complex. Such structures have been evidenced in metal oxide catalysts[48].

### 3.2.2.3 Iron Aluminium pillared systems

The amount of perylene adsorbed on the mixed pillared system and its transition metal exchanged analogues are presented in table 3.2.2.3. FeAl PM adsorbs significant amounts of perylene. Exchange with transition metals increases the one electron adsorption capacity of the pillared clay. However, vanadium and nickel incorporation into the porous network decreases the Lewis acidity.

| Catalyst | Perylene adsorbed ($\times 10^{-6}$ molg$^{-1}$) |
|----------|:---:|
| V/FeAl PM | 3.92 |
| Mn/FeAl PM | 6.40 |
| Co/FeAl PM | 6.08 |
| Ni/FeAl PM | 3.71 |
| Cu/FeAl PM | 5.47 |
| Zn/FeAl PM | 5.28 |
| FeAl PM | 5.10 |

Table 3.2.2.3 Perylene adsorption data for iron aluminium pillared systems

The substantial adsorption of perylene on FeAl PM indicates the high Lewis acidity of catalyst. The high accessibility of the bulky electron donor is an added evidence for the successful pillaring mechanism in this solid.

## 3.2.3 CUMENE CRACKING

The best method for characterising industrial acid catalysts is through model reactions. The exact nature, strength and density of the sites can be determined. The drawback of this method is that only the active sites for the particular reaction can be characterised. Thus, for a Brönsted acid catalysed reaction, density of Brönsted acid sites alone can be estimated. Cumene is a conventional model compound for testing the catalytic activity since it undergoes diverse reactions over different types of acid sites[49-51]. Major reactions taking place during cracking of cumene are dealkylation or cracking to benzene and propene and dehydrogenation to *a*-methyl styrene. Small amounts of ethylbenzene and toluene can be formed by cracking of side chain, which on dehydrogenation gives styrene. Cracking of cumene is generally attributed to Brönsted acid sites by a carbonium ion mechanism (Scheme 1). *a*-methyl styrene is formed on Lewis acid sites[52-55]. Mechanism of the reaction is given in scheme 3.2.3.
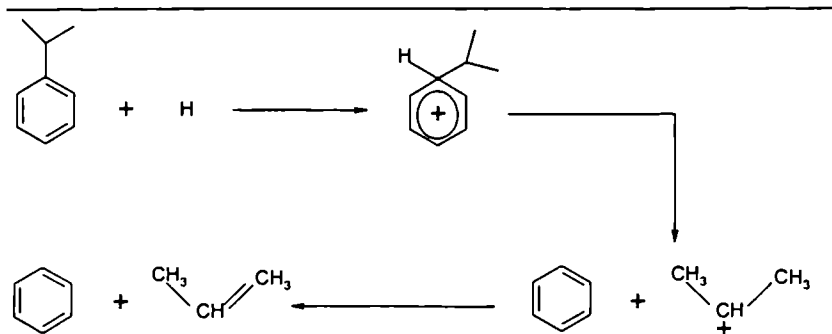
Scheme 1
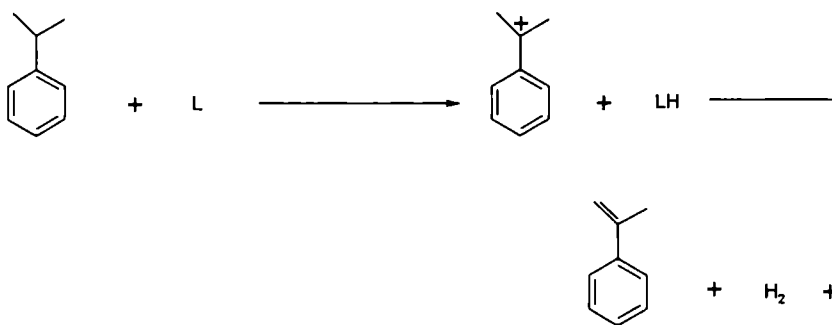


Scheme 2

Scheme 3.2.3. Mechanism of cumene cracking reaction

The cumene cracking reaction was performed over the prepared ca el reaction for characterising the acid sites present in the catalysts. Tl examination are presented in two sections; I) Catalytic activity c ıs and II) Effect of reaction variables.

## I CATALYTIC ACTIVITY OF VARIOUS SYSTEMS

The catalytic performance of the various pillared clays for the rea ect of transition metal exchange on pillared clays are given in table 3.:

| Catalyst | Conversion (%) | Selectivity (%) | | Lewis/ Brönsted |
| --- | --- | --- | --- | --- |
| | | α-methyl styrene | Dealkylation products | |
| V/Fe PM | 29.8 | 53.2 | 46.8 | 1.15 |
| Mn/Fe PM | 30.2 | 58.9 | 41.1 | 1.43 |
| Co/Fe PM | 21.8 | 59.7 | 40.3 | 1.48 |
| Ni/Fe PM | 31.7 | 64.7 | 35.3 | 1.83 |
| Cu/Fe PM | 28.9 | 60.0 | 40.0 | 1.5 |
| Zn/Fe PM | 24.5 | 48.2 | 51.8 | 0.94 |
| Fe PM | 25.6 | 58.3 | 42.7 | 1.37 |
| V/Al PM | 28.8 | 58.8 | 41.2 | 1.42 |
| Mn/Al PM | 26.0 | 55.4 | 44.6 | 1.24 |
| Co/Al PM | 31.4 | 50.8 | 41.7 | 1.22 |
| Ni/Al PM | 33.6 | 56.8 | 43.2 | 1.22 |
| Cu/Al PM | 19.2 | 44.9 | 55.1 | 0.81 |
| Zn/Al PM | 26.5 | 59.1 | 41.1 | 1.44 |
| Al PM | 28.5 | 58.6 | 41.4 | 1.42 |
| V/FeAl PM | 22.8 | 54.3 | 45.7 | 1.19 |
| Mn/FeAl PM | 22.5 | 53.2 | 46.8 | 1.14 |
| Co/FeAl PM | 32.5 | 54.2 | 45.8 | 1.18 |
| Ni/FeAl PM | 28.9 | 60.7 | 39.3 | 1.54 |
| Cu/FeAl PM | 19.5 | 50.2 | 49.8 | 1.0 |
| Zn/FeAl PM | 21.1 | 53.3 | 46.7 | 1.14 |
| FeAl PM | 20.7 | 62.7 | 36.3 | 1.73 |

Table 3.2.3.1 Catalytic activity of various systems towards cumene cracking

Temperature- 400°C, WHSV – 7 h$^{-1}$, time on stream- 2h

From table 3.2.3.1, it can be inferred that all pillared clays show considerable activity towards cumene cracking under the specified conditions. Appreciable selectivity towards the dehydrogenated product is obtained for all catalysts. Ethylbenzene and styrene appeared in minor quantities and in some cases toluene also was detected. All the dealkylated products are bannered together and Lewis to Brönsted ratio gives the ratio between the dehydrogenated and cracked products.

Iron pillared clay shows very good activity towards the reaction with high selectivity towards *a*-methyl styrene. Lewis/Brönsted acid ratio is 1.37 for Fe PM. Exchange with transition metals increases the activity except for Co/Fe PM and Zn/Fe PM. It has been well documented that the catalytic activity cumene cracking reaction can be correlated to the total acidity of the catalyst. Also, dehydrogenation to *a*-methyl styrene occurs over Lewis acid sites and cracking over Brönsted acid sites[56,57]. The decrease in activity for cobalt and zinc exchanged systems can be traced to the decrease in *a*-methyl styrene selectivity. Hence, decrease in the number of acid sites is mainly due to decrease in the number of Lewis acid sites.

Aluminium pillared clay exhibits high activity towards the reaction with Lewis/Brönsted acid ratio of 1.42. Exchange with transition metals results in reduction in acidity except for nickel and cobalt exchanged systems as indicated by conversion of cumene. A critical scrutiny of the table indicates that the decline in acid sites is mainly due to decrease in the number of Lewis acid sites.

FeAl PM shows conversion of 20.7% with a selectivity of 62.7% for *a*-methyl styrene. The high selectivity for the dehydrogenated product can be attributed to the effective pillaring. Transition metal exchange decreases the dehydrogenation activity with a concomitant decrease in catalytic activity. Exchange with transition metals brings about deposition of metal oxides inside the pores and this can be the reason for decrease in Lewis acidity.

An attempt was made to correlate observed dehydrogenation activities with limiting amount of perylene adsorbed on catalyst surface (Figures 3.2.3.1- 3.2.3.3).
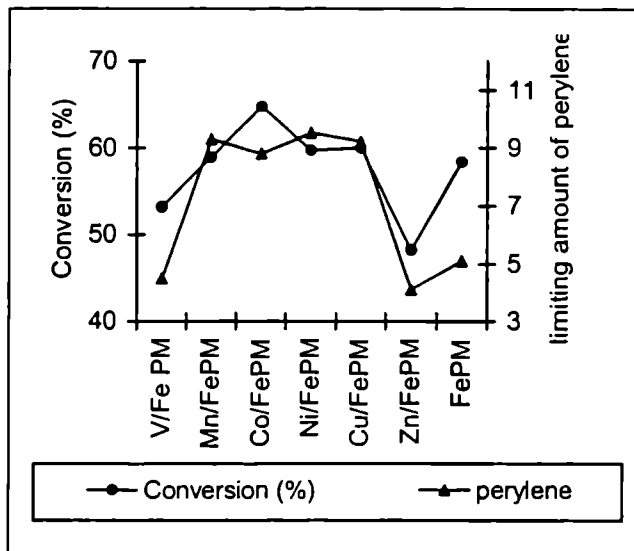


Figure 3.2.3.1 Correlation of $a$-methyl styrene with limiting value of perylene
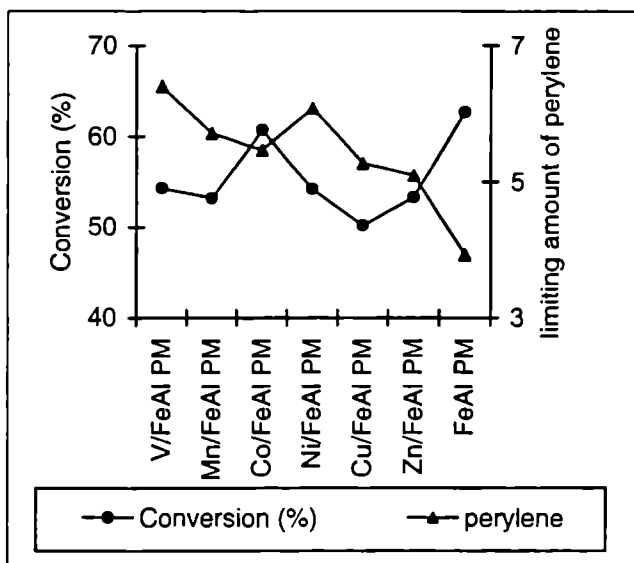


Figure 3.2.3.2 Correlation of $a$-methyl styrene with limiting value of perylene
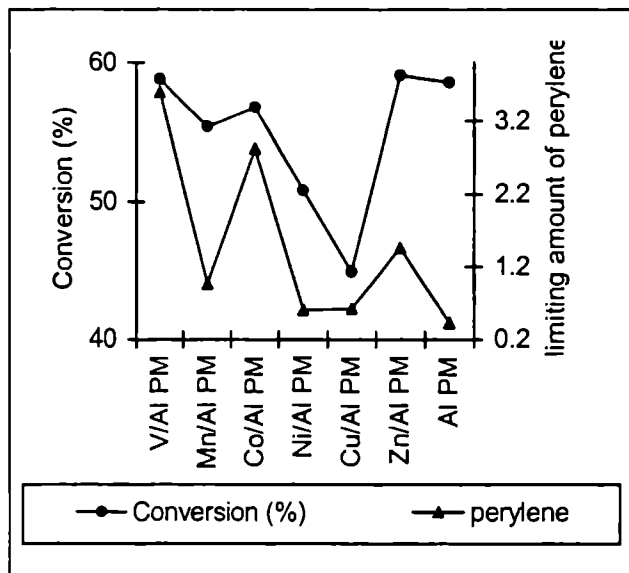
Figure 3.2.3.1 Correlation of $a$-methyl styrene with limiting value of perylene

Parallel relationship between the two parameters are obtained for iron and mixed iron aluminium pillared systems. However, discrepancies arise with aluminium pillared catalysts. This may be due to low surface area of these materials, restricting the passage of bulky perylene molecules to the Lewis acid sites (refer 3.2.2.2).

## 3.2.3.2 EFFECT OF REACTION VARIABLES

The influence of reaction variables on catalytic activity of the prepared systems was checked using Cu/Fe PM as reference catalyst. The results of the investigation are discussed in the proceeding sections.

Table 3.2.3.2 demonstrates the effect of temperature on cumene cracking reaction. Catalytic activity increases with temperature. The activity of the catalyst at a particular temperature can be related to the total acidity of the system at that temperature. Hence, increase in temperature denotes the high amount of acid sites in the system. Dealkylated product selectivity increases with a concomitant decrease

in α-methyl styrene selectivity. Thus, the Lewis/Brönsted acid ratio decreases and at 450°C, the number of Brönsted sites exceeds that of Lewis sites.

| Temperature (°C) | Conversion (%) | Selectivity (%) | | Lewis/ Brönsted |
|---|---|---|---|---|
| | | α-methyl styrene | Dealkylation products | |
| 300 | 18.5 | 60.2 | 39.8 | 1.5 |
| 350 | 21.8 | 59.7 | 40.3 | 1.48 |
| 400 | 28.9 | 50.4 | 49.6 | 1.02 |
| 450 | 35.6 | 44.2 | 55.8 | 0.80 |

Table 3.2.3.2 Effect of temperature

Catalyst- 0.5g, WHSV – 7 $h^{-1}$, time on stream- 2h

| WHSV ($h^{-1}$) | Conversion (%) | Selectivity (%) | | Lewis/ Brönsted |
|---|---|---|---|---|
| | | α-methyl styrene | Dealkylation Products | |
| 5.2 | 24.4 | 61.2 | 38.8 | 1.58 |
| 7.0 | 21.8 | 59.7 | 40.3 | 1.48 |
| 8.6 | 19.8 | 57.8 | 42.2 | 1.37 |
| 10.4 | 17.4 | 55.1 | 45.9 | 1.2 |

Figure 3.2.3.3. Effect of weight hourly space velocity

Catalyst- 0.5g, temperature- 400°C, time on stream- 2h

The influence of weight hourly space velocity on catalytic activity as well as selectivity pattern is illustrated in table 3.2.3.3. Increase in space velocity results in decreased reaction rate. Lower the weight hourly space velocity, higher the contact time that the reactant molecules get for interaction with catalyst active sites. Dealkylation product selectivity increases with decrease in contact time. The decrease in α-methyl styrene selectivity can be attributed to steric effect rather than

acidity. *a*-methyl styrene, due to its bulky nature may be experiencing difficulty in desorption from catalyst active site at larger space velocities.

Deactivation of catalyst active sites is a major problem encountered in heterogeneous catalysis. Hence, the effect of time on stream for the reaction was studied up to 5 hours. The results are tabulated in table 3.2.3.4. The catalyst shows considerable stability towards the reaction. There is a slight decrease in *a*-methyl styrene selectivity that can be due to poisoning of active sites by product molecules.

| Time on stream | Conversion (%) | Selectivity (%) | | Lewis/ Brönsted |
|---|---|---|---|---|
| | | *a*-methyl styrene | Dealkylation products | |
| 1 | 22.1 | 60.1 | 38.9 | 1.51 |
| 2 | 21.8 | 59.7 | 40.3 | 1.48 |
| 3 | 21.4 | 58.9 | 41.1 | 1.43 |
| 4 | 20.8 | 57.4 | 42.6 | 1.35 |
| 5 | 20.5 | 55.9 | 44.1 | 1.26 |

Table 3.2.3.4 Deactivation studies

Catalyst- 0.5g, temperature- 400°C, WHSV – 7 h$^{-1}$

## 3.2.4 CYCLOHEXANOL DECOMPOSITION

The multifunctional character of a catalyst system is manifested through the wide diversity of products obtained with a given reactant. The selectivity of the products exhibited by a catalyst can be related to its surface acid base and redox properties[58-61]. Alcohols, being amphoteric in nature can interact with both acidic and basic sites on the catalyst surface[62]. Cyclohexanol undergoes dehydration over acidic sites giving cyclohexene as the major product whereas a combination of acidic and basic sites is required for dehydrogenation yielding cyclohexanone. Cyclohexene on disproportionation yields benzene, cyclohexane and methylcyclopentane[72]. Thus,

product selectivity gives a quantitative estimate of surface acid base properties[63,64]. Moreover, cyclohexanone is the key intermediate for the manufacture of Nylon 6, Nylon 6,6 for synthetic fibre and tyre cord[65]. Present industrial practice of cyclohexanone production involves catalytic dehydrogenation of cyclohexanol over commercial grade copper oxide supported on zinc oxide (Girdler-G-66B)[66].
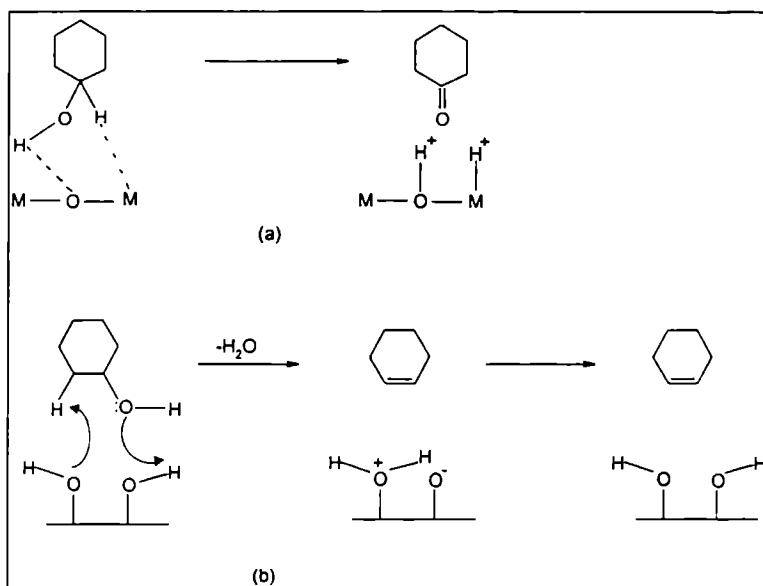


Scheme 3.2.4.1. Mechanism of a) dehydrogenation and
b) dehydration of cyclohexanol on catalyst surface

The exact mechanism of gas phase dehydration of cyclohexanol has been proved difficult to study. Two possible mechanistic schemes have been proposed[67,68]. One of these is similar to E2 elimination in which the catalyst provides both an acidic site to attack the hydroxyl group and a basic site to abstract a proton. The other is similar to E1 elimination in which the reaction proceeds through initial formation of a carbocation. Adsorption on acidic site is the rate determining step[69]. Dehydrogenation catalysed by the acid base sites takes place through a concerted

mechanism in which the metal cation acts as Lewis acid site accepting a hydride ion whereas the oxygen anion acts as Brönsted base accepting the proton of the alcohol group[70,71]. The mechanism for the reaction is given in scheme 3.2.4.1.

The dehydration-dehydrogenation activity of cyclohexanol was tested in the vapour phase at optimised conditions. It is assumed that dehydrogenation and dehydration processes represent a set of parallel reactions obeying first order kinetics. The formation of phenol has been reported by the further transformation of cyclohexanone[73] though this was not observed in the present study. Selectivity to the product is expressed as –one selectivity (cyclohexanone) and –ene selectivity (cyclohexene).

## 3.2.4.1 CATALYTIC ACTIVITY OF VARIOUS SYSTEMS

The catalytic performance of the various systems for the decomposition of cyclohexanol is presented in table 3.2.4. Table shows that pillared clay systems show exceptional activity towards cyclohexanol decomposition. Predominant dehydration of cyclohexanol to cyclohexene occurs over the catalysts. At first sight, this fact points towards the predominantly acidic nature of catalysts and the non existence of sufficient basic sites. Exchange with transition metals causes a noticeable enhancement in decomposition activities of all pillared systems, this influence being higher for iron containing systems and less for aluminium pillared ones. On the average, dehydrogenation activities and -ene/-one selectivities are higher for iron containing systems whereas dehydrogenation activities of aluminium pillared systems except Co/Al PM are monotonously much lower.

| Catalyst | Conversion (%) | Selectivity (%) | | | Benzene selectivity (%) |
|---|---|---|---|---|---|
| | | Cyclohexene | Cyclohexanone | Others | |
| V/Fe PM | 99.0 | 82.9 | 8.9 | 8.2 | 46.8 |
| Mn/Fe PM | 91.6 | 85.6 | 9.5 | 4.9 | 41.1 |
| Co/Fe PM | 89.5 | 87.4 | 5.2 | 7.4 | 40.3 |
| Ni/Fe PM | 97.5 | 80.6 | 12.9 | 8.5 | 35.3 |
| Cu/Fe PM | 97.1 | 90.7 | 6.5 | 2.8 | 40.0 |
| Zn/Fe PM | 99.8 | 81.9 | 8.2 | 9.9 | 51.8 |
| Fe PM | 60.3 | 84.0 | 8.2 | 11.8 | 42.7 |
| V/Al PM | 93.6 | 95.1 | 2.0 | 2.9 | 41.2 |
| Mn/Al PM | 95.1 | 96.2 | 2.8 | 1.0 | 44.6 |
| Co/Al PM | 94.6 | 82.6 | 9.4 | 8.0 | 41.7 |
| Ni/Al PM | 94.4 | 87.1 | 2.2 | 10.7 | 43.2 |
| Cu/Al PM | 92.3 | 95.3 | 2.7 | 2.0 | 55.1 |
| Zn/Al PM | 97.2 | 84.2 | 6.3 | 9.5 | 41.1 |
| Al PM | 58.3 | 87.4 | 1.8 | 10.8 | 41.4 |
| V/FeAl PM | 93.5 | 82.0 | 7.0 | 11.0 | 45.7 |
| Mn/FeAl PM | 95.5 | 82.3 | 7.9 | 7.8 | 46.8 |
| Co/FeAl PM | 98.1 | 84.9 | 7.2 | 7.9 | 45.8 |
| Ni/FeAl PM | 96.7 | 91.5 | 2.1 | 6.4 | 39.3 |
| Cu/FeAl PM | 95.3 | 83.1 | 7.1 | 9.8 | 49.8 |
| Zn/FeAl PM | 97.7 | 81.2 | 8.7 | 11.1 | 46.7 |
| FeAl PM | 59.2 | 87.5 | 5.2 | 12.0 | 36.3 |

Table 3.2.4. Activity of various systems towards cyclohexanol decomposition
Catalyst- 0.5g, WHSV- 9.9 $h^{-1}$, temperature-250°C, TOS-2h

The dehydration activities of various systems run almost parallel with the amount of Brönsted acid sites as obtained from cumene cracking test reaction. The

-ene selectivity for the reaction has been suggested as an index for the amount of Brönsted acidity[74,75]. Similar trends were obtained in the present case also but to a magnified extent. The dehydration activity is much higher than expected from benzene selectivity values and hence cannot be explained in terms of the amount of Brönsted sites alone. For clays, it has been postulated that a Brönsted acid site upon dehydroxylation yields a Lewis acid site. It has also been concluded that a Lewis acid site can be converted to a Brönsted site in presence of a water molecule[76]. Hence the effect of water formed by the dehydration of cyclohexanol has to be taken into account. Conversion of Lewis acid sites to Brönsted ones can occur on clays, with the absorption of water produced on dehydration. This can result in enhanced amounts of Brönsted acid sites, further increasing the dehydration activity of cyclohexanol. On the other hand, dehydrogenation to cyclohexanone takes place through a concerted mechanism of Lewis acid sites and Brönsted basic sites. Increase in the Brönsted acid sites at the expense of Lewis acid sites, decreases the dehydrogenation activity of the systems. The reduced -ene selectivity for the reaction can thus be attributed not only to a lower amount of basic sites but also to a decreased amount of Lewis acid sites as a result of hydroxylation.

### 3.2.4.2 EFFECT OF REACTION VARIABLES

The effect of various reaction variables on the reaction was checked using V/Al PM as the reference catalyst. Figure 3.2.4.2 shows the influence of temperature on the decomposition of cyclohexanol. The percentage conversion increases with increase in temperature. Almost complete conversion of cyclohexanol occurs at 250°C and above. This shows that the reaction has low activation energy. The dehydrogenation activity also increases with rise in temperature. Increase in cyclohexanone selectivity with temperature can be attributed to the increase in the amount of Lewis acid sites as a result of dehydroxylation of Brönsted acid sites occurring at higher temperatures. As expected, this has a diminutive effect on the

amount of Brönsted acid sites and hence the decrease in cyclohexene selectivity at higher temperatures.
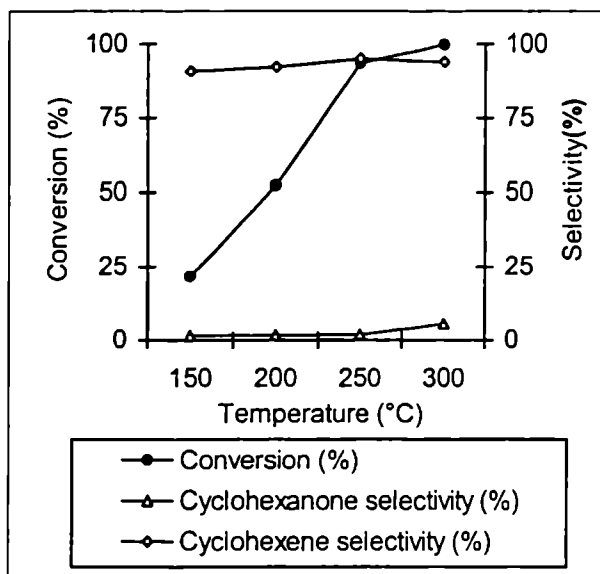


Figure 3.2.4.2 Effect of temperature

Catalyst- 0.5g, WHSV- 9.9 h$^{-1}$, TOS-2h

Figure 3.2.4.3 presents the decomposition activity and product selectivity of the catalyst as a function of feed rate of cyclohexanol. Increase in feed rate first increases the percentage conversion and after the optimum space velocity of 9.9 h$^{-1}$, the activity decreases. The lower yields at smaller feed rates can be attributed to the adsorbed product species at the catalyst surface blocking the active sites for further reaction. At higher feed rates the speedy desorption of the products can occur. At still higher space velocities, the reactant may not be getting sufficient contact time for reaction with the catalyst active site and hence the decrease in decomposition activity. Cyclohexanone selectivity remains the same throughout.
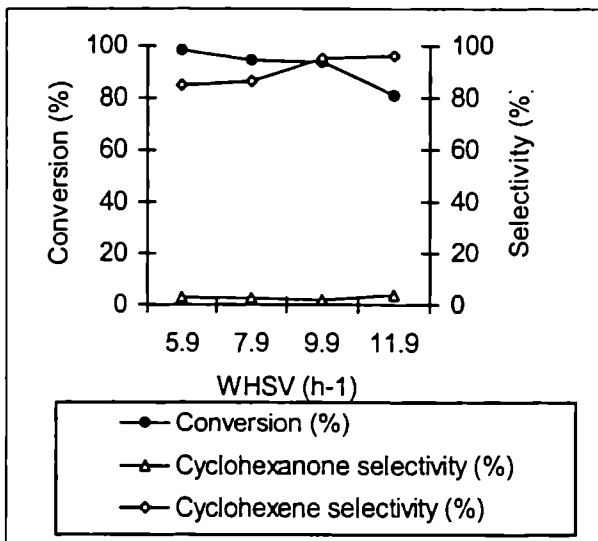
Figure 3.2.4.3 Effect of weight hourly space velocity

Catalyst- 0.5g, temperature- 250°C, TOS- 2h
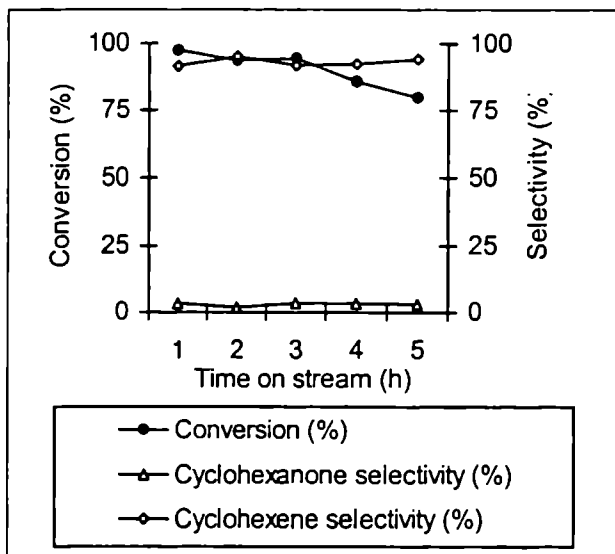


Figure 3.2.4.4 Effect of time on stream

Catalyst- 0.5g, WHSV- 9.9 $h^{-1}$, temperature-250°C

Deactivation of catalyst surface is a common problem encountered in heterogeneous catalysis. In the cyclohexanol decomposition reaction using pillared clays, this effect is pronounced. The –one selectivity also decreases with time on stream. This can be attributed to the pore blocking by the cyclohexanone molecule. Coke deposition can also be a reason for the decreased activity.

## 3.3 CONCLUSIONS

The various points that can be summarised from the examination of the structural characteristics of the prepared systems are,

❖ Residual CEC measurements indicate that 35-60% of the original CEC of the parent montmorillonite is retained after pillaring.

❖ Chemical composition of prepared systems as determined by EDX analysis reveals that an increase in the amount of pillared metal occurs at the expense of exchangeable cations. Si/Al ratio changes can be attributed to increase in the amount of aluminium rather than to structural instability of the clay on pillaring. 1-3% of the transition metals were incorporated on exchange.

❖ Surface area and pore volume measurements increases substantially upon pillaring. 60-70% of the total surface area can be attributed to micropores. Transition metal exchange decreases the surface area, especially the external surface area.

❖ Presence of X-ray diffraction peaks shows that long range face to face layer aggregation is present in pillared sample. Shifting of $2\theta$ values clearly suggest expansion of clay layer during pillaring process. The major intercalated species giving rise to stable basal spacing in aluminium pillared clay is the $Al_{13}$ polyhydroxy polymer or Keggin cation. Presence of Fe substituted $Al_{13}$ like polymers are detected in the mixed pillared system. Insertion of the

second metal after the formation of stable pillars does not destabilise the porous network.

❖ IR spectra of the various samples could be assigned properly. The vibrations on the framework region does not change on pillaring, indicating the structural integrity of the clay layers.

❖ $^{27}$Al NMR reveals unambiguously that the pillared species is the Keggin $Al_{13}$ polymer for Al pillared systems. For iron pillared systems, the peaks are broader due to the relaxation effects of the paramagnetic centres. The structure of iron aluminium mixed pillared systems is similar to Al polymeric species and not hydroxy iron oligomers. Incorporation of the transition metals does not affect the structural stability of the layers and pillars.

❖ $^{29}$Si NMR spectra reveals that majority of the silicon tetrahedra is linked to 3 Si atoms and one Al atom. A very small portion is linked to 2 Al atoms and 2 Si atoms while a part of the Si tetrahedra is linked to Si atoms alone. This distribution of silicon tetrahedra into various environments is not affected by pillaring. The shift in ppm, which indicates the strain in the local environment of the Si atoms, is proportional to the size of the intercalated species. As anticipated, pillaring which is only a cation exchange process does not affect the short range order within the clay layers. Incorporation of transition metals on the pillared systems does not alter the local environment of the Si atoms.

❖ The pillared clays possess substantial thermal stability. Dehydration and dehydroxylation of the clay layers occurs. The thermal stability of the pillared clays is in the order Al PM > FeAl PM > Fe PM.

❖ UV- DRS supports the presence of the Keggin cation in aluminium and mixed pillared systems. The spectrum for the iron pillared and mixed pillared systems shows a band that could be assigned to the polyoxoiron complexes.

❖ SEM images support the conclusion that the exchanged metal oxides are incorporated inside the porous network.

❖ TPD profiles show the presence of weak (ammonia desorbed between 35-200°C), medium (201-400°C) and strong (401-600°C) acid sites. All systems show considerable acidity. Weak and medium strength acid sites predominate the strong sites. Exchange with transition metals increases the amount of cumulative as well as strong acid sites. The increase in acidity, especially in the strong acidity region as a result of transition metal deposition is due to the increase in acidity of the pillars.

❖ Al PM shows much reduced Lewis acidity, when compared to Fe PM and FeAl PM. The decreased adsorption of perylene molecules into the Lewis acid sites of Al PM can be ascribed to the ineffectual pillaring in this material rather than the decreased amount of Lewis acid sites.

❖ Cumene cracking test reaction could differentiate between Lewis and Brönsted acid sites. Dehydrogenation activities could be well correlated with Lewis acidity as obtained from perylene adsorption studies.

❖ Cyclohexanol decomposition reaction indicated the presence of basic sites on pillared clays. Exchange with transition metals causes a noticeable enhancement in decomposition activities. On the average, dehydrogenation activities and -ene/-one selectivities are higher for iron containing systems whereas the dehydrogenation activities of aluminium pillared systems are monotonously much lower.

# REFERENCES

1.  A Gil, M.A Vicente, L.M Gandia, *Microporous. Mesoporous Mater.*, 34, 115-125 (2000).

2.  S Moreno, R SunKou, G Poncelot, *J. Phy. Chem. B.*, 101, 1569 (1997).

3.  S Moreno, R SunKou, R Molina, G Poncelot, *J. Catal.*, 182, 174-185 (1999).

4.  J.P Olivier, M.L Occelli, *J. Phy. Chem. B.*, 105, (2001)

5.  M.L Occelli, J.A Bertrand, S.A.C Gould, J.M Dominguez, *Microporous. Mesoporous Mater.*, 34, 195-206 (2000).

6.  D.W Rutherford, C.T Chiou, D.D Eberl, *Clays. Clay Miner.*, 45, 534-543 (1997).

7.  M.J Remy, G Poncelit, *J. Phy. Chem.*, 99, 773-779 (1995).

8.  S Narayanan, K Deshpande, *Appl. Catal. A: Gen.*, 193, 17-27 (2000).

9.  H.P Zhu, E.F Vansant, *J. Porous Mater.*, 2, 107 (1995).

10. K Bahranowski, A Kielski, E.M Serwicka, E.W Walsh, K Wodnicka, *Microporous Mesoporous Mater.*, 41, 201-215 (2000).

11. T Bakas, A Moukarika, V Papaefthymiou, A Ladavos, *Clays Clay Miner.*, 42, 634-642 (1994).

12. W.I Rausch, H.D Bale, *J. Chem. Phy.*, 40, 3391-3397 (1964).

13. A.K Helmy, E.A Ferreiro, S.G deBussetti, *Clays Clay Miner.*, 42, 444-450 (1994).

14. P.J Murphy, A.M Posner, J.P Quirk, *Aust. J. Soil Res.*, 13, 189 (1975).

15. P.J Murphy, A.M Posner, J.P Quirk, *J. Coll. Inter. Sci.*, 52, 229 (1975).

16. F Bergaua, N Hassoun, J Barraoult, L Gatineau, *Clay Miner.*, 28, 109 (1993).

17. J Barraoult, L Gatineau, N Hassoun, F Bergaua, *Energy Fuels*, 6, 760 (1992).

18. J Madejova, *Vibrational Spectroscopy*, 31, 1-10 (2003).

19. S Bodoardo, R Chiappetta, B Onida, F Figueras, E Garrone, *Microporous. Mesoporous Mater.*, 20, 187-196, (1998).

20. D Tichit, F Fajula, F Figueras, B Ducourant, G Mascerpa, C Guegen, J Bousquet, *Clays. Clay Miner.*, 36, 369-375 (1988).

21. L Li, X Liu, Y Ge, R Xu, J Rocha, J Klinowski, *J. Phy. Chem.*, 97, 10389-10393, (1993).

22. M.L Occelli, A Aurox, G.J Ray, *Microporous. Mesoporous Mater.*, 39, 43-56 (2000)

23. D Plee, F Borg, L Gatineau, J.J Fripiat, *J. Am. Chem. Soc.*, 107, 2362-2369 (1985).

24. I Palinko, A Molnar, J.B Nagy, J.C Bertrand, K Lazar, J Valyon, I Kiricsi, *J. Chem. Soc. Far.Trans.*,938, 1591-1599 (1997).

25. C.A Fyfe, G.J Kennedy, H Strobl, *J. Am. Cer. Soc.*, 69, 45-47 (1986).

26. D Zhao, G Wang, Y Yang, X Guo, Q Wang, J Ren, *Clays. Clay Miner.*, 41, 317 (1993).

27. P.B Malla, S Komemani, *Clays. Clay Miner.*, 38, 363-372 (1990).

28. D Zhao, G Wang, Y Yang, X Guo, Q Wang, *Clays Clay Miner.*, 41, 317 (1993).

29. X Gao, I.E Wachs, *J. Phy. Chem. B*, 104, 1261-1268 (2000).

30. A.C Scheinost, D.G Schulze, U Schwertmann, *Clays. Clay Miner.*, 47, 156-164 (1999).

31. R.G Burns, "Mineralogical Applications of Crystal Field Theory", A Putnis, R.C Lieberman (eds), Cambridge University Press, (1993).

32. M.C.M de Lucas, F Rodriguez, C Prieto, M Verdaguer, H U Gudel,. *J. Phy. Chem. Solids*, 56, 995-1001 (1995).

33. P Canizares, J.L Velverde, M.R Sun Kou, C.B Molina, *Microporous. Mesoporous Mater.*,, 29, 267-281 (1999).

34. E.G Rightor, M Tzou, T.J Pinnavia, *J. Catal.*, 130, 29 (1991).

35. M.R SunKou, S Mendioroz, V Munoz, *Clays. Clay Miner.*, 48, 528-536 (2000).

36. S.M Bradley, R.A Kydd, *J. Catal.*, 141, 239 (1993).

37. H.M Yuan, Z Liu, M Enze, *Catal. Today*, 2, 321-338 (1988).

38. D Plee, A Schutz, G Poncelot, J.J Fripiat, "Catalysis by acids and bases", B Imelik (eds), Elsevier science publishers B.V, Amsterdam (1985).

39. R Barthos, F Lonyi, G Onyestak, J Valyon, *J. Phy. Chem.*, 104, 7311-7319 (2000).

40. J Ravichandran, B Sivasankar, *Clays. Clay Miner.*, 45, 854-858 (1997).

41. J Ravichandran, B Sivasankar, *Indian J. Chem.*, 34, 127-130 (1995).

42. V.N Stathopoulos, A.K Ladavos, K.M Kolonia, S.P Skaribas D.E Petrakis, P.J Pomonis, *Microporous Mesoporous Mater.*, 31, 111-121 (1999).

43. F Arena, R Dario, A Parmaliano, *Appl. Catal. A: Gen.*, 170, 127-137 (1998).

44. A Aurox, A Gervasini, *J. Phy. Chem.*, 94, 6371 (1990).

45. H.M Yuan, Z Liu, M Enze, *Catal. Today*, 2, 321-338 (1988).

46. J Kijenski, *Catal. Today*, 1 (1989).

47. H Suja, C.S Deepa, K Sreeja Rani, S Sugunan, *Appl. Catal. A: Gen.*, 230, 233-243 (2002).

48. R.T Sanderson, "Chemical Bonds and Bond Energy", Academic Press, New York (1976).

49. A Gedson, A Lassoued, J.L Bonerdet, J Fraissard, *Microporous. Mesoporous Mater.*, 44-45, 801-806 (2001).

50. M.V Landau, E Dafa, M.L Kaliya, T Sen, M Herskowitz, *Microporous. Mesoporous Mater.*, 49, 65-81 (2001).

51. T Sano, Y Uno, Z.B Zang, C.H Ahn, K Soga, *Microporous. Mesoporous Mater.*, 31, 89-95 (1999).

52. T Misra, M Acharya, K.M Parida, 218-223, Narosa.

53. T Misra, K.M Parida, *Appl. Catal A: Gen.*, 174, 91-98 (1998).

54. A Corma, B.W Wojciechowski, *Catal. Rev. Sci. Eng.*, 24, 1 (1982).

55. R Mokaya, W Jones, *J. Catal*, 153, 76-85 (1995).

56. P.M Boorman, R.A Kydd, Z Sarbak, A Somogyvari, *J. Catal.*,96, 115 (1985).

57. P.M Boorman, R.A Kydd, Z Sarbak, A Somogyvari, *J. Catal.*,100, 287 (1985).

58. K Tanabe, M Misono, I Ono, N Hattori, *Stud. Surf. Sci. Catal.*, 51 (1989).

59. J.M Winterbottom, *Catalysis*, 4, 141 (1981).

60. A Ouquer, G Coudurier, J.C Vedrine, *J. Chem. Soc. Faraday Trans.*, 89. 3151 (1993).

61. F Figueras, L Morgues, Y Trambouze, *J. Catal.*, 14, 107 (1969).

62. C Shivaraj, B.M Reddy, P.K Rao, *Appl. Catal.*, 45, L11-14 (1988).

63. D Martin, Duprez, *J. Mol. Catal.*, 118, 113 (1997).

64. M.C.C Costa, L.F Hodson, R.A.W Johnstone, J.Y Liu, D Whitaker, *J. Mol. Catal.*, 142, 349 (1999).

65. K Othmer, "Encyclopedia of Chemical Technology", F.H Mark *et.al* (eds), John Wiley & Sons Inc, New York, 7, 410 (1979).

66. W.S Chen, M.D Lee, *Appl. Catal. A*, 83, 201 (1992).

67. J Blanc, H Pines, *J. Org. Chem.*, 33, 2035 (1968).

68. C.L Kibby, S.S Lande, W.K Hall, *J. Am. Chem. Soc.*, 94, 214 (1972).

69. J.C Luy, J.M Parera, *Appl. Catal*, 26, 299-304(1986).

70. M Ai, *J. Catal.*, 40, 318 (1975).

71. M Ai, *Bull. Chem. Soc. Jpn.*, 50, 2579 (1977).

72. M Dobrovolsky, P Tetenyi, Z Paal, *J. Catal.*, 74, 31 (1982).

73. N.J Feberathinam, V Krishnaswamy, "Catalysis: Present and Future", P.K Rao *et.al* (eds), Publication and Information Directorate, New Delhi (1995)

74. C.P Bezouhanova, M.A Al-Zihari, *Catal. Lett.*, 11, 245 (1991).

75. C.G Ramankutty, S Sugunan, B Thomas, *J. Mol. Catal. A: Chem.*, 187, 105-117 (2002).

76. J.P Rupert, W.T Granquist, T.J Pinnavia, " Chemistry of Clays and Clay Minerals", A.C.D Newman (ed) (1987).

# 4

# FRIEDEL CRAFTS ALKYLATIONS

*The development of cutting edge and cleaner processes is of topical interest to meet global competition and conform stringent environmental specifications. Friedel-Crafts alkylation is a very important tool for introducing alkyl substituents into the aromatic ring system. Conventionally, homogeneous acidic catalysts are used for the reaction. This presents several problems like tedious work up, use of corrossive chemicals, moisture sensitivity, decreased regioselectivity etc. The use of solid acids to replace waste generating soluble Lewis acids for the alkylation of arenes facilitates improved procedures. In this chapter, we introduce the use of cleaner, shape selective clay catalysts for Friedel-Crafts alkylations. The chapter is divided into four sections; viz., benzylation of benzene with benzyl chloride, benzylation of o-xylene with benzyl alcohol, single pot alkylation of o-xylene with benzyl alcohol and benzyl chloride and tert-butylation of phenol.*

## 4.0 INTRODUCTION

Friedel-Crafts alkylation is an important means of attaching alkyl chains to aromatic rings and hence is a key reaction in organic chemistry. Diphenylmethane and substituted diphenylmethanes are industrially significant compounds used as heat transfer fluids, aromatic solvents, fragrances and monomers for polycarbonate resins. They are also precursors to benzophenones, synthesised by an air oxidation step in acetic acid medium in presence of manganese based catalysts[1,2]. Traditionally, homogeneous acid catalysts like $AlCl_3$, $BF_3$ and $H_2SO_4$ are used for Friedel-Crafts alkylations[3]. However, use of Lewis acid catalysts is laden with several problems like difficulty in separation and recovery of products, disposal of spent catalyst, corrosion, high toxicity etc. These catalysts also catalyse other undesirable reactions like alkyl isomerisations and *trans* alkylation reactions[4]. In order to reduce isomerisation and disproportionation in aromatic alkylation catalysed by $AlCl_3$, the reactions are generally carried out at low temperature (below -10°C) and in solvents like carbon disulphide and nitromethane, which present hazards[5]. Moreover, these catalysts are moisture sensitive and hence demand moisture free solvent and reactants, anhydrous catalysts and dry atmosphere for their handling[6]. Most of the catalysts have to be added in stoichiometric amounts, thereby adding to the cost of the desired product. Hence worldwide efforts have been made to replace the present environmentally malignant catalysts with solid acid catalysts.

Clark *et.al* reported montmorillonite supported zinc (Clayzic) and nickel chlorides to be highly active and selective catalysts for Friedel-Crafts alkylations; this scheme was subsequently commercialised[7,8]. Rhodes *et.al* pointed out that alkylation activities were related to the pore diameter rather than their acidities[9]. However, Clayzic is limited in its applications. It is hygroscopic in nature and hence moisture sensitive. The metal ions leach readily in a polar solvent since they are held to the support through weak interactions[10]. Clayzic also shows poor regioselectivity towards

the *para* product[7]. Various other solid acids have been tested for the reaction and a brief review of the recent literature is presented.

Of all the new catalysts, clays have been the most promising and hence much of the active research has been concentrated in this field. Benzylation of benzene was carried out in presence of clay catalysts originating from K10 montmorillonite and Kunipia. It was found that iron pillared clays were the most efficient catalysts producing quantitative conversions with greatly reduced amounts of catalysts in lesser reaction times[11]. K10 modified with $SbCl_3$ through cation exchange and nonaqueous impregnation was very efficient with respect to catalytic activity and selectivity. The high activity was explained on the basis of reducible nature of $Sb^{3+}$ rather than the classical Lewis acid catalysed mechanism[12]. A comparative study of $H_2SO_4$, $HNO_3$ and $HClO_4$ treated metakaolinite revealed $HNO_3$ treated catalyst to be superior to others. Direct correlation with acidity was observed[13]. Iron exchanged K10 montmorillonite was successfully employed by Choudary *et.al* for one pot alkylation of arenes using secondary alcohols in presence of catalytic amounts of *p*-toluene sulphonic acid or methanesulphonic acid[14].

Ga containing MCM-41 was employed for the reaction by Okumura *et.al* under such low temperature as 313 K. The agglomerated $Ga_2O_3$ situated outside the MCM-41 network was considered to bear the weak Lewis acid sites responsible for the reaction[15]. Large pore zeolites were found to be highly active and regioselective towards the benzylation of bromobenzene. Regioselectivity was explained in terms of outer and inner surface[16]. Iron exchanged zeolites were employed for Friedel-Crafts alkylation of benzene by Bidart *et.al*. The catalysts showed high conversions and selectivity for monoalkylated products[17]. Jun *et.al* reported that the catalytic activity depended significantly on synthesis methods rather than structural differences for Al impregnated KIT-1, MCM-41 and MCM-48. Post synthesis impregnation of aqueous $AlCl_3$ solution followed by calcination turned out to be the most effective means for

increasing activity[18]. H-beta zeolite catalyses the benzylation of *o*-xylene efficiently. Conversion increases with $SiO_2/Al_2O_3$ ratio and degree of Na exchange of H-beta[19]. Kinetics of the reaction using $InCl_3$, $GaCl_3$, $FeCl_3$ and $ZnCl_2$ supported on K10 and Si MCM-41 was studied[20]. In and Ga catalysts showed superior activity.

Other than clays and zeolites, a variety of new and efficient catalysts have been successfully employed for Friedel-Crafts alkylations. $CuCr_{2-x}Fe_xO_4$ spinel catalysts were used for benzylation of benzene with benzyl chloride. Reactivity was found to be basically due to the surface Lewis acidity of spinels, which was promoted by the low values of activation energy that result in ease of electron movement[21]. $Cu(OTf)_2$ and $Sn(OTf)_2$ were employed for Friedel-Crafts alkylation by Singh *et.al.* Good catalytic activity was observed with a variety of substrates[22]. Sebti *et.al* compared the activities of $ZnCl_2$, $NiCl_2$ and $CuCl_2$ supported on hydroxyapatite for Friedel-Crafts alkylation of benzene, toluene and *p*-xylene by benzyl chloride. The reaction proceeds selectively to monoalkyl compounds in a short time. The best catalytic activities were observed with Zn catalysts[23]. Other catalysts for Friedel-Crafts alkylations include sulphated zirconia[24], sol gel derived silica[25] and rare earth oxides[26].

In the present study, Friedel-Crafts benzylation of arenes was done over iron, aluminium and mixed iron aluminium pillared montmorillonites exchanged with transition metals. The reaction was studied extensively with different substrates and benzylating agents. The chapter is divided into four sections; benzylation of benzene with benzyl chloride, benzylation of o-xylene with benzyl alcohol, single pot alkylation of o-xylene with benzyl alcohol and benzyl chloride and *tert*-butylation of phenol.

## 4.1 BENZYLATION OF BENZENE WITH BENZYL CHLORIDE

Benzylation of benzene is an important probe reaction to check the acidity of the catalysts since the ring itself is not activated or deactivated by substitution.

Moreover, the reaction gives diphenylmethane, an important synthetic intermediate as the product. The reaction is represented in scheme 4.1.
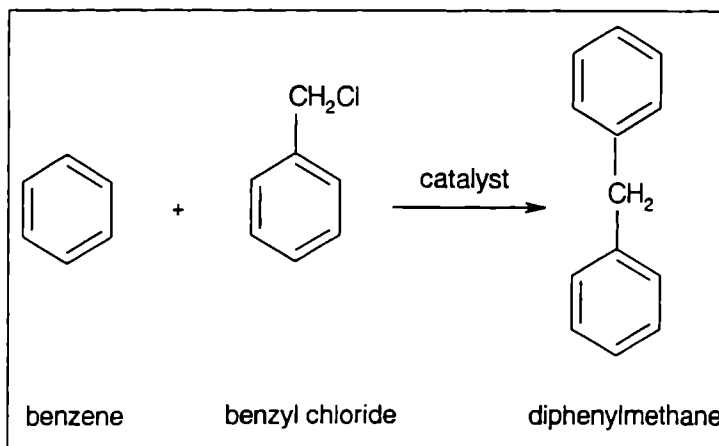


Scheme 4.1 Benzylation of benzene with benzyl chloride.

The liquid phase benzylation of benzene was carried out in a closed 50 mL round bottomed glass flask equipped with a reflux condenser, magnetic stirrer and provision for withdrawing product samples. The temperature of the reaction vessel was maintained using a thermostated oil bath. In a typical run, appropriate amounts of benzene, benzyl chloride and catalyst were allowed to react at specified temperatures under magnetic stirring. Reaction mixture was withdrawn at specific intervals and analysed by gas chromatography using SE-30 coloumn. The percentage conversion (wt%) of benzyl chloride is the total percentage of benzyl chloride transformed into the products. The selectivity to a product is the amount of that product divided by the total amount of products, expressed in percentage.

The reaction always gave monoalkylated product regardless of temperature, time and reactant molar ratio. Since the iron pillared and aluminium pillared samples performed differently in the mechanistic point of view, the reaction has been studied extensively using the two systems. The observations of the study and the inferences

drawn from it are given under three headings; I) Catalytic activity of various systems II) Structural stability of catalysts III) Effect of reaction variables.

## 4.1.1 CATALYTIC ACTIVITY OF VARIOUS SYSTEMS

Catalytic activity of the various transition metal doped pillared clays were tested for the benzylation of benzene at optimised reaction conditions. Considering the different pillars, no correlation is obtained between acidity and activity. Thus, Al pillared systems which are much more acidic, shows inferior activity. Presence of iron induces very high activity, which does not commensurate with acidity. Since the redox potential of $Fe^{2+}/Fe^{3+}$ is low, the activities, which are a measure of conversions, are higher for iron containing catalysts. Cent percent selectivity to monoalkylated product is little affected by change in catalyst.

### 4.1.1.1 Iron pillared systems

Iron pillared systems show very high activity to benzyl chloride(BC) when benzene is the substrate (Table 4.1.1.1).

| Catalyst | Time (minutes) | | | | | |
|---|---|---|---|---|---|---|
|  | 10 | 20 | 30 | 40 | 50 | 60 |
| V/Fe PM | 0.0 | 0.0 | 0.0 | 1.2 | 18.9 | 100 |
| Mn/Fe PM | 0.0 | 29.3 | 89.8 | 100 | 100 | 100 |
| Co/Fe PM | 0.0 | 0.0 | 0.0 | 31.9 | 95.0 | 100 |
| Ni/Fe PM | 0.0 | 31.2 | 95.0 | 100 | 100 | 100 |
| Cu/Fe PM | 0.0 | 0.0 | 0.0 | 9.1 | 27.4 | 100 |
| Zn/Fe PM | 0.0 | 0.0 | 0.0 | 27.6 | 100 | 100 |
| Fe PM | 0.0 | 0.0 | 0.0 | 4.2 | 83.2 | 100 |

Table 4.1.1.1. Activity of various iron pillared systems for benzylation of benzene

Temperature- 65°C, benzene/BC- 10, catalyst/BC- 0.1515

With Fe PM, the reaction proceed to completion in one hour at a surprisingly low temperature (65°C). Exchange of the pillared clay with transition metals of the first series improves the activity further. Thus, Mn/Fe PM and Ni/Fe PM shows maximum activity with almost 100% conversion of benzyl chloride in 30 minutes. An initial induction period when there is no reaction is found in all cases. Cent percent selectivity to the monobenzylated product remains the same.

The high activity of the iron pillared clay catalysts can be attributed to the iron oxide pillars present in the interlamellar space. The high surface area created by the pillars facilitate the easy diffusion of reactants in and products out of the catalyst active site. The three dimensional porous network also presents steric hindrance for further attack of carbocations on the product, inhibiting the formation of polyalkylated products. The effect of pillaring have been conclusively evidenced by comparing the reaction rates over pillared and exchanged clays[27].

Friedel-Crafts alkylation is an aromatic electrophilic substitution reaction in which the carbocation is formed by the complexation of alkyl halide with catalyst. The carbocation attacks the aromatic species for alkylation and hence formation of carbocation is an important step in the reaction mechanism. Lewis acidic centres on the catalyst surface facilitate the carbocation formation[21]. Hence, an attempt is made to correlate catalytic activity with the amount of Lewis acidity obtained by three independent acidity estimation techniques ellaborated in chapter 3. Figure 4.1.1.1 compares the activity of systems with limiting amount of perylene adsorbed on the catalyst surface. Perylene, being large in size may not be accessible to all the Lewis acid sites present inside the three dimensional network and hence the slight deterioration from perfect correlation. $a$-methyl styrene selectivity in the cumene cracking reaction can be considered as a measure of Lewis acidity. Figure 4.1.1.2 shows that catalytic activity of the prepared clay catalysts ties nicely with $a$-methyl styrene selectivity.

Figure 4.1.1.1. Correlation between activity and limiting value of perylene adsorbed



Figure 4.1.1.2. Correlation of conversion (%) with $a$-methyl styrene selectivity

A perfect correlation is obtained between catalytic activity and amount of strong acid sites (ammonia desorbed in the temperature region of 401-600°C). Thus strong acid sites may be considered to be involved in the benzylation of benzene with benzyl chloride. Though the pillared clay surface provides both Lewis and Brönsted acid sites, the above observations clearly indicate the dominating impact of Lewis/strong acid sites for the benzylation of benzene with benzyl chloride.
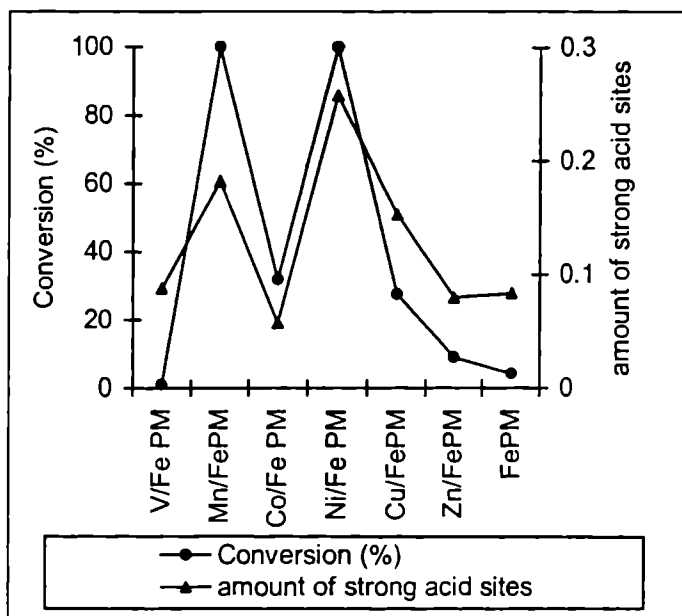


Figure 4.1.1.3. Dependence of activity on amount of strong acid sites from $NH_3$-TPD

## 4.1.1.2 Iron Aluminium pillared systems

The results of benzylation of benzene with benzyl chloride over iron aluminium mixed pillared systems are tabulated in table 4.1.1.2. Iron aluminium mixed pillared sytem show good catalytic activity towards benzyl chloride. Complete conversion of the benzylating agent occurs in 1 hour. A noticeable enhancement of the catalytic efficiency occurs as a result of exchange with transition metals for the

mixed pillared clay. An initial induction period is noticed with these systems also. Thus, it can be concluded that presence of iron increases the catalytic activity with benzyl chloride but imparts a certain inhibition for a short time, after which the reaction proceeds rapidly. Cent percent selectivity towards the monoalkylated product is not deteriorated.

| Catalyst | Time (minutes) | | | | | |
|---|---|---|---|---|---|---|
| | 10 | 20 | 30 | 40 | 50 | 60 |
| V/FeAl PM | 0.0 | 0.0 | 4.2 | 63.9 | 100 | 100 |
| Mn/FeAl PM | 0.0 | 0.0 | 0.0 | 21.6 | 99.1 | 100 |
| Co/FeAl PM | 0.0 | 0.0 | 0.0 | 21.3 | 92.3 | 100 |
| Ni/FeAl PM | 0.0 | 0.0 | 0.0 | 0.0 | 100 | 100 |
| Cu/FeAl PM | 0.0 | 0.0 | 0.6 | 64.6 | 100 | 100 |
| Zn/FeAl PM | 0.0 | 0.0 | 0.0 | 18.9 | 100 | 100 |
| FeAl PM | 0.0 | 0.0 | 0.0 | 3.5 | 17.5 | 68.9 |

Table 4.1.1.2. Activity of iron aluminium pillared systems for benzylation of benzene
Temperature- 70°C, benzene/BC- 10, catalyst/BC- 0.1515

The high activity of mixed pillared catalysts can be attributed to the presence of iron in the interlamellar space as well as to the porous network of the pillared clay. Shape selectivity imposed by the three dimensional network is responsible for the selectivity to monoalkylated product. The initial induction period is suggestive of a particular type of initiation, once the active site contains iron.

Since the reaction is reprted to be catalysed by Lewis acid sites, correlation between efficiency and number of Lewis acid sites have been attempted. (Figures 4.1.1.4 -4.1.1.5).
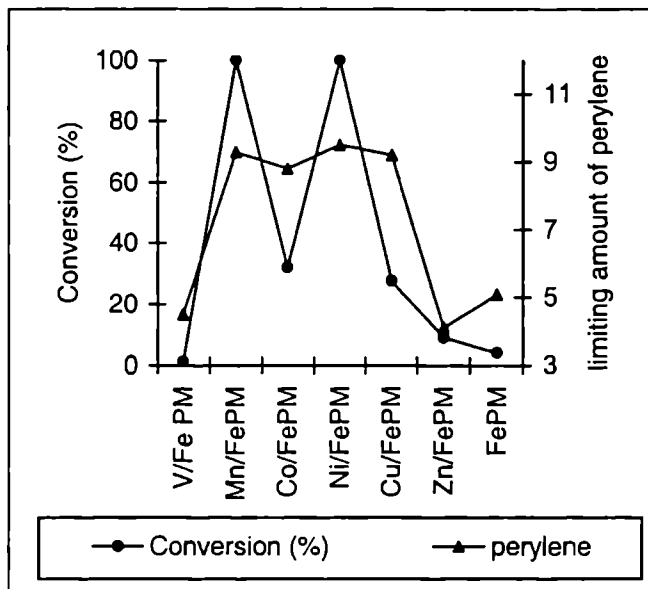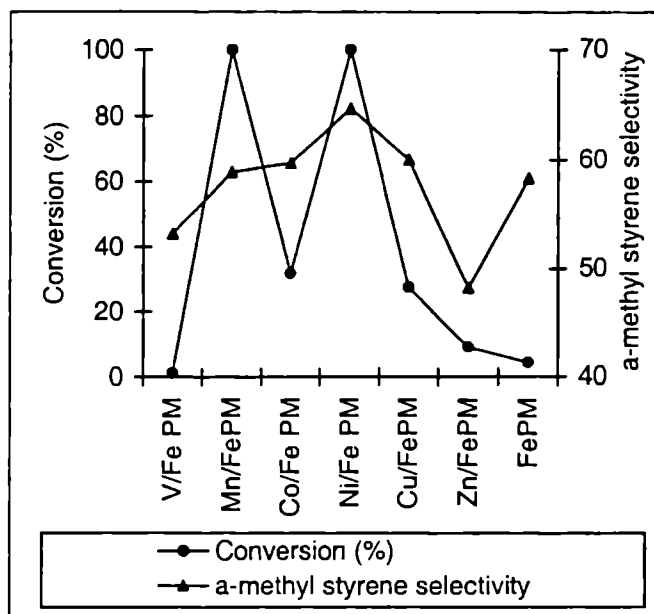
Figure 4.1.1.4. Correlation between activity and limiting value of perylene adsorbed
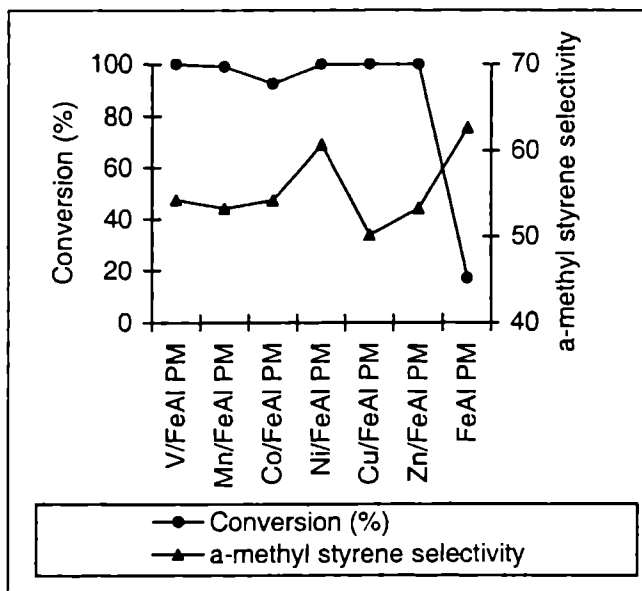


Figure 4.1.1.5. Correlation of conversion (%) with $a$-methyl styrene selectivity
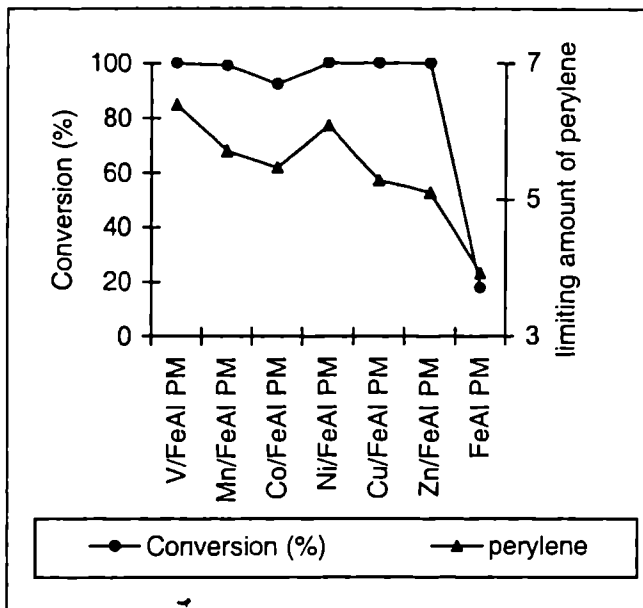
Appreciable correlation is obtained between catalytic performance of the catalysts of the mixed iron aluminium series with limiting values of perylene adsorbed on the catalyst surface. Figure 4.1.1.5 correlates the activity of the mixed pillared sytems with $a$- methyl styrene selectivity. Except the parent mixed pillared system, the activities are in accordance to the amount of Lewis acid sites. Thus, the results underline the involvement of Lewis acid sites in the benzylation of benzene, once benzyl chloride is the benzylating agent.

In order to get more insight on the mechanistic as well as kinetic properties of the reaction, the effects of various reaction variables were studied using a catalyst that shows moderate catalytic activity in the two series. The structural stability of the catalysts also was examined by the moisture sensitivity and metal leaching experiments. The catalyst Cu/FeAl PM was selected for this purpose.

## 4.1.2.A. STRUCTURAL STABILITY OF THE CATALYSTS

An essential requisite of a heterogeneous catalyst is the stability of active sites under the reaction conditions. The stability of the system can be lost during the course of the reaction. Reasons for this include thermal sintering, structural collapse and masking of active sites by impurities in product mixture. Leaching of certain metals like Fe in alkylation reactions and V in oxidation reactions have been reported[28,29]. This can lead to structural collapse as well as partly homogeneous reaction. Generally, Friedel-Crafts catalysts are highly moisture sensitive, another disadvantage of the conventional catalysts. The stability of the present catalysts was checked by metal leaching experiments as well as by moisture adsorption studies.

### 4.1.2.1.a. Effect of metal leaching

The question about the true nature of the reaction is a popular subject of concern for the scientific community. Leaching of metals from the catalyst surface can occur without much transformation in reaction profile, gradually changing the

nature of reaction from truly heterogeneous to partly homogeneous[30]. Fe in the clay can be reduced and this has every chance of combining with $Cl^-$ ions from benzyl chloride, forming $FeCl_3$. This fact questions the heterogeneous nature of the reaction. Hence, the effect of leaching of iron was studied at 35 minutes, by continuing the reaction for further 25 minutes, after filtering off the catalyst. The results are given in table 4.1.2.a. The presence of $Fe^{3+}$ was further examined qualitatively by addition of thiocyanate ions to the filtrate.

| Time (minutes) | Conversion % |
|---|---|
|  | 69.6 |
| 35 | 75.2 |
| 25* |  |
| (* after filtering off the catalyst) |  |

Table 4.1.2.a. Metal leaching studies.
Temperature- 70°C, benzene/BC- 10, catalyst/BC- 0.1515

For iron containing system, percentage conversion at the time of filtration of catalyst is 69.6, which increase to 75.2 on continuing the reaction for 25 minutes after the removal of the catalyst. On addition of thiocyanate ions, reaction mixture give blood red colour, confirming the presence of leached out iron ions.

The increase in product yield, though diminutive is significant. The result itself is suggestive of a partly homogeneous reaction. Fe from the pillaring species has been leached out into the reaction mixture, which then combines with chloride ions to give $FeCl_3$. The presence of blood red colour on addition of thiocyanate ions confirms the presence of $Fe^{3+}$ ions in the reaction mixture. This is responsible for the reaction even after the removal of the active catalyst. Similar results have been reported by Arata *et.al* for benzoylation reactions using benzoyl chloride over sulphate and tungstate modified $Fe_2O_3$[31].

## 4.1.2.2.a. Effect of moisture

The Lewis acid catalysts usually used for Friedel-Crafts alkylations are moisture sensitive. Hence, conventional catalysts demand moisture free solvent and reactants, anhydrous catalyst and dry atmosphere for their handling. In order to test the effect of moisture on catalyst performance, the catalyst and substrate were saturated with water vapour, by keeping them over deionised water in a dessicator for 72 hours at room temperature. The reaction was carried out as usual. The results are given in figure 4.1.2.a.
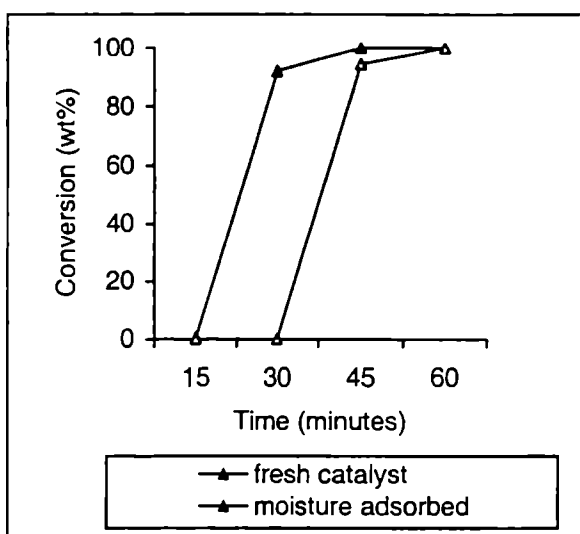


Figure 4.1.2.a. Moisture adsorption studies
Temperature- 70°C, benzene/BC- 10, catalyst/BC-0.1515

The induction period for the reaction increase in presence of moisture, after which, the reaction proceeds as in moisture free conditions. However, the increase in induction period is quite low (15 minutes).

The increase in induction period is suggestive of water molecules occupying the active sites prior to reaction, from where Cl⁻ ions displace them. Thus induction

period is the time required for replacing the adsorbed moisture by the reactants to start the reaction[6]. Once the sites are freed from water molecules, reaction goes on as in moisture free conditions. this leads us to the conclusion that the catalyst systems are active even in presence of moisture.The increase in reaction induction period was reported by Choudary *et.al* also[20].

## 4.1.3.A. EFFECT OF REACTION VARIABLES

Influence of various reaction variables like time, temperature, benzene to benzyl chloride ratio, substrate and catalyst concentration on the extent of reaction was studied extensively in order to arrive at a plausible mechanism for the reaction.

### 4.1.3.1.a. Effect of time

The results of the effect of time are given in figure 4.1.3.1.a. The figure shows the reaction rate is nominal for a particular period of time, after wcich, it continually increases. Further it is worth mentioning that no polyalkylated products are formed even after complete conversion of benzyl chloride unlike other reports[32].
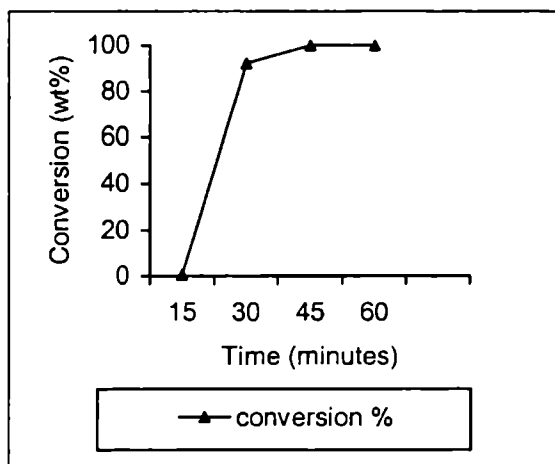


Figure 4.1.3.1.a. Dependence of time on conversion %

Temperature- 70°C, benzene/BC- 10, catalyst/BC- 0.1515

The continual increase in percentage conversion with time is indicative of the heterogeneous nature of the reaction. Selective formation of monoalkylated product can be attributed to the porous two dimensional structure of pillared clays restricting the attack of benzyl cation on the bulky product species. The side products are supposed to be dibenzyl benzene and higher products, which are formed through secondary reactions[33] and these were not observed. The presence of induction period is suggestive of a different type of mechanism for the reaction.

## 4.1.3.2.a. Effect of temperature

The effect of temperature on benzylation of benzene using transition metal doped pillared clays was studied. The results are presented in figure 4.1.3.2.a.
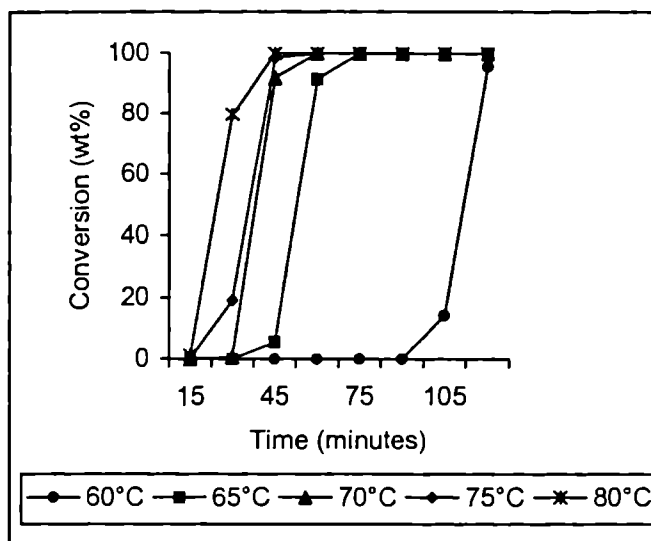


Figure 4.1.3.2.a. Dependence of activity on temperature.
benzene/BC- 10, catalyst/BC- 0.1515

It can be seen that temperature plays a prominent promotional role in the reaction. Alkylation of benzene with benzyl chloride proceed to completion at a low

temperature (60°C) in 2 hours. Even a slight increment in temperature has an extremely beneficial effect in the time required for complete conversion. The conversion at a given time as well as time required for complete conversion is most advantageous at the reflux temperature of benzene. At the reflux temperature of benzene, the reaction proceed to completion in 30 minutes. Thus, alkylation with benzyl chloride need much lower activation energy over iron pillared systems. Another interesting feature of the reaction is the initial induction period, when there is no reaction. This period, which is 90 minutes at 60°C reduce to 45 minutes as the temperature is enhanced by 5°C. Increase in temperature does not have any detrimental effect in the cent percentage selectivity to diphenylmethane.

It is evident from figure 4.1.3.2.a that the reaction temperature has a vital role in the benzylation of benzene. Increase in reaction rate with subsequent increase in temperature is probably due to speedy desorption of product at higher temperatures, thus exposing the catalyst active sites for further adsorption of reactants, resulting in enhanced reaction rates. The increase in alkylation activity can also be recognised with increase in intrinsic activity of acid sites on the bare catalyst surface. The initial induction period is suggestive of a particular mechanism, once benzyl chloride is the benzylating agent. Fe in the clay can be reduced at room temperature producing free radicals. Radicals are powerful reductants, oxidised in presence of reducible metallic ions like $Fe^{3+}$, $Sn^{4+}$ etc. The high activity observed with these cations could be ascribed to different initiation of the reaction, for instance, homolytic rupture of C - Cl bond followed by oxidation of radical[11,27,34].

$$C_6H_5 - CH_2Cl \quad\quad \rightarrow \quad\quad C_6H_5 - CH_2^{\cdot} + Cl^{\cdot} \quad\quad (I)$$

$$C_6H_5 - CH_2^{\cdot} + Fe^{3+} \quad\quad \rightarrow \quad\quad C_6H_5 - CH_2^{+} + Fe^{2+} \quad\quad (II)$$

$$Fe^{2+} + Cl^{\cdot} \quad\quad \rightarrow \quad\quad Fe^{3+} + Cl^{-} \quad\quad (III)$$
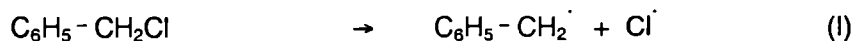
In this mechanism, homolytic rupture of the C - Cl bond should be the rate determining step. It can be deduced that the energy of rupture will prevent it from

taking place at lower temperatures. The benzyl carbocation attached to the catalyst surface facilitates the attack of the arene molecule.

### 4.1.3.3.a. Effect of benzene to benzyl chloride ratio

Benzene to benzylating agent molar ratio was studied by taking appropriate amounts of benzene, keeping the amount of catalyst and benzyl chloride fixed. The results are given in table 4.1.3.1.a. An inverse relationship is observed between benzene to benzyl chloride molar ratio and conversion % at any given time. Thus, higher amounts of benzene in the reaction mixture prolong the time required for complete conversion. It is worth mentioning that self condensation of the reagent or polyalkylation does not occur even at high concentrations of benzyl chloride.

| Benzene/BC | Time (minutes) | | | | | |
|---|---|---|---|---|---|---|
| | 15 | 30 | 45 | 60 | 75 | 90 |
| 5.0 | 3.2 | 90.8 | 100 | 100 | 100 | 100 |
| 7.5 | 4.7 | 58.9 | 100 | 100 | 100 | 100 |
| 10.0 | 0 | 5.5 | 91.5 | 100 | 100 | 100 |
| 12.5 | 0 | 0 | 0 | 0 | 2.3 | 84.6 |

Table 4.1.3.1.a. Dependence of activity on benzene to benzyl chloride ratio
Temperature- 70°C, catalyst/BC- 0.1515

Since benzene is taken in excess, the reaction is supposed to follow pseudo unimolecular mechanism. Therefore the reaction should have an equivalent relation with the amount of benzyl chloride. This can be explained as, lower the reactant molar ratio, higher the amount of benzylating agent and hence increase in reaction rate. Thus, the catalyst is very efficient for the creation of the benzyl carbocations even at high concentrations of the reagent. Higher reactant molar ratios result in insufficient interaction with catalyst surface for the formation of free radicals,

consequently prolonging the induction period. Thus, this result also is indicative of free radical type initiation reaction[35].

## 4.1.3.4.a. Effect of catalyst concentration

The effect of catalyst concentration on benzylation of benzene was scanned by varying the amount of catalyst, keeping the amount of reactants constant. The percentage conversions obtained at a time interval of 15 minutes are summarised in table 4.1.3.2.a. The amount of catalyst is expressed as wt% of benzyl chloride. The table shows that presence of catalyst even in trace amounts has marked influence in product yield. Increase in catalyst concentration, enhance the percentage conversion and at a stage, the reaction rate levels off. After this stage, increase in catalyst concentration has no pronounced effect in reaction rate. Thus, only a small amount of catalyst is needed for the easy completion of reaction. Cent percentage selectivity to monoalkylated product even at high catalyst concentrations is commendable.

| Catalyst/BC | Time (minutes) | | | |
|---|---|---|---|---|
|  | 15 | 30 | 45 | 60 |
| - | 0 | 0 | 0.9 | 2.8 |
| 0.0758 | 0 | 0 | 85.2 | 99.8 |
| 0.1515 | 0 | 0.6 | 92.0 | 100 |
| 0.227 | 0 | 3.6 | 96.5 | 100 |
| 0.303 | 0 | 14.5 | 95.8 | 100 |

Table 4.1.3.2.a. Dependence of catalyst concentration on conversion (%)
Temperature- 70°C, benzene/BC- 10/1.

Higher amounts of catalyst result in an enhanced amount of active sites and hence increase in reaction rate. Since the systems under study are very efficient Friedel-Crafts catalysts, only a small amount of catalyst is needed for the reaction. Speedy adsorption and desorption of the reactants and products from the catalyst

surface coupled with higher amount of strong acid sites may be responsible for the high catalytic performance.

### 4.1.3.5.a. Effect of substrate

The effect of substrate on percentage conversion was studied with different substrates, both activated and deactivated (table 4.1.3.3.a). Temperature for the reaction of fluorobenzene and chlorobenzene was respective refluxing temperatures. The observed order of reactivity of substrates is o-xylene > toluene > benzene > chlorobenzene > fluorobenzene. Also, the induction period for hydrocarbons is very low compared to halobenzenes.

| Substrate | Time (minutes) | | | | | | | | |
|---|---|---|---|---|---|---|---|---|---|
| | 15 | 30 | 45 | 60 | 75 | 90 | 105 | 120 | 135 |
| o-xylene | 74.3 | 100 | 100 | 100 | 100 | 100 | 100 | 100 | 100 |
| toluene | 61.2 | 100 | 100 | 100 | 100 | 100 | 100 | 100 | 100 |
| benzene | 0.0 | 4.6 | 92.0 | 100 | 100 | 100 | 100 | 100 | 100 |
| chlorobenzene | 0.0 | 0.0 | 30.9 | 63.5 | 96.1 | 100 | 100 | 100 | 100 |
| fluorobenzene | 0.0 | 0.0 | 0.0 | 0.0 | 0.0 | 0.0 | 5.73 | 39.9 | 100 |

Table 4.1.3.3.a. Dependence of substrate on conversion (%)
Temperature- 70°C, benzene/BC- 10, catalyst/BC- 0.1515

From the results it can be inferred that the activating and deactivating effect of substituting groups in the benzene ring has a profound influence on the rate of the reaction. The observed order of reactivity is exactly the same as the order of electron releasing effect of the substituting group in the benzene ring. The inductive effect of methyl group makes the reaction more facile with toluene and still higher for xylene due to the cumulative effect of two methyl groups. Similar results have been reported by Jun et.al[18].The electron withdrawing effect of halo group decreases the reaction rate for halobenzenes.

### 4.1.1.3 Aluminium pillared systems

The reaction was performed over aluminium pillared systems in optimised conditions (table 4.1.1.3). Al PM shows a conversion of 12% in 1 hour under refluxing conditions. However, catalytic activity increases as a result of transition metal exchange. V/Al PM exhibits 100% conversion of benzyl chloride in 1 hour matching the activity of iron pillared systems. Induction period is not observed with aluminium pillared systems. Cent percent selectivity to monoalkylated product is not altered.

| Catalyst | Conversion (%) | Selectivity (%) |
|----------|----------------|-----------------|
| V/Al PM  | 100            | 100             |
| Mn/Al PM | 72.3           | 100             |
| Ni/Al PM | 48.5           | 100             |
| Co/Al PM | 69.8           | 100             |
| Cu/Al PM | 24.8           | 100             |
| Zn/Al PM | 44.5           | 100             |
| Al PM    | 12.0           | 100             |

Table 4.1.1.3. Activity of aluminium pillared systems for benzylation of benzene.
Temperature- 80°C, benzene/BC- 5, time-1hour, catalyst/BC- 0.1515

The three dimensional porous network of pillared clay systems brings about the reaction between the aromatic species and benzyl chloride in a shape selective manner, leading to cent percent diphenylmethane selectivity. Presence of exchanged cations increases the catalytic efficiency. The usual carbocation mechanism can be visualised with these catalysts and hence absence of induction period.

Attempts are made to correlate Lewis acidity with catalytic activity. Lewis acidity as indicated by $\alpha$-methyl styrene selectivity in cumene cracking reaction ties nicely with catalytic performance of aluminium pillared systems (Figure 4.1.1.6).
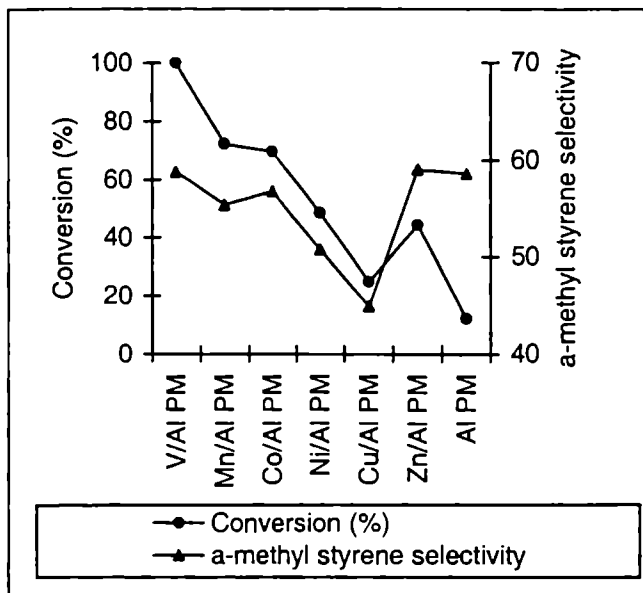
Figure 4.1.1.3. Correlation of conversion (%) with *α*-methyl styrene selectivity
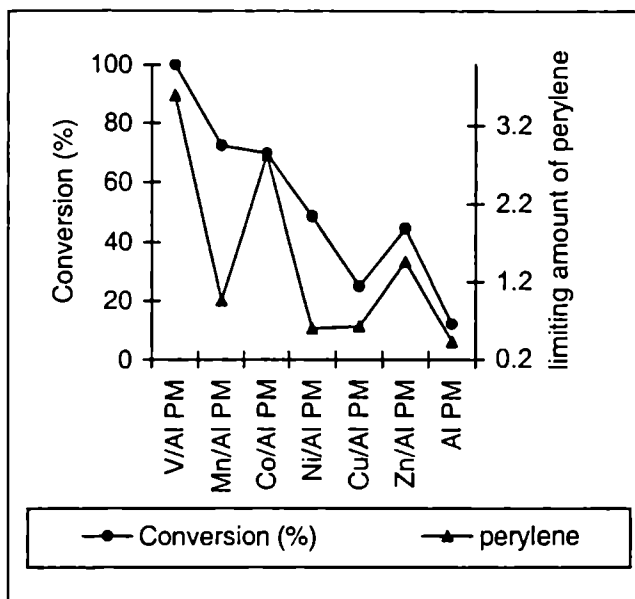


Figure 4.1.1.4. Correlation between activity and limiting value of perylene adsorbed

Perfect correlation is obtained between catalytic activity and limiting value of perylene adsorbed on catalyst surface as shown in figure 4.1.1.7. Figure 4.1.1.8 indicates that catalytic activity along the series follow the order of the amount of strong acid sites (ammonia desorbed in the temperature range of 401-600°C). Greater efficiency of V/Al PM is due to increase in amount of strong acid sites. Thus, conclusive confirmation of the relationship between the amount of strong/Lewis acid sites with catalytic activity has been evidenced.
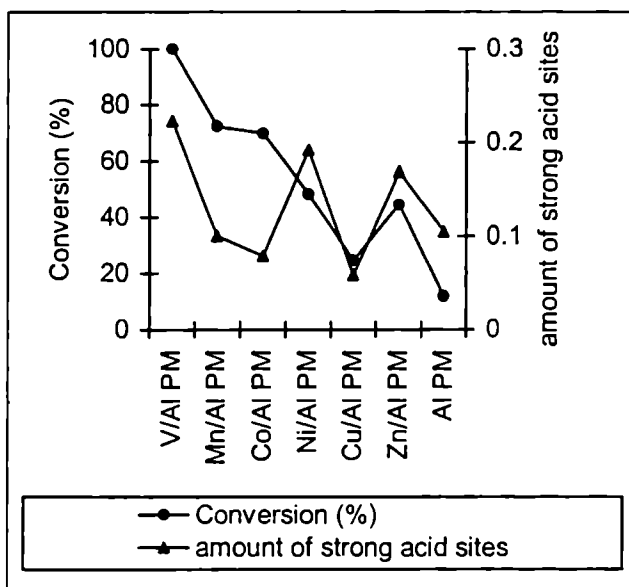


Figure 4.1.1.6. Dependence of activity on amount of strong acid sites from $NH_3$-TPD

A detailed investigation of the structural stability and the effect of various reaction variables were studied using Mn/Al PM as reference catalyst. The results helped in arriving at a reliable mechanism for the reaction.

## 4.1.2.B. STRUCTURAL STABILITY OF THE CATALYSTS

Crucial importance is given to the stability of active sites under the reaction conditions. Generally, Friedel-Crafts catalysts are highly moisture sensitive, another

disadvantage of the conventional catalysts. Hence stability of the catalysts was checked by metal leaching and moisture adsorption experiments.

### 4.1.2.1.b. Effect of metal leaching

Leaching of metals from the catalyst surface can occur without much transformation in the reaction profile, gradually changing the nature of reaction from truly heterogeneous to partly homogeneous[30]. The probability of aluminium leaching is remote and has not been reported so far. However, metal leaching was studied at 35 minutes, by continuing the reaction for further 25 minutes, after filtering off the catalyst. The results are given in table 4.1.2.

| Time (minutes) | Conversion (%) |
|----------------|----------------|
| 35 | 51.4 |
| 25* | 52.1 |
| (* after filtering off the catalyst) | |

Table 4.1.2.b. Metal leaching studies.
Temperature- 80°C, benzene/BC- 5, catalyst/BC- 0.1515

From the table it can be concluded that no noticeable change is observed even after 25 minutes of reaction, in the absence of catalyst. Hence a truly heterogeneous reaction can be envisaged with aluminium pillared systems.

### 4.1.2.2.b. Effect of moisture

In order to test the effect of moisture on catalyst performance, the catalyst and the substrate were saturated with water vapour, by keeping them over deionised water in a dessicator for 72 hours at room temperature. The reaction was carried out as usual. The results are given in figure 4.1.2.b. The induction period for the reaction

increase in presence of moisture. After this short span of time (1 hour), the reaction proceeds as in moisture free conditions.
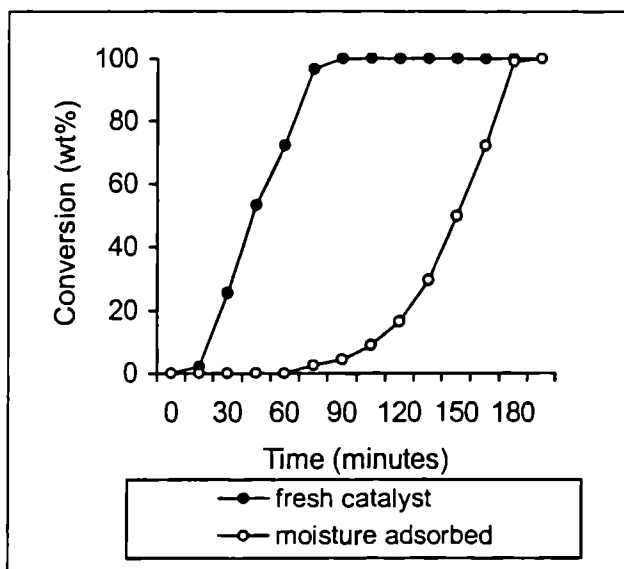


Figure 4.1.2. Moisture adsorption studies
Temperature- 80°C, benzene/BC- 5, catalyst/BC- 0.1515

Presence of induction period is suggestive of water molecules occupying the active sites prior to reaction, from where $Cl^-$ ions displace them. Induction period is the time required for replacing the adsorbed moisture by the reactants to start the catalytic reaction[6]. The high induction period can be attributed to the high activation energy over these catalysts.

## 4.1.3.B. EFFECT OF REACTION VARIABLES

Influence of various reaction variables like time, benzene to benzyl chloride ratio, substrate and catalyst concentration on the extent of reaction were studied extensively using Mn/Al PM as reference in order to arrive at a plausible mechanistic pathway for the reaction.

142

## 4.1.3.1.b. Effect of time

The results of the effect of time on the reaction are given in figure 4.1.3.1.b. The figure shows the reaction rate to be nominal for a particular period of time and then continually increasing with time. Thus time plays a decisive role in the reaction. Absence of polyalkylated products is a significant result.
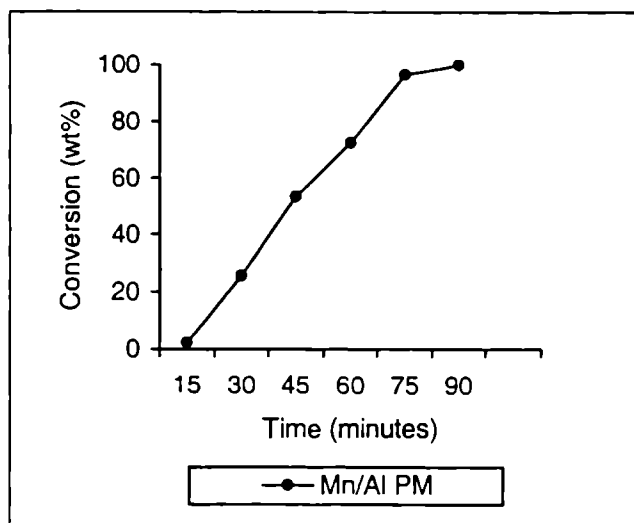


Figure 4.1.3.1.b. Dependence of time on conversion (%).
Temperature- 80°C, benzene/BC- 5, catalyst/BC- 0.1515

The continual increase in percentage conversion with time is indicative of heterogeneous nature of the reaction. Selective formation of the monoalkylated product can be attributed to the porous two dimensional structure of the pillared clays restricting the attack of the benzyl cation on the bulky product species.

## 4.1.3.3.b. Effect of benzene to benzyl chloride ratio

Benzene to benzylating agent molar ratio was studied by taking appropriate amounts of benzene, keeping the amount of catalyst and benzyl chloride fixed. The

results are given in table 4.1.3.1.b. An inverse relationship is observed between benzene to benzyl chloride molar ratio and conversion % at any given time. Thus higher amounts of benzene in the reaction mixture prolong the time required for complete conversion. It is worth mentioning that polyalkylation does not occur even at high concentrations of benzyl chloride.

| Benzene/BC | Time (minutes) | | | | | |
|---|---|---|---|---|---|---|
| | 15 | 30 | 45 | 60 | 75 | 90 |
| 5.0 | 2.3 | 25.6 | 52.3 | 72.3 | 96.6 | 100 |
| 7.5 | 0 | 18.7 | 34.5 | 53.9 | 78.9 | 93.6 |
| 10.0 | 0 | 15.6 | 28.4 | 41.9 | 69.8 | 79.8 |
| 12.5 | 0 | 12.7 | 24.3 | 34.0 | 56.3 | 71.3 |

Table 4.1.3.1.b. Dependence of activity on benzene to benzyl chloride ratio
Temperature- 80°C, catalyst/BC- 0.1515

Since benzene is taken in excess, the reaction is supposed to follow pseudo unimolecular mechanism. Therefore the reaction should have an equivalent relation with the amount of benzyl chloride. Thus the catalyst is very efficient for the creation of benzyl carbocations even at high concentrations of the reagent.

**4.1.3.4.b. Effect of catalyst concentration**

The effect of catalyst concentration on the reaction was studied by varying the amount of catalyst added, keeping the amount of reactants constant. The results obtained at a time interval of 15 minutes are summarised in table 4.1.3.2.b. The amount of catalyst is expressed as wt% of benzyl chloride. The table shows that the presence of catalyst even in trace amounts has a marked difference in the product yield. Increase in catalyst concentration, enhance the percentage conversion and at a stage, rate of the reaction levels off. After this stage, increase in catalyst concentration has no pronounced effect in the reaction rate. Thus, only a small

amount of catalyst is needed for easy completion of the reaction. Cent percentage selectivity to monoalkylated product even at high concentrations of the catalyst is commendable.

| Catalyst/BC | Time (minutes) | | | |
|---|---|---|---|---|
| | 15 | 30 | 45 | 60 |
| - | 0 | 0 | 0.3 | 1.6 |
| 0.0758 | 0 | 5.1 | 10.3 | 16.6 |
| 0.1515 | 2.3 | 25.6 | 52.3 | 72.3 |
| 0.227 | 3.6 | 32.3 | 53.3 | 74.8 |
| 0.303 | 3.9 | 35.6 | 55.2 | 76.4 |

Table 4.1.3.2.b. Dependence of catalyst concentration on conversion (%)
Temperature- 80°C, benzene/BC- 5

Increase in reaction rate with catalyst concentration is suggestive of heterogeneous mechanism for the reaction. Higher amounts of catalyst result in higher amounts of active sites and hence the increase in reaction rate. Since the systems under study are very efficient Friedel-Crafts catalysts, a small amount of catalyst is needed.

### 4.1.3.5.b. Effect of substrate

The effect of substrate on percentage conversion was studied with different substrates (Table 4.1.3.3.b). The observed order of reactivity of substrates is o-xylene > toluene > benzene. As expected, the reaction rate for hydrocarbons is lowered over aluminium pillared systems and halobenzenes do not react at all over these catalysts under the specified conditions.

From the results it can be inferred that the activating and deactivating effect of the substituting groups in the benzene ring has profound influence on reaction

rate. The observed order of reactivity is exactly the same order of electron releasing effect of the substituting group in the benzene ring. The inductive effect of methyl group makes the reaction more facile in the case of toluene and still higher for xylene due to the cumulative effect of two methyl groups. Similar results have been reported by Jun et.al[18]. The higher activation energy due to electron withdrawing effect of the halo group is responsible for the non occurrence of the reaction over these catalysts.

| Substrate | Time (minutes) | | | | | | | | |
|---|---|---|---|---|---|---|---|---|---|
| | 15 | 30 | 45 | 60 | 75 | 90 | 105 | 120 | 135 |
| o-xylene | 44.2 | 74.3 | 90.2 | 100 | 100 | 100 | 100 | 100 | 100 |
| toluene | 22.3 | 51.9 | 75.9 | 100 | 100 | 100 | 100 | 100 | 100 |
| benzene | 2.3 | 25.6 | 53.2 | 75.6 | 95.6 | 100 | 100 | 100 | 100 |

Table 4.1.3.3.b Dependence of substrate on conversion (%)

Temperature- 80°C, benzene/BC- 5, catalyst/BC- 0.1515

## 4.1.4 MECHANISM OF THE REACTION

Several mechanisms have been put forward by various authors for benzylation with benzyl chloride. Predominant among them are the classical carbocation mechanism and the redox mechanism involving free radicals. Yadav et.al investigated the alkylation of toluene by benzyl chloride on sulphated zirconia, a very strong Lewis acid and reported a surprisingly low activity[36]. Hence a redox mechanism was suggested for the reaction.

Based on the observations of present study, a plausible reaction mechanism is suggested for the reaction (Scheme 4.2). The mechanism is similar to the mechanism of alkylation reaction catalysed by an $M^+$-H species present on synthetic transition metal oxide $SiO_2$-$Al_2O_3$ systems[37,38]. The alkylating agent, benzyl chloride interacts with the active species and forms the alkylating moiety $M^+$-$CH_2$-$C_6H_5$ that in

ᅥ attacks the benzene molecule forming a pi-complex. This is possible due to t

tially filled p- orbitals of Al(III) and d- orbitals of Fe(III) present in the pillars.



pi complex

pi-sigma
rearrangement

sigma complex

diphenyl methane.
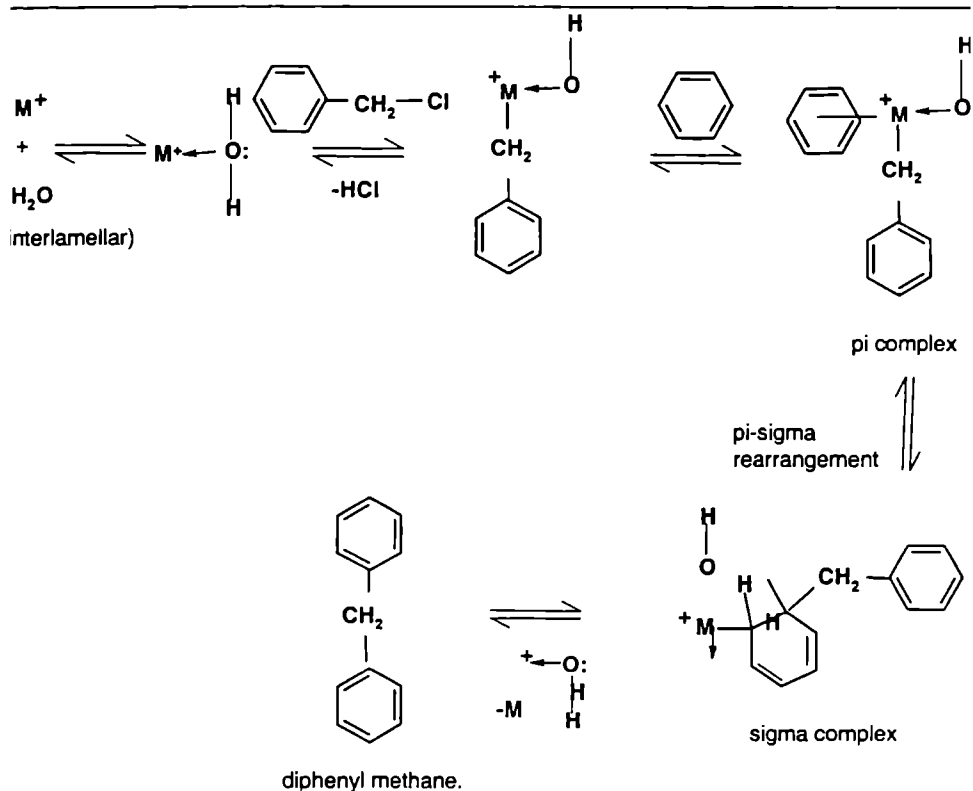
ᅥeme 4.2. A plausible mechanism for benzylation of benzene with benzyl chloride oᴠ
ᅥred clays. $M^+$ is $Al^{3+}$ or $Fe^{3+}$.

The framework Al and Fe does not contribute to the formation of pi compl

pure montmorillonite would have shown much better activity. The pi compl

rranges to give the alkylated product diphenylmethane. The platelets of cl

ᴣrcalated with transition metal oxide pillars are capable of stabilising highly poᴉ

ᴺsition states converting it into products whereas it is formed in lesser amounts

ᴣn not obtained in homogeneous conditions[39]. Thus the intermediate of tᴉ

alkylating moiety, the pi complex and the sigma complex could be stabilised which in turn enhances the conversion to diphenylmethane. When the reactants are constrained to diffuse in a porous solid, which have layered structure like clays, their encounter frequencies increase. Also, organic molecules congregate in the compartment like structures of the clay matrix. Thus, pores locally increase the interaction between reactants[40].

## 4.1.5 CONCLUSIONS

The important points that can be summarised from the above discussion are,

❖ All the pillared clays under study are efficient Friedel-Crafts benzylation catalysts with benzyl chloride. Appreciable conversions are obtained at shorter durations of reaction time. Thus pillared clays can contribute to the development of cleaner catalytic processes.

❖ The reaction is faster and conversions quantitative for iron containing catalysts.

❖ The procedure has the advantage of total simplicity; the aromatic hydrocarbon to be alkylated serves as its own solvent, the workup consists merely of filtration to remove the catalyst followed by solvent evaporation.

❖ Cent percent selectivity to monoalkylated product without any formation of di or poly products is a significant result. The high reactivity and specificity of these catalysts coupled with their ease of use and reduced environmental problems makes them attractive alternatives for the traditional catalysts.

❖ Acidity plays an important role in the reaction. The product yield obtained for the systems can be well correlated with the amount of Lewis acid sites.

❖ Detailed studies on reaction variables are suggestive of free radical type initiation for iron containing samples whereas usual carbocation mechanism is recommended for aluminium pillared systems.

❖ Studies on structural stability establish leaching of Fe into the reaction mixture for iron pillared samples while this effect is not shown by aluminium pillared systems. All the prepared systems are moisture sensitive. This effect is more pronounced for aluminium pillared systems compared to the iron containing counter parts.

## 4.2 BENZYLATION OF *O*-XYLENE WITH BENZYL ALCOHOL

Benzylation of *o*-xylene with benzyl alcohol, a typical example of Friedel-Crafts alkylation, produces dimethyldiphenylmethanes (DMDPM's) used as synthetic intermediates for production of dielectric fluid[41]. The reaction can be represented as,
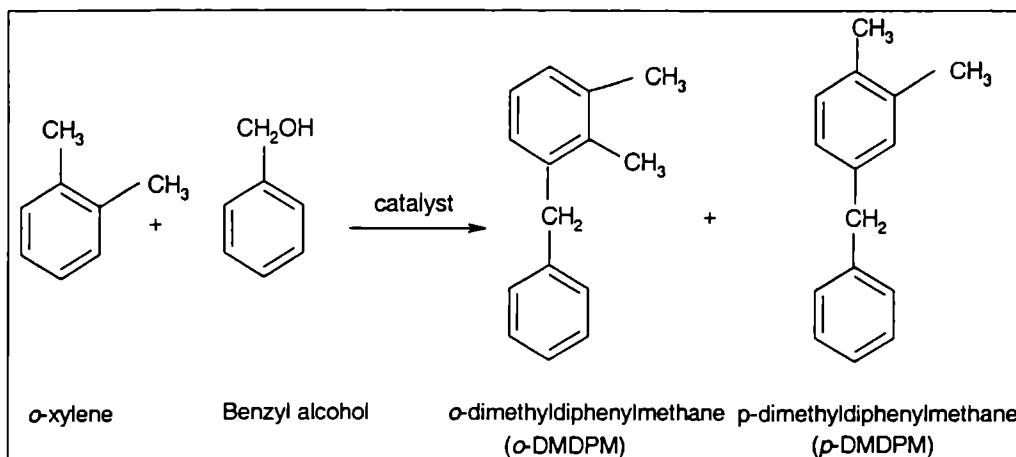


Scheme 4.2 Benzylation of *o*-xylene with benzyl alcohol.

The liquid phase benzylation of *o*-xylene was carried out in a closed 50 ml round bottomed glass flask equipped with a reflux condenser, magnetic stirrer and provision for withdrawing product samples. The temperature of reaction vessel was

maintained using a thermostated oil bath. In a typical run, appropriate amounts of *o*-xylene, benzyl alcohol and catalyst were allowed to react at specified temperatures under magnetic stirring. Reaction mixture was withdrawn at specific intervals and analysed using gas chromatography at conditions specified in chapter 2. The percentage conversion (wt%) of benzyl alcohol is the total percentage of benzyl alcohol transformed into the products. The selectivity to a product is the amount of that product divided by total amount of products, expressed as percentage.

The reaction always gave monoalkylated product regardless of time and reactant molar ratio. Another noteworthy point is the absence of dibenzyl ether in product mixture even at high concentrations of benzyl alcohol. The observations of the study and the conclusions drawn from it are given under three headings; I) Catalytic activity of various systems II) Structural stability of catalysts III) Effect of reaction variables.

## 4.2.1 CATALYTIC ACTIVITY OF VARIOUS SYSTEMS

The catalytic performance of various transition metal exchanged pillared montmorillonites towards benzylation of *o*-xylene was checked with benzyl alcohol. Iron containing systems exhibit better catalytic activity towards the reaction. The charge to ionic radius for $Fe^{3+}$ is higher than that for $Al^{3+}$. This induces better catalytic activity for iron and mixed iron aluminium pillared montmorillonites[42,43]. A detailed discussion of the activity of the prepared catalysts is presented in three sections. An attempt to correlate activity with acidity is also included.

### 4.2.1.1 Iron pillared systems

Iron pillared montmorillonite and its transition metal exchanged analogues were used for benzylation of *o*-xylene with benzyl alcohol. The results are tabulated in Table 4.2.1.1. Iron pillared systems prove to be efficient catalysts for benzylation of *o*-xylene with benzyl alcohol. 91.3% of the initial benzyl alcohol gets converted in

1 hour with o-DMDPM selectivity over 96%. Transition metal incorporation improves the activity considerably, except for Ni exchange. Selectivity to o-DMDPM decreases as a result of transition metal incorporation except for Co/Fe PM. Thus, Co/Fe PM proves to be the best catalyst in the series with respect to activity and selectivity.

| Catalyst | Conversion (%) | Selectivity (%) | |
|----------|----------------|-----------------|---|
|          |                | o-DMDPM | p-DMDPM |
| V/Fe PM | 99.8 | 75.7 | 24.3 |
| Mn/Fe PM | 98.8 | 72.9 | 27.1 |
| Co/Fe PM | 100 | 96.2 | 3.8 |
| Ni/Fe PM | 72.7 | 82.3 | 17.7 |
| Cu/Fe PM | 98.1 | 84.4 | 15.6 |
| Zn/Fe PM | 100 | 55.3 | 44.7 |
| Fe PM | 91.3 | 96.3 | 3.7 |

Table 4.2.1.1. Catalytic activity of iron pillared catalysts towards benzylation. o-xylene/BA- 10, temperature- gentle reflux, time- 60 minutes, catalyst/BA- 0.0859

Benzylation using benzyl alcohol has been reported to occur over Brönsted acid sites[12,27,44]. Dealkylated product selectivity in the cumene cracking test reaction is a measure of Brönsted acidity. Perfect correlation between activity and dealkylated product selectivity for cumene cracking reaction is obtained (Figure 4.2.1.1). Brönsted acidity of Fe PM increases as a result of transition metal exchange and this is reflected in the catalytic performance of the systems. Figure 4.2.1.2 shows the dependence of catalytic activity on the amount of weak and medium acid sites obtained from $NH_3$-TPD measurements. The $NH_3$-TPD method is widely employed to characterise the acidity of solid acids because ammonia can titrate acid sites of any strength and type. Catalytic activity can be associated with the cumulative amount of weak and medium sites. Thus, it can be well concluded that benzylation with benzyl alcohol occurs over weak and medium strength acid sites.
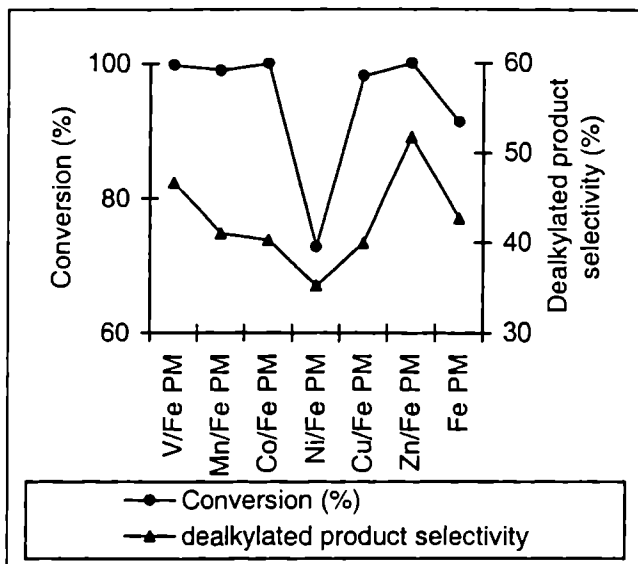
Figure 4.2.1.1. Dependence of activity on dealkylated product selectivity
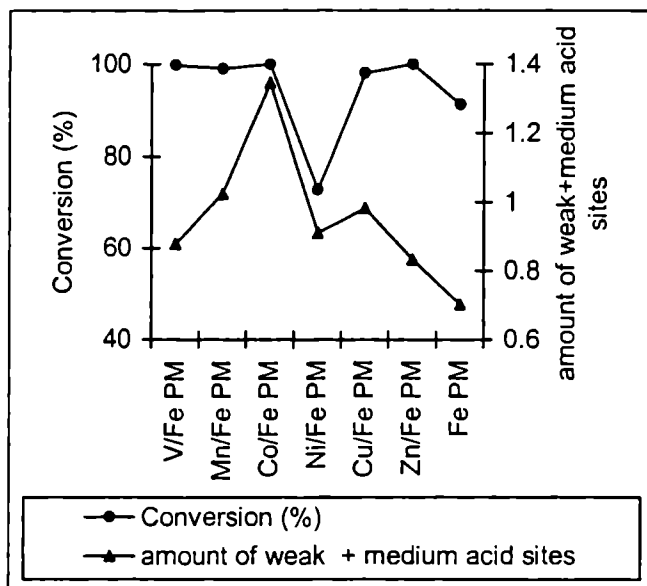


Figure 4.2.1.2. Dependence of activity on the amount of weak + medium acid sites

## 4.2.1.2 Aluminium pillared systems

A comparative evaluation of the activities of aluminium pillared systems is given in table 4.2.1.2. Al PM exhibits a conversion % of 66.3 with an $o$- to $p$- product ratio of 2:1. The results of our investigation on catalytic performance of different aluminium pillared systems suggest that exchange with transition metals significantly increases activity for Friedel-Crafts benzylation of $o$-xylene with benzyl alcohol. Almost complete conversion of benzyl alcohol occurs over Ni/Al PM with very high selectivity (around 90%). V/Al PM exhibits lowest activity with an inferior selectivity of isomeric products.

| Catalyst | Conversion (%) | Selectivity (%) | |
|----------|----------------|-----------------|-----------------|
|          |                | $o$-DMDPM | $p$-DMDPM |
| V/Al PM  | 52.7 | 50.6 | 49.4 |
| Mn/Al PM | 72.7 | 79.2 | 30.8 |
| Co/Al PM | 89.2 | 52.2 | 47.8 |
| Ni/Al PM | 99.0 | 88.3 | 11.7 |
| Cu/Al PM | 76.0 | 77.9 | 22.1 |
| Zn/Al PM | 71.0 | 78.2 | 21.8 |
| Al PM    | 66.3 | 67.2 | 32.8 |

Table 4.2.1.2. Catalytic activity of aluminium pillared systems.
$o$-xylene/BA- 10, temperature- gentle reflux, time- 60 minutes, catalyst/BA -0.0859

Figure 4.2.1.3 presents dependence of Brönsted acidity on the activities of various aluminium pillared catalysts. A rough correlation is observed between Brönsted acidity as obtained from dealkylated product selectivity in cumene cracking and catalytic activity. A discrepancy occurs as we move from Ni/Al PM to Cu/Al PM. Cu/Al PM, though exhibits higher dealkylated product selectivity, shows a much

lower conversion of cumene. Hence, it can be deduced that the number of acid sites present in the system is very low.



Figure 4.2.1.3. Dependence of activity on dealkylated product selectivity
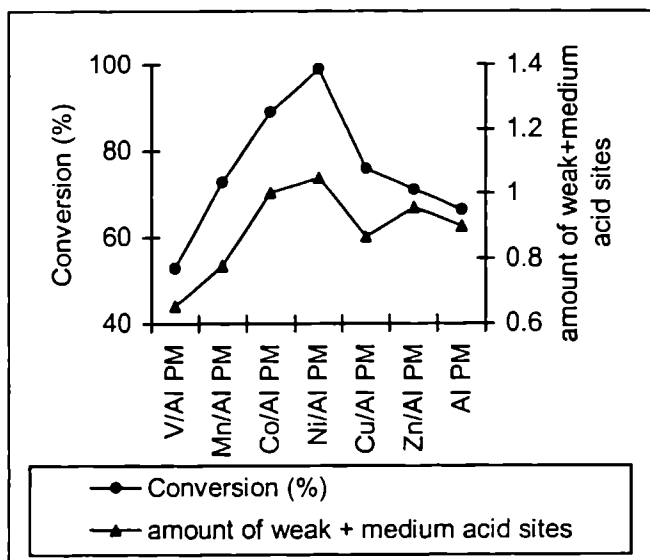


Figure 4.2.1.4. Dependence of activity on the amount of weak+ medium acid sites

Figure 4.2.1.4 gives the correlation between catalytic activities of aluminium pillared catalysts with the amount of weak and medium strength acid sites. Activity ties nicely with the results from $NH_3$-TPD measurements. Inferior activity of V/Al PM can be ascribed to lower amount of weak and medium acid sites.

### 4.2.1.3 Iron aluminium pillared systems

Table 4.2.1.3 gives the catalytic efficiency of various iron aluminium pillared montmorillonites for benzylation of o-xylene with benzyl alcohol. The parent mixed pillared system shows an efficiency of 93% with o-DMDPM selectivity of 84%. Incorporation of V, Co and Ni increases the activity and more than 97% of benzyl alcohol gets transformed over these catalysts, though with inferior product selectivity.

| Catalyst | Conversion (%) | Selectivity (%) | |
|---|---|---|---|
| | | o-DMDPM | p-DMDPM |
| V/FeAl PM | 99.7 | 61.6 | 38.4 |
| Mn/FeAl PM | 69.1 | 87.3 | 12.7 |
| Co/FeAl PM | 97.5 | 80.7 | 19.3 |
| Ni/FeAl PM | 97.3 | 68.9 | 31.1 |
| Cu/FeAl PM | 76.0 | 89.2 | 10.8 |
| Zn/FeAl PM | 83.0 | 68.4 | 31.6 |
| FeAl PM | 93.0 | 84.0 | 16.0 |

Table 4.2.1.3. Activity of iron aluminium pillared systems on benzylation of o-xylene. o-xylene/BA- 10, temperature- gentle reflux, time- 60 minutes, catalyst/ BA- 0.0859

Figure 4.2.1.5 shows the dependence of catalytic performance of various mixed pillared systems on Brönsted acidity. It can be concluded that activity depends to a great extent on the number of Brönsted acid sites. The meagre performance of Mn exchanged catalysts can be credited to low number of Brönsted acid sites.
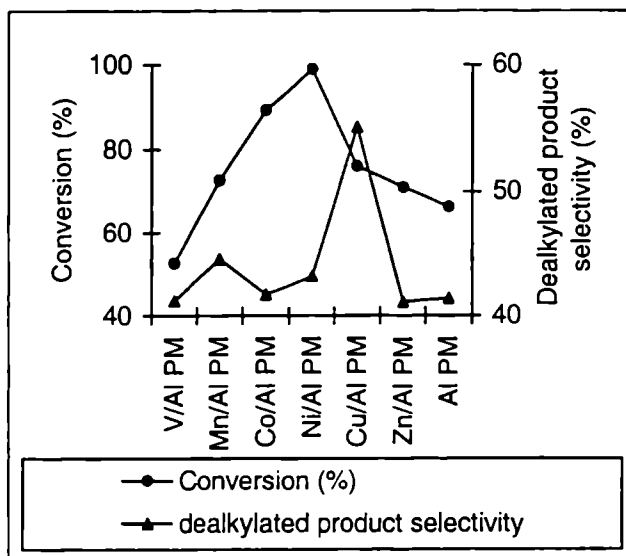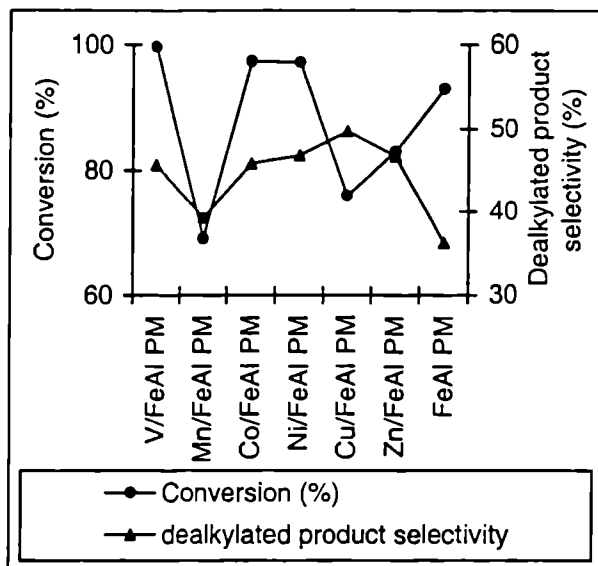
Figure 4.2.1.5. Dependence of activity on dealkylated product selectivity
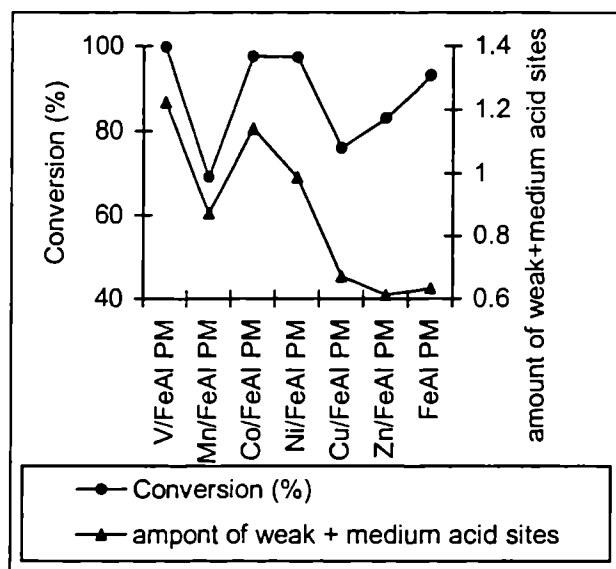


Figure 4.2.1.6. Dependence of activity on the amount of weak and medium acid sites

Direct correlation between activity and amount of weak + medium acid sites is obtained (Figure 4.2.1.6). Thus, the cumulative effect of weak and medium acid sites play an important role in the reaction. The higher number of these sites induces a higher activity to the V, Co and Ni exchanged systems.

## 4.2.2 STRUCTURAL STABILITY OF THE CATALYSTS

A fundamental requirement of a heterogeneous catalyst is the stability of the active sites under the reaction conditions. Leaching of certain metals like Fe in alkylation reactions and V in oxidation reactions have been reported[28,29]. This can lead to structural collapse as well as partly homogeneous reaction. Generally, Friedel-Crafts catalysts are highly moisture sensitive. The stability of the present catalysts was checked by leaching experiments as well as moisture adsorption studies by taking FeAl PM as reference catalyst.

### 4.2.2.1 Effect of leaching

In Friedel-Crafts reactions, use of iron containing solid acids questions the true nature of the reaction. Arata *et.al* reported leaching of Fe for benzoylation reactions using benzoyl chloride[31]. We obtained results indicative of iron leaching when benzylation of benzene was carried out using benzyl chloride. The results of iron leaching studies with benzyl alcohol are given in table 4.2.2.1.

| Time (minutes) | Conversion (%) | Selectivity (%) | |
|---|---|---|---|
| | | *o*-DMDPM | *p*-DMDPM |
| 60 | 93.0 | 84.0 | 16.0 |
| 30* | 93.9 | 84.4 | 15.5 |
| (* after filtering off the catalyst) | | | |

Table 4.2.2.1. Metal leaching studies

Temperature- gentle reflux, benzene/BA- 10, catalyst/BA- 0.859

The percentage conversion and selectivity pattern show only a nominal variation (within the limits of GC error) even after 30 minutes. The filtrate is colourless when tested for leached out metal ions. The diminutive increase in conversion % signifies heterogeneity of the reaction. Thus it is confirmed that the reaction occur exclusively on clay catalyst.

## 4.2.2.2 Effect of moisture

The Lewis acid catalysts usually used for Friedel-Crafts alkylations are moisture sensitive. In order to test the effect of moisture on catalyst performance, catalyst and substrate were saturated with water vapour, by keeping them over deionised water in a dessicator for two days. The reaction was carried out as usual. Dibenzyl ether was the only product formed even after 3 hours.

Deshpande et.al[12] reported benzylation of benzene with benzyl alcohol to be a multi step reaction in which the dibenzyl ether that is first formed, alkylate the benzene molecule via a cation mechanism. Formation of dibenzyl ether requires strong Brönsted acid sites. For clays, it has been postulated that a Brönsted acid site upon dehydroxylation yields a Lewis acid site. It has also been concluded that a Lewis acid site can be converted to a Brönsted site in presence of water molecule[45]. Interaction of activated clay catalyst with moisture causes conversion of Lewis acid sites to Brönsted sites and this can be the reason for exclusive formation of dibenzyl ether over moisture activated catalysts. Selective formation of ether signifies that benzyl alcohol is unable to displace the water molecules from the active sites for further reaction.

## 4.2.3 INFLUENCE OF REACTION VARIABLES

The influence of reaction conditions has been extensively studied by varying different reaction variables like time, catalyst concentration and o-xylene to benzyl

alcohol ratio with FeAl PM as reference catalyst. Based on the detailed study, a plausible reaction mechanism have been suggested for the reaction.

### 4.2.3.1 Effect of time

Effect of time on benzylation of $o$-xylene was studied for 90 minutes. The results are presented in figure 4.2.3.1. As the duration of run is increased, reaction show gradual increase in rate and 75 minutes is needed for complete conversion of benzyl alcohol. Another interesting point is that as time goes on, $o$- to $p$- product ratio increase from 1.1 to 9, indicative of preferential formation of $p$-DMDPM in initial stages. This is expected considering the steric hindrance at $o$- position. As reaction proceeds, $o$- position becomes more susceptible to attack by carbocation.
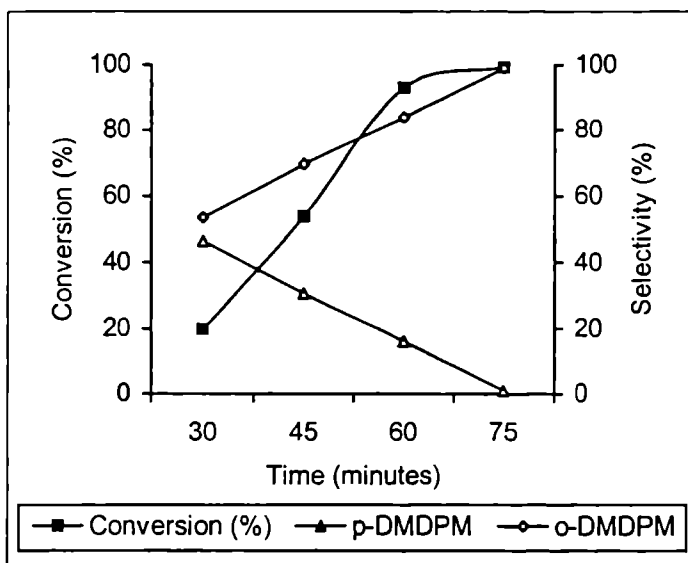


Figure 4.2.3.1. Dependence of conversion and selectivity on time.
$o$-xylene/BA– 10, temperature- gentle reflux, catalyst/BA- 0.0859

The continual increase in conversion % with time is indicative of the heterogeneous nature of the reaction. Selective formation of monoalkylated products,

even at high conversions can be ascribed to the shape selective effect of the pillared clay catalysts, restricting the further attack of carbocation on the aromatic species.

## 4.2.3.2 Effect of *o*-xylene to benzylating agent molar ratio

The ratio of reactants taken is very crucial in alkylations and this was checked by keeping the amount of catalyst and *o*-xylene fixed and varying the amount of benzyl alcohol. An inverse relationship is observed between *o*-xylene to benzylating agent molar ratio and conversion (Figure 4.2.3.1). Again, at higher amounts of *o*-xylene, the *o*- to *p*- product ratio is high and the ratio increases with *o*-xylene in the reaction mixture. It is noteworthy that no dibenzyl ether is formed even at high concentrations of benzyl alcohol.



Figure 4.2.3.1. Dependance of catalytic activity on *o*-xylene/benzyl alcohol ratio. Temperature- gentle reflux, time- 60 minutes, catalyst/BA- 0.0859

Since *o*-xylene is used in excess, the reaction is expected to follow psuedo first order kinetics. Selectivity to monoalkylated product can be ascribed to low

concentration of benzylating agent as well as on the shape selective nature of the catalyst.

### 4.2.3.3 Effect of catalyst concentration

The effect of the amount of the catalyst used for the reaction was studied by keeping the amount of reactants fixed and varying the amount of catalyst used. Figure 4.2.3.2 shows the effect of catalyst concentration on benzylation of *o*-xylene. Increase in catalyst concentration, enhance percentage conversion and at a stage reaction rate levels off. Thus, a small amount of catalyst is needed for the completion of reaction. Again, increase in catalyst concentration boost *o*-DMDPM selectivity.
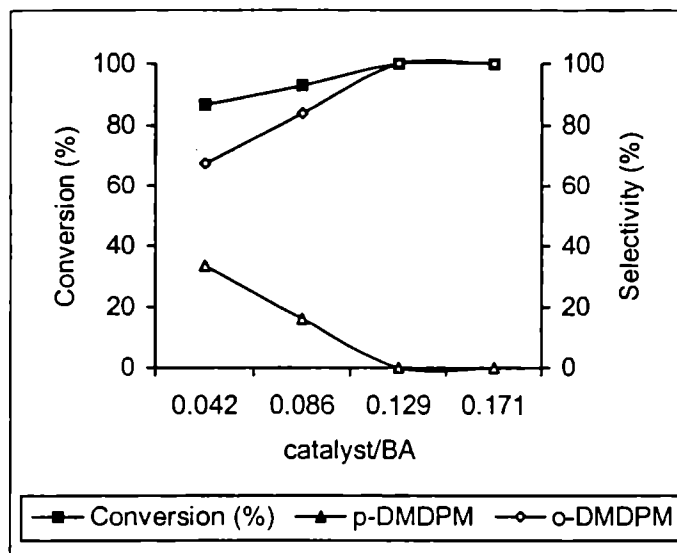


Figure 4.2.3.2. Effect of catalyst/benzyl alcohol ratio on catalytic activity

Temperature- gentle reflux, *o*- xylene/BA - 10,time- 60 minutes

### 4.2.4 MECHANISM OF THE REACTION

The trend in *o*-DMDPM selectivity leads to the conclusion that *o*- and *p*-DMDPM formation occurs by two different mechanisms. For *p*- product, the

generally accepted mechanism for Friedel-Crafts alkylations and acylations in which, the benzyl carbocation formed by the interaction with catalyst surface attacking the unadsorbed substrate molecules, forming product is appropriate (Scheme 4.2). Thus, the benzyl alcohol interacts with Brönsted acid sites on catalyst surface and in this case, substrate is unadsorbed. Possibility of attack on *p-* position of unadsorbed substrate is most feasible in this mechanism.
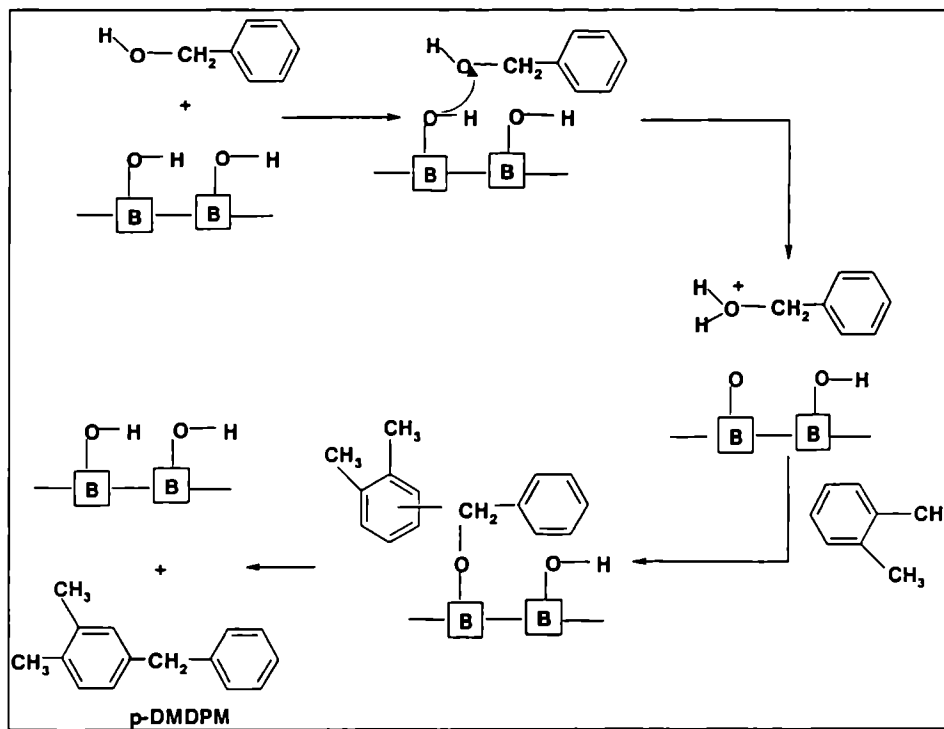


Scheme 4.2. Mechanism for *para* product formation in benzylation of *o-*xylene with benzyl alcohol.

Ortho product formation is more difficult in this case due to hindrance of three bulky functional groups attached at adjacent positions in the same ring. Nevertheless, increase in reaction time, catalyst concentration and decrease in reactant molar ratio favours *o-* product formation.

Therefore, for o-DMDPM formation, we propose a new mechanism in which the p- position of o-xylene is locked from attack by benzyl cations[35]. O-xylene has two electron releasing groups and this causes an accumulation of slight negative charge in the ring. Thus, o-xylene gets adsorbed to acidic sites on the catalyst surface, preferably at *para* position, considering steric factors. The p- position being blocked, the benzyl cation attacks the o- position. This is depicted in scheme 4.3.
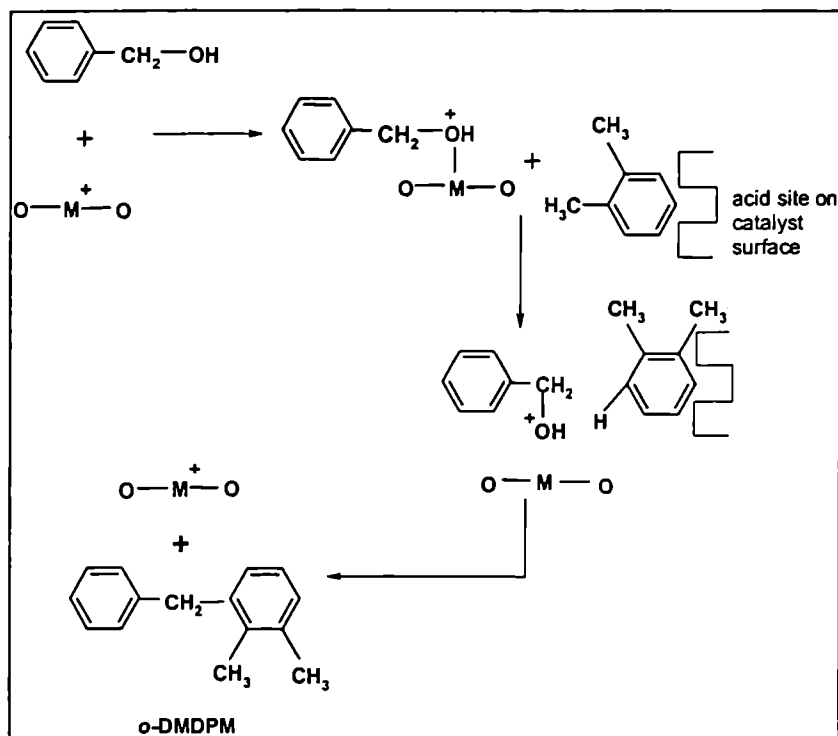


Scheme 4.3. Plausible mechanism for o- product formation over solid acids.

At lower reaction times, attack by benzyl cation occurs before the adsorption of o-xylene molecules to catalyst surface. Again at higher o-xylene concentrations, benzyl cation attacks the p- position of unadsorbed o-xylene molecules, which are greater in number. Higher catalyst concentrations lead to greater adsorption of

substrate molecules on catalyst surface and hence better $o$-DMDPM selectivity. Thus different mechanisms for $o$- and $p$- product formation based on the adsorption of $o$-xylene on catalyst surface clearly gives an explanation for the preferential formation of $p$-DMDPM when benzyl chloride is used as benzylating agent and $o$-DMDPM when benzyl alcohol is used[35].

## 4.2.5 CONCLUSIONS

The important points that can be summarised from the above discussion are,

- ❖ All pillared clays under study are efficient Friedel-Crafts benzylation catalysts when benzyl alcohol is the benzylating agent. Self condensation of benzyl alcohol giving dibenzyl ether does not occur over these catalysts.

- ❖ The procedure has the asset of total simplicity; the aromatic hydrocarbon to be alkylated serves as its own solvent, the workup consists merely of filtration of the catalyst followed by solvent evaporation.

- ❖ Cent percentage selectivity to monoalkylated products without formation of di or poly products is a significant result. The high reactivity and specificity of these catalysts coupled with ease of use and reduced environmental problems makes them attractive alternatives for the traditional catalysts.

- ❖ Acidity of the prepered systems plays an important role in the reaction. Product yield obtained for different systems can be well correlated with Brönsted acidity and the cumulative effect of weak and medium acid sites.

- ❖ Studies on structural stability establish the heterogenic nature of the reaction. Presence of moisture brings about self condensation of benzyl alcohol.

- ❖ Studies on various reaction variables are suggestive of the operation of two different mechanisms for the production of isomeric products.

## 4.3 SINGLE POT BENZYLATION OF O-XYLENE WITH BENZYL CHLORIDE AND BENZYL ALCOHOL

Selectivity improvement is the order of the day. When more than one reaction occurs in a single pot, the relative rates as well as product selectivities for the reactions can vary, than when they occur seperately. Potential applications of such reversals in reaction rates as well as product selectivities are numerous. Very high selectivities could be achieved without time consuming, costly and wasteful separations. Laszlo *et.al* documented first such a switch in relative reactivities when a substrate is reacted alone or in tandem with a co-reactant[46]. In the catalysed benzoylation of anisole and mesitylene in the temperature range of 120-130°C, mesitylene reacts faster by a factor three. However when the reactions are run jointly, competition favours anisole, again by a factor three. The reversal in reaction rate was attributed to the pore structural effects that appeared in microreactors capable of dynamic sieving[47].

Friedel-Crafts benzylation of toluene with benzyl chloride and benzyl alcohol was done in a single pot over clays, sulphated zirconia, Filtrol-24 and Amberlyst-15[48]. The reaction of toluene with benzyl alcohol proceeds fast in presence of benzyl chloride than when present alone as the benzylating species. This enhancement comes at the expense of no reaction of benzyl chloride, which when present alone reacts faster than benzyl alcohol. Preferential adsorption of benzyl alcohol to the catalyst active site was suggested as the mechanism for the reaction. Benzyl ether was used as co reactant in the before said reaction. Preferential adsorption mechanism was substantiated with relative rates of the reaction in the order of benzyl alcohol > benzyl ether > benzyl chloride[49].

The single pot benzylation of o-xylene with a combination of benzyl alcohol and benzyl chloride was carried out in a closed 50 mL round bottomed glass flask equipped with reflux condenser, magnetic stirrer and provision for withdrawing

product samples. In a typical run, appropriate amounts of o-xylene, benzyl chloride, benzyl alcohol and catalyst were allowed to react at specified temperatures under magnetic stirring. Reaction mixture was withdrawn at specific intervals and analysed by gas chromatography using SE-30 coloumn. The percentage conversion (wt%) of benzyl alcohol is the total percentage of benzyl alcohol transformed into products. The selectivity to a product is the amount of that product divided by total amount of products and is expressed as percentage.

The reaction has been studied extensively using iron, aluminium and mixed iron aluminium pillared systems. The observations of the study and the conclusions and inferences drawn from it are given under three headings; I) Catalytic activity of various systems II) Structural stability of catalysts III) Effect of reaction variables.

## 4.1.1 CATALYTIC ACTIVITY OF VARIOUS SYSTEMS

Catalytic activity of various transition metal doped pillared clays were tested for single pot benzylation of o-xylene under optimised conditions. Conversion of benzyl alcohol takes place at faster rate and lower temperatures in presence of benzyl chloride, than when present alone. No correlation is obtained between acidity and activity, considering the various pillars. Thus, Al pillared systems which are much more acidic, shows inferior activity. Presence of iron induces high activity, which does not correspond to acidity. This can be attributed to a difference in mechanism. Cent percent monoalkylated product selectivity is little affected by change in catalyst.

### 4.3.1.1 Iron pillared systems

The catalytic activities and selectivity patterns of iron pillared montmorillonite and its transition metal exchanged analogues are listed in table 4.3.1.1. Fe PM shows poor activity towards the reaction at specified conditions, with almost equal selectivity towards isomeric monoalkylated products. Transition metal incorporation enhances the activity greatly (almost fivefold enhancement), the effect being

166

minimum for vanadium exchanged species. From the table it can also be concluded that the ascend in activity comes mainly from increase in $p$- product concentration. Absence of polyalkylated products and dibenzyl ether are commendable observations for the reaction.

| Catalyst | Conversion (%) | Selectivity (%) | |
| --- | --- | --- | --- |
| | | $o$-DMDPM | $p$-DMDPM |
| V/Fe PM | 58.9 | 39.2 | 60.8 |
| Mn/Fe PM | 71.4 | 25.1 | 74.9 |
| Ni/Fe PM | 98.4 | 1.6 | 98.4 |
| Co/Fe PM | 96.6 | 2.9 | 97.1 |
| Cu/Fe PM | 71.9 | 16.0 | 84.0 |
| Zn/Fe PM | 100 | 2.5 | 97.5 |
| Fe PM | 16.5 | 56.2 | 43.4 |

Table 4.3.1.1. Activity of iron pillared series towards single pot benzylation of $o$-xylene $o$-xylene/BA- 10, temperature- 120°C, time- 30 minutes, catalyst/BA- 0.0859, BA/BC- 2

Selective formation of monoalkylated product can be assigned to the shape selective nature of the pillared clay catalyst, restricting further alkylation of the monoalkylated product. Friedel-Crafts alkylations generally prefer the $p$- product considering the steric factors. Hence, increased activity of the catalyst results in enhanced $p$- product concentrations.

### 4.3.1.2 Aluminium pillared systems

Table 4.3.1.2 illustrates the activity of aluminium pillared catalysts towards single pot alkylation of $o$-xylene with benzyl alcohol and benzyl chloride. Benzyl alcohol preferentially reacts with the substrate leading to the exclusive formation of monoalkylated products. Al PM exhibits considerable activity, with an $o$- to $p$- product ratio of 3:1. The activity and selectivity pattern of the transition metal exchanged

analogues do not vary much except for V/Al PM. V/Al PM shows an enhanced activity at the expense of selectivity. The inferior activity of aluminium pillared catalysts can be attributed to the low surface area of the catalysts.

| Catalyst | Conversion (%) | Selectivity (%) | |
|----------|----------------|-----------------|---------|
|          |                | o-DMDPM         | p-DMDPM |
| V/Al PM  | 46.8           | 52.3            | 47.7    |
| Mn/Al PM | 26.6           | 79.8            | 20.2    |
| Ni/Al PM | 22.1           | 81.2            | 18.8    |
| Co/Al PM | 18.7           | 79.5            | 20.5    |
| Cu/Al PM | 20.3           | 77.5            | 22.5    |
| Zn/Al PM | 19.3           | 78.9            | 20.1    |
| Al PM    | 25.3           | 74.3            | 25.7    |

Table 4.3.1.2. Activity of aluminium pillared catalysts

o-xylene/BA- 10, temperature- 130°C, time- 30 minutes,catalyst/BA- 0.0859, BA/BC- 2

### 4.3.1.3 Iron Aluminium pillared systems

The mixed iron aluminium pillared samples were employed for the benzylation of o-xylene with a combination of benzyl chloride and benzyl alcohol. The observations are given in table 4.3.1.3. The parent iron aluminium pillared clay shows conversion % of 20.2 with almost equal selectivity for the isomeric monobenzylated products. Incorporation of transition metals increase the catalytic activity as well as p- product selectivity. Thus, V/FeAl PM and Zn/FeAl PM act as the best catalysts in the series with cent percent conversion of benzyl alcohol and predominant selectivity towards p- product.

| Catalyst | Conversion (%) | Selectivity (%) | |
| --- | --- | --- | --- |
| | | o-DMDPM | p-DMDPM |
| V/FeAl PM | 100 | 4.7 | 95.3 |
| Mn/FeAl PM | 48.4 | 28.9 | 71.1 |
| Co/FeAl PM | 59.8 | 22.3 | 77.7 |
| Ni/FeAl PM | 42.4 | 24.4 | 75.6 |
| Cu/FeAl PM | 47.0 | 32.0 | 68.0 |
| Zn/FeAl PM | 100 | 3.7 | 96.3 |
| FeAl PM | 20.2 | 56.8 | 43.2 |

Table 4.3.1.3. Activity of iron aluminium pillared series

o-xylene/BA- 10, temperature- 120°C, time- 30 minutes, catalyst/BA- 0.0859, BA/BC- 2

High selectivity to p-DMDPM results from the high activity of prepared systems. O-DMDPM is produced by the adsorption of substrate to catalyst acid site. Preferential adsorption of benzyl alcohol has been proposed by Yadav et.al for the reaction[48,49]. Our own experiments with benzyl alcohol yield o-DMDPM as major product (refer 4.2.4) and hence high concentration of o- product in initial stages here also. As time goes by, as Friedel-Crafts reactions generally prefers, p- product concentration increases.

## 4.3.2 STRUCTURAL STABILITY OF THE CATALYSTS

Stability of catalyst active sites under the reaction conditions is fundamental for the selection of any catalyst. Deteriorations can occur in structure due to several reasons like thermal sintering, pore blocking due to coke deposition, poisoning by products and phase changes of active phase. The stability of prepared catalysts was checked against metal leaching as well as moisture adsorption by taking FeAl PM as reference at standard conditions.

## 4.3.2.1 Effect of metal leaching

The reference catalyst contains iron in the pillars. This has every chance of combining with $Cl^-$ ions from benzyl chloride forming $FeCl_3$, the traditional Friedel-Crafts catalyst. Thus, there is chance of the reaction becoming partly homogeneous in nature. Hence, the possibility of leached out iron was checked by two methods 1) by continuing the reaction for further 30 minutes after filtering off the catalyst at 30 minutes 2) testing the presence of iron in the reaction mixture with thiocyanate ions. The results of the investigation are given in table 4.3.2.1.

| Time (minutes) | Conversion (%) | Selectivity (%) | |
| --- | --- | --- | --- |
| | | o-DMDPM | p-DMDPM |
| 30 | | | |
| 30* | 62.5 | 72.9 | 27.1 |
| (*after filtering off the catalyst) | 63.9 | 71.5 | 28.5 |

Table 4.3.2.1. Effect of metal leaching.

o-xylene/BA- 10, temperature- 130°C, time- 30 minutes, catalyst/BA- 0.0859, BA/BC- 2

On continuing the reaction for further 30 minutes after filtering off the catalyst, almost same activity and product selectivity pattern is noticed. Addition of thiocyanate ions to the reaction mixture give no blood red colour, characteristic of $Fe^{3+}$ ions.

The data in table 4.3.2.1 reveals that leaching of Fe from the catalyst does not occur. This gives proof to the preferential adsorption mechanism of benzyl alcohol to catalyst active sites. Benzyl chloride, preferentially adsorbed to the catalyst active site, would have leached out Fe from the surface, thus increasing the reaction rate. Completely heterogeneous mechanism for the reaction, as described in section 4.2.2 is obtained.

## 4.3.2.2 Effect of moisture

Conventional Friedel-Crafts catalysts are extremely moisture sensive. The newly commercialised heterogeneous catalyst, clayzic also suffers from this drawback. Hence, moisture sensitivity of the catalysts was checked by saturating the catalyst and substrate with moisture and conducing the reaction as usual. The observations are presented in figure 4.3.2.1. Presence of benzyl chloride makes the catalyst indifferent to moisture. Percentage conversion does not alter much but product selectivity changes a good deal. Initial formation of $p$-DMDPM increases in presence of moisture. However, $p$-DMDPM selectivity at cent percent conversion of benzyl alcohol is much low in presence of moisture, than in its absence.
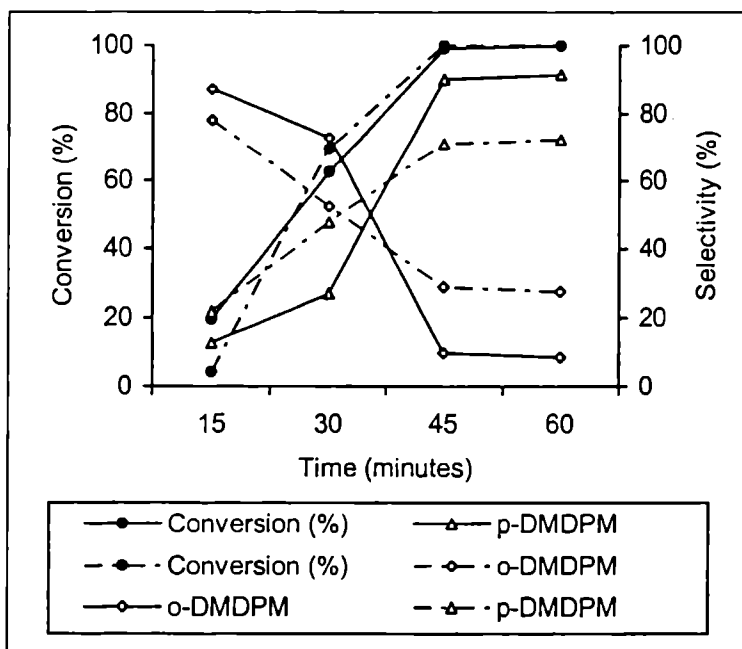


Figure 4.3.2.1. Effect of moisture on activity and product selectivity.

Temperature- 130°C, $o$-xylene/BA- 10, catalyst/BA- 0.0859, BA/BC- 2

(* Dotted lines refer to moisture adsorbed samples)

The data for moisture studies give further confirmation to preferential adsorption of benzyl alcohol to catalyst active sites. Moisture, which gets adsorbed to catalyst active site is displaced by benzyl alcohol molecule when benzyl chloride competes for the position. In the absence of benzyl chloride, this does not occur (refer 4.2.2.2). o-DMDPM is proposed to be formed by the preferential adsorption of substrate molecule to catalyst active site[35]. Moisture present in active sites prevent the interaction of substrate molecule with catalyst and hence increased p-DMDPM selectivity at initial stages. As time goes by, substrate molecules displace the water molecules present in active sites and this explains the better selectivity to o-DMDPM.

## 4.3.3 EFFECT OF REACTION VARIABLES

The reaction conditions play crucial role in determining catalytic activity as well as selectivity pattern for any reaction. Consequently, the influence of various reaction conditions like time, temperature, catalyst concentration, substrate-reactant ratio etc on the reaction was checked by taking FeAl PM as reference catalyst.

### 4.3.3.1 Effect of temperature

The influence of temperature on single pot alkylation of o-xylene with benzyl alcohol and benzyl chloride was investigated from 110°C to refluxing temperature. The results are tabulated in table 4.3.3.1.

| Temperature (°C) | Conversion (%) | Selectivity (%) | |
|---|---|---|---|
| | | o-DMDPM | p-DMDPM |
| 110 | 10.2 | 34.5 | 65.5 |
| 120 | 30.2 | 56.8 | 43.2 |
| 130 | 62.5 | 72.9 | 27.1 |
| gentle reflux | 100 | 85.6 | 14.4 |

Table 4.3.3.1 Effect of temperature.

o-xylene/BA- 10, time- 30 minutes, catalyst/BA- 0.0859, BA/BC- 2

Increase in reaction temperature has a boosting effect on catalytic efficiency. Cent percent conversion of benzyl alcohol is obtained in 30 minutes on gentle reflux. The p- product selectivity decreases with increase in temperature.

The linear increase in catalytic activity with temperature can be assigned to speedy desorption of the benzylated product from the catalyst surface at high temperatures.  This facilitates further adsorption of reactant molecules, resulting in enhanced conversion of benzyl alcohol. The increase in activity can also be ascribed to increase in intrinsic activity of the bare catalyst surface. Owing to steric factors, p- product formation is much easier in Friedel-Crafts alkylations. O- product formation requires adsorption of substrate molecule to the catalyst active site[35]. The rate of this will be lowered at high temperatures due to speedy desorption of substrate molecules and hence decreased selectivity to o-DMDPM.

## 4.3.3.2 Effect of time

The influence of time on single pot benzylation of o-xylene is tabulated in table 4.3.3.2. The table shows that conversion (%) increases linearly with time. The p- product selectivity though negligible initially, picks up with time. It seems that p -product alone is formed at longer duration of run.

| Time (minutes) | Conversion (%) | Selectivity (%) | |
| --- | --- | --- | --- |
| | | o-DMDPM | p-DMDPM |
| 15 | 19.6 | 87.2 | 12.8 |
| 30 | 62.5 | 72.9 | 27.1 |
| 45 | 99.2 | 9.9 | 90.1 |
| 60 | 100 | 8.6 | 91.4 |

Table 4.3.3.2 Effect of time on activity

o-xylene/BA- 10, temperature- 130°C, catalyst/ BA - 0.0859, BA/BC- 2

Increase in catalytic activity with time proves the heterogeneity of reaction. The adsorption and desorption of reactants and products occur fast over the clay catalyst and hence the easy completion of reaction.

### 4.3.3.3 Effect of benzyl alcohol/benzyl chloride ratio

Presence of benzyl chloride proves to be crucial in benzylation of aromatic species with benzyl alcohol. Hence, influence of the ratio of the two reagents was checked at standard conditions. The results are given in table 4.3.3.3. From the table, it can be summarised that catalytic activity increases with benzyl chloride. Presence of co reactant favours $p$- product formation. Cent percent monoalkylated product selectivity is not altered even at high concentrations of benzyl chloride.

| BC/BA | Conversion (%) | Selectivity (%) | |
|---|---|---|---|
| | | $o$-DMDPM | $p$-DMDPM |
| 1/6 | 12.1 | 82.5 | 17.5 |
| 2/6 | 38.2 | 77.4 | 22.6 |
| 3/6 | 62.5 | 72.9 | 27.1 |
| 4/6 | 77.5 | 60.5 | 39.5 |
| 5/6 | 100 | 54.5 | 45.5 |

Table 4.3.3.3. Effect of benzyl alcohol to benzyl chloride ratio.

$o$-xylene/BA- 10, temperature- 130°C, time- 30 minutes, catalyst/BA - 0.0859

Presence of benzyl chloride and benzyl alcohol imposes competition among the two reagents. Benzyl alcohol gets preferentially adsorbed on the catalyst surface. Increase in benzyl chloride thus increases competition and hence improved activities.

### 4.3.3.4 Effect of $o$-xylene/benzyl alcohol ratio

The effect of substrate to benzylating agent ratio is demonstrated in table 4.3.3.4. Catalytic activity first increases and after an optimum ratio of 10, decreases.

However, selectivity pattern does not show much variations with change in concentration of $o$-xylene.

| $o$-xylene/BA | Conversion (%) | Selectivity (%) | |
|---|---|---|---|
| | | $o$-DMDPM | $p$-DMDPM |
| 5 | 39.8 | 84.1 | 15.9 |
| 7.5 | 60.4 | 70.1 | 29.9 |
| 10 | 62.5 | 72.9 | 27.1 |
| 12.5 | 45.6 | 79.5 | 20.5 |
| 15 | 12.5 | 90.4 | 9.6 |

Table 4.3.3.4. Effect of $o$-xylene to benzyl alcohol molar ratio.
temperature- 130°C, time- 30 minutes, catalyst/BA- 0.0859, BA/BC- 2

Since $o$-xylene is taken in excess, the reaction is supposed to follow pseudo unimolecular mechanism. Therefore the reaction should have an equivalent relation with the amount of benzyl alcohol. Thus, the catalyst is very efficient for the creation of benzyl carbocations even at high concentrations of reagent. Higher reactant molar ratios result in insufficient interaction with catalyst surface for the formation of carbocations, consequently reducing catalytic activity.

## 4.3.3.5 Effect of catalyst concentration

The influence of catalyst to benzylating agent ratio was studied at four catalyst concentrations. The results are summarised in table 4.3.3.5. The table discloses that the amount of catalyst employed, has an optimum value. Increase in catalyst concentration has a beneficial effect at low concentrations. On the other hand, high amounts of catalyst has a detrimental effect on conversion %. The product selectivity also depends on the amount of catalyst. Thus, with increase in the quantity of catalyst, $p$- product selectivity increases. However, at high catalyst concentrations, $o$- product selectivity increases.

| catalyst/BA | Conversion (%) | Selectivity (%) | |
|:---:|:---:|:---:|:---:|
| | | *o*-DMDPM | *p*-DMDPM |
| 0.0429 | 25.8 | 85.4 | 14.6 |
| 0.0859 | 62.5 | 72.9 | 27.1 |
| 0.1288 | 65.2 | 70.1 | 29.9 |
| 0.1717 | 37.4 | 81.2 | 18.8 |

Table 4.3.3.5. Effect of catalyst concentration

*o*-xylene/BA- 10, temperature- 130°C, time- 30 minutes, BA/BC- 2

Increase in conversion % with catalyst concentration provides evidence for the heterogeneity of reaction. Thus, only a small amount of the catalyst is required. High concentrations causes slow diffusion and desorption of products, thus causing pore blocking of the catalyst. Increase in reaction rate enhances *p*- product concentration. *O*-DMDPM is proposed to be formed by adsorption of substrate to catalyst active site and hence, increased production of *o*- product at high catalyst concentrations.

## 4.3.4 MECHANISM OF THE REACTION

Yadav *et.al* formulated a mechanism to account for the inversion phenomenon observed in single pot alkylation of toluene with benzyl chloride and benzyl alcohol[51]. It was proposed that benzyl alcohol gets preferentially adsorbed on the acid site of catalyst and forms a benzyloxonium species. The interaction of the lone pair of electrons associated with chlorine in benzyl chloride then forms a polar complex with the species leading to the formation of a super electrophile. This species then affects the alkylation of toluene at a much faster rate than when benzyl alcohol is present alone.

A similar mechanism can explain the observed facts in our study. In the single pot alkylation of *o*-xylene with benzyl alcohol and benzyl chloride, competition

occurs between the two reagents. Benzyl alcohol gets the upper hand and gets adsorbed on catalyst active sites. Benzyl carbocations are formed according to the usual Friedel-Crafts mechanism. The substrate, due to the presence of two electron releasing methyl groups also gets attached to the catalyst surface. Alkylation occurs preferentially on *o*- position considering steric factors and hence increased concentrations of *o*- product at initial stages (refer 4.2.4).

## 4.3.5 CONCLUSIONS

The various points that can be summarised from the foregoing discussion are,

- ❖ Single pot benzylation of *o*-xylene with benzyl chloride and benzyl alcohol occurs efficiently over the prepared clay catalysts with cent percent monoalkylated product selectivity. This can be attributed to the shape selective nature of the pillared clay.

- ❖ No correlation could be obtained between activity and intrinsic acidity of catalysts.

- ❖ Metal leaching and moisture adsorption studies confirm the preferential adsorption of benzyl alcohol to catalyst active sites. The prepared catalysts are not moisture sensitive.The reaction occurs by a truly heterogeneous mechanism.

- ❖ Reaction variables like time, temperature, substrate to benzyl alcohol ratio, catalyst concentration and ratio of the two benzylating agents had profound influence on catalytic activity. The observed activities and product selectivity pattern can be well explained in terms preferential adsorption mechanism of benzyl alcohol.

- ❖ In the absence of benzyl chloride, preferential formation of *p*-DMDPM occurs where as in its presence *o*-DMDPM is formed first.

## 4.4 *TERT-* BUTYLATION OF PHENOL

Alkylation of hydroxy aromatic derivatives to prepare alkyl substituted phenols is an important area of fine chemical synthesis[51,52]. *Tert*-butylation of phenol is a key reaction in this category as the products, *tert*-butyl phenols (TBP) find wide variety of applications in industry[53,54]. 2-TBP is used for the synthesis of antioxidants and agrochemicals. 4-TBP is used on a large scale for the production of phenol formaldehyde resins, used as binders in paints and varnishes and calixeranes used as clathrates. 4-TBP find extensive applications as stabilisers in rubber and chlorinated hydrocarbons, chain length regulator in the production of polycarbonate resins and antioxidants. 2,4-DTBP is expansively used in the production of UV absorbers and stabilisers and is an indispensable building block in high molecular mass light protection agents and antioxidants.

Numerous studies have been reported on *t*-butylation of phenol, both in homogeneous and heterogeneous using several acid catalysts like $H_2SO_4$, $H_3PO_4$[55], arene sulphonic acid and cation exchange resins[56]. However, homogeneous catalysts have difficulties such as tedious work up for the separation of catalyst and are corrosive. On the other hand, cation exchange resins cannot be used at higher temperatures. Therefore, in recent years, considerable attention has been focussed on using heterogeneous catalysts for the reaction.

*T*-butylation of phenol just like alkylation of any other aromatic compound follows Friedel-Crafts mechanism. A schematic representation of the reaction is given in scheme 4.4. Depending on the nature of catalyst, alkylation of phenol can take place at the oxygen (O- alkylation) and/or at the ring carbon atoms (C- alkylation). In C- alkylation, the presence of phenolic group kinetically favours *ortho* alkylation[57,58]. However, due to steric hindrance, thermodynamically unfavoured *o*- isomer isomerises to less hindered partially kinetically favourable *p*- isomer[59].
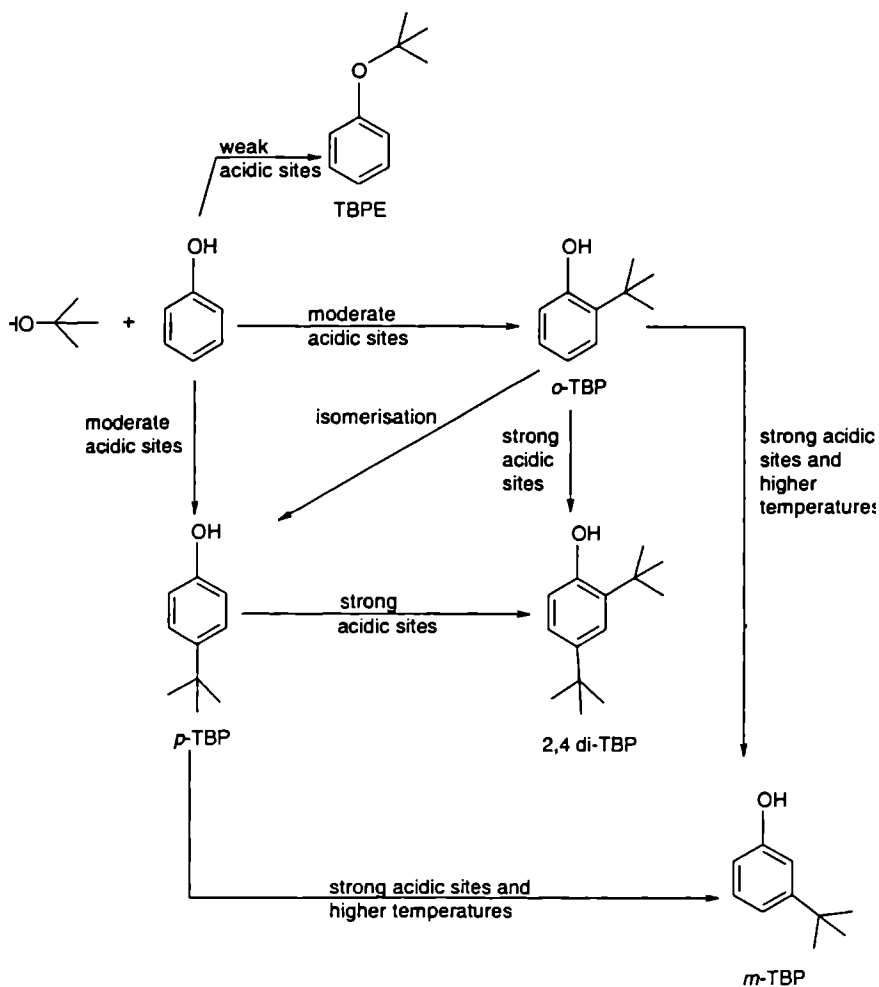
Scheme 4.4. Alkylation of phenol with *t*-butyl alcohol

Selectivity of the product depends on the nature of acidic sites pre:
:ts as well as reaction temperature. Thus, the weakly acidic catalyst lil
⁺ ion exchanged zeolite-Y leads to oxygen alkylated product (phen)
TBPE) as major product[60]. The strong acidic catalyst like zeolite β an
·atures favour carbon alkylated product, *m*-TBP by secondary isomerisa
tially formed *o*- and *p*- isomers[61,62]. On the other hand, moderately

catalysts like ZSM-12[63], SAPO-11[64] and zeolite Y[65] are suitable for the formation of *p-* isomer. A direct relationship between catalytic activity and basicity of the catalysts was obtained over hydrotalcites[66].

Tert-butylation of phenol was done in vapour phase. In a typical experiment, the reactor was charged with the activated catalyst, sandwiched between silica beads. The liquid reactants were fed into the reactor by a syringe pump. The products of the reaction were collected downstream from the reactor at specified intervals and analysed by gas chromatography. The percentage conversion (wt%) is the total percentage of phenol transformed into products. The selectivity to a product is the amount of that product divided by total amount of products, expressed in percentage. The reaction has been studied extensively using the prepared catalysts. The observations of the study and the conclusions drawn from it are given under two headings; I) Catalytic activity of various systems II) Effect of reaction variables.

## 4.4.1 CATALYTIC ACTIVITY OF VARIOUS SYSTEMS

We attempted to determine how the pillared clays as well as their transition metal exchanged analogues catalysed *tert*-butylation of phenol. A detailed investigation of conversion % and product selectivity on the amount and availability of surface acid sites also is included.

### 4.4.1.1 Iron pillared systems

Table 4.4.1.1 depicts the activity and selectivity pattern exhibited by Fe PM and its transition metal exchanged analogues. Fe PM proves to be efficient catalyst for *tert*-butylation of phenol. Monoalkylated product selectivity of 96.4% is obtained. Incorporation of transition metal decreases the activity except for Ni/Fe PM. The increase in activity for nickel exchanged catalyst is due to increase in disubstituted product concentration. The selectivity for monoalkylated product does not alter much from the parent pillared system for other catalysts in the series.

| Catalyst | Conversion (%) | Selectivity (%) | |
| --- | --- | --- | --- |
| | | TBP | 2,4 di TBP |
| V/Fe PM | 32.2 | 93.2 | 6.8 |
| Mn/Fe PM | 39.6 | 89.2 | 10.8 |
| Co/Fe PM | 25.2 | 91.7 | 8.3 |
| Ni/Fe PM | 58.1 | 78.6 | 21.4 |
| Cu/Fe PM | 34.2 | 94.9 | 5.1 |
| Zn/Fe PM | 46.1 | 94.4 | 5.6 |
| Fe PM | 54.0 | 96.4 | 3.6 |

Table 4.4.1.1. Activity of iron pillared systems for *tert*-butylation of phenol. Phenol/*tert*-butyl alcohol- 1/3, temperature- 200°C, WHSV- 2.6h$^{-1}$, TOS- 2h

The *tert*-butylation of phenol occurs over acidic sites present in the catalyst[67]. Hence an attempt was made to correlate catalytic activity of the systems with total amount of acid sites present in iron pillared systems. Figure 4.4.1.1 unambigously shows that the reaction occurs over acidic sites. The superior activity of Ni/Fe PM can be attributed to higher amount of acidic sites on the catalyst surface.

Product selectivity shown by a catalyst depends on acid site distribution on catalyst surface. The di substituted product is suggested to be formed by the alkylation of monoalkylated product. Zhang *et.al* proposed that strong acid sites are required for the formation of 2,4 di TBP[66]. Hence selectivity of di substituted product was correlated to the amount of strong acid sites, obtained from $NH_3$-TPD measurements (Figure 4.4.1.2). Enhanced formation of 2,4 di TBP over Ni/Fe PM and Mn/Fe PM can be traced to higher amount of strong acid sites.
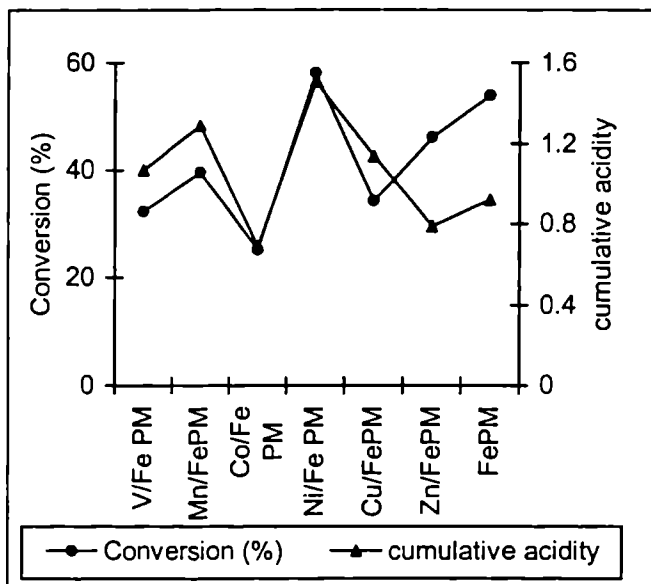
Figure 4.4.1.1. Correlation of conversion (%) on the cumulative acidity
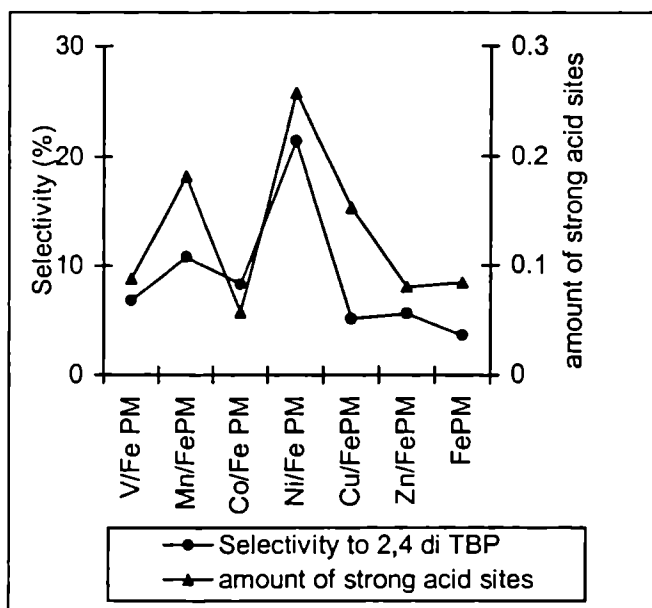


Figure 4.4.1.2. Correlation of 2,4 di TBP selectivity on the amount of strong acid sites.

### 4.4.1.2 Aluminium pillared systems

The catalytic activity of aluminium pillared systems were tested for t-butylation of phenol at standard reaction conditions. The results are tabulated in table 4.4.1.2. All aluminium pillared catalysts exhibit mediocre activity towards the reaction with the exception of Ni/Al PM. However, high concentrations of the di substituted product is obtained over these catalysts.

| Catalyst | Conversion (%) | Selectivity (%) | |
|---|---|---|---|
| | | TBP | 2,4 di TBP |
| V/Al PM | 19.9 | 80.3 | 19.7 |
| Mn/Al PM | 14.1 | 85.7 | 14.3 |
| Co/Al PM | 16.2 | 89.2 | 10.8 |
| Ni/Al PM | 51.2 | 78.8 | 21.2 |
| Cu/Al PM | 16.5 | 92.9 | 7.1 |
| Zn/Al PM | 15.9 | 92.5 | 7.5 |
| Al PM | 14.4 | 84.5 | 15.5 |

Table 4.4.1.2. Activity of aluminium pillared systems for tert-butylation of phenol. Phenol/tert-butyl alcohol- 1/3, temperature- 200°C, WHSV- 2.6h$^{-1}$, TOS- 2h

The inferior activity of the aluminium pillared sytems can be ascribed to the low surface area of the catalysts. The disubstituted products may be formed in active sites in the outer surface of catalyst.

Figure 4.4.1.3 illustrates the dependence of cumulative acidity on catalytic activity of aluminium pillared series. Though inferior in activity, the exhibited activity is almost proportional to the total acidity of the systems. Ammonia being small in size, can titrate with acid sites situated at the inner pores also. This may be the reason for the slight variations in the correlation.
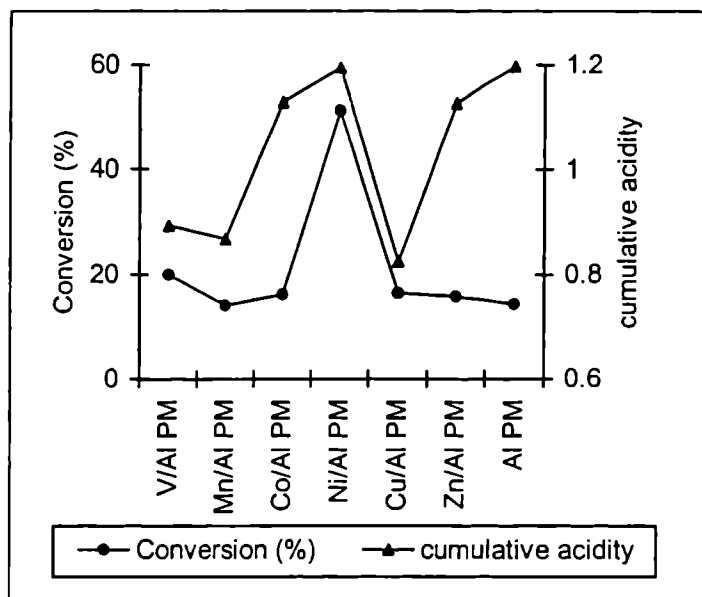
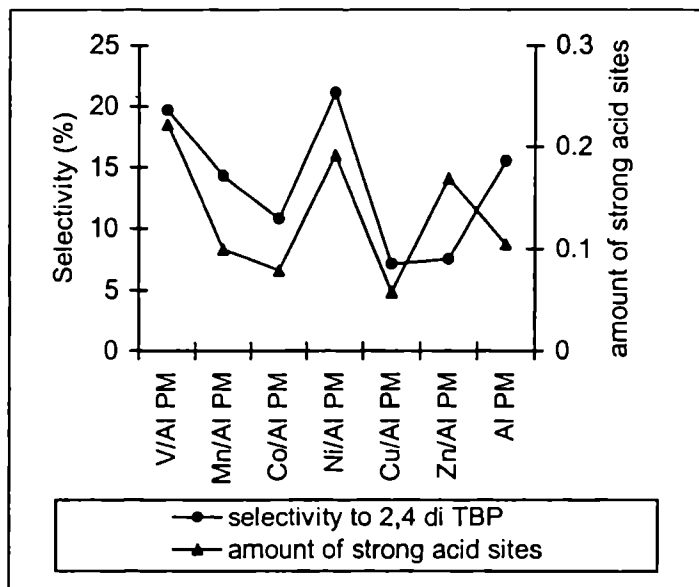Figure 4.4.1.3. Dependence of catalytic activity on total acidity.



Figure 4.4.1.4. Dependence of 2,4 di TBP on the amount of strong acid sites.

A direct dependence of di substituted product selectivity on the amount of strong acid sites is obtained (Figure 4.4.1.4). The strong sites are present mainly in the outer surface of the clay. Aluminium in threefold coordination, perhaps occurring at an edge, or arising from a Si-O-Al rupturing dehydroxylation of the Brönsted site, would correspond to Lewis site. An octahedral $Al^{3+}$, located at a platelet edge, also function as Lewis site after thorough dehydration. Hence, the strong sites which are present mainly in the outer surface, catalyses conversion of produced monoalkylated products to di substituted ones.

### 4.4.1.3 Iron Aluminium pillared systems

The activity profiles of FeAl PM and its transition metal exchanged analogues at standard conditions are demonstrated in table 4.4.1.3. The parent pillared clay exhibits phenol conversion of 32.3% with high selectivity towards di substituted product. All systems in the series are efficient catalysts towards $t$-butylation of phenol with the exception of Ni/FeAl PM. Higher concentrations of 2,4 di TBP is obtained in all cases.

| Catalyst | Conversion (%) | Selectivity (%) | |
|---|---|---|---|
| | | TBP | 2,4 di TBP |
| V/FeAl PM | 45.3 | 84.7 | 15.3 |
| Mn/FeAl PM | 48.5 | 75.6 | 24.4 |
| Co/FeAl PM | 48.3 | 91.7 | 8.3 |
| Ni/FeAl PM | 16.6 | 70.1 | 29.1 |
| Cu/FeAl PM | 45.6 | 85.6 | 14.4 |
| Zn/FeAl PM | 51.0 | 68.8 | 31.2 |
| FeAl PM | 32.3 | 71.2 | 28.8 |

Table 4.4.1.3. Activity of iron aluminium pillared systems for $tert$-butylation of phenol.
Phenol/$tert$-butyl alcohol- 1/3, temperature- 200°C, WHSV- $2.6h^{-1}$, TOS- 2h

The high activity of the mixed pillared systems can be credited to their high surface area. The reactants have nonrestricted access to active sites resulting in better yield. The high selectivity towards dialkylated product also confirms this observation. However, no correlation could be obtained between total acidity and conversion %.

Figure 4.4.1.5 reveals the dependence of di substituted product selectivity on the amount of strong acid sites. Thus, strong acidity plays a key role in the alkylation of monobutylated product. Lower amounts of strong acid sites on catalyst surface of Co/FeAl PM and Cu/FeAl PM explains the diminutive selectivity towards 2,4 di TBP.

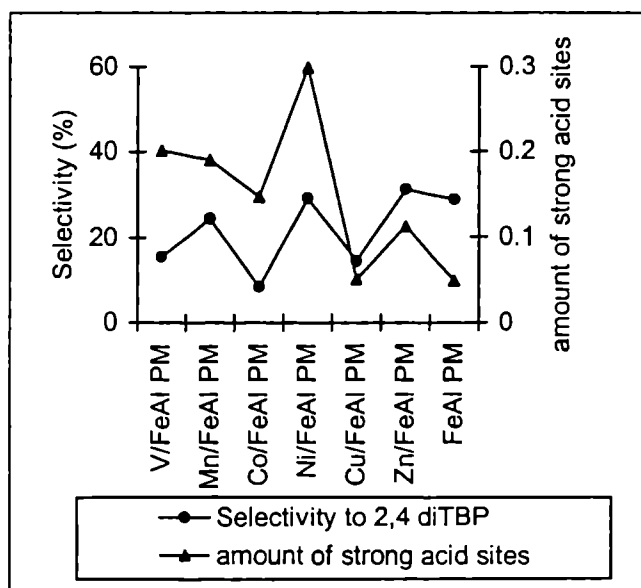

Figure 4.4.1.3. Dependence of 2,4 di TBP on the amount of strong acid sites.

## 4.4.2 EFFECT OF REACTION VARIABLES

The reaction conditions play an imperative role in deciding the catalytic activity and product distribution. Hence, the effect of operating parameters such as

reaction temperature, molar ratio, weight hourly space velocity and time on stream has been the subject of meticulous investigation using Fe PM as reference catalyst.

### 4.4.2.1 Effect of temperature

The effect of temperature on $t$-butylation of phenol was studied by performing a set of reactions in the temperature range of 160-240°C at an interval of 20°C. The activity and selectivity pattern obtained are presented in table 4.4.2.1. Temperature plays a vital role in $t$-butylation of phenol. Increase in temperature increases phenol conversion and selectivity to monoalkylated product. Maximum conversion occurs at 200°C, after which, activity decreses with no apparent change in product selectivity.

| Temperature (°C) | Conversion (%) | Selectivity (%) | |
| :---: | :---: | :---: | :---: |
| | | TBP | 2,4 di TBP |
| 160 | 37.5 | 65.0 | 35.0 |
| 180 | 48.2 | 74.3 | 25.7 |
| 200 | 54.0 | 96.4 | 3.6 |
| 220 | 31.7 | 95.9 | 4.1 |
| 240 | 23.2 | 97.7 | 2.3 |

Table 4.4.2.1. Effect of temperature on activity.

Phenol/$tert$- butyl alcohol- 1/3, WHSV- 2.6h$^{-1}$, TOS- 2h.

The decrease in phenol conversion at high temperatures can be due to dealkylation of di substituted product. Similar observations were reported by Subramanian $et.al$[64]. Decrease in conversion can also be due to the side reaction (oligomerisation) of $t$-butyl alcohol at high temperatures as suggested by Liu $et.al$[69].

### 4.4.2.2 Effect of molar ratio

The ratio of the reactants can be very crucial in deciding the result of a reaction. Hence the effect of molar ratio of the reactants on phenol conversion was

scrutinised in a wide range of phenol/t-butyl alcohol ratios from 2 to 0.2. The results are tabulated in table 4.4.2.2. The reactant molar ratio has profound influence on catalytic activity as well as product selectivity. At high phenol concentrations, conversion to butyl phenols is less. Increase in t-butyl alcohol in the reaction mixture increases phenol conversion as expected. The activity reduces at still higher t-butyl alcohol concentrations. The selectivity to di substituted product is high at large concentrations of t-butyl alcohol.

| Phenol:TBA | Conversion (%) | Selectivity (%) | |
| --- | --- | --- | --- |
| | | TBP | 2,4 di TBP |
| 2:1 | 30.2 | 98.3 | 1.7 |
| 1:1 | 48.7 | 93.5 | 6.5 |
| 1:2 | 44.0 | 92.9 | 7.1 |
| 1:3 | 54.0 | 96.4 | 3.6 |
| 1:5 | 41.4 | 86.3 | 13.7 |

Table 4.4.2.2. Effect of molar ratio on catalytic activity.
Temperature- 200°C, WHSV- 2.6 h$^{-1}$, TOS- 2h

Low conversion of phenol at phenol/t-butyl alcohol ratio of 2 can be attributed to high amount of phenol. It has been demonstrated that polar molecules such as methanol and higher alcohols compete with phenol for adsorption sites, and with increasing molar excess of alkylating agent, phenol conversion increases[70]. Increase in di substituted product at high t-butyl alcohol ratios can be attributed to high concentrations of t-butyl carbenium ions in the reaction mixture, bringing about alkylation of monobutylated product.

## 4.4.2.3 Effect of weight hourly space velocity

Feed rate is another important parameter that influences the activity as well as selectivity pattern in gas phase reactions. The results of the variation in activity

with weight hourly space velocity at four different space velocities have been investigated. The results are given in table 4.4.2.3. Increase in space velocity increases the phenol conversion in *t*-butylation of phenol. Maximum conversion is shown at space velocity of $2.6h^{-1}$, whereafter, conversion decreases. Thus, there is an optimum contact time for *t*-butylation to occur over clays. The selectivity to monoalkylated product also shows a decrease first followed by an increase.

| WHSV ($h^{-1}$) | Conversion (%) | Selectivity (%) | |
| --- | --- | --- | --- |
| | | TBP | 2,4 di TBP |
| 1.7 | 44.5 | 88.3 | 11.7 |
| 2.6 | 54.0 | 96.4 | 3.6 |
| 3.5 | 33.8 | 94.1 | 5.9 |
| 4.3 | 34.0 | 89.1 | 10.9 |

Table 4.4.2.3. Effect of weight hourly space velocity on catalytic activity

Phenol/*tert*-butyl alcohol- 1/3, Temperature- 200°C, TOS- 2h

The reduction in conversion at high space velocities can be simply due to low contact time for reactant molecules. On the other hand, low conversion at low space velocity can be attributed to dealkylation of butyl phenols to phenol as well as coke formation at higher contact time. Sakthivel *et.al* also reported in similar lines[67].

## 4.4.2.4 Effect of time on stream

Another set of experiments were conducted to evaluate the stability of the systems with reaction time. In order to obtain a trend in the deactivation of catalyst, the reaction was carried out continously for 5 hours (Table 4.4.2.4). From the table it is clear that the prepared clay catalysts show appreciable activity for the reaction even after 5 hours. The selectivity to di substituted product increases with time on stream.

| Time on stream (h) | Conversion (%) | Selectivity (%) | |
| --- | --- | --- | --- |
| | | TBP | 2,4 di TBP |
| 1 | 52.5 | 97.3 | 2.7 |
| 2 | 54.0 | 96.4 | 3.6 |
| 3 | 53.8 | 94.1 | 5.9 |
| 4 | 51.2 | 92.1 | 7.9 |
| 5 | 50.0 | 91.5 | 8.5 |

Table 4.4.2.4. Effect of time on stream on activity.

Phenol/tert-butyl alcohol- 1/3, Temperature- 200°C, WHSV- 2.6h$^{-1}$

The slight decrease in catalytic activity with increase in time on stream can be due to deactivation of active sites. This can be attributed to either coke formation or poisoning of active sites with products. However, poisoning of active sites by products seem to be more feasible because there is an increase in di substituted product with increase in time. It has been reported that disubstituted product is formed by further alkylation of o- and p- t-butyl phenols.

## 4.4.3 MECHANISM OF THE REACTION

T-butylation of phenol just like alkylation of any other aromatic compound follows Friedel-Crafts mechanism. The generally accepted mechanism for the reaction is that the carbenium ion interacts with adsorbed phenol forming the pi complex, which then rearranges to sigma complex by the electrophilic attack at a ring carbon atom. The sigma complex on proton elimination gives t-butyl phenol. It has been suggested that the Brönsted acid site interacts with the pi cloud of aromatic ring bringing the molecule parallel to the surface[71,72]. This allows alkylation at p- position. Also it has been reported that steric hindrance due to the substitution of bulkier t-butyl group at ortho position enhances para selectivity[61]. The disubstituted product is formed by the alkylation of o- and p- tert butyl phenols.

## 4.4.5 CONCLUSIONS

The various points that can be summarised from a systematic study of the catalytic activity and product selectivity towards *t*-butylation of phenol are,

- ❖ Iron pillared and mixed iron pillared sytems are efficient catalysts for *t*-butylation of phenol in the gas phase.

- ❖ In spite of high acidity, aluminium pillared systems show inferior activity. This can be due to the lower surface area of these catalysts.

- ❖ Catalytic activity of the systems can be correlated to cumulative acidity of the catalysts.

- ❖ Di substituted product selectivity exhibited direct correlation with amount of strong acid sites.

- ❖ The reaction is highly sensitive towards reaction temperature. An optimum temperature of 200°C was detected.

- ❖ Increase in amount of *t*-butyl alcohol increases the conversion.

- ❖ An optimum feed rate of 2.6 h$^{-1}$ is required for maximum conversion of *t*-butyl alcohol as well as monoalkylated product selectivity.

- ❖ The prepared clay catalysts show appreciable activity even after 5 hours. This can be ascribed to the stability of active sites under the reaction conditions.

# REFERENCES

1. D.E James, N.R Nowicki, US Patent 4,822,527 (1989).

2. L.A DeWitt, H Su, C.T Mathew, US Patent 5,723,676 (1998).

3. G.A Olah, "Friedel-Crafts Chemistry", Wiley, New York (1973).

4. P Ratnaswamy, A.P Singh, S Sharma, *Appl. Catal. A: Gen.*, 135, 25 (1996).

5. F.P DeHaan, W.H Chan, J Chang, D.M Ferrera, L.A Wainschel., *J. Org. Chem.*, 51, 1591 (1986).

6. V.R Choudhary, S.K Jana, B.P Kiran, *J. Catal.*, 192, 257-261 (2000)

7. J.H Clark, S.R Cullen, S.J Barlow, T.W Bastock, *J. Chem. Soc. Perkin Trans.*, 2, 1117 (1994).

8. J.H Clark, A.P Kybett, D.J Macquerrie, S.J Barlow, P Landan, *J. Chem. Soc. Chem. Commun.*, 1353 (1989).

9. C.N Rhodes, D.R Brown, *J. Chem. Soc. Faraday Trans.*, 89, 1387 (1993).

10. J.H Clark, J.H Macquerrie, *Chem. Commun.*, 853 (1998).

11. B.M Choudhary, M.L Kantam, M Sateesh, K.K Rao, P.L Santhi, *Appl. Catal A: Gen.*, 149, 257-264 (1997).

12. A.B Deshpande, A.R Bajpai, S.D Samant, *Appl. Catal. A: Gen.*, 209, 229-235 (2001).

13. K.R Sabu, R Sukumar, R Rekha, M Lalithambika, *Catal. Today*, 49, 321-326 (1999).

14. B.M Choudhary, B.P.C Rao, N.S Chowdri, M.L Kantam, *Catal. Commun.*, 3, 363-367 (2002).

15. K Okumura, K Nishigaki, M Niwa., *Microporous. Mesoporous Mater.*, 44-45, 509-516 (2001).

16. X Chu, G.K Chuah, S Jaenicke, *Microporous. Mesoporous Mater.*, 53, 153-161 (2002).

17. A.M.F Bidart, A.P.S Borges, L Nogueira, E.R Lachter, C.J.A Mota, *Catal. Lett.*, 75, 155-157 (2001).

18. S Jun, R Ryoo., *J. Catal.*, 185, 237-243 (2000).

19. A.P Singh, B Jacob, S Sugunan, *Appl. Catal. A: Gen.*, 174, 51-60 (1998).

20. V.R Choudhary, S.K Jana, *J. Mol. Catal. A: Chem.*, 180, 267-276 (2002).

21. S.P Ghorpade, V.S Dharsane, S.G Dixit, *Appl. Catal. A: Gen.*, 166, 135-142 (1998).

22. R.P Singh, R.M Kamble, K.L Chandra, P Saravanan, V.K Singh, *Tetrahedron Lett.*, 57, 241-247 (2001).

23. S Sebti, R Tahir, R Nazih, S Boulaajaj, *Appl. Catal. A: Gen.*, 218, 25-30 (2001).

24. S.N Koyande, R.G Jaiswal, R.V Jayaram, *Ind. Eng. Chem. Res.*, 37, 98 (1998).

25. J Miller, M Goodchild, J.L Lakshmi, D Wails, J.S Hartman, *Catal. Lett.*, 63, 199 (1999).

26. K.B Sherly, V.T Bhatt, *React. Kin. Catal. Lett.*, 75, 239-243 (2002).

27. T Cseri, S Bekassy, F Figueras, S Rizner, *J. Mol. Catal. A: Chem.*, 98, 101-107 (1995).

28. D Rohan, B.K Hodnett, *Appl. Catal. A: Gen.*, 151, 409 (1997).

29. B.J Wittingtton, J.R Anderson, *J. Phy. Chem.*, 97, 1032 (1993).

30. Y Deng, C Lettmann, W.F Maier, *Appl. Catal A: Gen.*, 214, 31-45 (2001).

31. K Arata, H Nakamura, M Shouji, *Appl. Catal. A: Gen.*, 197, 213 (2000).

32. P Botella, A Corma, J.M Lopez Nieto, S Valentia, R Jacquot, *J. Catal.*, 195, 161 (2000).

33. B Coq, V Gourves, F Figueras, *Appl. Catal. A: Gen.*, 100, 69 (1993).

34. N He, S Bao, Q Xu, *Appl. Catal A: Gen.*, 169, 29-36, (1998).

35. Manju Kurian, S Sugunan, *Ind. J. Chem.*, 42, 2480-2486 (2003).

36. G.D Yadav, T.S Thorat, P.S Khumbar, *Tetrahedron Lett.*, 34, 529 (1993).

37. K.R Sabu, K.V.C Rao, C.G.R Nair, *Bull. Chem. Soc. Jpn.*, 64, 1920 (1991).

38. K.R Sabu, K.V.C Rao, C.G.R Nair, *Bull. Chem. Soc. Jpn.*, 64, 1926 (1991).

39. P Laszlo, *Pure Appl. Chem.*, 62, 2027 (1990).

40. P Laszlo, *Acc. Chem. Res.*, 19, 121 (1986).

41. R Commanduer, N Berger, P Jay, J Kervannal, EP 0,442,986 (1991).

42. R.D Laura, *Clay Miner.*, 11, 331 (1976).

43. T.J Pinnavia, *Science*, 220, 365 (1983).

44. H.H.P Yiu, D.R Brown, *Catal. Lett.*, 56, 57-64 (1998).

45. J.P Rupert, W.T Granquist, T.J Pinnavia, " Chemistry of Clays and Clay Minerals", A.C.D Newman (ed) (1987).

46. P Laszlo, M.T Montaufier, *Tetrahedron Lett.*, 32, 1561-1564 (1991).

47. P Laszlo, A Coenelis, C Dony, K.M Nsunda, *Tetrahedron Lett.*, 32, 2903-2904 (1991).

48. G.D Yadav, T.S Thorat, P.S Khumbhar, *Tetrahedron Lett.*, 34, 529-532 (1993).

49. G.D Yadav, T.S Thorat, *Tetrahedron Lett.*, 37, 5405-5408 (1996).

50. G.D Yadav, J.J Nair, *Microporous. Mesoporous Mater.*, 33, 1-48 (1999).

51. R Anand, R Maheswari, K.U Gore, V.R Chumbale, *Catal. Commun.*, 3, 321-326, (2002).

52. "Ullmann's Encyclopeadia of Industrial Chemistry", B Elvers, S Hawkins, G Schulz (eds), 5th ed, 19, 325-341.

53. G Kamalakar, M.R Prasad, S.J Kulkarni, K.V Raghavan, *Microporous. Mesoporous Mater.*, 52, 151-158 (2002).

54. A Knop, L.A Pilato, "Phenolic Resins Chemistry", Springer, Berlin (1985).

55. J.F Lorenc, G Lambeth, W Scheffer, "Kirk-Othmer Encyclopedia of Chemical Technology", M.H Grant, J.I Kroshwitz (eds), 4th ed., Wiley, New York (1992).

56. P.B Venuto, *Microporous Mater.*, 2, 297 (1994).

57. B Love, J.T Messangale, *J. Org. Chem.*, 22, 642 (1957).

58. A.J Kolka, J.P Napolitano, G.G Elike, *J. Org. Chem.*, 21, 712 (1956).

59. E.A Goldsmith, M.J Schlatter, W.J Toland, *J. Org. Chem.*, 23, 1871 (1958).

60. A Corma, H Garcia, J Primo, *J. Chem. Res.* (S), 40 (1988).

61. R.F Parton, J.M Jacobs, D.R Huybrechts, P.A Jacobs, *Stud. Surf. Sci. Catal.*, 46, 163 (1989).

62. N.S Chang, C.C Chen, S.J Chu, P.Y Chen, T.K Chuang, *Stud. Surf. Sci. Catal.*, 46, 163 (1989).

63. C.D Chang, S.D Hellring, US Patent 5288927 (1994).

64. S Subramanian, A Mitra, C.V.V Satyanarayana, D.K Chakrabarty, *Appl. Catal. A,* 159, 229 (1997)

65. S Namba, T Yashima, Y Itaba, N Hara, *Stud. Surf. Sci. Catal.,* 5, 105 (1980).

66. A.H Padmasri, V.D Kumari, P.K Rao, "Recent trends in Catalysis", V Murugesan *et.al* (eds), Narosa Publishing house, New Delhi (1999)

67. A Sakthivel, S.K Badamali, P Selvam, *Microporous. Mesoporous Mater.,* 39, 457-463 (2000).

68. K Zhang, H Zhang, C Huang, S Liu, D Xu, H Li, *Appl. Catal. A,* 166, 89-95 (1998).

69. Z Liu, P Moreau, F Fajula, *Appl. Catal. A,* 159, 305 (1997).

70. A Sakthivel, N Saritha, P Selvam, *Catal. Lett.,* 72, 225-228 (2001).

71. R.F Parton, J.M Jacobs, H Van Ootehem, P.A Jacobs, *Stud. Surf. Sci. Catal.,* 46, 211 (1989).

72. K Tanabe, *Stud. Surf. Sci. Catal.,* 20 (1985).

# 5

# PHENOL HYDROXYLATION

*The strong demand in the chemical industry for phenolic compounds have led to the development of improved catalyst based technologies for partial oxidation reactions. Moreover, phenol is a major water pollutant. The complete oxidation of phenol and other organic compounds in the wastewater stream is achieving considerable attention in recent years. The potential application of pillared clays in the oxidation of phenol to catechol and hydroquinone was studied in aqueous medium. The influence of various reaction conditions was thoroughly studied. A plausible mechanism for the reaction, considering the various inferences has also been proposed.*

## 5.0 INTRODUCTION

Water is an increasingly coveted commodity. As a result, regional and planetary policies are being implemented for the effective and parsimonious exploitation of water resources. Nevertheless, management of toxic and hazardous waste water streams is still a perennial problem facing industries, governments and environmental and health protection agencies. Wastewater effluents that are too dilute to incinerate and yet too toxic to biotreat can suitably be dealt with by catalysed wet oxidation (CWO). The recourse with solid catalysts offers a suitable technological alternative to conventional homogeneously catalysed or noncatalytic routes because the treatment takes place at much milder conditions and the catalyst can be easily recovered and reused[1]. Among catalysed wet oxidations, Wet Peroxide Oxidation (WPO) is preferred because the active oxygen content of hydrogen peroxide is much higher than other oxidants. Water is the only bye product formed and the oxidant is inexpensive. Also, aqueous hydrogen peroxide is a stable reagent, provided it is handled and stored in the proper manner[2].

Phenol is a major water pollutant. The presence of phenol even in trace amounts has been proven fatal to living beings. Removal of phenol from effluents can be brought about by oxidation with hydrogen peroxide. An added advantage of the reaction is that oxidation of phenol produces catechol and hydroquinone, two important intermediates in agrochemical and fine chemical industries. Catechol and hydroquinone are also used as photographic developers and antioxidants. Conventionally, $HClO_4$-$H_3PO_4$ and Fe(III)/Co(II) catalysts were used for oxidation of phenol[3,4]. But obvious shortcomings of these homogeneous catalysts prevent their wide use in diphenol production.

Titanium silicate-1 (TS-I), a titanium containing zeolite was found superior to other catalysts for phenol hydroxylation, due to decreased formation of tar and polluting bye products and subsequently the method was commercialised. Extensive

study of the reaction has been conducted using this catalyst. The extent of phenol hydroxylation over TS-I is determined by the pore geometry, external surface Ti sites, crystal size of Ti containing molecular sieve and the nature of the solvent. Smaller pore dimensions led to decreased conversion and enhanced selectivity to hydroquinone. The phenol hydroxylation was strongly diffusion limited and small crystals are preferred[5]. Hydroquinone was formed inside the zeolite channels, where as catechol and tarry products were produced in the external surface[6]. Thangaraj et.al observed a significant effect of solvent on product selectivity and conversion percentage. A considerable amount of benzoquinone at lower phenol conversions was also observed[7]. The higher catalytic activity of smaller particles was not caused by a larger contribution of the outer surface but by higher catalyst efficiency as a result of pore diffusion limitation[8]. Co existence of benzene or cyclohexane along with phenol improved hydroquinone selectivity and this was attributed to the coexistent bulky molecules imposing steric restriction on the transition state, which prefers products with relatively small molecular dimensions[9]. Though TS-I is an excellent catalyst for phenol hydroxylation, lack of thermal stability and somewhat complex preparation method have led researchers to develop other cheaper catalysts for the hydroxylation of phenol.

Since peroxide is used, free radical mechanism can be expected for the reaction and hence various iron and copper containing catalysts have been employed. Cu, Zn and Al bearing zeolites proved to be very efficient catalysts for oxidation of organic compounds in water, of which Cu containing zeolite was most active[10]. An appropriate amount and strength of acid sites was a prerequisite for an optimised generation of active cationic species. A novel catalyst $Cu_2(OH)PO_4$ was found to be very active towards phenol hydroxylation by $H_2O_2$. ESR spectrum of $H_2O_2$ with DMPO over this catalyst showed typical signals assigned to hydroxyl radicals suggesting that hydroxyl radicals were major active intermediates[11]. Santos et.al compared the reaction in acidic and basic media using $CuO-2(CuO).Cr_2O_3$-

198

$CrO_4Ba-Al_2O_3$, a commercial catalyst. Acidic media favoured the reaction to greater extent while an inhibitor effect of $OH^-$ anion was observed in basic media. A homogeneous contribution for the phenol oxidation rate was observed, indicative of a free radical mechanism[12]. A novel Cu-Bi-V-O complex oxide was found very active for the reaction. Investigations using ESR spin trapping technique suggested $Cu^{2+}$ species to be the major active site and hydroxyl radicals, major reaction intermediates[13]. Santos *et.al* explored the reaction using four copper based commercial catalysts and found Engelhard Cu-0203T to be the most active catalyst with good thermal and chemical stability[14]. A lower limit of catalyst leaching was observed at high catalyst concentrations. Copper modified MCM 41 catalysts confirmed the reaction to occur by a radical substitution mechanism[15].

The catalytic activities of Si MCM 41s chemically modified with iron have been evaluated and compared for hydroxylation of phenol[16]. 10-15% Fe leaching was reported. Grafting of iron was superior to coupling in Si MCM 41. Fe based complex oxides of Si and Mg exhibited high activity, selectivity, short induction period and reaction time[17]. The induction period was shortened by increase in surface area and a free radical mechanism was suggested for the reaction. Highly ordered Fe MCM-48 synthesised by mixed templation was found to be active towards phenol with high selectivity for catechol[18]. The active centres were framework isolated $Fe^{3+}$.

Pillared clays have been successfully employed for the hydroxylation of phenol. Castillo *et.al* found a relation between the amount of Brönsted acid sites and catalytic activity, in aprotic solvents like acetone using Ti pillared montmorillonites. A correlation between total acidity and over oxidation of phenol was also obtained[19]. Boudali *et.al* employed Ti pillared clays for the reaction and proposed the availability of Brönsted acid sites for better performance of the catalyst[20]. Mixed Fe-Al and Al-Cu pillared clays were employed to study the reaction by Barrault *et.al*[21,22]. In mild reaction conditions, about 80% of the initial amount of phenol was converted in 2

hours and catalyst leaching remained very low even after recycling the catalyst three times. Completely heterogeneous reaction was observed for Al-Cu pillared clays, rather than a homogenous Fenton like oxidation. Bahranowski *et.al* showed that the yield of dihydroxybenzenes was almost near to TS-I catalyst with Cu doped Al pillared clays. Experiments with change of substrate dosing indicated that adsorption and activation of phenol molecules is necessary for the reaction to occur[23].

A wide range of other catalysts has also been employed for phenol hydroxylation. These include vanadium silicate with MEL structure[24], TS-II[25], VS-2[26], TAPO-II[27] and $Pt_xAg_{1-x}MnO_2/CeO_2$[28]. A novel complex oxide, $H_xV_2Zr_2O_9H_2O$ was used and $V^{5+}$ was detected to be the active species. Recycling of catalyst did not decrease activity and conversion of phenol was found to be proportional to polarity of solvent used[29]. The heteropoly compound, $K_{0.5}(NH_4)_{5.5}[MnMo_9O_{32}].6H_2O$ showed dependence on pH when methanol was the solvent. Mn(V)Mo was detected to be the active species[30]. Transition metal incorporated ternary hydrotalcites were also employed for phenol hydroxylation with $H_2O_2$. Other oxidants like air, oxygen and *t*-butyl peroxide did not hydroxylate phenol to a significant extent due to lack of generation of active oxidant species and solubility problems[31].

The liquid phase hydroxylation of phenol was carried out in a 50 mL round bottomed flask equipped with air condenser and magnetic stirrer. 0.1g of the catalyst, preactivated at 500°C for 2 hours was added to calculated amounts of phenol and solvent. Required amounts of 30% $H_2O_2$ was added drop wise to the reaction medium and reaction ensued at specified temperatures. Reaction mixture was periodically analysed using gas chromatography at conditions specified in chapter 2. Benzoquinone was not detected in any case. Tarry products were observed in all runs. Quantitative estimation of tarry products was not pursued and conversion of phenol refers to conversion to diphenols. Thus, percentage conversion (wt%) of

phenol is the total percentage of phenol transformed into diphenols. A representation of the reaction pathways for phenol hydroxylation is given in scheme 5.1.
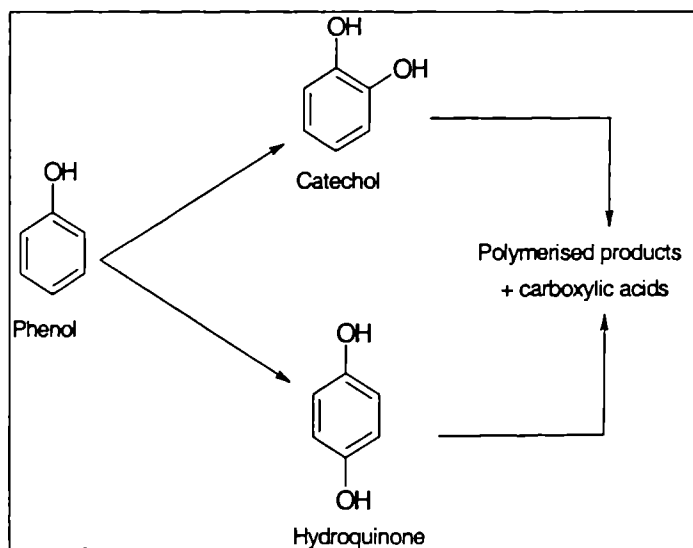


Scheme 5.1 Reaction pathways for the hydroxylation of phenol.

The objectives of the current study are to investigate the reaction pathways and associated mechanisms of the reaction and to correlate product selectivity with external as well as internal surface area of catalysts. In addition, influence of various reaction variables like time, temperature, solvent, solvent concentration and amount of oxidant have been taken into account. The observations and conclusions of the study are given under two headings; I) Catalytic activity of various systems II) Effect of reaction variables. Finally, a plausible mechanism is proposed for the reaction.

## 5.1 CATALYTIC ACTIVITY OF VARIOUS SYSTEMS

The catalytic efficiency of prepared pillared clays and their transition metal exchanged analogues for wet peroxide oxidation of phenol was investigated at

standard reaction conditions. Presence of tarry products was detected in all cases. The results are presented in the proceeding sections of the chapter.

### 5.1.1 Iron pillared systems

Table 5.1.1 indicates the catalytic activity of iron pillared series for the oxidation of phenol. The parent pillared clay exhibits very good activity towards the reaction. 74.3% of the phenol gets converted over Fe PM with hydroquinone selectivity of more than one third of the produced diphenols. Presence of transition metals in the porous network does not alter catalytic efficiency and product selectivity much. However Cu/Fe PM exhibits increased catechol selectivity.

| Catalyst | Conversion (%) | Selectivity (%) | |
|----------|----------------|----------|--------------|
|          |                | Catechol | Hydroquinone |
| V/Fe PM  | 75.0 | 61.9 | 38.1 |
| Mn/Fe PM | 70.3 | 66.1 | 33.9 |
| Co/Fe PM | 73.5 | 59.2 | 40.8 |
| Ni/Fe PM | 76.5 | 58.0 | 42.0 |
| Cu/Fe PM | 73.5 | 72.6 | 27.4 |
| Zn/Fe PM | 77.6 | 59.8 | 40.2 |
| Fe PM    | 74.3 | 61.3 | 38.7 |

Table 5.1.1 Activity of iron pillared systems towards phenol hydroxylation

Phenol: solvent: $H_2O_2$- 1:5:5, catalyst- 0.1g, temperature- 80°C, time- 45 minutes.

The high activity of iron containing systems can be attributed to the redox nature of iron. Since hydrogen peroxide is used, there is possibility for involvement of free radicals and presence of iron in the catalyst can produce free radicals. Catechol has been postulated to be formed in the external surface of the catalyst where as hydroquinone is formed inside the pores[6,33]. The hindrance in diffusion of reactants into the porous network of the pillared clay can be the reason for reduced

hydroquinone selectivity, though thermodynamically o- and p- products have equal probability.

Though acidity is not an important parameter for oxidation reactions, several reports are present in literature suggesting the participation of Brönsted acid sites in hydroxylation of phenol[19,20]. The availability of structural OH species (Brönsted acidity) in zeolites has been correlated with catalytic efficiency. In clays, Brönsted acidity stems mainly from structural OH groups. Hence an attempt is made to correlate observed activities with Brönsted acidity as obtained from cumene cracking reaction (Figure 5.1.1). Very good correlation could be obtained between the two.


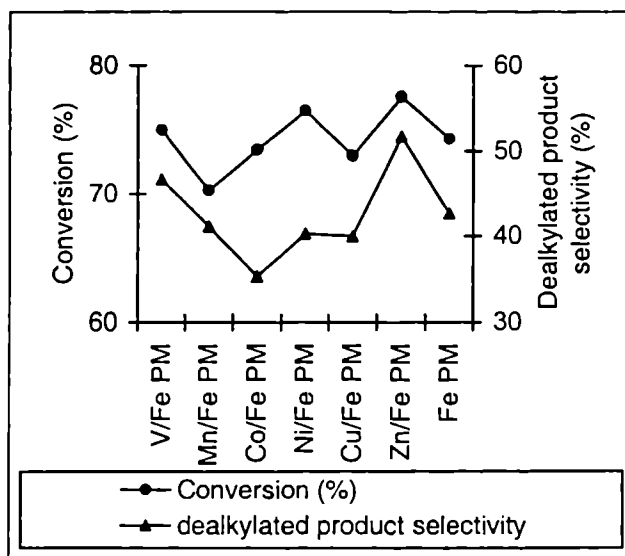
Figure 5.1.1 Dependence of activity on benzene selectivity for the iron pillared series.

## 5.1.2 Aluminium pillared systems

The catalytic efficacy of various aluminium pillared systems was tested at standard conditions. The results are tabulated in table 5.1.2. Al PM shows phenol conversion of 68.5% with hydroquinone selectivity to 32%. Exchange with transition

metals increases the activity of Al PM. Hydroquinone selectivity also improves as a result of modification by metal oxides. Cu/Al PM shows surprisingly low activity, though copper containing catalysts have been widely reported for the reaction. However, product selectivity for this catalyst does not deteriorate to a large extent from others.

| Catalyst | Conversion (%) | Selectivity (%) | |
|----------|----------------|-----------------|--------------|
|          |                | Catechol | Hydroquinone |
| V/Al PM  | 68.9 | 69.6 | 30.4 |
| Mn/Al PM | 72.3 | 67.1 | 32.9 |
| Co/Al PM | 70.4 | 60.1 | 39.9 |
| Ni/Al PM | 71.6 | 66.4 | 33.6 |
| Cu/Al PM | 59.0 | 61.6 | 38.4 |
| Zn/Al PM | 70.4 | 64.3 | 35.7 |
| Al PM    | 68.5 | 68.1 | 31.9 |

Table 5.1.2 Activity of aluminium pillared systems towards phenol hydroxylation
Phenol: solvent: $H_2O_2$- 1:5:5, catalyst- 0.1g, temperature- 80°C, time- 45 minutes.

Aluminium pillared clays perform well for the reaction. Decreased selectivity for hydroquinone can be ascribed to the shape selective nature of pillared clay. Presence of transition metals in the catalyst surface improves catalytic activity.

Figure 5.1.2 illustrates the dependence of activity on the amount of Brönsted acid sites. Good agreement could be obtained between dealkylated product selectivity in cumene cracking test reaction and oxidation efficiency of various catalysts. A discrepancy occurs with Cu/Al PM. This system, though exhibits higher selectivity for dealkylated products, shows much lower conversion of cumene. Hence total number of acid sites is very less for this system. Thus, it can be concluded that structural OH species in pillared clays play a major role in the reaction.
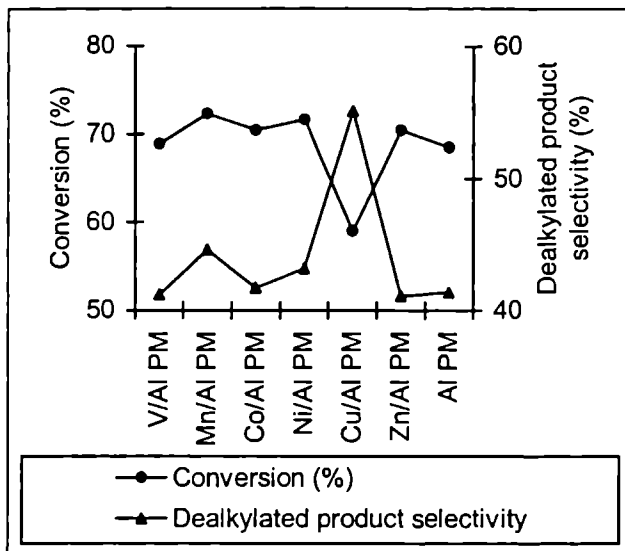
Figure 5.1.2 Dependence of activity on benzene selectivity for aluminium pillared series.

### 5.1.3 Iron Aluminium pillared systems

Table 5.1.3 discloses the catalytic performances of various mixed pillared systems towards hydroxylation of phenol with hydrogen peroxide. FeAl PM exhibits very high activity for the reaction. Almost 80% of the phenol gets converted over this catalyst within 45 minutes, with 38% selectivity towards hydroquinone. Incorporation of transition metals into the porous network reduces the activity of pillared clay especially for copper and zinc exchanged systems. The product selectivity however remains almost the same.

Iron containing systems, due to its redox nature are good oxidation catalysts. The exchange of mixed pillared system with transition metals incorporates the corresponding metal oxide inside the pores. This can block the active sites for the reaction and hence reduced activity. Pore blocking due to the deposition of incorporated metals can be the reason for reduced hydroquinone selectivity.

| Catalyst | Conversion (%) | Selectivity (%) | |
|---|---|---|---|
| | | Catechol | Hydroquinone |
| V/FeAl PM | 77.2 | 64.1 | 35.9 |
| Mn/FeAl PM | 72.3 | 63.4 | 36.6 |
| Co/FeAl PM | 77.1 | 66.0 | 34.0 |
| Ni/FeAl PM | 71.1 | 63.8 | 36.2 |
| Cu/FeAl PM | 58.2 | 67.7 | 32.3 |
| Zn/FeAl PM | 58.9 | 63.5 | 36.5 |
| FeAl PM | 79.0 | 62.0 | 38.0 |

Table 5.1.3 Activity of iron aluminium pillared systems towards phenol hydroxylation
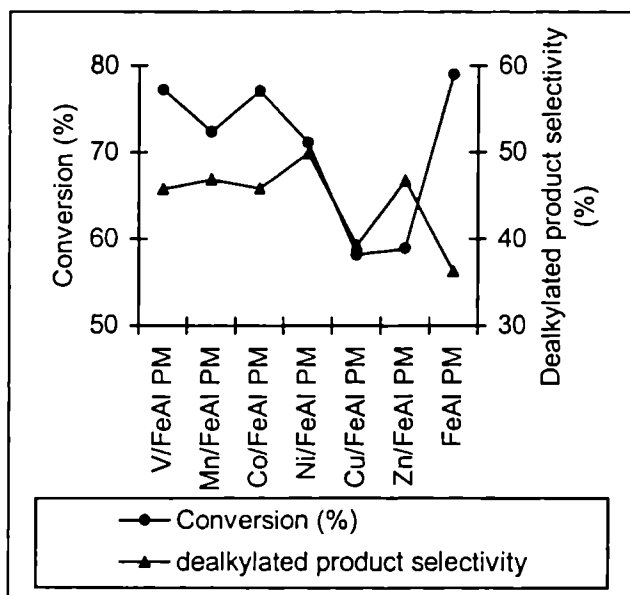Phenol: solvent: $H_2O_2$- 1:5:5, catalyst- 0.1g, temperature- 80°C, time- 45 minutes.



Figure 5.1.3 Dependence of catalytic activity on Brönsted acidity.

Figure 5.1.3 correlates the catalytic activity of various systems in the iron aluminium pillared series with Brönsted acidity. Brönsted acidity ties well with

catalytic activity. An inconsistency is observed for FeAl PM that can be explained on the basis of increased hydroquinone formation inside pores. Thus, it can be conclusively noted that Brönsted acidity play prominent role in phenol hydroxylation.

## 5.2 EFFECT OF REACTION VARIABLES

Hydroxylation of phenol is extremely sensitive to reaction conditions as well as quality of the catalyst. Hence the influence of various reaction variables like time, temperature, phenol concentration, oxidant concentration, solvent, solvent concentration and catalyst concentration was extensively studied using V/FeAl PM as reference catalyst. The observations and conclusions drawn from the study are presented in subsequent portions of the chapter.

### 5.2.1 Effect of time

The effect of time on wet peroxide oxidation of phenol was studied at a range of 90 minutes. The results are given in figure 5.2.1. From the figure it can be deduced that excellent conversion occurs even at 15 minutes. However, an induction period of about 5 minutes was noticed, after which violent reaction starts, turning the reaction mixture black. This was observed at all temperatures. The conversion % does not alter much with increase in duration of run. After 45 minutes, reaction rate drops. Regarding selectivity pattern, as time increases, hydroquinone selectivity improves.

The results indicate that, an optimum reaction time is needed for substantial phenol conversion. After a particular period, activity of surface sites practically drops. This change in activity pattern may be attributed to poisoning of surface sites by reaction products[32]. Tar, produced by over oxidation of diphenols is a major poison for surface sites. It has been reported that with zeolites and molecular sieve catalysts, catechol is formed in the external surface of catalyst, whereas hydroquinone is formed inside pores[6,33]. Since pillared clays also possess a porous

network, shape selective nature can be assigned for this type of catalysts also. Hence, formation of catechol is low in the pores. As time goes by, more and more reactants diffuse in and out of pores leading to increased hydroquinone selectivity.
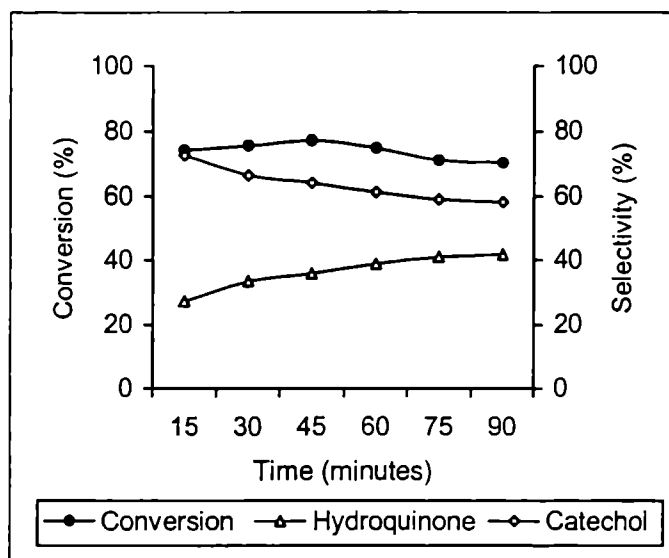


Figure 5.2.1 Effect of time

Phenol: $H_2O$: $H_2O_2$- 1:5:5, catalyst- 0.1g, temperature- 80°C

## 5.2.2 Effect of temperature

The effect of temperature was checked in a range of 50-90°C at an interval of 10°C. On an average, conversion of phenol increases with temperature. At room temperature, reaction does not occur even after one hour. As the temperature is increased by 10°C, drastic change occurs in reaction rate. Maximum conversion is observed at 80°C and at 90°C, reaction rate drops. Regarding selectivity pattern, low temperatures favour high yields of hydroquinone. Another remarkable point is that at low temperatures, hydroquinone selectivity decreases with time. As the temperature is raised, hydroquinone selectivity suffers but increases with time at a particular temperature.

| Temperature (°C) | Time (minutes) | Conversion (%) | Selectivity (%) | |
|---|---|---|---|---|
| | | | Catechol | Hydroquinone |
| 50 | 30 | 17.4 | 28.8 | 71.2 |
| | 45 | 27.5 | 40.3 | 59.7 |
| | 60 | 29.6 | 46.3 | 53.7 |
| | 75 | 31.8 | 64.7 | 35.3 |
| | 90 | 29.9 | 51.3 | 48.7 |
| 60 | 30 | 29.4 | 38.5 | 61.5 |
| | 45 | 52.2 | 53.9 | 36.1 |
| | 60 | 60.6 | 65.3 | 34.7 |
| | 75 | 57.2 | 63.4 | 34.6 |
| | 90 | 54.6 | 61.2 | 38.8 |
| 70 | 30 | 64.3 | 69.6 | 30.4 |
| | 45 | 66.1 | 67.0 | 33.0 |
| | 60 | 61.3 | 58.2 | 41.8 |
| | 75 | 69.9 | 65.1 | 34.9 |
| | 90 | 71.0 | 68.1 | 31.9 |
| 80 | 15 | 74.4 | 72.8 | 27.2 |
| | 30 | 75.6 | 66.5 | 33.5 |
| | 45 | 77.2 | 64.1 | 35.9 |
| | 60 | 74.9 | 61.1 | 38.9 |
| | 75 | 71.2 | 59.0 | 41.0 |
| | 90 | 70.3 | 58.3 | 41.7 |
| 90 | 15 | 62.7 | 54.2 | 45.8 |
| | 30 | 67.6 | 61.4 | 38.6 |
| | 45 | 69.9 | 62.8 | 37.2 |
| | 60 | 70.8 | 62.7 | 37.3 |
| | 75 | 72.9 | 58.8 | 41.2 |
| | 90 | 74.8 | 62.4 | 37.6 |

Table 5.2.2. Effect of time. Phenol: $H_2O$: $H_2O_2$- 1:5:5, catalyst- 0.1g

Induction period was noticed for the reaction at all temperatures, suggestive of free radical mechanism. The induction period shows inverse relationship with temperature. Hence, the non-occurrence of the reaction at room temperature may be due to prolonged induction period. The sweeping enhancement in reaction rate with temperature again is suggestive of free radical mechanism for the reaction. At higher temperatures, the formation of free radicals occurs to greater extent and hence the sudden boost in reaction rate. The decrease in rate at 90°C can be recognised with high rate of $H_2O_2$ decomposition. This side reaction suppresses the availability of sufficient peroxide for the reaction and is indicative of decreased activation energy for hydrogen peroxide decomposition compared to the oxidation reaction[34].

### 5.2.3 Effect of phenol concentration

The influence of the amount of phenol in reaction mixture was studied by keeping the amount of water and hydrogen peroxide constant and altering the amount of phenol. The observations are presented in figure 5.2.3. From the figure, it can be noticed that a minimum phenol concentration is required for good conversions. The rate of reaction increases with increase in the amount of phenol. Nevertheless, after an optimum phenol level, reaction rate again drops. Commenting on selectivity pattern, one can easily notice that hydroquinone selectivity improves steadily with increase in the amount of phenol. Thus, at a phenol: water: hydrogen peroxide ratio of 4: 5: 5, almost an equal ratio of isomeric products is obtained.

At lower concentrations, due to solvent effects, phenol molecules may be experiencing difficulty in approaching active sites and hence the reduced rate. The decrease in phenol conversion at high concentrations can be attributed to the fact that conversions are calculated as weight % of unreacted phenol. Increase in phenol concentration increases the rate of diffusion of reactants into the pores and hence the increase in hydroquinone selectivity.
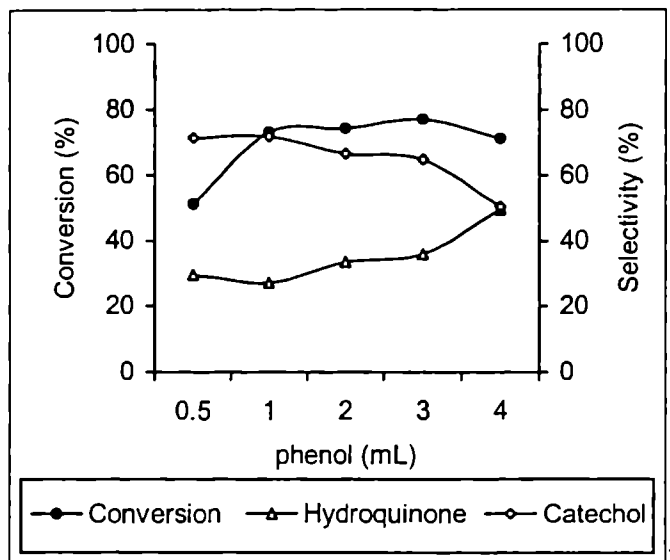
Figure 5.2.3 Effect of phenol concentration

Water: $H_2O_2$- 5:5, catalyst- 0.1g, temperature- 80°C, time- 45 minutes

## 5.2.4 Effect of peroxide concentration

The amount of oxidant used up is an essential parameter for oxidation reactions. The influence of phenol to hydrogen peroxide ratio was studied and the results are illustrated in figure 5.2.4. Oxidant present even in trace quantities can bring about oxidation of phenol to diphenols over pillared clay catalysts. Increase in amount of peroxide increases the reaction rate. However, after an optimum amount of oxidant, reaction rate falls. Hydroquinone selectivity also follows the same trend.

The proficient conversion of phenol over pillared clay catalysts depicts their superior ability for oxidation reactions. The presence of iron may be a reason for this. Maximum conversion of phenol to diphenols was observed at a peroxide to phenol ratio of 7. Several authors reported decrease in the reaction rate at high oxidant concentrations[28]. Neumann *et.al* proposed large excess of water accompanying

hydrogen peroxide as possible reason for this[35]. This seems to be an unsatisfactory explanation since the reaction rate was unaffected by solvent concentration (refer 5.2.6). The increase in oxidant concentration increases the rate of deep oxidation of produced diphenols to tar and this can be a possible explanation for decreased conversion. The high concentration of $H_2O_2$ can also accelerate self decomposition of oxidant, reducing the reaction rate.
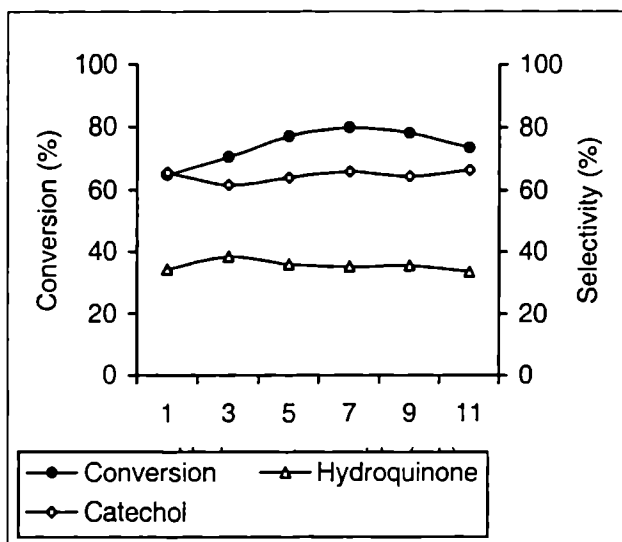


Figure 5.2.4 Effect of oxidant concentration

Phenol: solvent - 1:5, catalyst- 0.1g, temperature- 80°C, time- 45 minutes

## 5.2.5 Effect of solvent

Selection of appropriate solvent is an essential requisite for any reaction. The right solvent was selected by examining the activity in different solvents of varying polarity. The results are tabulated in table 5.2.5. From the table, it can be deduced that reaction proceeds with great vigour in aqueous medium. Other solvents like isopropanol, acetone and dioxan permit the reaction to occur only in a nominal rate. However, high hydroquinone selectivity is observed with isopropanol and dioxan.

| Solvent | Conversion (%) | Selectivity (%) | |
| --- | --- | --- | --- |
| | | Catechol | Hydroquinone |
| water | 77.2 | 64.1 | 35.9 |
| isopropanol | 3.4 | 36.7 | 63.3 |
| acetone | 5.5 | 69.0 | 31.0 |
| dioxan | 4.9 | 36.3 | 63.7 |

Table 5.2.5 Effect of solvent

Phenol: solvent: $H_2O_2$- 1:5:5, catalyst- 0.1g, temperature- 80°C, time- 45 minutes

The high activity in aqueous medium can be recognised with strong adsorption of phenol on the catalyst in this solvent, which is driven by nonideality of water phenol system. At the same mole fraction, the calculated activity coefficient of phenol is much higher in water than in other solvents[36].

## 5.2.6 Effect of solvent concentration

Oxidation of phenol using pillared clays was undertaken as a means for removing the organic pollutant from water streams. Thus the amount of water in the system becomes critical. Hence, influence of water concentration was studied by varying the amount of water used, keeping the amount of phenol, oxidant and catalyst constant. The observations are outlined in figure 5.2.6. From the figure it can be inferred that at low concentrations, the amount of solvent plays a critical role. Phenol conversion increases with increase in the amount of water and after an optimum phenol to water ratio of 1/5, it remains constant.

The influence of water concentration has been studied using organic peroxides in hydrocarbon oxidation[37]. It was concluded that active water species interacts with peroxy radicals. The propagation and termination steps are influenced by water via hydrogen bond interaction of peroxy radicals. The same is applicable in oxidation of phenol also. The interaction of active water species with peroxy radicals

increases with water concentration and hence the increased conversions at high amounts of solvent.
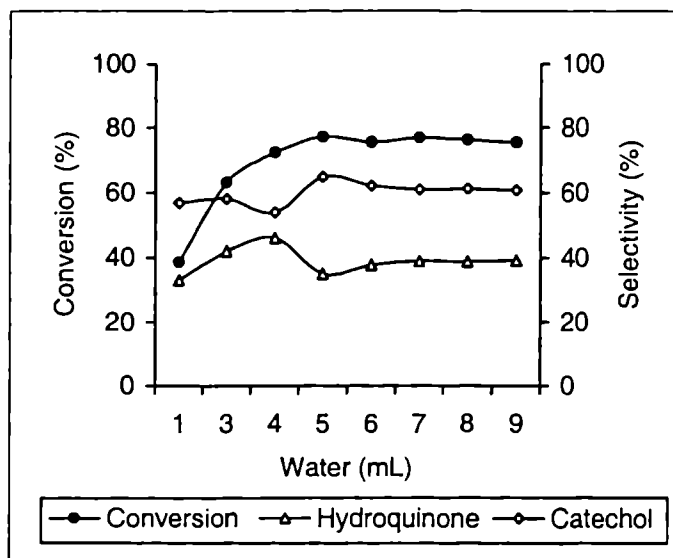


Figure 5.2.6 Effect of solvent concentration

Phenol: $H_2O_2$- 1: 5, catalyst- 0.1g, temperature- 80°C, time- 45 minutes.

### 5.2.7 Effect of catalyst concentration

The catalyst amount required for maximum conversion of phenol was found out in the specified reaction conditions. The observations of the study are sketched in figure 5.2.7. From the figure, it can be noted that phenol oxidation increases with catalyst concentration. However, after an optimum amount of catalyst, reaction rate falls. Catechol selectivity also increases with increase in catalyst and then levels off.

From the figure, it can be concluded that a minimum amount of catalyst sites is required for the easy occurence of reaction. Increase in catalyst concentration accelerates decomposition of hydrogen peroxide[13]. The increased amounts of active sites in concurrence with increase in catalyst concentration can also lead to readsorption of products to active sites. Santos *et.al* reported a vital contribution of

homogeneous reaction at low catalyst loadings[12]. They suggested a homogeneous reaction for oxidation of phenol, while oxidation of intermediates is mainly due to heterogeneous mechanism. Yu *et.al* reported that excess of catalyst has no benefit on phenol hydroxylation and large excess of catalyst reduced the yield significantly[34].
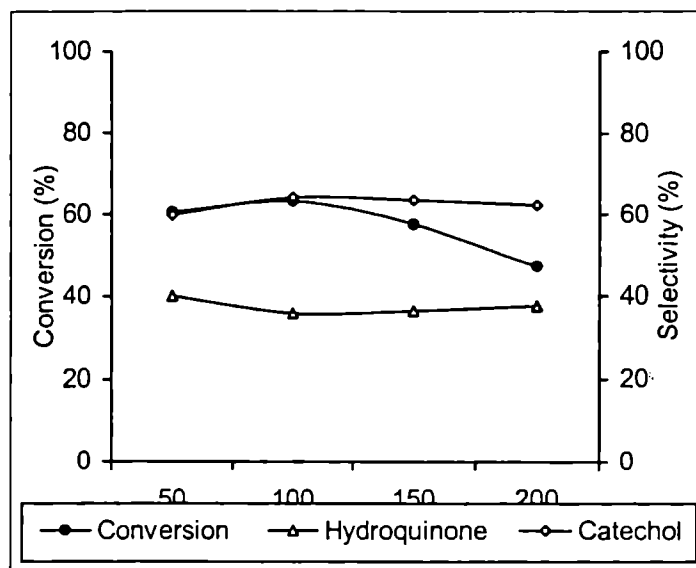


Figure 5.2.7 Effect of catalyst concentration

Phenol: solvent: $H_2O_2$- 1:5:5, temperature- 80°C, time- 45 minutes.

## 5.3 MECHANISM OF THE REACTION

Several mechanisms have been proposed for the hydroxylation of phenol. Since the oxidant is hydrogen peroxide, most of them are based on free radicals, though elecrophilic mechanism has been postulated over titano silicates[5]. Meyer *et.al* suggested a heterogeneous- homogenous free radical mechanism for liquid phase oxidations over solid acid catalysts[38]. This mechanism was applied for phenol successfully by Sadana *et.al*[39] and Lui *et.al*[40]. In this mechanism, free radicals are formed on the surface of solid acids, which subsequently undergo propagation and termination in solution. Two ways have been suggested for the generation of free

215

radicals on catalyst surface[17]. In the first mechanism, catalyst accelerates the decomposition of hydrogen peroxide into radicals. This initiation step is followed by the propagation step in solution. In the second mechanism, catalyst activates the phenol molecules directly and facilitates formation of phenoxy radicals, bringing about initiation. Franco *et.al* proposed that thermodynamically *o-* and *p-* substitutions are equally feasible; kinetically substitution at *o-* position is more favoured. This suggests a steric effect on reaction, which can be explained in terms of a transition stage involving a complex with the OH of phenol and OH radical of the peroxide[15].
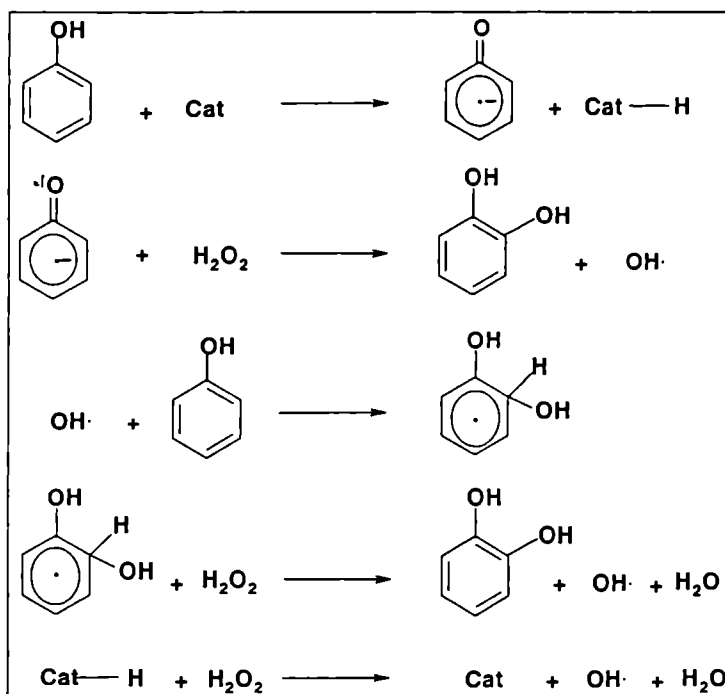


Scheme 5.3.1 Plausible mechanism for phenol hydroxylation with hydrogen peroxide

In the present study, an initial induction period was noticed in all cases, after which the reaction occurred violently with bursting of reaction mixture. Also, slight increase in temperature resulted in several fold enhancement in reaction rate.

Hence, a free radical mechanism can be envisaged for the reaction. From solvent effect studies, it was concluded that adsorption of phenol on catalyst surface was favoured in aqueous medium. This suggests that formation of phenoxy radical in the catalyst surface is the rate determining step. Also, homogeneous contribution was not observed from catalyst concentration studies. The suggested mechanism involves formation of phenoxy radical on catalyst surface, which then reacts with peroxide giving OH free radical and diphenol. The produced free radical propagates the chain by attacking phenol molecule, forming diphenols. Same mechanism is proposed for the formation of isomeric products. The kinetic preference for catechol is explained by selective formation of hydroquinone inside the porous network of pillared clay. The proposed mechanism is sketched in scheme 5.3.1. Intermediates formed in propagation step can lead to side reactions, forming polymerised products and this accounts for tar formation. This is depicted in scheme 5.3.2.
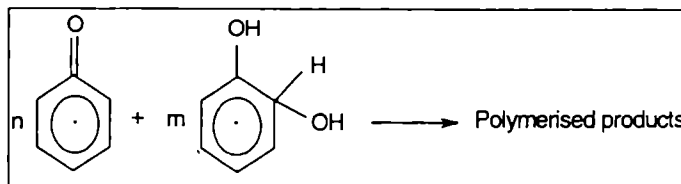


Scheme 5.3.2 Plausible side reaction during phenol hydroxylation

## 5.4 CONCLUSIONS

Important outcomes that can be summarised from a systematic study of the reaction are,

❖    Iron, aluminium and mixed iron aluminium pillared clays and their transition metal exchanged analogues are good oxidation catalysts. The decrease in hydroquinone selectivity can be attributed to the shape selective nature of pillared clays.

❖   Correlation of catalytic activity with Brönsted acidity of the catalysts yields excellent results for single pillared systems.

❖   Time has a promotional effect on the rate of hydroxylation of phenol. An induction period of about 10-15 minutes is observed. Hydroquinone selectivity increases with time. Reaction rate increases with temperature and maximum conversion of phenol is observed at 80°C. After this, the reaction rate drops. Hydroquinone selectivity decreases with temperature.

❖   Water was the best solvent for the reaction over pillared clays. Other solvents like acetone, dioxan and isopropanol show nominal conversion. Reaction rate increases linearly with solvent concentration. After an optimum value of solvent, the rate levels off.

❖   Phenol conversion is almost independent of concentration of phenol. However, hydroquinone selectivity increases at higher amounts of phenol. After an initial increase, the reaction rate decreases with increase in catalyst concentration. Selectivity is independent of the amount of catalyst.

❖   Hydrogen peroxide concentration plays an important promotional role on hydroxylation of phenol. After an optimum concentration of the oxidant, the rate levels off. Hydroquinone selectivity is independent of oxidant taken.

# REFERENCES

1. K Belkacemi, F Larachi, A Sayari, *J. Catal.*, 193, 224-237 (2000).

2. M.G Clerici, "Heterogeneous Catalysis and Fine Chemicals", Vol. III M Guisnet, J Baebier (eds).

3. H Jeifert, W Wldmann, W Sch Weidel, Ger. Patent 2,410,742 (1975).

4. P Maggioni, US Patent 3,914,323 (1975).

5. U Wilkenhoner, G Langhendries, F van Laar, G.V Baron, D.W Gammon, P.A Jacobs, E van Steen, *J. Catal.*, 203, 201-212 (2001).

6. A Tuel, S.M Khouzami, Y.B Taarit, C Naccache, *J. Mol. Catal.*, 68, 45-52 (1991).

7. A Thangaraj, R Kumar, P Ratnaswamy, *J. Catal.*, 131, 294-297 (1991).

8. A.J.H.P van der Pol, A.J Verduyn, J.H.C van Hooff, *Appl. Catal: A*, 92, 113-130 (1992).

9. T Yokoiu, P Weng, T Tatsumi, *Catal. Commun.*, 4, 11-15 (2003).

10. S Valage, Z Gabelicia, M Abdellaoni, J.M Clacens, J Barrault, *Microporous. Mesoporous Mater.*, 30, 177-185 (1999).

11. F.S Xiao, J Sun, X Meng, R Yu, H Yuan, J Xu, T Song, D Jiang, R Xu, *J. Catal.*, 199, 273-281 (2001).

12. A Santos, E Barrasso, F.G Ochoa, *Catal. Today*, 48,109-117 (1999).

13. J Sun, X Meng, Y Shi, R Wang, S Feng, D Jiang, R Xu, F-S Xiao *J. Catal.*, 193, 199-206 (2000)

14. A Santos, P Yustos, B Durban, F.G Ochoa, *Catal. Today*, 66, 511-517 (2001).

15. C.W Lee, D.W Ahn, B Wang, J.S Hwang, S-E Park, *Microporous. Mesoporous Mater.*, 44-45, 587-592 (2001).

16. L.N Franco, I.H Perez, A Pliego, A.M Franco, *Catal. Today*, 75 189-195 (2002).

17. C Xiong, Q Chen, W Lu, H Gao, W Lu, Z Gao. *Catal. Lett.*, 69, 231-236 (2000).

18. W Zhao, Y Luo, P Deng, Q Li. *Catal. Lett.*, 73, 199-202 (2001).

19. H.L del Castillo, A Gil, P Grange, *Clays. Clay Miner.*, 44(5), 706-709 (1996).

20. L.K Boudali, A Ghorbel, D Tichit, B Chiche, R Dutartre, F Figueras, *Microporous Mater.*, 2, 525-535 (1994).

21. J Barrault, M Abdellaou, C Bouchoule, A Majeste, J.M Tatibouet, A Louloudi, N Pappayannakos, N.H Gangas, *Appl. Catal: B*, 27, 225-230 (2000).

22. J Barrault, C Bouchoule, K Echachoui, N.F Srasra, M Trabelsi, F Bergaya, *Appl. Catal: B*, 15, 269-274 (1998).

23. K Bahranowski, M Gasior, A Kielski, J Podobinski, E.M Serwicka, L.A Vartikian, K Wodnicka, *Clays. Clay Miner.*, 46, 98-102 (1998).

24. P.H.P Rao, A.V Ramaswamy, P Ratnaswamy, *J. Catal.*, 137, 225-231 (1992).

25. J.S Reddy, S Shivashankar, *Catal. Lett.*, 11, 241 (1992).

26. N Vlagappan, V Rishani, *J. Chem. Soc. Chem. Commun.*, 374 (1995).

27. P.H.P Rao, P Ratnaswamy, *Appl. Catal.*, 93,123 (1993).

28. S Hamoudi, A Sayari, K Belkacemi, L Bonneviot, F Larachi, *Catal. Today*, 62, 379-384 (2000).

29. R Yu, F-S Xiao, D Wang, J Sun, Y Liu, G Pang, S Feng, S Qiu, R Xu, C Fang, *Catal. Today*, 51, 39-46 (1999).

30. S Lin, Y Zhen, S-M Wang, Y-M Dai, *J. Mol. Catal: A*, 156, 113-120 (2000).

31. A Dubey, S Kannan, S Velu, K Susuki, *Appl. Catal: A*, 238, 319-326 (2003).

32. T Blasco, J.M Nieto, *Appl. Catal. A: Gen.*, 127, 117-142 (1995).

33. J.A Martens, P Buskens, P.A Jacobs, A vander Pol, J.H.C vant Hoff, C Ferrini, H.W Kowenhoven, P.J Koyman, H Bekkum, *Appl. Catal. A: Gen.*, 99, 71 (1992).

34. R Yu, F-S Xiao, D Wang, G Pang, S Feng, S Qiu, R Xu, *Catal. Lett.*, 49, 49 (1997).

35. R Neumann, M Levin Elad, *Appl. Catal. A Gen.*, 122, 85 (1995).

36. S.I Saudler, "Chemical and Engineering Thermodynamics", 2nd ed, Elsevier (1992).

37. L.J Csanyi, K Jakey, *J. Catal.*, 141, 721-724 (1993).

38. C Meyer, G Clement, J.C Balaceanu, "Proc. 3rd Int. Congres on Catalysis", Vol.I (1965).

39. A Sadana, J.R Katzer, *J. Catal.*, 35, 140 (1974).

40. C.B Lui, Z Zhang, X.G Yang, Y Wu, *J. Chem. Soc. Chem. Commun.*, 1019 (1996).

# 6

# METHYL *TERT*-BUTYL ETHER

# SYNTHESIS

*Due to its high octane number, MTBE (methyl tert- butyl ether) is presently the most widely used additive for improving the quality of unleaded gasoline. The decomposition of the ether is also of industrial interest as it represents a route for the production of pure isobutene. Worldwide production of MTBE has increased faster than most other commodity chemicals and in US the annual production of MTBE stands eighth in the industrial production chart with an estimated increasing yearly demand of 15%. Commercial catalysts are cation exchange resins, which require tedious work up and low reaction temperatures, resulting in low selectivity. The prepared clay catalysts were employed for gas phase MTBE synthesis and were found to be good alternatives for resin catalysts, permitting the reaction at higher temperatures. The effect of various reaction variables on the reaction was also dealt with extensively.*

## 6.0 INTRODUCTION

Combustion of fossil fuels for the purpose of transport and heating contributes significantly to problems like global warming, hazardous carbon monoxide pollution and other toxic pollutants. Due to strong environmental concerns about fuel emissions, use of metal octane enhancers such as tetraethyl lead (TEL), tetramethyl lead (TML) and methyl cyclopentadienyl manganese tricarbonyl (MMT) in gasoline has been phased out in many countries. The addition of fuel oxygenates to gasoline for increased octane number resulted in higher engine efficiency and reduction of polluting components in exhaust, thereby significantly reducing toxic tailpipe pollution[1]. Among many oxygenated compounds, methyl *tert* butyl ether (MTBE) has been widely utilised as a gasoline additive due to its good antiknocking properties, lower production cost, outstanding physical properties such as volatility, miscibility in gasoline and reduction of environmentally hazardous emissions.

The current commercial MTBE synthesis is a liquid phase reaction of methanol and isobutene over sulphonated ion exchange resins, mainly Amberlyst 15 or Lewatit SPC 118 (Bayer) at low temperatures (30-100°C) and moderately high pressures (usually up to 2.0 MPa). Although resin catalysts are very active, they have some major drawbacks like fragility, sensitivity to methanol to isobutene ratios, corrosive problems, loss of acid sites due to leaching and need of large excess of methanol over isobutene necessitating recycle in industrial installations. In addition, deactivated resin catalyst cannot be regenerated and must be properly disposed under current environmental regulations[2]. Use of resin catalysts leads to undesirable bye products like diisobutenes, dimethyl ether etc[3]. Alternate catalysts like zeolites[4-8], sulphated zirconia, heteropoly acids and clays have been developed[9-11]. However, a problem concerning MTBE production from isobutene is that the source of isobutene is limited to catalytic cracking and steam cracking fractions of petroleum refining. Another possible source of isobutene is isobutane dehydrogenation[12].

Commercially, MTBE can also be produced by reaction between methanol and *t*-butanol. The obvious advantage of this process is the direct use of *t*-butanol, a bye product in a number of reaction processes such as Halcon process (propylene oxide synthesis), where 3.5 kg of *t*-butanol is produced per kg of propylene oxide[13]. There are two ways to produce MTBE from *t*-butanol; the indirect and the direct method. In the former reaction, *t*-butanol is dehydrated to isobutene in the first reactor followed by reaction with methanol in the second reactor[14]. In the direct method, MTBE can be produced by reacting *t*-butanol directly with methanol in one reactor in presence of an acid catalyst in which water is also formed as co product. The choices of solid acid catalyst for the reaction are a variety of heteropolyacids[15], hydrogen ion exchange acid resins like Amberlyst 15[16], protonated zeolites[17] and inorganic oxides like $Nb_2O_5$, $TiO_2$, $ZrO_2$, $H_3PO_4$ treated oxides[18].

Mineral acid treated montmorillonite and heteropolyacids of group III and IV have been employed for the reaction in direct method[19]. An unexpected, in situ, phase separation of desired MTBE plus isobutene products from aqueous methanol has been observed at high *t*-butanol conversions. Even crude stock of *t*-butanol containing impurities like peroxides could be used. An alternative catalyst for MTBE production by direct method is provided by the as synthesised microporous niobium silicate AM-11. Higher MTBE selectivity could be attained at low temperatures. At high temperatures MTBE selectivity decreases as a result of extensive dehydration reactions[20]. HPW/MCM 41 was reported as potential catalyst for the reaction[21]. The observed activities could be related to catalyst structure as well as Brönsted acidity. Yadav *et.al* studied the reaction over different catalysts like Amberlyst 15, aluminium and zirconium exchanged K10, sulphated zirconia etc. Dodecatungstophosphoric acid doped K10 gave very high conversion and better selectivity[22].

Pillared clays have been suggested as potential catalysts for the reaction because etherification can occur more readily in the inner layer space[23]. In fact

pillaring of clay with chlorhydrol plus certain phosphates have led to improved MTBE selectivities[24]. Moreover, the reaction can also be thought as a model reaction for understanding the potential use of clays for etherification reactions. Hence, synthesis of MTBE by direct method was attempted over the prepared transition metal exchanged iron, aluminium and iron aluminium mixed pillared systems. The reaction can be represented as,
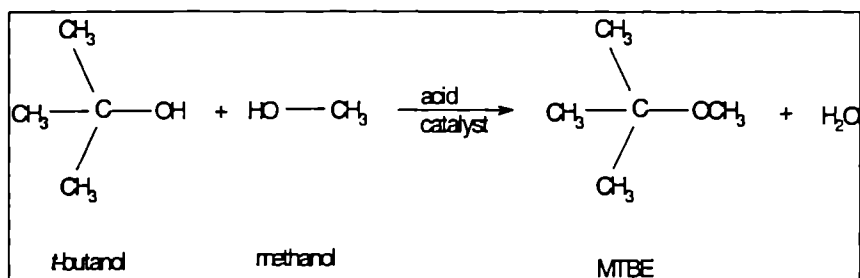


Scheme 6.1 MTBE synthesis from methanol and _t_-butanol.

_Tert_-butylation of methanol was done in the vapour phase. In a typical experiment, the reactor was charged with activated catalyst, sandwiched between silica beads. The liquid reactants were fed into the reactor by a syringe pump. Products of the reaction were collected downstream from the reactor at specified intervals and analysed by gas chromatography at analysis conditions specified in chapter 2. The percentage conversion (wt%) is the total percentage of _t_-butanol transformed into products. The reaction has been studied extensively using prepared clay catalysts. Observations and conclusions drawn from the study are given under two headings; I) Catalytic activity of various systems II) Effect of reaction variables.

## 6.1 CATALYTIC ACTIVITY OF VARIOUS SYSTEMS

A comparative evaluation of the catalytic activity of prepared pillared clay systems at standard conditions for vapour phase MTBE synthesis is given in this section. The performance of catalysts of iron, aluminium and iron aluminium mixed

pillared series are given separately. An attempt to correlate Brönsted acidity with catalyst efficiency is also presented.

### 6.1.1 Iron pillared systems

Table 6.1.1 shows the catalytic activities of various iron pillared catalysts for MTBE synthesis. The parent pillared clay shows a percentage conversion of 26.5 in the specified reaction conditions. Exchange with transition metals increases the activity considerably. Thus, Co/Fe PM shows the maximum activity of 93.5%. The cent percent selectivity to MTBE is observed with all catalytic systems.

| Catalyst | Conversion (%) | Selectivity (%) |
|----------|----------------|-----------------|
| V/Fe PM  | 66.5           | 100             |
| Mn/Fe PM | 79.5           | 100             |
| Ni/Fe PM | 53.1           | 100             |
| Co/Fe PM | 93.5           | 100             |
| Cu/Fe PM | 52.1           | 100             |
| Zn/Fe PM | 36.3           | 100             |
| Fe PM    | 26.5           | 100             |

Table 6.1.1 Activity of iron pillared system towards MTBE synthesis.

Methanol/tert-butyl alcohol- 10, temperature- 180°C, WHSV- 2.4h$^{-1}$, TOS- 2 hours

From the table, it can be concluded that iron pillared systems are efficient catalysts for gas phase synthesis of MTBE. The higher efficiency can be attributed to co-ordinately unsaturated nature of Fe in the pillars, facilitating nucleophilic attack of isobutyl carbonium ion on methanol. The diffusion rate of MTBE could depend on the porous network and fine pores seem to fill the effective role of diffusion. The high selectivity can also be attributed to the porous structure of clay catalyst. Mesoporous, shape selective catalysts like zeolites also give high MTBE selectivity[21].

The rate of etherification reaction has been reported to be dependant on the Brönsted acidity of catalyst[12,21]. Hence, an effort was made to correlate activities with Brönsted acidity as obtained from cumene cracking test reaction (Figure 6.1.1). A rough correlation between the two parameters can be obtained from the figure. A slight discrepancy occurs at Ni/FePM. The system should have been more active for the reaction, considering the surface acidity. The low activity for Ni/Fe PM and Zn/Fe PM can be explained in terms of low pore volume. The product may be experiencing difficulty for diffusing out of the interlayers of catalyst.
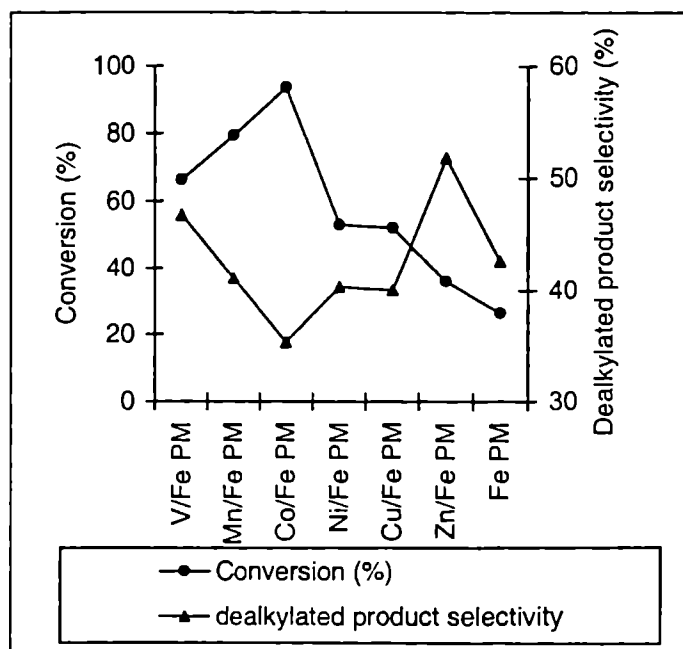


Figure 6.1.1 Dependence of activity on dealkylated product selectivity

The catalytic performance of various samples is correlated with cumulative amount of weak and medium acid sites obtained from temperature programmed desorption of ammonia (ammonia desorbed in the temperature range of 100-400°C). Figure 6.1.2 shows that perfect correlation could be arrived at, between the two

parameters. The high activity of Co/Fe PM can be attributed to larger amount of weak and medium acid sites. Thus, it can be concluded that gas phase etherification of methanol with *t*-butanol occurs over weak and medium acid sites.
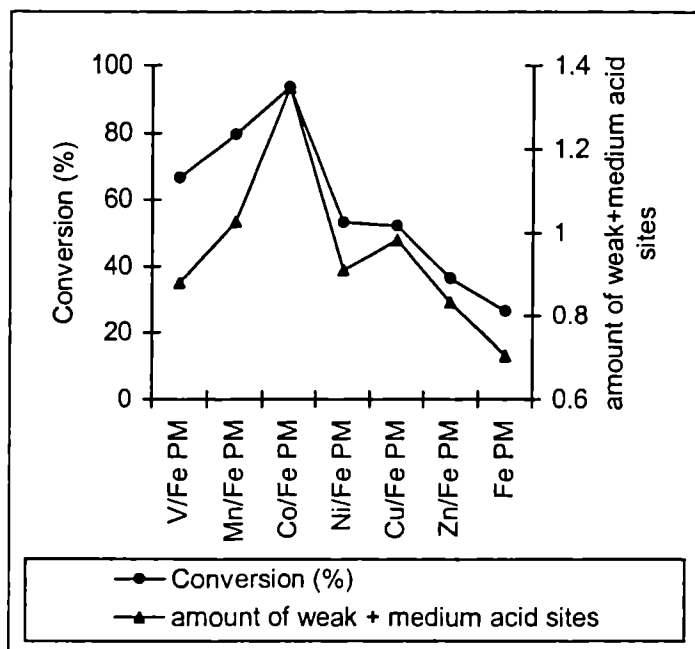


Figure 6.1.2 Dependence of activity on the amount of weak + medium acid sites

## 6.1.2 Aluminium pillared systems

The catalytic performance of various aluminium pillared catalysts for gas phase MTBE synthesis was evaluated. The *t*-butanol conversion as well as MTBE selectivity is listed in table 6.1.2. Al PM shows inferior activity for the reaction and this can be ascribed to the low surface area of these catalysts. Transition metal exchange improves the activity of the system and maximum activity is exhibited by Mn/Al PM.

| Catalyst | Conversion (%) | Selectivity (%) |
|----------|----------------|-----------------|
| V/Al PM | 28.8 | 100 |
| Mn/Al PM | 32.1 | 100 |
| Ni/Al PM | 26.4 | 100 |
| Co/Al PM | 12.3 | 100 |
| Cu/Al PM | 22.8 | 100 |
| Zn/Al PM | 21.0 | 100 |
| Al PM | 13.0 | 100 |

Table 6.1.2 Activity of aluminium pillared systems towards MTBE synthesis.
Methanol/tert-butyl alcohol- 10, temperature- 180°C, WHSV- 2.4h$^{-1}$, TOS- 2 hours



Figure 6.1.3 Dependence of activity on dealkylated product selectivity

Figure 6.1.3 shows the dependence of catalytic activity of various systems on dealkylated product selectivity. An inconsistency is revealed in the series at Co/Al PM. This discrepancy can be attributed to lower conversion rate of Cu/Al PM

towards cumene cracking. The observed activities of all other systems can be recognised with Brönsted acidity.
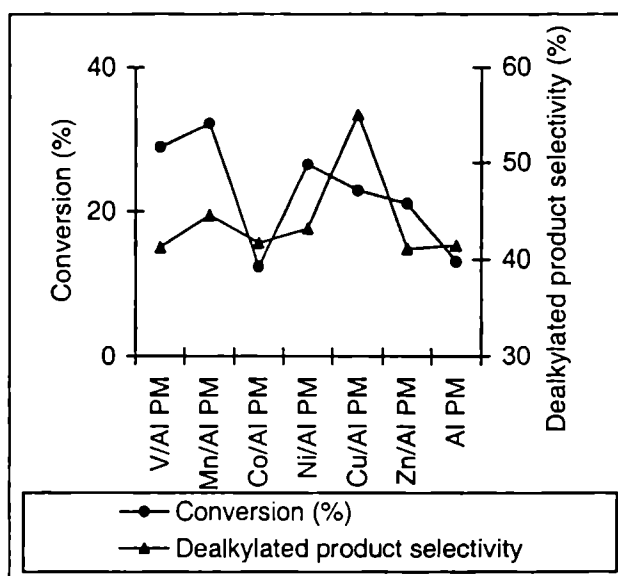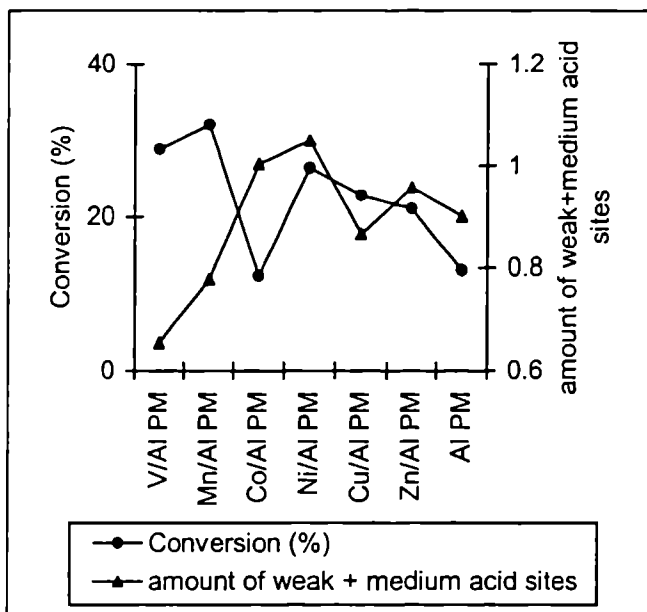


Figure 6.1.4 Dependence of activity on the amount of weak + medium acid sites

Correlation between catalytic activities of various aluminium pillared samples with amount of weak and medium strength acid sites is depicted in figure 6.1.4. As can be seen from figure, no conclusion can be made between the two parameters. Aluminium pillars exhibit high acidity but inferior activity for MTBE synthesis.

### 6.1.3 Iron Aluminium pillared systems

Table 6.1.3 describes the catalytic efficiency of various iron aluminium mixed pillared systems towards gas phase etherification of methanol with t-butanol under standard conditions. FeAl PM shows mediocre activity of 24.8% with cent percent selectivity for MTBE. Transition metal exchange increases the activity greatly while selectivity remains the same. The high activity of the mixed pillared systems can be

attributed to the finer three dimensional porous network. Speedy adsorption and desorption of reactants and products occur and hence the superior activity.

| Catalyst | Conversion (%) | Selectivity (%) |
|----------|----------------|-----------------|
| V/FeAl PM | 69.5 | 100 |
| Mn/FeAl PM | 64.1 | 100 |
| Ni/FeAl PM | 79.7 | 100 |
| Co/FeAl PM | 78.8 | 100 |
| Cu/FeAl PM | 42.4 | 100 |
| Zn/FeAl PM | 49.8 | 100 |
| FeAl PM | 24.8 | 100 |

Table 6.1.3 Activity of iron aluminium pillared systems towards MTBE synthesis.
Methanol/*tert*-butyl alcohol- 10, temperature- 180°C, WHSV- 2.4h$^{-1}$, TOS- 2 hours
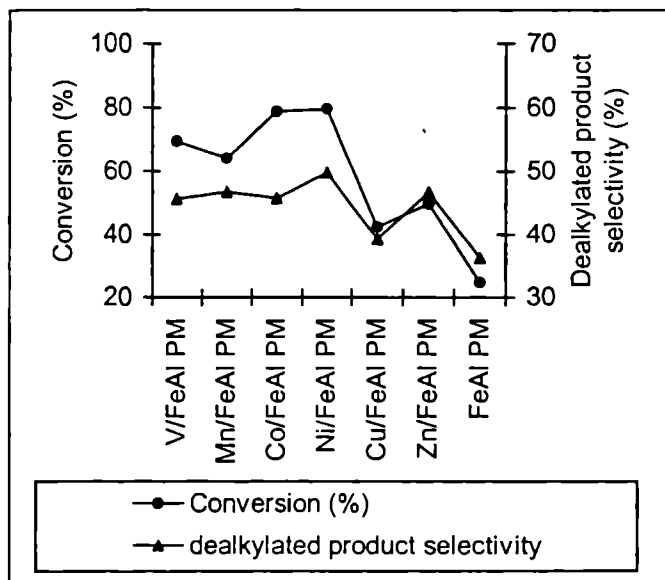


Figure 6.1.5 Dependence of activity on dealkylated product selectivity

The catalytic activities of mixed pillared systems can be correlated to dealkylated product selectivity in cumene cracking reaction, a measure of Brönsted acidity (Figure 6.1.5) and total amount of weak and medium acid sites from $NH_3$-TPD measurements (Figure 6.1.6). Excellent rapport is obtained between acidity and catalytic activity throughout the series. Hence, presence of appropriate amounts of acid sites can be cited as another reason for the activity of mixed pillared systems.
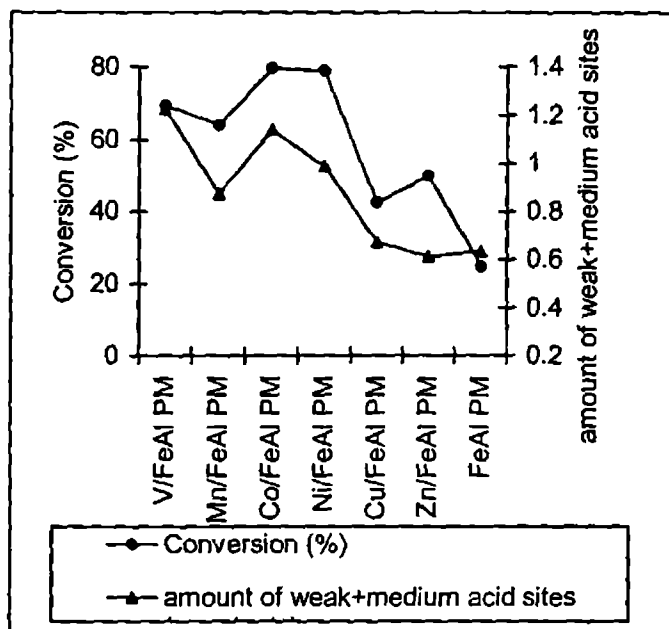


Figure 6.1.6 Dependence of activity on the amount of weak + medium acid sites

## 6.2 EFFECT OF REACTION VARIABLES

Gas phase MTBE synthesis by direct method is highly sensitive to reaction conditions. The influence of reaction variables like temperature, molar ratio, weight hourly space velocity and time on stream on the catalytic activity was probed out by taking Co/Fe PM as reference catalyst. The observations of the systematic study are listed in the subsequent portions of the chapter.

### 6.2.1 Effect of temperature

Table 6.2.1 illustrates the influence of temperature on the reaction in the range of 110-190°C. Temperature plays a decisive role in MTBE synthesis. A notable increase in *t*-butanol conversion is observed up to 180°C followed by decay at higher temperatures. However, deviation from the cent percent selectivity to MTBE was not observed even at high temperatures.

| Temperature (°C) | Conversion (%) | Selectivity (%) |
|---|---|---|
| 110 | 14.6 | 100 |
| 130 | 51.6 | 100 |
| 150 | 62.3 | 100 |
| 170 | 79.6 | 100 |
| 180 | 93.5 | 100 |
| 190 | 78.9 | 100 |

Table 6.2.1 Effect of temperature

Methanol/*tert*-butyl alcohol- 10, WHSV- 2.4h$^{-1}$, TOS- 2 hours

The data on temperature study indicates the reaction to be extremely sensitive to temperature. The decay in reaction rate above 180°C can be attributed to extensive dehydration of *t*-butanol which results in decreased amounts of *t*-butanol. Higher reaction temperatures also lead to side reactions producing hydrocarbons and other oxygenates[21].

### 6.2.2 Effect of molar ratio

Methanol to *t*-butanol ratio plays an important role in the reaction. Methanol is used as both reactant and solvent. Hence the reaction was studied at various methanol- *t*-butanol concentrations. The observations of the study are presented in table 6.2.2. The data shows that increase in methanol increases the activity of

catalyst. With an equimolar mixture of methanol and *t*-butanol, only 14.8% of *t*-butanol gets converted. A twofold enhancement in methanol concentration increases the activity almost three times. Tenfold enhancement of methanol concentration increases the activity by eight times. Nonetheless, cent percent selectivity to MTBE remains constant at all reactant ratios.

| Methanol: TBA | Conversion (%) | Selectivity (%) |
|:---:|:---:|:---:|
| 1:1 | 14.8 | 100 |
| 2:1 | 36.5 | 100 |
| 5:1 | 56.8 | 100 |
| 10:1 | 93.5 | 100 |

Table 6.2.2 Effect of molar ratio

Temperature- 180°C, WHSV- 2.4h$^{-1}$, TOS- 2 hours

The increase in activity with methanol concentration denotes the importance of solvent. Higher amounts of methanol suppresses the conversion of *t*-butanol to isobutene. The decrease in activity at low methanol to *t*-butanol ratio can be attributed to high concentrations of *t*-butanol in the feed. The percentage conversion is calculated on the basis of *t*-butanol and high excess of it, increases the calculated conversions as expected.

**6.2.3 Effect of weight hourly space velocity**

Feed rate is an important parameter in vapour phase reactions. The influence of weight hourly space velocity on catalytic activity was checked by conducting reactions at four different space velocities. The results are tabulated in table 6.2.3. From the table, it can be concluded that activity of catalyst increases with decrease in feed rate. Higher space velocities decrease the reaction rate. However, selectivity to MTBE remains the same irrespective of feed rate.

| WHSV (h$^{-1}$) | Conversion (%) | Selectivity (%) |
|:---:|:---:|:---:|
| 1.6 | 98.9 | 100 |
| 2.4 | 93.5 | 100 |
| 4.0 | 44.9 | 100 |
| 5.5 | 43.8 | 100 |

Table 6.2.3 Effect of weight hourly space velocity

Methanol/*tert*-butyl alcohol- 10, Temperature- 180°C, TOS- 2 hours

The table describes the significance of space velocity. Lower space velocity implies higher residence times for reactants in active sites and hence increased conversions. Increase in space velocity refers to insufficient contact time for reactants. This leads to speedy desorption of the reactant molecules from catalyst site before the completion of reaction and therefore lowered reaction rate.

## 6.2.4 Deactivation studies

Stability of the catalyst can be lost at increased durations of run. The performance of the reaction for a continuous 9 hours run tests the susceptibility of catalyst. The products were collected and analysed at an interval of 1 hour. The results are tabulated in table 6.2.4. From the table it is clear that activity declines steadily with time. Thus conversion % that is 93.5 at the second hour, becomes 82.8 at the end of ninth hour. However, cent percent selectivity towards MTBE remains the same throughout.

The lowering of activity with time is a common problem associated with solid acids. Literature suggests that zeolites are more resistant to this effect. The resistance was attributed to the relatively small diffusion hindrance of these microporous catalysts and to their high hydrophobicity[21]. The prepared pillared clays

have pore volumes much smaller than reported zeolites and hence difficulty in diffusion of the product due to pore blocking can be the reason for deactivation.

| Time on stream (h) | Conversion (%) | Selectivity (%) |
|:---:|:---:|:---:|
| 1 | 76.3 | 100 |
| 2 | 93.5 | 100 |
| 3 | 90.3 | 100 |
| 4 | 89.3 | 100 |
| 5 | 88.5 | 100 |
| 6 | 87.0 | 100 |
| 7 | 83.4 | 100 |
| 8 | 83.8 | 100 |
| 9 | 82.8 | 100 |

Table 6.2.4 Deactivation studies

Methanol/*tert*-butyl alcohol- 1/10, Temperature- 180°C, WHSV- 2.4h$^{-1}$

## 6.3 MECHANISM OF THE REACTION

Over cation exchange resins, the reaction is considered to occur by intermediate formation of isobutene (IB). For TBA-methanol-acid ion exchange system, following three reactions can take place.

TBA  →  IB + $H_2O$                              (I)

IB  +  MeOH →    MTBE                         (II)

TBA  +  MeOH →    MTBE + $H_2O$       (III)

If isobutene produced in the second reaction is consumed simultaneously and completely, then the reaction can be represented by the third equation. For cation exchange resins, Ancillotti *et.al* proposed that the reaction is catalysed mainly by solvated proton when methanol is present in large excess[25,26]. Thus, the reaction

is quasi homogeneous or quasi heterogeneous depending on reactant concentrations. The use of molecular modelling techniques was made with silicalite and H ZSM 5 catalysts. The adsorbate and adsorbent interaction energy values along with combination of energy minimisation and molecular dynamics were used for studying the adsorptive and diffusive behaviour of different species involved in the reaction. The energy barrier value of isobutene is the lowest as it diffuses even through the sinusoidal channel. This indicates the strong probability of dehydration of t-butanol to give isobutene, which further react with methanol to give MTBE. The heat of formation of isobutene from diffusion calculations also supports this view[27].

However, recent literature suggests an ionic mechanism for the reaction over solid acids. The reaction mechanism involves the formation of isobutyl carbonium ion intermediates followed by the nucleophilic attack of methanol molecules[28,29]. A similar mechanism can be envisaged in the present study also. Dependence of catalytic activity on acidity confirms the ionic mechanism.

## 6.4 CONCLUSIONS

The various points that can be summarised from the preceding discussion are,

❖   Iron containing pillared clay catalysts are efficient catalysts for gas phase MTBE synthesis from methanol and t-butanol by direct method. Cent percent selectivity to MTBE was observed in all cases.

❖   The activities could be well correlated with Brönsted acidities and/or the amount of weak and medium sites for iron and mixed pillared systems.

❖   The reaction variables like temperature, space velocity and molar ratio prove to be critical for vapour phase MTBE synthesis.

❖   Deactivation of the catalyst occurs on longer durations of run. However selectivity to MTBE remains the same throughout.

# REFERENCES

1.  G.R Hadder, *Energy*, 21, 118 (1992).

2.  J.G Goodwin Jr., S Natesakhawat, A.A Nikolopoulos, S.Y Kim, *Catal. Rev. Sci. Eng.*, 44, 287-320 (2002).

3.  M Vila, F Cunill, J.P Izquiredo, J Gonzalez, A Hernandez, *Appl. Catal.*, 117, L99 (1994).

4.  M Hunger, T Horvath, J Weitkamp, *Microporous. Mesoporous Mater.*, 22, 357-367 (1998).

5.  F Colignon, M Mariani, S Moreno, M Remy, G Poncelet, *J. Catal*, 166, 53 (1997).

6.  M.A Ali, B.J Bridson, W.J Thomas, *Appl. Catal. A: Gen.*, 197, 303 (2000).

7.  F Colignon, R Launders, J.A Martens, P.A Jacobs, G Poncelet, *J. Catal.*, 182, 302 (1999).

8.  T Horwath, M Seiler, M Hunger, *Appl. Catal. A: Gen.*, 193, 227 (2000).

9.  J.S Kim, J.M Kim, G Seo, N.C Park, S Niiyama, *Appl. Catal.*, 37, 45 (1988).

10. M.E Quiroga, N.S Figoli, U.A Sedran, *J. Chem. Eng.*, 67, 199 (1997).

11. J.M Adams, K Martin, R.W McCabe, S Murray, *Clays. Clay Miner.*, 34, 597-603 (1986).

12. Z Ziang, K Hidajat, A.K Ray, *J. Catal.*, 200, 209-221 (2001).

13. P Wiseman, "Petrochemicals", Ellis Horwood, Chichester (1986).

14. A Ali, S Bhatia, *J. Chem. Eng.*, 44, 97 (1990).

15. K Sugiyama, K Kato, H Miura, T Matsuda, *J. Jpn. Petro. Inst.*, 26, 243 (1983).

16. M.H Matouq, G Shigeo, *Int. J. Chem. Kinet.*, 25, 925 (1993).

17. C.P Nicolaides, C.J Stotgin, E.R.A vanderVeen, M.S Wisser, *Appl. Catal.*, 103, 223 (1993).

18. S Okazaki, N Wada, *Catal. Today*, 16, 349 (1993).

19. J.F Knifton, J.C Edwards, *Appl. Catal. A: Gen.*, 183, 1-13 (1999).

20. P Brandao, A Philippou, J Rocha, M.W Anderson, *Catal. Lett.*, 73, 59-62 (2001).

21. Q.H Xia, K Hidajat, S Kawi, *J. Catal.*, 209, 433-444 (2002).

22. G.D Yadav, N Kirthivasan, *J. Chem. Soc. Chem. Commun.*, 203 (1995).

23. J.M Adams, *Appl. Clay Sci.*, 2, 309 (1987).

24. J.F Knifton, US Patent 5,352,847 (1994).

25. F Ancillotti, M Massi Mauri, E Pescarallo, *J. Catal.*, 46, 49 (1977).

26. F Ancillotti, M Massi Mauri, E Pescarallo, L Romagnoni, *J. Mol. Catal.*, 4, 37 (1978).

27. S.C Desai, G.D Yadav, "Recent trends in Catalysis", V Murugesan *et.al* (eds), 224-229, Narosa Publishing house, New Delhi (1999)

28. G.J Hutchings, C.P Nicolaides, M.S Scurrell, *Catal. Today*, 15, 23 (1992).

29. van Le, R Mao, T.S Le, M Faibairn, A Muntasar, S Xiao, S Denes, *Appl. Catal. A: Gen.*, 185, 221 (1999).

# 7

# SUMMARY

# AND CONCLUSIONS

*The present work engrosses a thrust area in the field of chemical engineering, viz., catalysis by newer mesoporous clay catalysts. The venture consists of three main parts; preparation of the pillared clay catalyst, physicochemical characterisation by various techniques and application of the prepared systems for industrially important reactions like Friedel Crafts alkylations, tert-butylation of phenol, phenol hydroxylation and MTBE synthesis. This chapter reviews the summary of the work detailed in the preceding chapters. Important conclusions that can be made from the study are also included. Finally, the scope for the further work on the ever-expanding field is also outlined.*

The intercalation of clays with large, oxygen containing cations to produce pillared clays has been investigated for nearly twenty years. Montmorillonite is a common starting material because of its favourable characteristics of expandability, cation exchange capacity and its widespread availability. Many porous compounds have been synthesised with a variety of textural and surface chemistry characteristics thereby producing a wide range of adsorption and catalytic applications. These materials result from a two step modification of swelling clay minerals; insertion of polyoxocations into the interlamellar space and stabilisation of the polymeric species by subsequent thermal treatment.

## 7.1 SUMMARY OF THE WORK

The present work is dedicated to the synthesis and modification of different pillared montmorillonites. Iron, aluminium and mixed iron aluminium pillared montmorillonites were prepared by standard methods. The pillared clays were exchanged with transition metals of the first series. The prepared systems were characterised by different spectroscopic techniques. Acid structure of the samples was also followed by independent methods. The catalytic activities of the prepared systems were probed out by industrially important reactions. The present thesis comprises of seven chapters expliciting the introduction, experimental, results and discussion parts.

**Chapter 1** gives a brief account on catalysis, especially heterogeneous catalysis. A short but concise review on clays, different modifications on clays and the pillaring process is also covered. The structure of clays and the nature and different mechanisms of acidity generation are also demonstrated. Doping of pillared clays with transition metals and their applications are given special importance. The chapter also includes a brief outline on the reactions selected for the catalytic activity studies.

**Chapter 2** deals with the materials and methods employed for the preparation and characterisation of the different pillared montmorillonites and their transition metal exchanged analogues. A brief description of the various techniques adopted for the characterisation is sketched out. The experimental details for the evaluation of catalytic activity are also incorporated in this chapter.

**Chapter 3** describes the physicochemical characteristics of the prepared catalytic systems. The elemental composition and surface area and pore volume of individual systems were found out. Representative characterisation of the three series by cation exchange capacity determination, X ray diffraction, infrared spectroscopy, Al and Si NMR spectroscopy, thermogravimetry, UV diffuse reflectance spectroscopy and scanning electron microscopy was done. The nature and density of the acidic sites were examined by three independent techniques, viz., ammonia TPD, perylene adsorption and cumene cracking test reaction. The acid base property of the systems was evaluated by cyclohexanol decomposition reaction.

**Chapter 4** focuses on the application of the prepared systems for Friedel Crafts alkylations of arenes. The reactions achieved were benzylation of benzene with benzyl chloride, benzylation of *o*-xylene with benzyl alcohol, single pot benzylation of *o*-xylene with benzyl chloride and benzyl alcohol and *t*-butylation of phenol. The dependence of the catalytic activity on textural properties and surface acidity is given special importance. The structural stability of the catalysts was examined. The influence of different reaction variables on catalytic activity was studied extensively. On the basis of the various observations, plausible mechanisms for each reaction over the clay catalysts have been suggested.

**Chapter 5** discusses the significance of the prepared systems on the catalytic wet peroxide oxidation of phenol in aqueous solutions. A detailed study of the various reaction variables including the solvent and solvent concentrations revealed the

prepared pillared clay catalysts to be highly efficient in the oxidation of phenol. A plausible reaction mechanism also is suggested to explain the various facts.

**Chapter 6** establishes pillared clays to be effectual catalysts for the gas phase synthesis of MTBE with cent percent product selectivity. The observed activities could be recognised with Brönsted acidity of the catalysts. The influence of the reaction conditions on the catalytic performance is also furnished.

Each chapter is provided with a brief introduction. The key points emerging from the investigations are given at the end of each chapter as conclusions. Each chapter is provided with a reference list at the end.

**Chapter 7** outlines the summary and important conclusions of the work. Further scope of the study is also given at the end of the chapter.

## 7.2 CONCLUSIONS

The general conclusions that can be drawn from the present investigation are,

* Insertion of montmorillonites with iron, aluminium and mixed iron aluminium polyoxocations resulted in effective pillaring of the original clay. XRD, surface area and FTIR profiles confirmed this fact. As a result of pillaring, the basal spacing increased twofold. Surface area and pore volume of the clay increased drastically. However, the basic structural characteristics of the parent montmorillonite remained the same as indicated by FTIR spectroscopy.

* Exchange of the pillared clays with transition metals of the first series incorporated 1-3% of the metal, as revealed by the EDX measurements. However, NMR and FTIR spectra proved that the structural properties of the pillared clay were not altered as a result of this exchange. Surface area and pore volume measurements suggested that the incorporated metals were present in the pores.

❈       $^{27}Al$ NMR spectra reveal the presence of the Keggin cation in aluminium
        pillared samples. The pillaring species present in the mixed pillared system
        is the Keggin cation in which Fe replaces some of the Al. Iron pillared
        species show broadening of peaks due to relaxation effects. $^{29}Si$ NMR
        spectra indicate strain in the local environment. No inversion of silicon
        tetrahedra occurs as a result of pillaring. Exchange with transition metals
        had no effect on the structural details of the pillared clay.

❈       The prepared systems exhibited good thermal stability. Dehydroxylation of
        the pillar occurs up to temperatures above 500°C. SEM pictures and UV
        DRS shows no structural change on exchange.

❈       Transition metal exchanged pillared samples were efficient Friedel Crafts
        catalysts. Cent percent monoalkylated product selectivity was obtained in
        all cases. This can be attributed to the shape selective nature of the
        pillared clay catalysts. With benzyl chloride, iron containing systems show
        free radical based initiation. Lewis acid sites were responsible for the
        benzylation with benzyl chloride while Brönsted sites catalysed benzylation
        with benzyl alcohol. Single pot benzylation of o-xylene with benzyl alcohol
        and benzyl chloride led to the preferential adsorption and hence reaction of
        benzyl alcohol.

❈       T-butylation of phenol proceeded over the catalysts effectively. The
        conversions as well as product selectivities could be explained in terms of
        acidity.

❈       Pillared clays were found to be superior catalysts for the wet peroxide
        oxidation of phenol. Water was the most effective solvent for the reaction.

❈       Gas phase MTBE synthesis by direct method proceeds smoothly over the
        clay catalysts. Cent percent selectivity to the product is found. The
        activities can be recognised with Brönsted acidity.

## 7.3 FUTURE OUTLOOK

Pillared clays present a novel class of microporous materials that can be prepared easily. The most appreciable advantage of this type of catalysts is the large number of polymeric species that can be intercalated. Thus, the nature and extent of the pillars can be varied. This provides us with an important benefit, viz., the tuning of the pore sizes. Hence, other intercalants that have interesting properties; for example, sulphated zirconia or high surface area rare earth oxides prepared by surfactant method can also be intercalated.

The acidic properties of the catalyst alone have been exploited so far. Though the number of basic sites present in the prepared systems is nominal as indicated by the cyclohexanol decomposition reaction, its strength indicates that base catalysed reactions can take place over the catalysts effectively. This aspect combined with the shape selective nature of the porous network suggests potential applications.

The prepared systems were effective alkylation catalysts. Complex alkylations involving alkylating agents like styrene and MTBE can also be tried over the catalysts. Important alkylations like cumene synthesis and production of linear alkyl benzenes can be brought about over this group of catalysts.

Cracking and isomerisation reactions of hydrocarbons require acidic sites of the type possessed by the prepared catalysts. This field of catalysis is mainly governed by zeolites due to their much better thermal stability. However, since the pore volumes of the pillared clays are much larger, they can compliment zeolites in these reactions.

Oxidation of an important pollutant, viz., phenol occurs effectively over the prepared systems. Hence, oxidation of other organic pollutants also can be carried out successfully using the catalysts.